CONCEPTS OF OPERATIONAL AMPLIFIER

Vivek Jain
Dr. Pradeepa P

ALEXIS PRESS
JERSEY CITY, USA

CONCEPTS OF OPERATIONAL AMPLIFIER

CONCEPTS OF OPERATIONAL AMPLIFIER

Vivek Jain

Dr. Pradeepa P

ALEXIS PRESS

ALEXIS PRESS

Published by: Alexis Press, LLC, Jersey City, USA
www.alexispress.us

First Published 2022

A catalogue record for this publication is available from the British Library

Library of Congress Cataloguing in Publication Data

Includes bibliographical references and index.

Concepts of Operational Amplifier by *Vivek Jain, Dr. Pradeepa P*

ISBN 978-1-64532-887-2

CONTENTS

CHAPTER 1

COMPREHENSIVE STUDY ON THE OPERATIONAL AMPLIFIER

Mr. Vivek Jain, Associate Professor,
Department of Electrical Engineering, Jaipur National University, Jaipur India
Email Id- vivekkumar@jnujaipur.ac.in

Abstract

An integrated circuit (IC) known as an operational amplifier (op-amp) amplifies the voltage difference between two different inputs. It has the ability set up to execute arithmetic operations, thus its name. In this chapter author is discusses the open loop gain and bandwidth gain product.One of the most popular building blocks for linear designs, the op amp, will have its fundamental function covered in this chapter. The fundamental functioning of the op amp will be covered in section 1. We'll focus on the op amp from a black box perspective. While there are several literature that detail an op amp's internal operations, a more broad perspective will be used in this study. But, there are a few occasions when we shall discuss the internals of the op amp. It cannot be avoided.

Keywords

Bandwidth, Gain, Operational Amplifier, Network, Signal.

INTRODUCTION

One of the fundamental components of linear design is the op amp. The device contains two input terminals, the one of which inverts the signal's phase while the other retains it, and an output terminal. Figure 1provides the op amp's standard symbol. The power supply connections, which are unquestionably necessary for functioning, are disregarded in this.

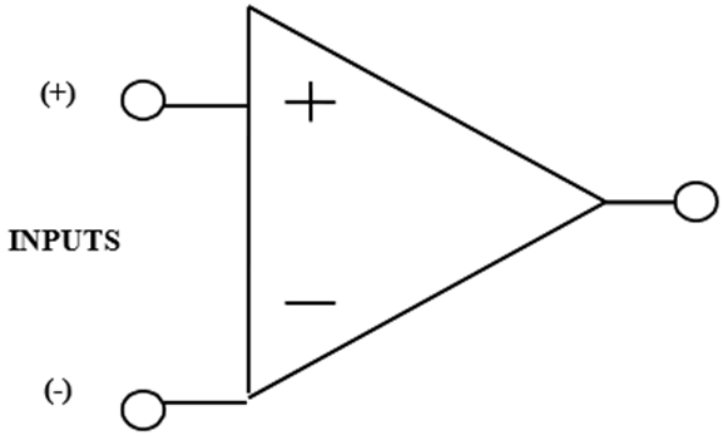

Figure1:Standardopampsymbol

Operational amplifier is often referred to by the acronym "op amp". Its moniker dates back to the early days of amplifier development, when analog computers employed op amps. (Sure, the first computers weren't digital; they were analog.) Many mathematical "operations" could be carried out when the fundamental amplifier was combined with a few external parts. Plotting the trajectories of munitions was one of the main applications of analog computers during World War Two.

VoltageFeedback(VFB)Model

Theclassicmodelofthevoltagefeedbackopampincorporatesthefollowingcharacteristics:

1. Infiniteinputimpedance
2. Infinite bandwidth
3. Infinitegain
4. Zerooutputimpedance
5. Zeropowerconsumption

Naturally, none of these are possible in their true form. The level of the op amp depends on how closely we adhere to these standards. The voltage feedback model is what is used to describe this. Almost all op amps with bandwidths under 10 MHz and over 90% of those with greater bandwidths belong to this category.

BasicOperation

It is simple to condense the op amp's fundamental mode of operation. In order to get the fixed gain for the amplifier, we first assume that some of the output is sent back to the inverting terminal. This is unfavorable commentary. The open-loop gain of the amplifier is doubled by any differential voltage between the input terminals of both the op amp. The output will become more negative if the magnitude of just this differential voltage is greater on the inverting (-) terminal than that on the noninverting (+) terminal. The output voltage will become more positive if indeed the magnitude of the differential voltage is greater on the noninverting (+) terminal compared to the inverting (-) terminal. The amplifier's open-loop gain will make an effort to reduce the differential voltage to zero. The differential voltage will remain at zero as long as the input and output remain within the operating range of the amplifier, and the output will consist of the input voltage multiplied by that of the gain specified by the feedback. This demonstrates that the inputs react to differential mode input voltage rather than common-mode input voltage.

Configurations in Inverting and Non-inverting

The voltage feedback operational amplifier may be set up as an amplifier in one of two ways at a minimum. As the inverting arrangement the output and input of this circuit are not in phase. The ratio of the employed resistors, which determines the gain of such a circuit (Figure 2), is given by:

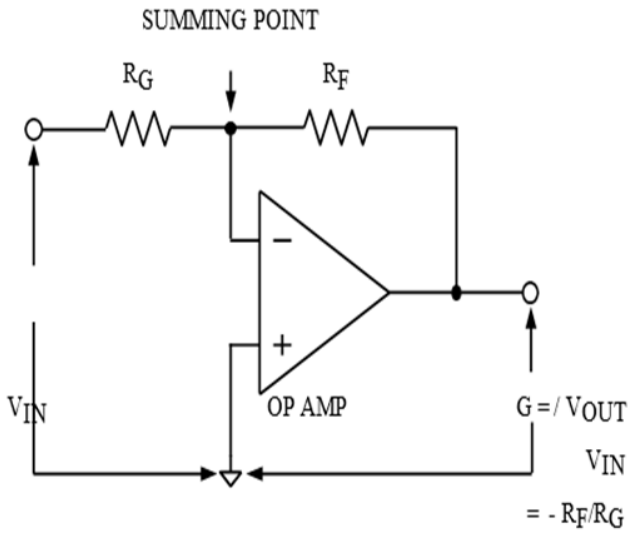

Figure 2: Illustrates the InvertingModeOpAmpStage.

It isknownastheNon-invertingconfiguration.Withthiscircuittheoutput is in phase with the input. The gain of the circuit is also determined by the ratio oftheresistorsusedandisgivenby (Figure 3):

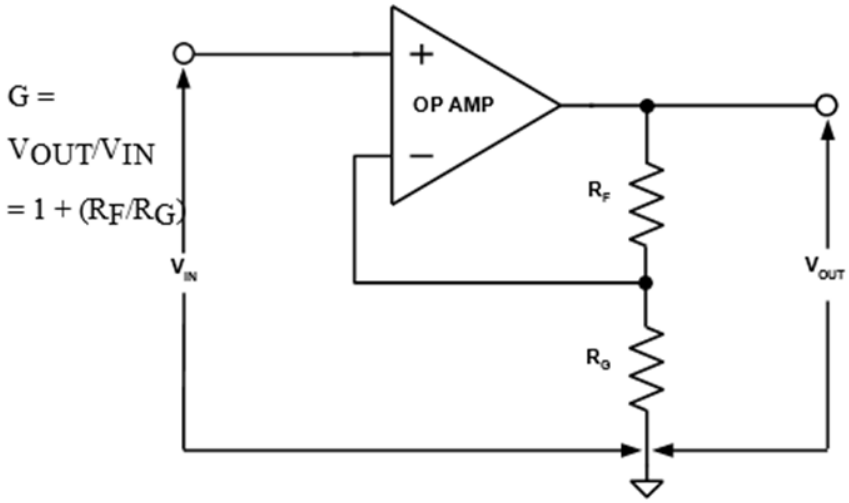

Figure 3: Illustrates the Non-invertingModeOpAmpStage

The greatest voltage available at the inverting terminal is the whole output voltage since the output drives a voltage divider (the gain setting network), which results in a minimum gain of 1. Keep in mind that the inverting terminal receives feedback in both circumstances from the output. This is unfavorable criticism, and the designer will benefit much from it. They will be covered in further depth in the next chapters. It should be remembered that the gain is determined by the resistor ratio rather than their actual values. This implies that, within reasonable bounds, the designer may choose pretty much any value. A lot of current would be needed from the op amps output to operate if the resistor values are too low. This results in high dissipation in the op amp, which has a number of drawbacks. The higher dissipation causes the chip to self-heat, which might alter the dc characteristics of the op amp. Moreover,

the heat produced by dissipation may ultimately lead the junction temperature to exceed 150 C, which is the generally acknowledged upper limit as with most semiconductors. The temperature of the silicon chip itself is the junction temperature. On the other extreme, if the resistor values are excessively high, noise will grow and the system will be more vulnerable to parasitic capacitances, which also will reduce bandwidth and may even result in instability and oscillation.Practically speaking, it becomes harder and harder to get resistors below 10 and above 1 M, particularly if precise resistors are needed (Figure 4).

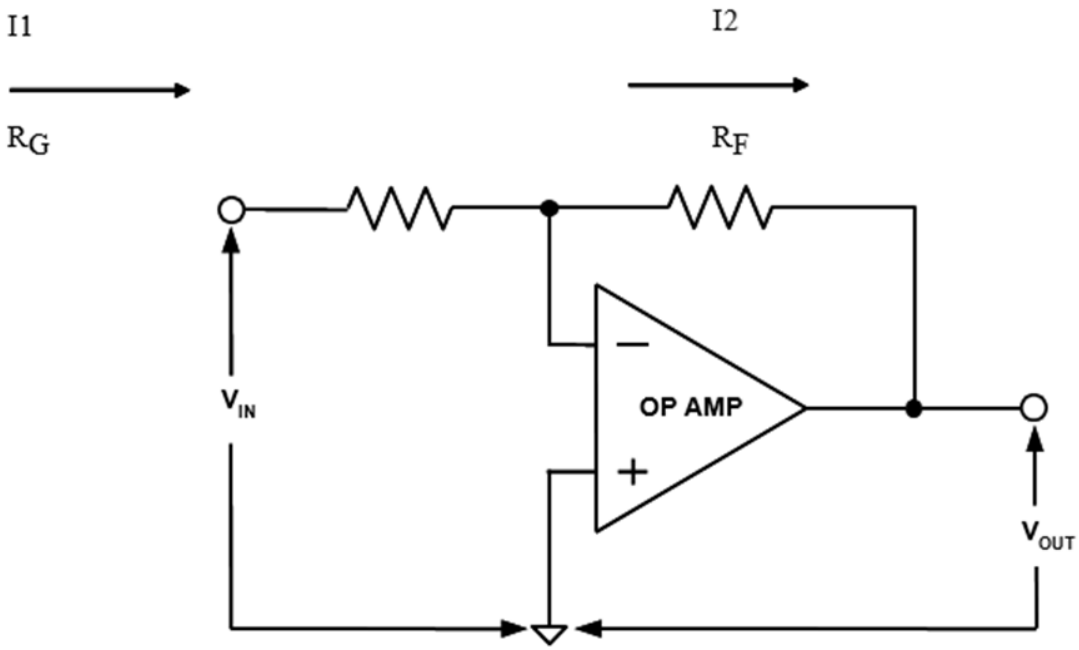

Figure 4: Illustrates the InvertingAmplifierGain

Let's take a closer look at the case of such an inverting amplifier. The noninverting terminal was linked to ground. The inverting input will also seem to be at ground since the op amp will drive the differential voltage across the inputs to zero. This node is really often referred to as the "virtual ground." A voltage (Vin) supplied to the input resistor will cause a current (I1) to flow through the resistor (Rin), creating the conditions for No current will flow into to the inverting input because the op amp's input impedance is infinite. Thus, the feedback resistor must be contacted by the same current (I1) (Rfb). The output would assume a voltage because the amplifier will drive the inverting connection to ground (Vout). We now look more closely at the noninverting scenario. The noninverting terminal receives the input voltage. The voltage divider made up of Rfb and Rin is driven by the output voltage. Although the resistor isn't really connected towards the input in this case, the word "Rin" is a little misleading. Nonetheless, we stick with it since it describes the inverting arrangement and has subsequently established a de facto standard. The voltage (Va) there at junction of the two resistors' inverting terminals.

LITERATURE REVIEW

According to the X. Chen et al. [1]capacitive power transfer (CPT) circuits' open-loop gain is sensitive to variations in coupling capacitance, which makes it challenging to regulate output voltage and output power, particularly for applications like wirelessly charging a laptop or keyboard. It has been shown that a hybrid coupler may combine the benefits of both CPT and inductive power transfer (IPT). A hybrid coupler is created in this research with the intention

of maintaining a constant open-loop gain whenever the coupling capacitance varies. The hybrid coupler's construction and operating principles are first described. Subsequently, using the suggested hybrid coupler, the open-loop gains of CPT, IPT, and hybrid wireless power transfer (HWPT) are computed, which is followed by a condensed design guideline for the whole HWPT system. Ultimately, a 40 W, 6.78 GHz experimental prototype is used to validate the suggested coupler.

In addition to taking into account the feedforward effects of heart rate on BP, closed-loop models of both the interactions between changes in blood pressure (BP) and pulse rate allow for assessment of baroreflex sensitivity by G. Paratiet al. [2]. By analyzing closed-loop baroreflex models under ambulatory settings, our work aims to compare modulations of feedback and feedback control couplings across 24 h in normotensive and hypertension people. Eight normotensive and eight hypertensive participants had continuous intra-arterial BP measurements for 24 hours. A moving average autoregressive model was used to assess the beat-by-beat sequence of systolic blood pressure (SBP) and pulse interval (PI), predicting closed-loop feedback but also feedforward gains within every window. As a result, the closed-loop SBP-PI model may identify hypertension-related changes in spontaneous baroreflex sensitivity and diurnal changes in the feedforward gain for PI on SBP that are not observable using the open-loop method. These results may contribute to a more thorough understanding of the autonomic dysfunction that underlies hypertension as well as a more thorough analysis of the advantages of rehabilitation techniques on autonomic cardiovascular regulation.

R. Moradi et al. [3] stated an innovative passive-active modulator with high-resolution and low-power applications is presented in this research. A passive switch capacitor integrator's performance is enhanced with an open-loop unity gain buffer. There is no requirement for big capacitors with this approach since it corrects phase and gain problems, which greatly reduces the chip footprint. As the first filter is passive, the amplifier's output swing is minimal but sufficient to provide linearity and just a relaxed slew rate inside the modulator structure, which results in the amplifier's low power. The needed SNR is achieved by employing the second-order modulation with a suitable oversampling ratio. The second-order passive-active modulator's post-layout simulation is carried out using the electrical simulator Spectre/Cadence utilizing the TSMC 0.18 CMOS model in the common 0.18 m CMOS process. In a 500 Hz signal bandwidth at 1.5 V supply, the frequency response of 92.4 dB, peak signal to noise ratio of 88.6 dB, peak signal to noisy plus distortions of 82.7 dB, and FoMWalden of 0.173 pJ/ conv-step were obtained while using 1.93 w. The FoMSchreier is 176.53 dB.

M. S. MurshithaShajahanet al. [4]in this work, a controller design that can withstand parameter changes in a thermal power plant process is proposed. The 500 MW Tuticorin facility of NLC Tamilnadu Power Limited (NTPL) provides real-time cold starting data. The coal flow rate, air flow rate, and feed water flow rate loops that will be managed to eventually control the produced electric power are modelled using this data. Quantitative Feedback Theory is a method for getting the parameters of both the PD controller that supports resilience in the stated performance even with changes in the plant parameters. It is utilized for controller design. The open loop gain and phase curve's magnitude and phase are measured at a certain frequency, and by resolving the ensuing equations, we are given the tuning parameters of both the controller. It is clear from either the simulation results that the controller functions rather well.

D. Valério[5] et al. gain may drop with frequency as phase rises in a controller whose frequency response is a complicated order derivative. To achieve simultaneous rejection of

high-frequency noise and resilience to changes in the open-loop gain, this behavior may be desired. The literature has implementations of such complicated order controllers, but they are unsatisfactory for a number of reasons, including the possibility of non-minimum phase zeros, unstable open-loop poles, or difficulty in obtaining the appropriate gain behavior. We provide a different nonlinear approximation that does not have these issues by combining a CRONE approximations of a fractional derivative with reset control. The favorable results of this approximation are confirmed by an experimental proof of concept, which also demonstrates that nonlinear effects do not prevent the required performance.

J. Lagos et al.[6]the design of ADCs in deep nanoscale CMOS technologies is highly difficult since low-voltage operation and limited inherent gain sometimes require the use of power-hungry analog circuitry and extensive digital calibration. In order to solve these issues, this study introduces a pipelined ADC that takes use of the ring amplifier's (ringamp) low but extremely consistent open-loop gain vs output voltage property in order to achieve high speed and linearity in low-voltage nanoscale CMOS systems. Moreover, an active ringamp-based common-mode feedback system and an adjustable ringamp biasing approach employing an anti-parallel arrangement of CMOS transistors are described. The implementation of a single-channel prototype ADC in a conventional 28-nm CMOS process yields Walden and Schreier figure-of-merit (FoM) values of 34.4 fJ/conv.-step and 161.9 dB, respectively, whereas the achieving 58.7-dB SNDR and 72.4-dB SFDR at 600 MS/s whilst also consuming 14.5 mW from a single 0.9-V supply.

According to the G. Royo[7] et al. usage in the downlink receiver of a remote antenna unit, this paper proposes an improved design of a low-noise transimpedance amplifier (TIA) with good linearity (RAU). The purpose of this design is to be implemented in a combined fiber-wireless indoor distributed antenna system (DAS) for WLAN transmission. A completely differential shunt-shunt responses TIA with digitally controllable transimpedance makes up the circuit architecture. Stability and continuous bandwidth are maintained by using an open-loop gain compensation approach (BW). A 1.2 V voltage supply and 65 nm CMOS technology were used to construct the TIA. The TIA uses 6 mW of electricity in its whole. For the purpose of demonstrating the dependable 54 Mb/s 802.11a WLAN transmission accomplished with just an error vector magnitude (EVM) lower than 3% over a 20 dB optical input range, a thorough electrical and optical evaluation using a 1550 nm PIN photodiode has been carried out.

Y. Du [8] et al. front-end receiver amplifier design for a capacitive micro-machined ultrasonic transducer is discussed in this study (CMUT). The proposed operational amplifier (op amp) has a class AB output stage after a complete differential folded-cascode instrumentation amplifier. A transimpedance amplifier is created by adding a feedback resistor between the op amp's input and output. We determined the static output impedance and center frequency characteristics of the CMUT by analyzing the equivalent circuit model of the CMUT element operating throughout the receiving mode. There includes a thorough discussion of the tradeoffs between op amp gain, bandwidth, distortion, and power usage. The complementary metal-oxide semiconductor (CMOS) 0.18-m technology from GlobalFoundries was used to create the amplifier. The amplifier's gain bandwidth combination is around 29.5 MHz, and its open loop gain is about 65 dB. 56 nA/Hz@3 MHz was the observed input reference noise current. The op amp is driven by 3.3 V, has a static power consumption of 11 mW, and has an area of 325 m 150 m. We used CMUT to confirm that our amplifier was functioning properly, and echo-pulse results showed that the CMUT's center frequency approximately 3 MHz with a 92% fractional bandwidth.

Y. T. Ku [9] et al. that work presents a novel fully differential operational Trans resistance amplifier (FDOTRA)-based current-mode Wheatstone bridge (CMWB). With its benefits of low input and output impedances, input voltage adjustment, high transimpedance (R m), a broad input range, and low input and output impedances, this suggested FDOTRA is an active component of the proposed CMWB. The performance of the proposed CMWB is unaffected by the usage of only one active component, the FDOTRA, and four resistors. The suggested CMWB features a straightforward design, excellent accuracy, a broad operating range, a compact volume, and cheap cost. Thus, the suggested CMWB has two distinct benefits. First of all, it lessens the quantity of passive and active sensing components. Second, compared to previous CMWB integrated circuits, the proposed CMWB circuit delivers a significant accuracy enhancement (IC). It has been evaluated, simulated, and implemented to use the suggested CMWB. The proposed FDOTRA was created using 2P4M CMOS technologies at TSMC's 0.35 mm pitch. 1.65 V is what its supply voltages are. The proposed FDOTRA has an open-loop gain of 69.2 dB and a 3-dB bandwidth of 16 MHz, respectively. The FDOTRA based CMWB has an open-loop gain of 24.6 dB and a 3-dB frequency of 16 MHz, respectively. The experimental findings indicate that the FDOTRA-based CMWB's accuracy is 92.4%.

Paul [10] et al. that work presents a straightforward method to create class AB Miller op-amps, which are very power efficient. With just a slight increase in power dissipation, it effectively increases the op-effective amp's transconductance gain, the dc open-loop gain, the gain-bandwidth product, effects on the psychological rate. It does this by using a composite input stage with resistive local common mode feedback, which gives the input stage class AB operation. The suggested strategy is validated by the experimental findings of op-amps in strong inversion as well as subthreshold built using a 130-nm CMOS standard technology. The op-amp features a 1.2-V supply voltage, a 9 VpF/sW large-signal figure of merit (FOM), and a 17 MHz pF/W small-signal FOM. The op-amp features a 0.5-V supply voltage, 10 V pF/s/W large-signal FOM, and 92 MHz pF/W small-signal FOM under subthreshold.

DISCUSSION

As the feedback loop is not closed, the gain of the amplifier is known as the open-loop gain (sometimes abbreviated as AVOL). Its gain may go as high as 160 dB or more for just a precision op amp. This is a 100 million dollar gain. From dc to what is known as the dominating pole, this increase is flat. The drop-off from there is 6 dB/octave or 20 dB/decade. (An octave doubles frequency; a decade multiplies frequency by ten). A single-pole reaction is what is used to describe this. Unless it collides with another pole inside the response, it will keep falling at this pace. This second pole will cause the open-loop gain to decline at a rate that is twice as fast, or 12 dB/octave or 40 dB/decade. The op amp would be unconditionally stable at any level if the open-loop gain has fallen below 0 dB (unity gain) before something reaches the second pole. On the fact sheet, this will often be referred to this as unity gain steady (Figure 5). The amplifier could not be stable if the second pole is reached whereas the loop gain is higher than 1 (0 dB).

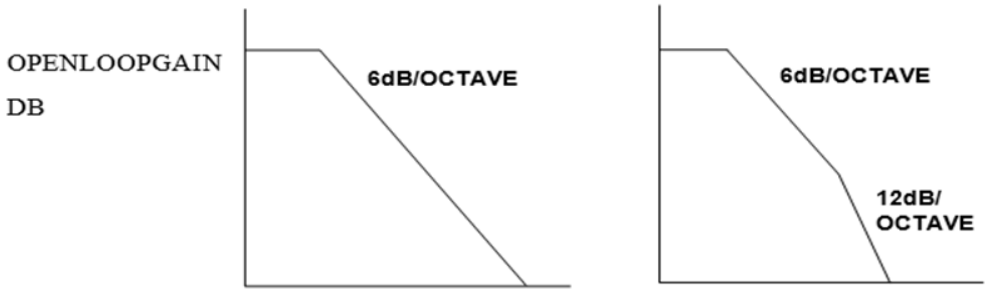

Figure 5: Illustrates the Open-LoopGain(BodePlot)

The distinctions between open-loop gain, closed-loop gain, loop gain, signal gain, and noise gain must be understood. They are distinct yet similar in nature and connected. We'll go into great depth on each of them. Open-loop gain is not a well-regulated specification. In most circumstances, it will be stated in the specifications as a typical number rather than a min/max figure since it may and often does have a very wide range (Figure 6). The specification will be a minimum in certain circumstances, generally high accuracy op amps. The output voltage levels and loading may also alter the open-loop gain. Temperature has some influence as well. These effects often have a very low impact and may be disregarded in most circumstances. In actuality, the data sheet for the component doesn't always mention this nonlinearity (Figure 7).

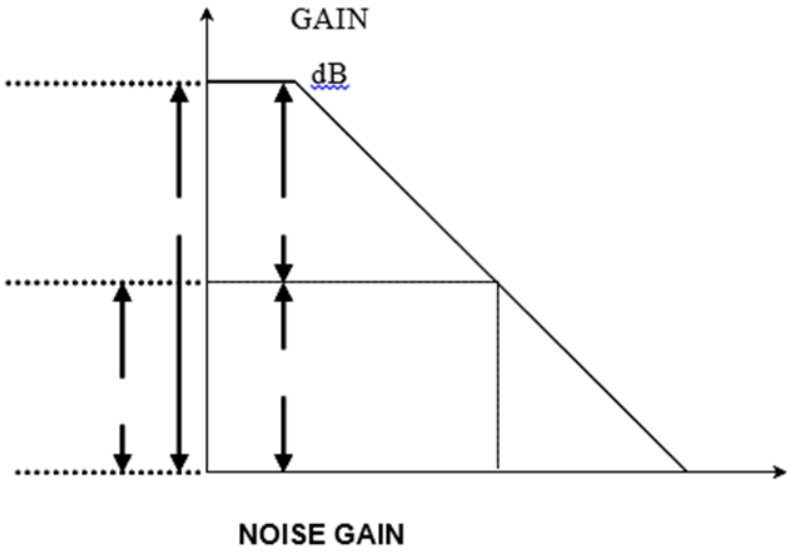

Figure 6: Illustrates the overall noise gain.

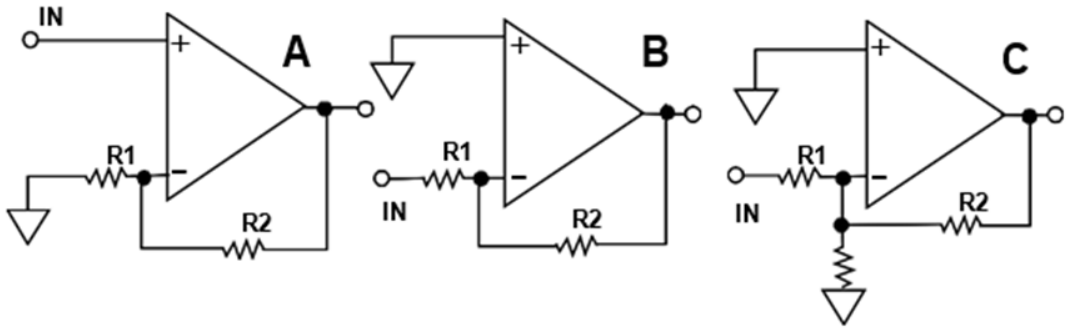

Figure 7: Represent the Circuit of Signal gain

Signal Gain =- R2/R1 NoiseGain=1+R2/R1

Voltage The Noise Gain of the op amp reflects noise and offset voltage to the output. When evaluating stability, noise gain—and not signal gain—is important. Circuit C's Signal Gain remains constant, but its Noise Gain is larger, improving stability, reducing noise, and increasing output offset voltage.

Bandwidth-Gain Product

The open-loop gain declines at a rate of 6 dB/octave. Hence, doubling the frequency will result in a gain that is only half of what it was before. The open-loop gain will double if the frequency is cut in half. As a result, the Gain- Bandwidth Product is created. The result of multiplying the frequency by the open-loop gain is always a constant. We must be in the portion of the curve that is dropping at 6 dB/octave in order for this to apply. This provides us with a useful figure of merit to assess if a certain op amp is appropriate for a given application.

For instance, suppose we need an op amp with a gain-bandwidth product of 1 MHz for an application that calls for a gain of 10 and a bandwidth of 100 kHz. This may be too simplistic. A little buffer should be included due to the unpredictability of the gain-bandwidth product and the fact that the response is really 3 dB lower at the point where the closed-loop gain crosses the open-loop gain. An op amp with such a gain-bandwidth product of 1 MHz would be insignificant in the aforementioned application. There would be greater insurance that the intended performance is realized if the safety factor were at least 5.

Stability Criteria

According to feedback theory, for a system to be stable, the closed-loop gain must intersect the open-loop gain at such a rate of 6 dB/octave (single-pole response). The op amp will oscillate if the response exceeds 12 dB/octave (2 pole response). Each pole contributes 90 of phase shift, which is the simplest way to conceptualize this. When two poles are present, the phase shift is 180 degrees, which causes oscillations when negative input is converted to positive feedback.

An amplifier that does not have unity gain steady, one would wonder. The explanation is that if an amplifier is not stable at unity gain, the bandwidth may be expanded for that amplifier. While the gain criterion must be satisfied, this is sometimes considered to as decompensated. The closed-loop gain should intercept the open-loop gain at a slope of 6 dB/oct in order to meet this requirement (single-pole response). Should this happen, the amplifier will vibrate.

Compare the open-loop gain diagrams in Figures 1.11, 1.12, and 1.13 as an example. The AD847, AD848, and AD849, the three components that are shown, are essentially the same part. The AD847 has a steady unity gain. Gains of at least two remain steady for the AD848. With a gain of ten or more, the AD849 is steady. This demonstrates how much wider bandwidth the AD849 has. Hence, if you operate at a high gain, you obtain a larger bandwidth.

There are a couple of tricks that you can use to help out in this regard in the circuit trickssection, which we will cover later.

Phase Margin

Phase margin is one way to gauge stability. The phase will likewise shift gradually, beginning as long as a decade away from the corner frequency, just as the magnitude response doesn't remain flat and then abruptly change. Phase margin, evaluated at the unity gain point, is the remaining amount of phase shift before you reach 180 degrees. Low phase margin manifests as an increase in output peaking shortly before the close-loop gain crosses the open-loop gain.

Gain in a Closed-Loop

In contrast to open-loop gain, which refers to the gain with said feedback loop open, this is, of course, the gain of the amplifier with both the feedback loop closed. Signal gain and noise gain are the two variations. Here are descriptions and distinctions of these. The open-loop gain is a factor in the formula for the gain of such a closed-loop amplifier. If AVOL is indeed the amplifier's open-loop gain and G is its actual gain, NG is its noise gain (see below), then:

Signal Gain

With the feedback loop linked, this is the gain that has been applied to the input signal. While discussing the gain of the inverting and noninverting circuits in the fundamental operating section above, we were really speaking more accurately about the closed-loop signal gain. It may invert or might not. In the inverting instance, it may even be less than one. While designing circuits, we are mainly concerned with signal gain. A noninverting amp's signal gain is the same as its noise gain. The situation is the same whether the stage is inverted or not. The stability is assessed using the noise gain. Moreover, Bode graphs use the closed-loop gain. While we utilized resistances in the calculation for noise gain, keep in mind that they are really impedances.

For best results, the feedback resistor was corrected. Smaller numbers may result in instability while larger values decrease bandwidth. The bandwidth is not significantly impacted by adjusting gain for fixed feedback resistors. Present-day feedback amplifiers lack a fixed gain-bandwidth product (Table 1).

Table 1: Illustrates the CurrentFeedbackAmplifierFrequencyResponse

	AD8001AN(PDIP) Gain					AD8001AR(SOIC) Gain					AD8001ART(SOT-23-5) Gain				
Component	−1	+1	+2	+10	+100	−1	+1	+2	+10	+100	−1	+1	+2	+10	+100

$R_F(\Omega)$	649	1050	750	470	1000	604	953	681	470	1000	845	1000	768	470	1000
$R_G(\Omega)$	649		750	51	10	604		681	51	10	845		768	51	10
R_O(Nominal)(Ω)	49.9	49.9	49.9	49.9	49.9	49.9	49.9	49.9	49.9	49.9	49.9	49.9	49.9	49.9	49.9
$R_S(\Omega)$	0					0					0				
R_T(Nominal)(Ω)	54.9	49.9	49.9	49.9	49.9	54.9	49.9	49.9	49.9	49.9	54.9	49.9	49.9	49.9	49.9
SmallSignal BW(MHz)	340	880	460	260	20	370	710	440	260	20	240	795	380	260	20
).1dbFlatness (MHz)	105	70	105			130	100	120			110	300	145		

Moreover, there shouldn't be a capacitor in the feedback loop of a CFB amplifier. An op amp will oscillate if a capacitor is employed in the feedback loop because it lowers the feedback impedance as frequency rises. For the same reason, you must be cautious about stray capacitances near the op amp's inverting input. In an effort to create a voltage follower with unity gain, it's standard practice to short the inverting input straight to the output when utilizing a current feedback op amp (buffer). It will oscillate in this circuit. Naturally, the feedback resistor value in this situation will be lower than the suggested value. If the specified feedback resistor of the right value is substituted for the short, the circuit is totally stable. The inverting input of the CFB amplifier has low impedance, which is another distinction between the VFB and CFB amplifiers. Low here often refers to 50 to 100. As a result, the inputs are not naturally balanced as the VFB circuit indicates. The CFB topology also improves slew rate efficiency. The internal compensating capacitor may be charged with a dynamic current. As is often the case with VFB topologies, it is not constrained to any set value. The current is raised (current-on-demand) using a step input or overload condition until the overdriven state is eliminated. There is no fundamental slew-rate restriction for the fundamental current feedback amplifier. Limitations are solely caused by parasitic internal capacitances, and significant progress has been made to lessen their impact.

Higher bandwidths and faster slew rates work together to provide CFB devices excellent distortion performance at lesser power. The amplifier's open loop distortion and the closed-loop circuit's loop gain have an effect on an amplifier's distortion. Due to the internal topology's fundamental symmetry, a CFB amplifier contributes only a modest amount of open-loop distortion. The other major cause of distortion is speed. A CFB amplifier often has a wider bandwidth than its VFB equivalent. As a result, the quicker portion has higher loop-gain and hence reduced distortion at a given signal frequency.

CONCLUSION

Operational amplifiers are crucial in the creation of the fundamental elements of several electronic circuits. Since there are external components that are connected to the system

characteristics, certain operational amplifier components are involved. An inverted output having negative polarity is produced by the inverting amplifier. Positive polarity and non-inversion characterize the output that a noninverting amplifier generates. Thus, the inverting amplifier's gain is merely a function of the resistances.

REFERENCES

[1] X. Chen, S. Yu, S. Song, R. T. H. Li, X. Yang, and Z. Zhang, "Hybrid coupler for 6.78 MHz desktop wireless power transfer applications with stable open-loop gain," *IET Power Electron.*, 2019, doi: 10.1049/iet-pel.2018.6199.

[2] G. Parati *et al.*, "Closed-loop cardiovascular interactions and the baroreflex cardiac arm: Modulations over the 24 h and the effect of hypertension," *Front. Physiol.*, 2019, doi: 10.3389/fphys.2019.00477.

[3] R. Moradi, E. Farshidi, and M. Soroosh, "A low power passive-active ΔΣ modulator with high-resolution employing an integrator with open-loop unity-gain buffer," *Integration*, 2019, doi: 10.1016/j.vlsi.2018.09.006.

[4] M. S. Murshitha Shajahan, D. Najumnissa Jamal, and V. Aparna, "Controller design using quantitative feedback theory for thermal power plant process," *Case Stud. Therm. Eng.*, 2019, doi: 10.1016/j.csite.2019.100441.

[5] D. Valério, N. Saikumar, A. A. Dastjerdi, N. Karbasizadeh, and S. H. HosseinNia, "Reset control approximates complex order transfer functions," *Nonlinear Dyn.*, 2019, doi: 10.1007/s11071-019-05130-2.

[6] J. Lagos, B. Hershberg, E. Martens, P. Wambacq, and J. Craninckx, "A single-channel, 600-MS/s, 12-b, ringamp-based pipelined ADC in 28-nm CMOS," *IEEE J. Solid-State Circuits*, 2019, doi: 10.1109/JSSC.2018.2879923.

[7] G. Royo, A. D. Martinez-Perez, C. Sanchez-Azqueta, C. Aldea, and S. Celma, "A highly linear low-noise transimpedance amplifier for indoor fiber-wireless remote antenna units," *Electron.*, 2019, doi: 10.3390/electronics8040437.

[8] Y. Du, C. He, G. Hao, W. Zhang, and C. Xue, "Full-differential folded-cascode front-end receiver amplifier integrated circuit for capacitive micromachined ultrasonic transducers," *Micromachines*, 2019, doi: 10.3390/mi10020088.

[9] Y. T. Ku, Y. S. Hwang, J. J. Chen, C. C. Shih, and D. Cheng, "A new current-mode wheatstone bridge based on a new fully differential operational transresistance amplifier," *AEU - Int. J. Electron. Commun.*, 2019, doi: 10.1016/j.aeue.2019.01.032.

[10] A. Paul, J. Ramirez-Angulo, A. J. Lopez-Martin, R. G. Carvajal, and J. M. Rocha-Perez, "Pseudo-three-stage miller op-amp with enhanced small-signal and large-signal performance," *IEEE Trans. Very Large Scale Integr. Syst.*, 2019, doi: 10.1109/TVLSI.2019.2918235.

CHAPTER 2

OVERVIEW ON VOLTAGE FEEDBACK AND CURRENT FEEDBACK

Mr. Sunil Dubey, Associate Professor,
Department of Electrical Engineering, Jaipur National University, Jaipur India
Email Id- sunildubey@jnujaipur.ac.in

Abstract

As the name suggests, voltage feedback describes a closed-loop setup where the error signal takes the form of a voltage. Conventional op amps employ voltage feedback, which means that when the input voltage changes, its output voltage also changes in response. In this chapter author is discusses effects of overdrive on Op Amp Inputs.

Keywords

Bandwidth, Gain, Operational Amplifier, Network, Signal.

INTRODUCTION

Several applications benefit from voltage and current feedback. The distinctions between CFB and VFB are not always obvious in applications. The performance of modern CFB and VFB amplifiers is similar, yet each architecture has certain distinct benefits. The option to choose the feedback resistor (or impedance) with voltage feedback comes at the cost of giving up bandwidth for gain. Current feedback restricts the options for the feedback impedance while maintaining excellent bandwidth across a broad range of strengths.

Ingeneral,VFBamplifiersoffer:

LowerNoise, BetterDCPerformance, FeedbackComponentFreedom whileCFBamplifiersoffer, FasterSlewRates, Lower Distortion, FeedbackComponentRestrictions

SupplyVoltages

Op amp supply voltage in the past was normally about 15 V. The range of the operating input and output was about 10 V. Yet these levels had no strict requirements. The maximum supply was typically 18 V. The internal structures established the lowest limit. You could probably get down to around 8 V supplies and still have an acceptable dynamic range since you could generally go within 1.5 or 2 V of each supply rail.

Nonetheless, a trend toward lower supply voltages has recently emerged. There are a few causes for why this has occurred. Secondly, the whole scale range of high speed circuits is often smaller. The amplifier's capacity to swing high voltages is the main explanation behind this. Every amplifier has a slew rate limit that is quantified as a certain number of volts per microsecond. If all else is equal, reducing your voltage range will allow you to go more quickly. The requirement to lower circuit impedance levels in order to lessen the effects of stray capacitance on them is a second factor. Pushing lower impedances puts more strain on the output stage and the amplifier package's capacity for dissipating power. Smaller voltage swings necessitate supplying smaller currents, which reduces the package's dissipation. The fact that the geometries of the components within the amplifier tended to shrink as their speed

rose is a further factor. Reduced breakdown voltages are often associated with these components' smaller geometries. The supply voltages had to decrease since the breakdown voltages were. The supplies are normally 5 V or even lower since high speed op amps nowadays typically have a breakdown voltage of 7 V.

In certain instances, using batteries created a need for lower supply voltages. As a result of fewer batteries being available, the final product's size, weight, and price would decrease. Single supply systems were being embraced at the same time. Op amps work with a single positive supply and ground instead of the usual plus and minus supplies, with the ground acting as the negative supply.

Factors for Single Supplies

The op amp's circuitry doesn't need ground in any way. In reality, you could just as easily use a single supply of +30 V (ground being the negative supply) in place of a bipolar (+ and) supply of 15 V as long as the rest of the circuit was biased properly and the signal remained within the op amp's common mode range. Alternatively, the supply might very well be -30 V. (ground being the most positive supply). One may encounter issues if you mix the single supply function with lower supply voltages. In the typical op amp architecture, the input stage is an NPN differential pair and the output stage is an emitter follower. You cannot run "rail-to-rail," that is, from one supply to the other, using any of these circuits. There must be some circuit adjustments. Using a PNP differential output was the first of these improvements (Figure 1). The LM324 was one of the first instances of this input arrangement. The input was able to approach the negative rail thanks to this setup (ground). But, it was unable to move to the positive rail. Yet, this was sufficient in many systems, particularly in mixed-signal ones that were mostly digital. The 324 is not a very accurate performer.

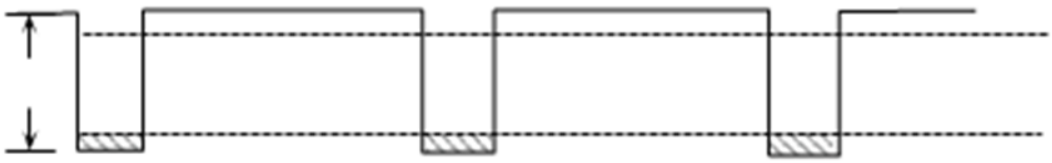

Figure 1: Illustrates the HeadroomIssueswithSingle-SupplyBiasing

The output signal will swing symmetrically around the bias point for a waveform with a symmetric (50% duty cycle) output level of 2 V p-p, or nominally 2.5 V 1 V. (using the values give). The ac averaged effect of CIN and R4 || R5 will move the effective maximum level either high or low, depending on the duty cycle, if the pulsed waveform has a very high (or low) duty cycle. This situation, which is seen, has the overall effect of decreasing the amplifier's operational headroom. A sample 50% duty cycle square wave with a bias between the upper and lower clip positions of a 5 V supply amplifier at a level of roughly 2 V p-p. For instance, this amplifier is only able to swing to the restricted dc values shown, which around 1 V from each rail are. Cases (B) and (C) both preserve the same peak-to-peak input level while adjusting the input waveform's duty cycle to the low and high duty cycle extremes. In (B) and (C), respectively, the waveform is observed to clip either negatively or positively at the amplifier output.

Rail-to-Rail

"Rail-to-rail" refers to a situation where the input and/or output may swing extremely near to the supply rails. There is no accepted definition in the business for this. This is what Analog

Devices considers swinging to within 100 mV of either rail. As the output current will determine the real maximum output level, this is driving a standard load for the output. You should be aware that not all amplifiers advertised as single supply are rail-to-rail. Moreover, not all rail-to-rail amplifiers have rail-to-rail input and output configurations. Either, both, neither, or neither might apply. In conclusion, students must read the data sheet. The output can never truly swing all the way to the rails.

Change of Phase

When the op amp's common-mode range is surpassed, an unusual occurrence may take place. Certain internal nodes have the potential to shut down, in which case the output will be dragged to the opposing rail until the input returns to a usable range. Several contemporary designs make efforts to solve this issue. This is often mentioned in the bullets on the cover page. Look at Figure 2. The most frequent phase reversal occurs when the amplifier is operating in follower mode.

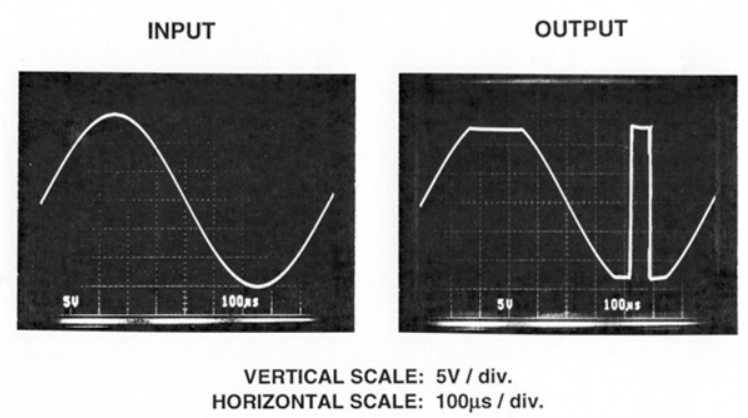

Figure 2: Illustrates the PhaseReversal.

LowPowerandMicro-power

The shift toward single suppliers is mirrored by the trend away from quiescent power. The amp itself is using this amount of power. Now that we've reached this stage, whole amplifiers can run on the bias current of the 741. Low power, but, comes with certain compromises.Lowering the output stage's bias current is one method of reducing the quiescent power. This translates into a stronger shift toward class B operation (and away from class A). The distortion of the output stage will thus have a tendency to increase. Reduce the input stage's standing current as another way to cut down on electricity. As a consequence, the bandwidth is decreased and the noise level is raised. But depending on the application, the word "low power" may signify a variety of various things. Op amps have a defined meaning at Analog Devices. Low power amplifiers have quiescent currents of less than 1 mA each. Micropower is described as having a quiescent current per amplifier of less than 100 A. This concept does not apply to the whole business, as was the case with "rail-to-rail".

Processes

Most contemporary op amps are constructed using bipolar transistors. On occasion, the input stage of a FET is a junction. Typically, this is referred to as a Bi-Fet (for Bipolar-FET). This

is often done to either reduce the input bias currents or raise the op amp's input impedance. Just the input stage normally makes use of the FET devices. The FETs used in single-supply applications may either be N-channel or P-channel. This permits input ranges that reach the positive and negative rails, respectively. Op amplifiers also undergo CMOS processing. While traditionally CMOS hasn't been a very appealing manufacturing technology for linear amplifiers, technology and circuit design have advanced to the point where CMOS op amps can now provide pretty respectable performance.

The ease with which CMOS lends itself to mixed mode (analog and digital) applications makes it a particularly appealing feature. The Digi-Trim and chopper stabilized op amps are two instances of this. The "Digi-Trim" method enables the offset voltage of op amps to be eliminated during final testing. This substitutes the wafer-level zener-zapping or laser trimming methods that are more widely used. The issue with trimming somewhere at wafer level is that after trimming, some parameter changes occur as a result of packing, etc. Trimming at the last test is a highly appealing choice, even if the change in parameters is rather well known and part of it may be expected. The Digi-trim amplifiers essentially have a tiny DAC that is used to change the offset.

Chopper stabilized amplifiers use methods to continually correct the offset. To do this, the offset of a larger bandwidth amp is adjusted using a dc precision amp. The input and a reference node (often ground) are alternated by the dc precision amp. This is then used to modify the "primary" amp's offset.

LITERATURE REVIEW

S. Bayhan[1] et al. for three-phase uninterruptible power supply (UPS) inverters, a Lyapunov energy function based control approach with output voltage feedback loops is suggested in this paper. The study that is being given shows that the conventional Lyapunov-energy function-based control approach not only causes significant steady-state output voltage inaccuracy, but also distorts the waveforms of the output voltage. Consequently, by including the output voltage feedback loops inside the control variables, the conventional Lyapunov-energy-function-based control has been modified. Analytical analysis of transfer functions, which are defined as the ratio of both the output voltage towards its reference, has been done to determine the resilience of the suggested control mechanism. These analytical findings are experimentally supported. Moreover, a three-phase UPS inverter running with linear (resistive) and nonlinear (diode-bridge rectifier) loads is used to experimentally assess the steady-state and dynamic performances of the proposed control approach. The proposed control method offers strong robustness against changes throughout LC filter parameters, high-quality sinusoidal waveform voltage with acceptable total harmonic distortion (THD) values under both linear and nonlinear loads, fast dynamic responding under abrupt load changes, and a negligibly small steady-state terminal voltage error as a result of including output voltage feedback loops inside the control variables.

H. C. Chen [2] et al. dual power source design is often utilized to guarantee that the equipment functions continuously even when the main power supply is turned off in various industries and medical power system applications. Yet, low loss output and voltage feedback between two separate power sources are significant problems for the system's energy dissipation. In this research, a novel mutual blocking control method is developed to efficiently address the voltage feedback issue present in the traditional dual power system without the need of a specialized microprocessor. Moreover, the suggested dual power switch design may totally eliminate voltage feedback and achieve a low voltage loss of roughly 30 mV when the load current is less than 0.5 A without significantly increasing hardware costs.

J. Yu [3] et al. that study suggests a virtual impedance-based bandwidth control technique for grid-connected inverters with multiple parallel harmonic compensators (HCGIs). The control bandwidth narrows as a consequence of the emergence of a new resonance point, according to an examination of the resonance points influenced by the interaction of numerous HCGIs on the control bandwidth. Next, six various kinds of virtual impedance circuits are built and evaluated in order to enhance the control bandwidth for multi-parallel HCGIs, and a virtual impedance via capacitor voltage feedback bandwidth control approach is suggested. The link between the feedback coefficient and bandwidth is then established, and the strategy for designing the method's parameters is then described. Ultimately, modeling and experimental testing support the suggested methodology. The calculation and experimental findings demonstrate that, without impacting the low-frequency current harmonic compensation, the proposed control approach may successfully shift resonant frequency right to address the problem of control bandwidth reduction throughout multi-parallel HCGIs systems.

J. Landaw and Z. Qu [4] explained the bifurcations and intricate dynamics brought on by the feedback between voltages and intracellular Ca2+ and Na+ concentrations in paced ventricular myocytes, we create an iterated map model. Whereas voltage and Na+ create a negative feedback loop, voltage and Ca2+ may form either a positive or negative feedback loop. Whenever the feedback between voltage and Ca2+ becomes positive under specific pathological circumstances, Hopf bifurcations can occur, resulting in periodic oscillatory behaviors. Period-doubling bifurcation paths to alternans and chaos happen whenever this feedback is negative.

M. Sulowicz[5] et al. that project proposal for a low-cost transducer with a Hall-effect sensor positioned in the air gap of a ferromagnetic core is presented in this paper. This device allows for the measurement of the distorted voltage instantaneous values even without feedback loop typically used for measurements in electrical machines. The transducer that is being used today provides for electrical isolation between both the measured voltage and the output voltage. Also, the effects of frequency, extra resistance, and the winding circuit's reactance on the amplitude and voltage phase shift brought on by the winding capacitance with ferrite core are explored. Finite element analysis is used to compute the outcome of modeling the leakage inductance of a measuring coil with a ferrite core and an air gap. In order to account for the linear core magnetization characteristic, experimental studies of the voltage phase shift angle but also output voltage amplitude drop for the voltage transducers with just an open feedback loop are conducted.

X. Hu [6] et al. stated the distribution of foot pressure is a crucial characteristic that is often used to gauge the pressure and load here on feet. Several plantar pressure measuring devices based on insoles have been developed in recent years. They are, however, limited by the data resolution end terms of the quantity of pressure sensing units. This research introduces a novel concept for a smart, portable insole that really can track measurements of the foot's plantar pressure. A pressure-sensitive E-textile is used to create this instrumented insole. The presence of 360 sensor arrays improves the resolution of pressure. To get rid of the cross-talk effect brought on by the interconnected sensing units, a VF-NSE technique was applied. The result demonstrates that this inexpensive instrumented insole can detect the foot pressure distribution fairly precisely.

According to the Y. Li, L. Fan, and Z. Miao [7]with poor grid connectivity, 4 Hz and 30 Hz oscillations have been seen in actual wind farms. Delivery of wind energy is constrained by such stability difficulties. To improve overall system stability, this research suggests

mechanism-based feedback control solutions appropriate for vector control based voltage source converters used in Type-3 and Type-4 wind. We first show that the coupling of power supply and voltage at the point of common connection is the primary source of the poor grid stability problem (PCC). The PCC voltage decreases when power supply is increased. Under poor grid conditions, this link creates a mechanism that might result in instability. The connection between power and voltage is lessened by the suggested control measures. Using the d-axis current or PCC voltage as the input signal, two feedback control algorithms are presented to modify the power order or dc-link voltage order. Analytical models and MATLAB/SimPower Systems testbeds of Type-3 and Type-4 wind are used to test the control techniques. The PCC voltage feedback control has good stability enhancing capabilities. The suggested regulation may greatly enhance the wind's ability to provide electricity.

X. Wu [8] et al. fuel cell electric cars need DC/DC converters with robust anti-jamming capabilities in addition to high boost ratio and efficiency. As a result, it is crucial to design a robust control technique that is based on the assumption of an acceptable topology. A straightforward dual-switch boost converter architecture is used in this research. We create a tiny signal model for continuous conduction mode (CCM) mode using the state space averaging approach, and then we suggest a feedforward-double feedback control system based on this model. The suggested feedforward-double feedback control method increases the resilience of the system while assuring a high boost ratio and efficiency, and addresses the issue of the weak output characteristics of fuel cells, according to simulation and experimental findings. Although the rising time of the step response is just a tenth of that of the voltage feedback control system, the control impact is comparable to the robust sliding mode control. The DC/DC converter utilizing feedforward-double feedback control system is much more resilient than the voltage feedback control system against unexpected changes in load when the output voltage of a DC/DC converter is 55 V.

Z. Guo [9] et al. in cascaded DC-DC converters, the interplay of the source and load converters may result in instability. So, it's crucial to increase the stability of cascaded DC-DC converters. By computing the eigenvalue sensitivity of a time-domain model for cascaded DC-DC converters, the aforementioned issue is resolved and a flowchart to enhance the control technique is produced. To further enhance the stability of cascaded DC-DC converters, an additional voltage-error mutual feedback control mechanism is first suggested based on the flowchart presented in this paper. The impact of the suggested mutual feedback control is next examined with regard to the stability of cascaded DC-DC converters. Lastly, simulation and experimentation are used to confirm the efficacy of the suggested control approach.

J. Ko and M. Lee [10]for the purpose of compensating for circuit delay, an on-chip resistor capacitor (RC) oscillator incorporating logic transition voltage (LTV) tracking feedback is provided. The suggested method uses the whole inverter chain as a comparator block and modifies the LTV to regulate the oscillation frequency in order to obtain excellent frequency stability. Additionally, low-frequency offset phase noise is reduced by the negative feedback structure. The proposed oscillator runs at 18.13 MHz and 245.7 W at room temperature with a 1.8 V supply. At 100 Hz and 1 kHz, respectively, the suggested approach decreases phase noise by 7.7 dB and 5.45 dB comparing to the free-running scenario. The observed phase noise values were 106.27 dBc/Hz at 100 KHz with a FOM of 157.53 dBc/Hz and 60.09 dBc/Hz at 1 kHz with such a figure of merit (FOM) of 151.35 dB/Hz. In a typical 0.18 mm CMOS process, the suggested oscillator takes up 0.056 mm2.

DISCUSSION

EffectsofOverdriveonOpAmpInputs

Regarding the effects of overdrive on op amp inputs, there are a number of crucial factors to keep in mind. Damage is undoubtedly the first. The "absolute maximum" input ratings for an op amp are listed on the data sheet of the component. They are normally written in terms of the supply voltage, however, unless the data sheet specifically states otherwise, maximum ratings only apply while the supplies are available. In the absence of supplies, the input voltages should be kept close to zero. The maximum input voltage is often expressed in terms of the supply, Vss 0.3 V, in a rating. Whether they are on or off, neither input is really allowed to move more than 0.3 V beyond the supply rails. In general, it doesn't matter if inputs do go outside 0.3 V while the supply is off if current is restricted to 5 mA or less (provided that no base- emitter reverse breakdown occurs). When the supplies are switched on, issues could develop if the input is outside of this range since this might activate parasitic SCRs within the device structure and cause it to malfunction within microseconds. Latch-up is a phenomenon that occurs far more often in digital CMOS than in the linear techniques used to make op amps. Avoid the potential of signals emerging before supplies are established if a device is prone to latch-up. (There is seldom, if ever, an issue when signals originate from other circuits utilizing the same source.) Thankfully, the majority of contemporary IC op amps are quite resistant to latch-up.

If the input current is restricted, input stage damage will be kept to a minimum. The general recommendation is to keep the current under 5 mA. At all costs, reverse bias junction breakage must be prevented. Keep in mind that the specifications for differential and common modes may vary. Moreover, not all overvoltage harm is severe. Consistent overvoltage of the op amp might cause minor deterioration of certain of the specifications. Schottky diodes are a typical way to clamp the signal to the supplies, in order to retain the signal inside the supplies. Nevertheless, if the Schottky diodes are located at the same temperature as the op amp, they will restrict the voltage to a safe level even if they do not limit it at all times to stay within the data sheet value. This does not, in reality, limit the signal to 0.3 V at all temperatures. Because diodes and op amps are constantly at the same temperature at turn-on and overvoltage is only conceivable then, this is readily done. Nevertheless, precautions must be made to guarantee that the diodes and op amp remain at the same temperature when this happens if the op amp may still be heated when it is repowered. The common-mode or differential input voltage ratings of many op amps are constrained. Limitations on common-mode differ from device to device and are often brought on by complicated architectures in extremely fast op amps. Limitations on differential input prevent the input transistors from experiencing a destructive reverse breakdown (especially super-beta transistors). Despite the extremely low current levels, this harm is still possible. In order to avoid internal protective circuitry from overheating at high current levels while it is conducting to prevent failures, limits on differential inputs may also be necessary. In this situation, a few hundred microseconds of overvoltage may not be harmful. Engineers should be aware of the rationale behind any "absolute maximum" rating in order to make accurate evaluations of the danger of long-term harm should the unexpected occur.

An op amp shouldn't be permanently damaged if it is overdriven within its ratings, although some of the internal stages could get saturated. With the exception of certain "clamped" op amps designed expressly for quick over-drive recovery, recovery following saturation is often lengthy. Hence, overdriven amplifiers could be quite sluggish.It is typically not a good idea to use an op amp as a comparator due to this decrease in speed with saturation (as well as output stages unsuitable to driving logic). However there are situations in which op amps may be used as comparators (Figure 3).

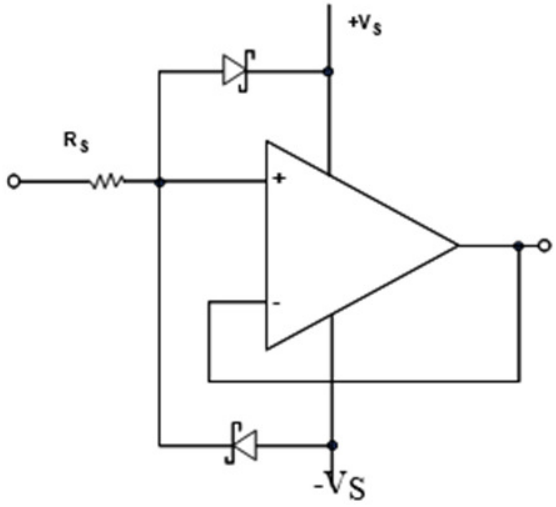

Figure 3: Illustrates the Input Over voltage Protection.

OP AMP Specifications

Basic op amp specifications will be covered in this section. Naturally, the application determines how significant each of these specifications is. For instance, in precision sensor signal conditioning circuits, dc specifications like offset voltage, offset voltage drift, and open-loop gain are crucial, but ac specifications like bandwidth, slew rate, and distortion may not be as crucial in high-speed applications. Op amp specifications are generally topology agnostic. While the error terminology and specifications for voltage feedback (VFB) and current feedback (CFB) op amps are identical, the application of each component justifies addressing parts of the specifications separately. This will be done in the talks that follow when there are big disparities. It should be noted that not all data sheets will necessarily provide all of these specifications. The more specifications an op amp has and the more stringent the specifications are, the better it performs. Remember the distinction between normal and min/max as well. A test at Analog Devices ensures that a specification is min/max. Typ specifications often aren't tested.

DC Requirements the Open-Loop Gain

The amplifier's gain while the feedback loop is open is known as the open-loop gain. Nonetheless, it is often measured at a very high gain with the feedback loop closed. It is unlimited with infinite bandwidth in a perfect op amp. It may be quite loud at dc (up to 160 dB) in actual use. It begins to decline at a certain frequency (the dominating pole) at a rate of 6 dB/octave or 20 dB/decade. (An octave doubles frequency; a decade is frequency divided by ten.) A single-pole reaction is what is used to describe this. For certain high precision

amplifiers, the dominating pole frequency will be about 10 Hz, whereas for some high speed amplifiers, it will be several kHz. It will keep dropping until it hits a different pole in the reaction, at which point it will stop. To 12 dB/octave or 40 dB/decade, or a factor of two, this second pole will twice the pace at which the open-loop gain declines. The op amp will be unconditionally stable anywhere at level if the open-loop gain has fallen below 0 dB (unity gain) before the amp reaches the second pole. In the data sheet, this will be referred to this as unity gain steady (Figure 4). The amplifier may not be stable if the second pole is reached whereas the loop gain is higher than 1 (0 db).

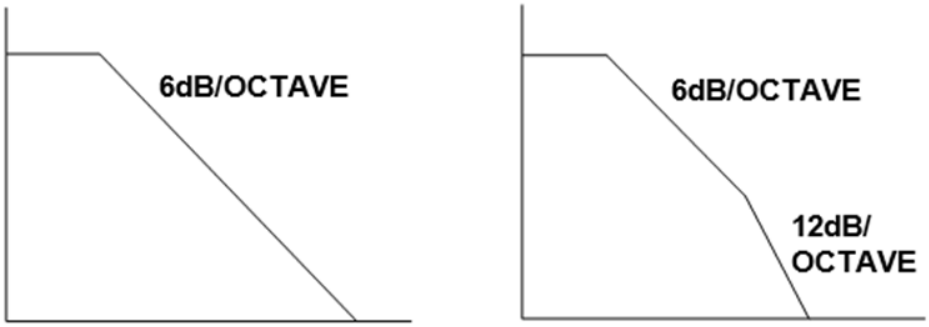

Figure 4: Illustrates the single pole response and two pole response.

With a single pole response, the open-loop gain decreases by 50% with a frequency doubling, resulting in what is known as a constant gain-bandwidth product. If indeed the frequency is multiplied by that of the gain at that frequency anywhere at point along the curve, the result is a constant. As an example, the open-loop gain of an amplifier with a 1 MHz gain bandwidth product will be 10 (20 dB) at 100 kHz, 100 (40 dB) at 10 kHz, etc. In a Bode plot, which graphs gain vs. frequency on such a log-log scale, this is easily visible.The open-loop gain of a voltage feedback op amp is a dimensionless ratio since it functions as a voltage in/voltage out transistor, hence no unit is required. In order to save space, data sheets may sometimes use V/mV or V/V instead of V/V to describe gain. Since gain in dB = 20 logAVOL, voltage gain may also be stated in dB terms. As a result, an open-loop gain of 1 V/V (or 1000 V/mV, 1,000,000 V/V, etc.) is comparable to 120 dB. The nonlinearity of the open-loop gain must be taken into account for extremely high precision operations. The most frequent reasons for variations in the open-loop gain of op amps are changes in the output voltage level and output loading. The closed-loop gain transfer function exhibits nonlinearity due to a change in open-loop gain with signal level, which cannot be corrected during system calibration. Although constant loads are common for op amps, AVOL fluctuations with load are often not significant. Yet for increasing load currents, AVOL's sensitivity to output signal level could rise.

The degree of this nonlinearity varies significantly across different device types and is often not included on the data sheet. The gain nonlinearity error probability will be reduced by selecting an op amp with a high AVOL because the minimum AVOL is always set. The AVOL nonlinearity cannot be made up for.

A CFB Op Amp's Open-Loop Trans-resistance

The open-loop response of current feedback amplifiers is voltage out for a current in, hence it is a trans-resistance (expressed in ohms) instead of a gain. As there is both a dc and an ac component, this is often known as a trans-impedance. A CFB amplifier's transimpedance will

typically fall between 500 k and 1 M. The open-loop transimpedance of a CFB op amp does not fluctuate in the same manner that a VFB open-loop gain does. The gain-bandwidth product of a CFB op amp will thus differ from that of VFB amps. A CFB amp's frequency response does vary somewhat with frequency, but not by more than 6 dB/octave. There may be some misunderstanding when the phrase "transimpedance amplifier" is used. Transimpedance amplifier is another name for an amplifier that is set up as a current to voltage (I/V) converter, commonly in photodiode circuits. Yet a FET input VFB amp rather than a CFB amp will typically be used in the photodiode application. This is due to the fact that the photodiode applications' current levels will be extremely low, making them less compatible with a CDB op amp's low impedance input.

Off set Voltage

The output of an op amp should be zero volts even when both inputs are precisely the same voltage since a difference of zero volts should result in a zero volt output. Nevertheless, in actual use, the output usually has some voltage. The offset voltage, or VOS, is referred to as this. The amount of voltage that must be applied to the input to force 0 V out is the traditional method to express offset voltage. The input offset voltage, also known as the input referred offset voltage, would this be voltage divided by that of the noise gain of the circuit. It is common practice to refer to the offset voltage as the input in order to remove the influence of circuit gain and facilitate comparisons. The offset voltage is represented mathematically as a voltage source, VOS, connected in series with the op amp's inverting input (Figure 5).

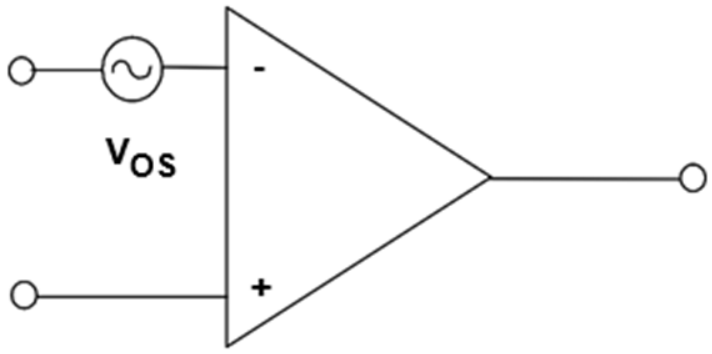

Figure 5: Illustrates the offsetVoltage

Off set Voltage Drift

The input offset voltage varies with temperature. Several times, drift or TCVOS are used to refer to the temperature coefficient. Drift in the offset could only be 0.1 V/oC. (Standard value for the very high accuracy op amp, OP177F). Common drift values range from 1 V/°C to 10 V/oC for a variety of general-purpose precision op amps. Most op amps have a predetermined TCVOS value, but others include a second, guaranteed maximum VOS value that applies across the operating temperature range. Such a definition is less useful since there is no guarantee that TCVOS is continuous or monotonic.

Eventually, Drift

The offset voltage also deteriorates or varies over time. V/month or V/1000 hours are typical measurements for characterizing aging, albeit they may be misleading. Instead of being linear, aging is a nonlinear phenomenon that is inversely proportional to the square root of the passage of time. So, instead of 9 V/year, a drift rate of 1 V/1000 hours becomes closer to 3 V/year. Long-term drift for the OP177F is around 0.3 V/month. This period is referred to after the first 30 days of operation. With the exception of the first hour of operation, the offset voltage of these devices typically varies throughout the first 30 hours of operation by less than 2 V. The long-term drift of offset voltage over time is often not specified, even with precision op amps.

Adjusting the voltage offset

Early op amps often included accessible pins for canceling offset voltages. By attaching a potentiometer to all of these pins and a wiper to either of the supply voltages, it was feasible to balance the input stage, eliminating the offset voltage. Several different input architectures were internally balanced by manufacturers of high precision op amps, such as Analog Devices (ADI) and Precision Monolithics (PMI). ADI used laser cutting on the input stage load resistors to achieve balance. PMI used a technique known as "zener zapping" to accomplish what was basically the same objective.During laser trimming, a portion of the collector resistors was eaten away by lasers in order to change their value. A series of resistors that were all bypassed by a semiconductor device that is essentially a zener diode were used in zener zapping. These zener diodes would indeed be shorted off by a voltage pulse (zapped). This modifies the resistor string's resistance value.

CONCLUSION

An amplifier performs better when there is negative feedback, but the overall gain is decreased. It ensures the circuit's performance repeatability, boosts bandwidth, lowers distortions, and aids in gain stabilization. A signal may be created from output and then returned to input in a variety of ways. Electronics circuits often use signal feedback to alter circuit behavior. If an amplifier has a gain more than unity, adding some of the output in phase to the input may raise gain, decrease linearity, therefore make the amplifier unstable, perhaps leading to oscillation.

REFERENCES

[1] S. Bayhan, S. S. Seyedalipour, H. Komurcugil, and H. Abu-Rub, “Lyapunov Energy Function Based Control Method for Three-Phase UPS Inverters with Output Voltage Feedback Loops,” *IEEE Access*, 2019, doi: 10.1109/ACCESS.2019.2934404.

[2] H. C. Chen, P. H. Kuo, and C. J. Huang, “A mutual blocking technology applied to dual power source switching control,” *Energies*, 2019, doi: 10.3390/en12040576.

[3] J. Yu, L. Deng, D. Song, and M. Pei, “Wide bandwidth control for multi-parallel grid-connected inverters with harmonic compensation,” *Energies*, 2019, doi: 10.3390/en12030571.

[4] J. Landaw and Z. Qu, “Bifurcations Caused by Feedback between Voltage and Intracellular Ion Concentrations in Ventricular Myocytes,” *Phys. Rev. Lett.*, 2019, doi: 10.1103/PhysRevLett.123.218101.

[5] M. Sulowicz, K. Ludwinek, J. Tulicki, W. Depczynski, and L. Nowakowski, “Practical adaptation of a low-cost voltage transducer with an open feedback loop for precise measurement of distorted voltages,” *Sensors (Switzerland)*, 2019, doi: 10.3390/s19051071.

[6] X. Hu, F. Shen, D. Peng, C. Luo, S. Mo, and X. Qu, "A Portable Insole for Foot Plantar Pressure Measurement Based on A Pressure Sensitive Etextile and Voltage Feedback Method," 2019. doi: 10.1109/ICDSP.2018.8631870.

[7] Y. Li, L. Fan, and Z. Miao, "Stability Control for Wind in Weak Grids," *IEEE Trans. Sustain. Energy*, 2019, doi: 10.1109/TSTE.2018.2878745.

[8] X. Wu, B. Yu, J. Du, and W. Shi, "Feedforward-double feedback control system of dual-switch boost DC/DC converters for fuel cell vehicles," *Energies*, 2019, doi: 10.3390/en12152886.

[9] Z. Guo, H. Li, C. Liu, Y. Zhao, and W. Su, "Stability-improvement method of cascaded DC-DC converters with additional voltage-error mutual feedback control," *Chinese J. Electr. Eng.*, 2019, doi: 10.23919/CJEE.2019.000012.

[10] J. Ko and M. Lee, "A 1.8 v 18.13 mhz inverter-based on-chip RC oscillator with flicker noise suppression using logic transition voltage feedback," *Electron.*, 2019, doi: 10.3390/electronics8111353.

CHAPTER 3

EXPLORATION ON THE TECHNOLOGY FROM DIGI-TRIM

Mr. Vivek Jain, Associate Professor,
Department of Electrical Engineering, Jaipur National University, Jaipur India
Email Id- vivekkumar@jnujaipur.ac.in

Abstract

Precision CMOS amplifiers may be produced using the Digi-Trim method for up to 30% less money and with more accuracy than other methods. Input offset voltage is the primary amplifier parameter for system accuracy. There are several methods for adjusting amplifier offset voltage and other parameters. In this chapter author is discusses Total Output Offset Error Calculation for IB and VOS.

Keywords

Bandwidth, Gain, Operational Amplifier, Network, Signal.

INTRODUCTION

Essentially a DAC, the DigiTrim method modifies the performance of circuit offsets by digitally weighting current sources. The CMOS process's mixed signal capabilities are used in this method. CMOS hasn't traditionally been the first option for precision amplifiers, however recent process advances and the DigiTrim technology have led to a highly acceptable level of precise performance. The trim data is input utilizing existing analog pins and a unique digital keyword sequence in this newly-patentable trim approach. Before making a permanent modification, the adjustment values may be temporarily programmed, assessed, and readjusted for maximum precision. The trim circuit is shut out after the trim is finished to avoid any chance of unintentional re-trimming by the end user. This process is distinctive in that the correction is made after the chip has been packed. The offset has to be changed at the die level for laser trimming and zener zapping. The offset shifts as a result of further processing, putting the chip on a header, and plastic encapsulation. This is brought on by both the heat used in the package molding process and the mechanical tension of the mounting (strain gauge effect). The ability to trim at the package level as opposed to the chip level is a considerable benefit, even though the amount of the shift is well characterized. By blowing polysilicon fuses, physical trimming may be accomplished with high reliability. With this trim technique, no additional pads or pins are needed, and no specialized test tools are necessary.

Using the input pins, the trimming is performed. Wafer-level testing is not necessary, given appropriate die yields. No unique wafer manufacturing method is needed, and our foundry partners can even create circuits. As every component of the trim circuit tends to scale with the characteristics of the process, the trim circuit likewise tends to scale proportionately with the process and amplifier circuit. The trim circuits contribute very little to the cost of the die since they are far smaller than typical amplifier circuits. The trims are discrete, similar to those used in link trimming and zener zapping, yet they may nevertheless easily provide the requisite precision at a very little cost premium over untrimmed parts. With a different

amplifier design, the DigiTrim technique might potentially permit user trimming of system offsets. While it hasn't yet been done so in a production section, this is still a possibility (Figure 1).

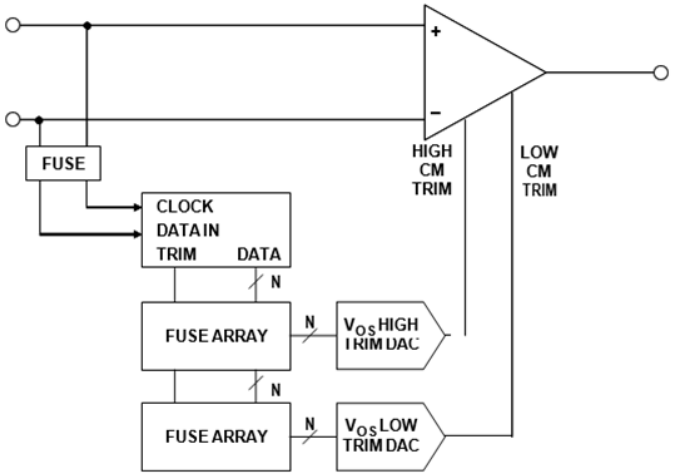

Figure 1: The Simplified Schematic of the Digi-Trim Technology.

Exterior Trim

With the introduction of twin op amps, the offset adjustment pins began to vanish since the 8-pin package was no longer large enough to accommodate them. Techniques for external adjustment were thus needed. In order to externally trim out the offset, a little voltage is essentially added to the input. The manufacturing technique utilized to make the component as well as the polarity of the input devices will determine the polarity of the voltage delivered to the offset potentiometer (NPN or PNP). Potentiometers, digital potentiometers, and DACs may all be used to adjust the offset. The primary issue with external trimming is that it's quite likely that the temperature coefficients of the inside and exterior components won't coincide. The efficiency of the temperature adjustment will be limited as a result. The mechanical potentiometer is also vulnerable to age and mechanical vibration. Due to the additional resistance and potentiometer resistance, there is an increase in noise gain. Making R3 significantly bigger than R1 will help to decrease the rise in noise gain that results. Notice that if the offset potentiometer is not changed, the signal gain may be impacted. Nevertheless, if R3 is linked to a constant low impedance reference voltage supply, VR, the gain may be stabilized.

Current Input Bias

As the inputs possess infinite impedance inside the ideal op amp model, there is no current flowing into the input terminals. Nevertheless, since bipolar junction transistors (BJTs), the most popular input structure, are current-controlled devices, there is always some current needed for operation. Input bias current (IB) or bias current is the term used, there are always two input bias currents, IB+ and IB, one for each input. IB values vary from 60 fA in the AD549 electrometer, or about one electron per three microseconds, to tens of microamperes in certain high-speed op amps. These bias currents tend to be equal because of the fundamental structure of monolithic op amp manufacturing processes, although this isn't always the case. Moreover, the nonsymmetrical character of the inputs in the case of current feedback amplifiers ensures that the bias currents are varied. Since input bias current flows

through external impedances and generates offset voltages that increase system defects, input bias current is an issue for op amp users. Imagine a unity gain noninverting source with a 1 M source impedance. IB will add an extra 10 mV of inaccuracy if it is 10 nA. Conversely, the circuit won't function at all if the designer just disregards IB and employs capacitive coupling. This is because a DC return channel from the bias currents to ground is required. The input of the op amp will veer toward one of the rails if the dc return route is absent. However, if IB is low enough, it could temporarily function while the capacitor charges, producing even more false findings. The lesson learned from this is to always consider the impacts of IB in op amp circuits (Figure 2).

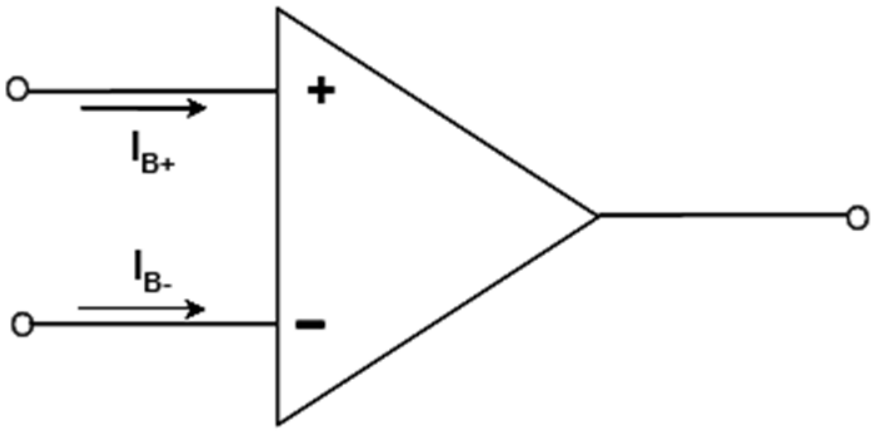

Figure 2: the InputBiasCurrent

InputOffsetCurrent

The input offset current is the difference between the bias currents. The offset current is often minor since the bias current differences are typically tiny as well. The offset current in bias-compensated op amps (see the next section) is almost equal to the bias current.

Taking into Account Input Bias Current

Bias currents may be compensated for in a variety of ways. The manufacturer can take care of it, or other methods may be used. Bias currents may be managed by an IC maker in essentially two distinct methods. The first is the input stage's usage of "super-beta" transistors. Specially processed transistors with an extremely thin base area are known as super-beta transistors. Often, they have a current gain () of tens of thousands or thousands (rather than the more usual hundreds for standard BJT transistors). While bias currents in op amps having super-beta input stages are substantially lower, their frequency response is also more constrained. Super-beta devices need extra circuitry to prevent the input stage from harm caused by input overvoltage since their breakdown voltages are often relatively low.

The employment of a bias compensated input structure is the second strategy for addressing bias currents. Small current sources are introduced to the input device bases with such a bias current compensated input. The concept is that the current sources will provide the bias currents needed by the input devices, greatly reducing the net current observed by the external circuit (Figure 3).

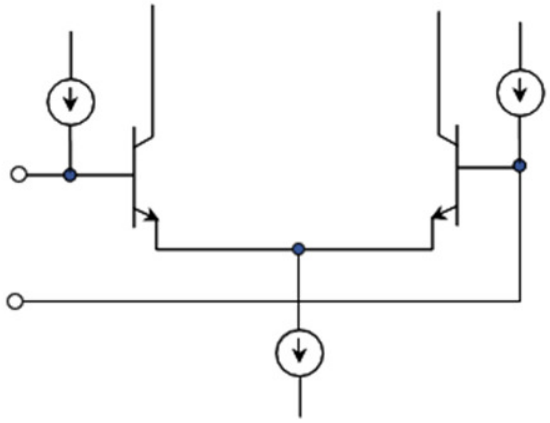

Figure 3: the InputBiasCurrentCompensation.

Several of the positive characteristics of the straightforward bipolar input stage, such as low voltage noise, low offset, and low drift, are also present in bias current compensated input stages. They also feature a low bias current that is mostly temperature stable. Unfortunately, since current sources are added to the input, their present noise is not very good. They also have poor bias current matching. The external bias current, which is the difference between the compensating current source and also the input transistor base current, is what causes the latter two undesirable side effects. There will always be noise in each of these currents. The two sounds accumulate in a root-sum-of-squares pattern since they are not connected (even though the dc currents subtract). Be aware that this is simple to confirm by looking at the offset current standard (the difference in the bias currents). The offset current will be the exact size as the bias current when internal bias current correction is present. The offset current will typically be at least 10 times less than the bias current without bias current adjustment. It should be noted that these correlations often persist regardless of the precise amount of the bias currents.

There is no justification for the net current to have a specified polarity since the resultant external bias current is indeed the difference between two virtually equal currents. Because of this, a bias-compensated op amp's bias currents may not only be out of phase, but they may also flow in the wrong direction! The droop (change in voltage in the hold mode) of a sample-and-hold amplifier (SHA) constructed using a bias-compensated op amp may have either polarity, for example, but in certain applications it might have unanticipated consequences. In an op amp data sheet, the bias current correction function is often absent. By looking at the bias current spec, it is simple to tell whether bias current compensation has been employed. The op amp is probably compensated for bias current if the bias current is stated as a "" value. By adjusting the impedances perceived by the two inputs equally, the designer can offset the effects of a bias current. If the impedances are equivalent, the bias currents that flow through them will also typically have equal values, resulting in the same offset voltage, where it will be seen as a common-mode signal. As it is a common-mode signal, the amplifier's common-mode rejection (CMRR, to also be explained later in this section) would tend to prevent it from adding to the error (Figure 4).

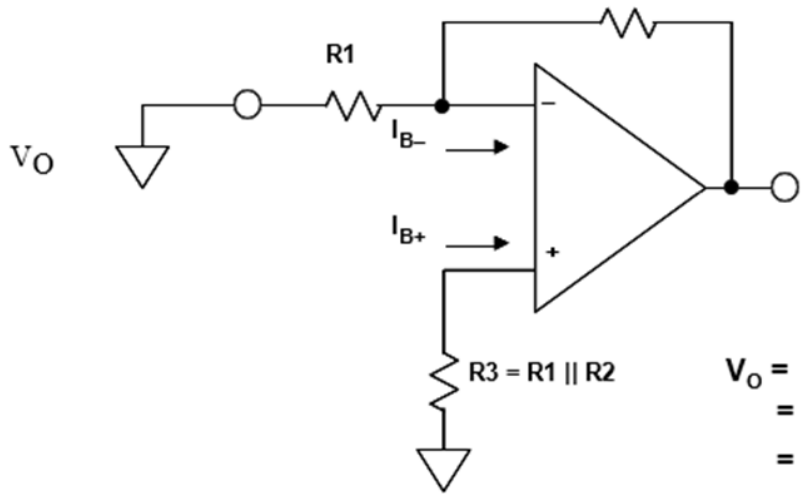

Figure 4: the BiasCurrentCompensation.

This method should be used with caution. As the bias currents aren't equal, it is evident that it won't operate with a bias compensated op amp. Due to the high input impedance levels and low bias currents that characterize FET input amplifiers, the effects of the Johnson noise may be higher than those of the bias current passing through them. Analysis must be carried out.

LITERATURE REVIEW

A. E. Urai[1] et al. stated the behavioral context, such as a person's past behavioral decisions, as well as the present sensory input influence perception. Yet, it is still unclear how these historical signals affect how decisions are made afterwards. The beginning point of accumulation is often considered in models of decision formation to move toward the bound reflecting the prior choice. Here, we offer findings that refute this notion. We computed bias parameters that were dependent on the observers' prior decisions by fitting bounded-accumulation decision models to data on human perceptual choice. Individual history biases affecting overt behavior were consistently explained by a history-dependent shift in the evidence accumulation, as opposed to its beginning point, across a variety of task procedures and sensory modalities. Hence, choice history signals seem to influence how present sensory information is interpreted, acting as a change in endogenous attention in favor of (or against) the previously chosen interpretation.

M. Fritsche and F. P. de Lange [2]serial dependency refers to the tendency for perceptions of present sensory information to favor input from the recent past. In the presence of both internal and external noise, serial reliance may help to stabilize neuronal representations. It is unclear, nevertheless, under what conditions prior information draws future perceptual choices and whether serial dependency represents a general smoothing or a more focused stabilizing process. Here, we looked at whether serial dependency may be modified by focusing on certain aspects of the preceding stimulus. When the orientations of the prior and present stimuli were identical, we discovered an attractive bias in orientation estimates, and a repulsive bias when they were different. When observers focused on the size rather than the direction of the prior stimulus, the attractive bias was significantly diminished—to less than half of its initial amplitude. The repulsive bias, on the other hand, was not affected by feature-based attention for stimuli with significant orientation disparities. This shows that the causes of these favorable and unfavorable perceptual biases are distinct.

H. P. Chen[3] et al. conducted a research to suggests employing two multi-output voltage difference transconductance amplifiers (VDTAs), three grounded capacitors, and a novel third-order quadrature oscillator that is electrically controllable. Three quadrature voltage outputs, two high-impedance quadrature current outputs, and one high-impedance vout with configurable amplitude are all provided by the proposed circuit. Whenever the input bias current of the second VDTA is indeed a modulating signal, the proposed circuit may produce amplitude modulation/amplitude shift keying signals. Two multi-output VDTAs' input bias currents allow for the independent adjustment of the oscillation conditions and frequency, making it appropriate for use with customized sensor networks. Results from experiments and H-Spice simulations are provided to support theoretical analysis.

Y. Zhang[4] et al. in a vertical-cavity surface-emitting laser (VCSEL) with just an integrated saturable absorber, a polarization-mode competition (PMC)-based all-optical spike inhibition technique is presented and statistically evaluated. To the best of our understanding, the inhibitory dynamics is defined by spike amplitude and first-spike latency (FSL) when the first time. Upon that spike amplitude and FSL, the impacts of input strengths, bias current, input strengths with time, and noise are all investigated. The findings demonstrate that an excitatory input may cause a spike to occur in the y-polarization mode, and that an inhibitory input from PMC can prevent a spike.

D. Bannister[5] et al. in order to assess hydrological and water resource systems, it is crucial to provide accurate estimation of precipitation over catchment areas in the Hindu Kush, Karakoram, but also Himalaya mountain ranges. It is also important to identify precipitation extremes in order to evaluate hydro-meteorological hazards. Here, we examine whether bias-corrected Weather Research and Forecasting model at a 5-km grid spacing can replicate the spatiotemporal variability of precipitation again for Beas and Sutlej river basins in the Himalaya, observed by 44 stations dispersed during the period from 1980 to 2012. We found that within the Sutlej basin, precipitation levels predicted by the raw (uncorrected) model output were often too low for yearly, monthly, and (especially low-intensity) daily precipitation. While biases persisted, the model's performance for the Beas basin was superior. An early-morning optimum in precipitation during in the monsoon season, which is associated to excessive precipitation dropping upwind, is thought to be the source of the dry bias and over Sutlej basin. The model output, however, produced much better results when a nonlinear bias-correction approach was used, outperforming precipitation predictions from retrospective study and two gridded datasets. Our results show that existing gridded datasets are not suitable for hydrological modeling across Himalayan catchments and that output from bias-corrected high-resolution regional climate change models is really required. Furthermore, the gridded datasets significantly underestimated precipitation extremes across the Beas and Sutlej basins, indicating that bias-corrected regional climate developed model is also required for hydro-meteorological vulnerability assessment in Himalayan catchments.

D. Luo [6] et al. In that study, a low-noise, low total harmonic distortion (THD) chopper amplifier concept was put forward for neural signal collection. To reject the electrode-dcoffset, a dc servo loop (DSL) based on an active Gm-C integrator is presented (EDO). To increase linearity and lower noise, a supplemental input very low-transconductance (VLT) operational transconductance amplifier (OTA) with a transconductance range of 45 pS to a few nS was developed and incorporated into the active Gm-C integrator. The suggested amplifier was created using a TSMC 0.18-m CMOS process, taking up 0.2 mm2 of space and requiring a 1.8-V supply voltage to operate at 3.24 W/channel. A 5-mVpp input has a THD that is less than -61 dB. It is determined that the input-referred thermal noise PSD is 39 nV/Hz. The observed input-referred noise is 0.65 Vrms inside the frequency range of 0.3-200

Hz and 2.14 Vrms in the range of 200 Hz to 5 kHz, resulting in noise-efficiency factors of 2.37 (0.3-200 Hz) and 1.56, respectively (0.2 k-5 kHz). Moreover, the external bias current allows the high-pass corner frequencies to be accurately set and linearly varied from 0.35 to 54.5 Hz.

According to the A. Gaur [7] et al. as a result of global climate change, residences and buildings in Canada may soon be subjected to climatic conditions that have never been seen before. It's crucial to assess how well new and existing structures operate in current and predicted future climates in order to increase their climate resilience. Input for the types of models that connect to solar radiation, cloud cover, wind, humidity, flash flooding, temperature, and snow cover must come from continuous climatic change records at high temporal frequency range of a wide range of climate variables. These models include hydrothermal and whole building simulations, which are crucial tools for evaluating performance. In this research, climatic data are created for 11 major Canadian cities that may be used to evaluate the performance of building envelopes under present and anticipated future climates, contemporaneous with 2C and 3.5C rises in world temperatures. The datasets, which are made up of 15 future climate realizations created by dynamically downscaling future forecasts from the CanESM2 global climate modeling and then bias-correcting with reference to observations, represent the internal variability of the climate. According to an analysis of the bias-corrected forecasts, future temperature and precipitation increases and reductions in snow cover and wind speed are predicted for all cities as a result of global warming.

A. Ghorbani[8] et al. it is essential to be able to accurately explain why the machine learning algorithm generates certain predictions if machine learning is to be believed in many applications. Because of this, a number of techniques have recently been created to interpret neural network projections by offering, for instance, feature significance maps. Knowing how much tiny systematic changes to the input data, such as those produced by adversaries or measurement biases, might change the interpretations is crucial for scientific robustness as well as security reasons. In this research, we show how to create adversarial perturbations that provide perceptually similar inputs that get the same predicted label but are interpreted significantly differently. Using ImageNet and CIFAR-10, we comprehensively evaluate the reliability of the interpretations produced by three popular feature significance interpretation techniques (feature importance maps, integrated gradients, and DeepLIFT). Our tests demonstrate that systematic perturbations may produce radically different interpretations in all situations while maintaining the label. We build on these findings to demonstrate how interpretations based on exemplars, like influence functions, are also vulnerable to hostile assault. Our examination of the Hessian matrix's geometry sheds light on why existing interpretation techniques often struggle with resilience.

In study H. Chen [9] et al. for both algorithm developers and data consumers, it is currently unknown how relevant geographic and climatic parameters affect the input source errors of integrated multi-satellite precipitation estimations. The consequences of the twelve input sources utilized in the most recent Global Satellite Mapping of Precipitation for Global Precipitation Measurement (GPM-GSMaP) for various climatic areas, altitudes, and seasons across mainland China were the major focus of this work. Our assessment findings demonstrate a relationship between the accuracy of GPM-GSMaP precipitation estimations and the error characteristics of the input sources from various passive microwave and infrared sensors. Throughout the semi-arid and dry areas, where the false bias was especially severe, the input sources exhibit greater hits, misses, and false biases. In terms of seasonality, the input data sources perform much better in the summer and have comparatively fewer hits and

more biases throughout the winter. Also, we discovered that geography had varying degrees of influence on the input sources' retrievals of precipitation. Conical-scanning imagers often outperform cross-track-scanning sounders in characteristics of passive microwave sensors, but the sounders-based precipitation predictions have a substantially greater detection capacity. One of the primary GPM sensors, the microwave imager GMI, has shortcomings in capturing areal rainfall patterns and exhibits rather substantial biases, particularly in the winter and spring. This suggests that the GMI algorithm may need additional development.

K. Turbett[10] et al. discussed the serial reliance is a perceptual bias in which the perception of the present is skewed toward the information of the past. It has been suggested that this bias plays a crucial functional role throughout vision, stabilizing the impression of objects via integration, when it perceives visual features, such as facial identity. This bias may help create reliable representations of facial identity when recognizing faces. If true, then the capacity to recognize faces may be influenced by individual variance in serial reliance. We used a novel measure of serial dependency of facial identity to quantify the intensity of serial dependence as well as the range across which people displayed this bias (the tuning) in 219 adults in order to explore this possibility. We discovered that larger serial reliance and tighter tuning were related with improved face recognition, mainly when successive faces were substantially similar. Also, it was shown that serial reliance tuning, rather than both object identification and facial identity aftereffects, was a major predictor of face recognition skills. These results imply that face recognition depends on how much serial dependency is applied selectively for comparable faces. Our findings support the idea that serial dependency has a practical use in face recognition.

DISCUSSION

Total Output Offset Error Calculation for IB and VOS

The formulae in Figure 5 below may be used to refer all offset voltage and bias current error-induced offset voltage to the input (RTI) or output (RTO) of the op amp. RTI or RTO might be chosen according on personal taste. When comparing the input signal towards the cumulative op amp offset error, the RTI value is helpful. If the op amp drives extra circuitry, the RTO value is more helpful for comparing the net faults with those of the subsequent stage.

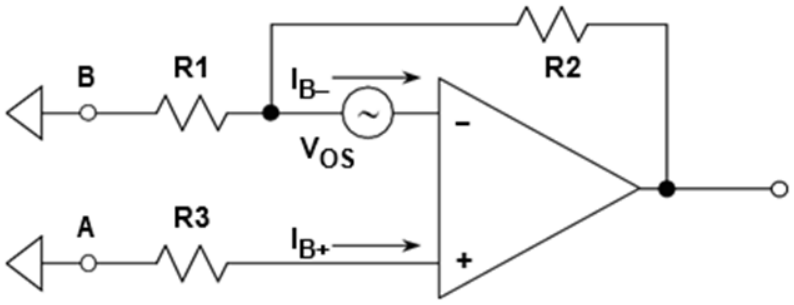

Figure 5: Offset voltage and bias current error-induced offset voltage to the input (RTI)

In either scenario, the stage noise gain, approximately equals 1 + R2/R1, is multiplied by the RTI value to get the RTO value. Offset voltage and bias current mistakes may be minimized by following a few simple guidelines. Keep input/feedback resistance settings low to reduce offset voltage brought on the impacts of bias current. Use bias compensation resistors second.

Bypass these resistors using capacitance that has quite high values. This minimizes noise at higher frequencies by shorting out the resistances at higher frequencies to offer the benefit of resistors at dc for bias currents. Also, it is probably not a good idea to use this approach to FET input devices since the compensation resistor's value is likely to increase noise rather than decrease the need for bias current compensation. Use of the compensation resistance will result in the bias currents not matching if an op amp utilizes internal bias current compensation. Use external offset trim networks as required to reduce induced drift. Instead of trimming, use a suitable precision op amp designed for minimal offset and drift.

Source Impedance

Both differential and common-mode input impedances are often provided for VFB op amps. The impedance to grounding at each input is often specified by current feedback op amps. While other models may be used for various voltage feedback op amps, it is often safe to utilize the model shown in Figure 6 throughout the absence of any additional information. In this concept, infinite impedance current sources provide the inputs from which bias currents flow.

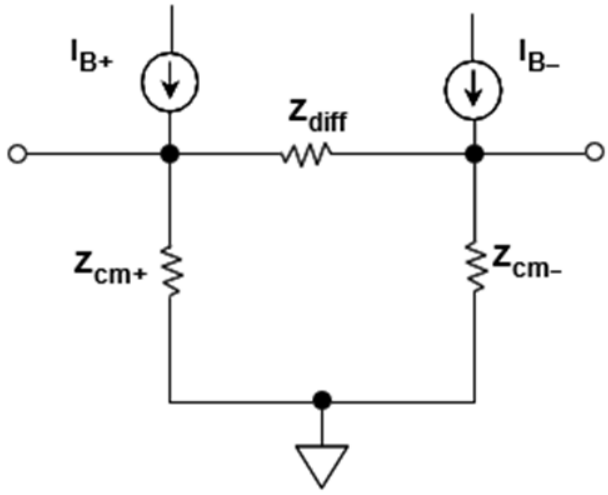

Figure 6: Illustrates the InputImpedance.

The impedance from either input to ground is indeed the common-mode input impedance data sheet specification (Zcm+ and Zcm-) (NOT from both to ground). The impedance between the two inputs is known as the differential input impedance (Zdiff). Typicallyresistive and high (105 to 1012), with considerable shunt capacitance, those impedances (generally a few pF, sometimes 20 pF to 25 pF). Negative feedback drives the inverting input impedance down to a relatively low value in the majority of op amp circuits, leaving just Zcm+ and Zdiff to be significant. Even more straightforward is a current feedback op amp. Z- is reactive (L r C, depending on the device) but contains a resistive component of 10 to 100, ranging from type to type, whereas Z+ is resistive, often with some shunt capacitance, relatively high (105 to 109).

Capacitance at Input

In general, high speed op amps do not encounter problems with input capacitance. It could be relevant in certain situations, such in a photodiode amp when the source impedance is high. A very tiny capacitance might provide a zero inside the transmission function with a very high

source impedance. Instability might result from this. The intersection will occur at 12 dB/octave, which really is unstable since the amplifier's noise gain is increasing at 6 dB/octave while the open-loop gain is decreasing at the same rate.

The modulation of the input capacitance by both the common-mode voltage is another concern with FET input devices powered from a high impedance source in the noninverting arrangement. A level-dependent distortion occurs as a result. Impedances as perceived by the inputs are balanced to counteract this impact. Similar to how input bias current is balanced, but with a balance that includes dc as well.

Range of the input common-mode voltage

The permitted voltage on the input pins is known as the input common-mode range. The supply range is often not complete. The inputs actually only required to span those ranges since traditional system design employed 15 V supplies with an estimated dynamic range of 10 V. The present trend, nevertheless, is toward steadily lower supply voltages. The need to improve input dynamic range grows as a result. "Rail-to-rail" inputs are used by several low voltage op amps. While "rail-to-rail" has no agreed-upon meaning in the industry, Analog Devices defines it as swinging within 100 mV from either rail. It's important to keep in mind that not all products sold as single supply are rail-to-rail, and not every products marketed as rail-to-rail can swing to the rails on both input and output. The data sheet has to be carefully read. The input voltage range will also be further constrained by certain inputs, such as bias compensated as well as super beta op amps.

Various Input Voltage

To avoid damage, certain input topologies need differential input voltage limiting. The inputs of these op amps often feature back-to-back diodes. The amps' simplified schematics may not always reflect this. Nonetheless, it will manifest as a maximum differential input voltage spec of 700 mV. A specification for the maximum input differential current may also be provided. While some amplifiers come with built-in current limiters, low noise operational amplifiers don't use them since they increase noise.

Power Voltage

The traditional system design used 15 V supplies and a 10 V predicted signal dynamic range. The majority of early op amps were designed to run at these voltages. Typically, the supply voltage range was fairly large. A range of permitted supply voltages was often specified on the data sheet. It could range from 4.5 to 18 volts, which is the range specified for the AD712. For the same op amp operated on various sources, there are often a few minor differences in the specifications. This often manifests as many spec pages, each at a unique set of circumstances, which typically denotes various supply. There is no reason why the voltage specification had to be either symmetrical or bipolar, despite the fact that it was often described as a symmetrical bipolar voltage. If the inputs are biased in the active zone, an op amp will treat a 15 V supply the same as a +30 V/0 V supply or a +20 V/10 V supply (within the common-mode range).

The supply voltages are being decreased as of late. Process restrictions are partly to blame for this in high speed amps. Smaller physical structures at higher speeds suggest smaller breakdown voltages, and vice versa. Reduced supply voltages suggest lower breakdown voltages. The majority of high speed op amps now in use need a single +5 V or 5 V supply. Supplies for general-purpose op amps are falling to as low as +1.8 V. Be aware that the phrase "single-supply" may also refer to lower supply voltages. While the two ideas are

connected, single-supply does not always imply low voltage, as was already mentioned. Keep the ideas distinct.Moreover, lower supplies are often used to run CMOS op amps. Again being driven by digital circuits, the trend in CMOS techniques stresses ever-tinier geometries with correspondingly lower breakdown voltages.

Peaceful Current

The internal current that the op amp consumes is known as the quiescent current (no load). High speed amplifiers often use more quiescent current than general-purpose amplifiers. Moreover, several performance metrics (noise and distortion in particular) for general-purpose op amps tend to become better with increased current. The lowest quiescent current amps, on the other hand, have a very constrained bandwidth. The OP290 from Analog Devices has the lowest quiescent current device available right now at 3.5 A. Op amps with low quiescent current are in high demand. Equipment that is powered by batteries is one driving application. While the definition of "low power" is not standardized throughout the industry, Analog Devices defines it as quiescent current of less than 1 mA. Quiescent current of less than 100 A is referred to as "micropower." Keep be mind that this is per amplifier, thus a quad op amp will need 4. And keep in mind that this only applies to amplifiers. For many individuals, low power might signify a variety of things. For instance, an extremely fast ADC may emit more than 1 W! While competing solutions might be more than 4 W, this can still be regarded as low power.

Swing in output voltage (High Output Voltage/Low Output Voltage)

As previously mentioned, the traditional system design used 15 V supplies with a 10 V predicted dynamic range. An emitter follower (common collector) circuit served as the default output structure. The output is above the base, which is a diode drop. For biasing the drive signal, there must be some voltage above that. Thus, a specification of the output voltage is required. This overhead specification will not change if lower supply voltages are used. We should anticipate achieving 6 V on a 9 V supply, for instance, if the specification calls for 12 V (min) on a 15 V supply. Again, we must increase the output dynamic range when the source voltage is decreased. For all, if we operate on a 3 V supply and lose 3 V to each of the supply rails, as in the case above, we will have a severely constricted dynamic range. The output stage's design is generally changed from an emitter follower to something like a common emitter in order to expand the dynamic range. The output will then be able to swing to the output transistor's VCEsat.

"Rail-to-rail" refers to allowing the output to swing almost in line with the rail. There is no industry-standard rail-to-rail specification, as we described in the input voltage section. The definition used by Analog Devices is the same as before: the ability to swing between 100 mV of either rail with the additional requirement of driving a 10 k load. The load's value is crucial because output current affects the output transistor's VCEsat. Keep in mind that not all "single-supply" op amps are "rail-to-rail" and not all "rail-to-rail" devices are input- and output-only.

Current Output (Short-Circuit Current)

The majority of general-purpose op amps feature output stages that are shielded against short circuits to either the supply or the ground. As the amplifier can continuously push that amount of current into in the short circuit, this is also known as "infinite" short-circuit protection. The output current that the op amp is capable of delivering is the output current. For general-purpose op amps, the limit is often set such that the op amp can produce 10 mA. It is suggested to utilize a separate output stage (inside the feedback loop) if an op amp is

needed to have both high accuracy and a big output current in order to reduce self-heating of the precision op amp. As this additional amplifier normally has a voltage gain of 1, it is often referred to as a buffer.

Certain operational amplifiers (op amps) are made to provide enormous output currents. The AD8534, a quad device with an output current of 250 mA for each of the four portions, serves as an example. A word of caution: you will go above the package dissipation spec if you attempt to provide 250 mA simultaneously from all four areas. The amplifier may self-destruct if it overheats. Smaller packages, which have less dissipation, exacerbate this issue. Since it would slow down their slew rate and hinder their ability to drive low impedances, high speed op amps normally do not have their output currents restricted to a low value. While a few are restricted to fewer than 30 mA, the majority of high speed op amps may source and sink between 50 mA and 100 mA. Because of the large short-circuit current, junction temperatures may be surpassed even by high-speed op amps with short-circuit protection, leading to device damage for extended shorts.

Noise AC Specs

In contrast to any outside noise that op amps may take up, internal noise is discussed in this section. While external noise is significant and is covered in depth in other publications, we are only interested in internal noise in this section. In an op amp, there are three main types of noise: current noise in each input, differential voltage noise between the two inputs. Effectively, these sources are unrelated (independent of each other). While there is a little link between the two noise currents, it is not significant enough to be taken into account in actual noise investigations. The Johnson noise of the external resistors, which are employed with the op amp in the feedback network, must also be taken into account in addition to these three internal noise sources.

Electrical noise

Different op amps' voltage noise may range from less than 1 nV/Hz to 20 nV/Hz or even more. Compared to JFET amps, bipolar op amps often exhibit reduced voltage noise. Voltage noise is described on the data sheet, and other factors cannot anticipate it (Figure 7).

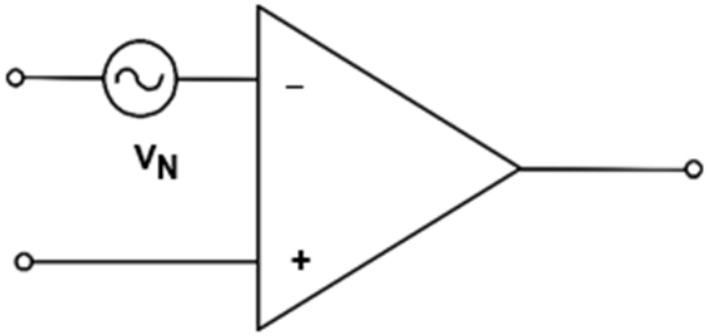

Figure 7: Illustrates the VoltageNoise.

JFET input amplifiers have historically had rather high voltage noise (while having very low current noise), making them more appropriate for low noise applications in high- impedance circuitry as opposed to low impedance circuitry. Voltage and current noise are quite minimal in the AD645 and AD743/AD745 devices. The specifications for the AD645 at 10 kHz are 10 nV/Hz and 0.6 fA/Hz, whereas the specifications for the AD743/AD745 are 2.9 nV/Hz and

6.9 fA/Hz. They allow for the creation of low noise amplifier circuits that exhibit low noise over a broad variety of source impedances. Large input devices and, thus, big input capacitance are the price of the reduced voltage noise.

Sound Wave width

We usually use a bandwidth of 1.57 fc to determine the noise contribution when determining the bandwidth. Since a single pole filter with a cutoff frequency of Fc possesses the same spectral energy as either a brick wall filter with a cutoff frequency of 1.57 fc, a resource of Gaussian (white) noise may be routed through it with the same spectral energy. An infinitely attenuating brick wall filter does have a smooth response up towards the cutoff frequency. A two pole filter has a similar apparent corner frequency, which is around 1.2 fc. When there are more than two poles in a filter, the error correction factor is often insignificant.

NoiseFigure

Op amps seldom use noise figure. The noise figure of an amplifier is the difference between the noise of the amplifier and an ideal noise-free amplifier in the same environment, expressed in decibels (dB). While 50 or 75 transmission lines and terminations were common in RF and TV applications, the idea is worthless for op amps since they may operate with a broad range of impedances. Even more helpful specifications are the voltage noise spectrum density and the current noise spectral density.

Current Activity

The range of current noise is substantially wider, ranging from around 0.1 fA/Hz (in JFET electrometer op amps) to several pA/Hz (in high speed bipolar op amps). It may be estimated in situations (such basic BJT or JFET input devices) where all of the bias current flows in the input junction since in these situations it is just the Schottky (or shot) noise of the bias current, even if it is not usually reported on data sheets. With current-feedback or bias-compensated op amps, in which the external bias current seems to be the difference of multiple internal current sources, it cannot be determined. The bias current in amps is denoted by Ib, and the charges on an electron is denoted by q, which is equal to 1.6 10-19 C. The shot noise spectral density is simply 2I bq Hz (Figure 8).

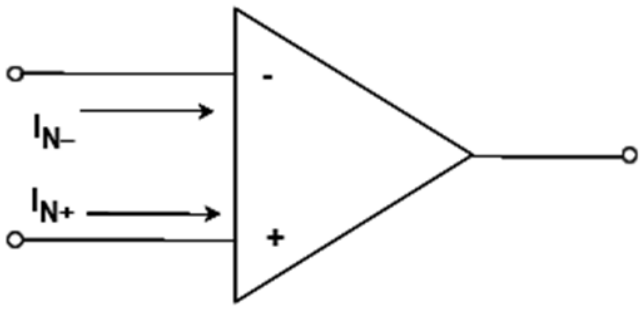

Figure 8: Illustrates the CurrentNoise.

A VFB op amp's input current noise is uncorrelated and generally equal in value. The current noise in simple input structures is the shot noise of the input bias current. The current noise in such a bias-compensated op amp cannot be estimated. Moreover, since a CFB op amp has distinct inputs, the current noise for such two inputs might vary significantly. Usually, neither the 1/f corners nor the angles will match. Only when current noise travels through an

impedance and produces noise voltage is it significant. Hence, the impedances surrounding it determine the low noise op amp to choose. A bias-compensated op amp having low voltage noise (3 nV/Hz) but rather high current noise (1 pA/Hz) is the OP-27. Voltage noise will predominate when the source impedance is zero. With the a source resistance of 3 k, the voltage noise will be equal to the current noise (1 pA/Hz flowing through 3 k), but the 3 k resistor's Johnson noise, which is 7 nV/Hz and hence dominating, will be equal to the current noise. With a source resistance of 300 k, the voltage noise remains unaltered, the Johnson noise (which really is proportional to the square root of the resistance) only rises tenfold, and the current noise multiplies by 100 to reach 300 nV/Hz. Current noise is prevalent here.

CONCLUSION

Personal computers and mobile phones, two of today's most widely used electronics applications, are moving to lower operating voltages. As a result, there is less room for mistake and component accuracy standards are raised. For the amplifiers employed in these applications, this is particularly true. Also, as demand for these items grows, suppliers are under more pressure to lower component prices. A brand-new, patented trimming technique created by Analog Devices provides the necessary precision and performance at a very affordable price. Input offset voltage is the primary amplifier parameter for system accuracy. There are several methods for adjusting amplifier offset voltage and other parameters. In fact, the existence of the whole class of precision amplifiers today is due to trimming procedures. Yet until recently, offset trimming as well as the increased precision it produces were mostly unknown in the high volume, low cost CMOS amplifier market.

REFERENCES

[1] A. E. Urai, J. W. De Gee, K. Tsetsos, and T. H. Donner, “Choice history biases subsequent evidence accumulation,” *Elife*, 2019, doi: 10.7554/eLife.46331.

[2] M. Fritsche and F. P. de Lange, “The role of feature-based attention in visual serial dependence,” *J. Vis.*, 2019, doi: 10.1167/19.13.21.

[3] H. P. Chen, S. F. Wang, Y. N. Chen, and Q. G. Huang, “Electronically tunable third-order quadrature oscillator using VDTAs,” *J. Circuits, Syst. Comput.*, 2019, doi: 10.1142/S021812661950066X.

[4] Y. Zhang, S. Xiang, X. Guo, A. Wen, and Y. Hao, “All-optical inhibitory dynamics in photonic neuron based on polarization mode competition in a VCSEL with an embedded saturable absorber,” *Opt. Lett.*, 2019, doi: 10.1364/ol.44.001548.

[5] D. Bannister *et al.*, “Bias Correction of High-Resolution Regional Climate Model Precipitation Output Gives the Best Estimates of Precipitation in Himalayan Catchments,” *J. Geophys. Res. Atmos.*, 2019, doi: 10.1029/2019JD030804.

[6] D. Luo, M. Zhang, and Z. Wang, “A Low-Noise Chopper Amplifier Designed for Multi-Channel Neural Signal Acquisition,” *IEEE J. Solid-State Circuits*, 2019, doi: 10.1109/JSSC.2019.2913101.

[7] A. Gaur, M. Lacasse, and M. Armstrong, “Climate data to undertake hygrothermal and whole building simulations under projected climate change influences for 11 Canadian cities,” *Data*, 2019, doi: 10.3390/data4020072.

[8] A. Ghorbani, A. Abid, and J. Zou, “Interpretation of neural networks is fragile,” 2019. doi: 10.1609/aaai.v33i01.33013681.

[9] H. Chen *et al.*, "Impact of the crucial geographic and climatic factors on the input source errors of GPM-based global satellite precipitation estimates," *J. Hydrol.*, 2019, doi: 10.1016/j.jhydrol.2019.05.020.

[10] K. Turbett, R. Palermo, J. Bell, J. Burton, and L. Jeffery, "Individual Differences in Serial Dependence of Facial Identity are Associated with Face Recognition Abilities," *Sci. Rep.*, 2019, doi: 10.1038/s41598-019-53282-3.

CHAPTER 4

OVERVIEW ON THE SUMOFNOISESOURCES

Mr. Sunil Dubey, Associate Professor,
Department of Electrical Engineering, Jaipur National University, Jaipur India
Email Id- sunildubey@jnujaipur.ac.in

Abstract

Electrical noise is indeed a collection of errant current and voltage oscillations. They exist in every electronic system and are brought about by the thermal mobility of the electrons and the quantized character of electric charge. In this chapter author is discusses calculations for total output noise

Keywords

Bandwidth, Gain, Operational Amplifier, Network, Signal.

INTRODUCTION

Uncorrelated noise voltages add in a "root-sum-of-squares" manner; i.e., noise voltages V_1, V_2, V_3 give a summed result of the sum of $(V_1^2+V_2^2+V_3^2)$. Noise powers, of course, add normally. Thus, any noise voltage that is more than 3 to 5 times any of the others is dominant, and the others may generally be ignored. This simplifies noise assessment. Current noises flowing through resistance equal noise voltage (Figure 1).

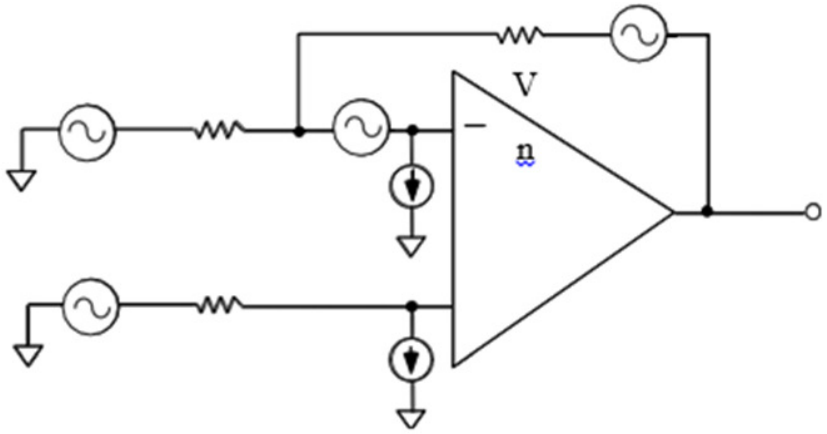

Figure 1: Illustrates the Total Noise Calculation.

Amplifiers with low voltage noise, like the OP-27, will be the natural option for low impedance circuits since they are affordable and their relatively high current noise won't interfere with the application. Johnson noise from resistors predominates at medium resistances, but at extremely high resistances, we have to choose an op amp with the least amount of current noise, such the FET input devices AD549 or AD645.

Noise, 1/f (Flicker Noise)

We've assumed that noise is white thus far (i.e., its spectral density does not vary with frequency). This is true for the majority of an op amp's frequency range at low frequencies,

the noise spectral density increases at a rate of 3 dB/octave. The voltage noise spectral density in this area is inversely related to the square root of the frequency because the power spectral density throughout this region is inversely proportional to frequency. Because of this, this noise is sometimes known as 1/f noise. However keep in mind that certain textbooks still refer to flicker noise. The 1/f corner frequency (FC), which is a measure of merit—the lower it is, the better—is the frequency at which this noise begins to increase. A current feedback op amp may well have three 1/f corners: because of its voltage noise, overall inverting input current noise, as well as its noninverting input current noise. The 1/f corner frequencies are not always the same for the voltage noise as well as the current noise of a specific amplifier.

PopcornNoise

Popcorn noise is so named because it has the same sound as popping popcorn when it is played via an audio system. It is made up of arbitrary step changes in offset voltage that happen at arbitrary intervals over a span of 10+ milliseconds. Such noise is caused by excessive contamination levels and crystal lattice dislocation at the silicon chip's surface, which are brought on by improper processing methods or subpar raw materials. Popcorn noise predominated when monolithic op amps was initially introduced in the 1960s. But, today's manufacturing testing for it are accurate, the reasons of popcorn noise are well known, raw materials are very pure, contamination is minimal, and no op amp manufacturer should experience any trouble providing products that are mostly free of it. It is not even addressed in the majority of current op amp textbooks or safety data sheet because of this.

Factors for RMS Noise

As was said before, frequency affects the noise spectral density. The noise spectral density curve must always be integrated across the desired bandwidth in order to get the rms noise. When k is the noise spectral density at 1 Hz, the rms noise inside the bandwidth f1 to f2 in the 1/f area is given by: As the actual frequency cancels away, the overall 1/f noise in a particular band depends on the ratio of the low to high band edges. Therefore, for the above calculation to be true, the top band edge must still be in the 1/f area.

Peak-to-peak measurements of rms noise are often desired. One needs some knowledge of the statistical makeup of noise to be able to perform this. Statistics show that for Gaussian noise with a given magnitude of rms noise, the likelihood of exceeding a certain peak-to-peak value dramatically reduces as that value grows, but this probability always hits zero (Table 1).

Table 1: Percentageofthetimenoisewillexceednominalpeak-to-peakvalue

Nominalpeak-to-peak	**Percentageofthetimenoisewillexceednominalpeak-to-peakvalue**
2×rms	32%
3×rms	13%
4×rms	4.6%
5×rms	1.2%
6×rms	0.27%

6.6×rms**	0.10%
7×rms	0.046%
8×rms	0.006%

It is conceivable to predict the percentage of times that a specific peak-to-peak value will be exceeded for a given rms noise, but it is not practical to produce a peak-to-peak value that would never be exceeded. Hence, peak-to-peak noise parameters for a certain time period must always be supplied. The most common setting assures that the peak-to-peak level will be only exceeded 0.1% of the time since the peak-to-peak noise is 6.6 times the rms value. Peak-to-peak measurements of the low frequency noise are often said to range between 0.1 Hz and 10 Hz. In order to ascertain this, a 0.1 Hz to 10 Hz band-pass filter is positioned in between the op amp and the measuring apparatus. The measurement is often represented as a scope shot with a time scale of one second per division, for the OP-213.

As real filters have limited roll-off characteristics, it is practically impossible to detect noise within certain frequency ranges without any contribution from beyond those limits. Thankfully, it is simple to calculate the measurement error caused by a single-pole low-pass filter. see the noise bandwidth part earlier.Wide bandwidth op amps' 1/f noise becomes comparatively minor when calculating rms noise. White or Gaussian noise is the predominant kind of noise. Across a broad frequency range, the noise spectral density of this noise is remarkably steady. The noise spectral density is multiplied by the square root of the equivalent noise bandwidth to get the rms noise.

LITERATURE REVIEW

P. Chiariotti et al.[1] conducted a review of acoustic beamforming for noise source identification and related applications is presented in this study. In order to provide the reader the chance to recognize ideas and references that can be relevant for her/his work, the key principles of beamforming are given, going from the most fundamental concepts and processes to more complex concepts and methods. There are also examples of how to use this strategy practically in various situations. The goal is to familiarize the reader with the subject and highlight the variety of stimuli that a technology like acoustic beamforming may provide to researchers.

O. Rikhotso et al. [2] discussed the industry of chemical manufacturing uses high-tech mechanical equipment to turn feedstock, such as natural gas, into raw materials that may be used in downstream industries. These facilities expose workers to risks to their health that are inherent in the workplace, such as noise. Searches for online and grey literature on noise emission sources in the industrial sector were done using specified keywords on ScienceDirect, Oxford Journals Online, PubMed, Medline, Jstor, and regulatory agencies. In order to effectively manage the hearing conservation program, this study focuses on the noise sources and associated control within chemical manufacturing facilities as well as the receptors of the produced noise. According to the literature, chemical production facilities use noise-emitting machinery, which exposes a variety of occupational types, including maintenance workers, process operators, and machine operators. Compressors, pumps, motors, fans, turbines, vents, steam leaks, and control valves are common sources of noise in the chemical production sector. Specific industries within the chemical manufacturing sector produce noise levels between 85 and 115 dBA (A-weighted sound pressure level), exceeding the noise rating limit of 85 dBA used in South Africa, the United Kingdom, and also the

United States, as well as the 90 dBA occupational exposure level used in that country. Levels above this limit necessitate workplace control. It is possible to install engineering noise control solutions with plant machinery and equipment used in chemical production facilities.

G. Burella et al. [3]in the Canadian province of Newfoundland and Labrador (NL), fishing is one of the most significant and dangerous occupations. In fishing boats, fish harvesters are subject to a variety of occupational risks. The combination of loud noise and extended exposure aboard fishing boats is one of them, and it is assumed to be the cause of noise-induced hearing loss. High noise levels in the crew quarters are also known to make them less comfortable. This study offers a preliminary analysis of the noise sources and noise levels aboard fishing boats in Newfoundland. In order to identify the features of the most prevalent fishing boats, the research first examined data on fishing vessel types. By vessel type, noise sources and structural layouts were discovered during vessel inspections. The next step was running an in-situ program to measure noise during seven fishing excursions aboard various boats for cod, whelk, lobster, and crab, each with a unique set of fishing activities and equipment. Noise levels were monitored during the journeys and afterwards analyzed to isolate the primary noise sources. The study determined that the primary steady state noise sources aboard the boats are the propulsion engine and auxiliary equipment, and it shown that these noise levels are above that advised for most places.

D. H. Kim et al. [4] that research focused on the discrete blade passing frequency (BPF) tone and its harmonics at shorter wavelengths less than 1000 Hz in order to better understand the tiny drone propeller noise. To study the stable and unsteady loading noise sources surrounding the blades with such a radius of 17 cm spinning at 5000 rpm, classical unsteady Reynolds-averaged Navier-Stokes equations were solved (a blade tip Mach number is 0.264). The top and lower blade surfaces of the drone propeller were found to have eccentric ellipsoidal isobaric surfaces according to the uRANS simulations, which were identified as the cause of steady loading noise. The BPF tone and even-number harmonics were predicted by a straightforward mathematical model of an ellipsoidal constant loading noise using the lattice Boltzmann technique, and they were similar to NASA's SPL measurements of two distinct APC 1147 SF and DJI 9443 CF drone propellers. During the first two discrete tones, the declining rate of - 6 in the SPL spectrum were pretty well matched. The unstable loading noise caused by blade-vortex interactions is determined to be most closely connected to the third and sixth harmonics of the circular per second noise, according to the transient pressure fluctuation features on the top surface of spinning blades. Due to the random nature of a phase difference of pressure difference, despite the identical locations of the two propeller blades, an unanticipated fifth component also appeared in some other rotating speeds.

J. C. A. Gonçalves et al.[5] studied for outlines the design and characterization of a silicon-based integrated millimeter-wave (mmW) noise source for applications up to 260 GHz. The designed integrated noise source was based on p-n and Schottky junction throughout series and is implemented using STMicroelectronics' SiGeBiCMOS 55-nm technology. This integrated diode noise generator, which is biased in the avalanche domain, produces a tunable excess noise ratio (ENR) ranging between 0 dB and 15 dB, in the frequency range of 130-260 GHz. The noise figure of two amplifiers was tested in order to demonstrate the value of the integrated noise source. The first amplifier is indeed an integrated low-noise amplifier (LNA) working in the D-band (130-170 GHz), while the second amplifier is packed and works from 220 to 260 GHz. That noise source offers a significant desire to conduct out high-frequency in situ noise evaluation of innovative Si CMOS or BiCMOS technology inside the mmW range due to its ability to just be naturally integrated on silicon.

Y. Liu et al. [6]the design process for an electromagnetic interference (EMI) filter for a single-phase SiC MOSFET inverter is presented in this work. The equivalent noise source capacitance and inductance of the common mode (CM) but also differential mode (DM) noise models are calculated to make sure the EMI filter performance is both precise and effective. Next, based on the known impedances of the CM and DM noise sources, respectively, the CM and DM EMI filters may be built. Both simulation and experimentation are used to verify the EMI filter design based just on suggested methodology. The efficiency of the suggested strategy has been confirmed by the simulation and testing findings.

J. Yao et al. [7]the emphasis and hot point in the field for internal combustion engine noise research is the separating and identification technologies of noise sources. The primary sources of noise in an internal combustion engine are combustion noises and piston slap noise. Yet, the top dead center is practically exactly where combustion noise and piston slap sounds occur. Both the time domain and also the frequency domain are combined. Separating them precisely and successfully is challenging. It is suggested to separate them using a single-channel approach that combines robust independent component analysis (RobustICA) and time-varying filtering-based empirical mode decomposition (TVF-EMD) techniques. Initially, the single-channel noise signals is divided into a number of intrinsic mode functions using the TVF-EMD approach (IMFs). The independent components are then extracted using the RobustICA approach. In order to identify noise sources, associated previous information and time-frequency analysis are being used. In order to confirm the accuracy of the separation findings, more work is done using the spectral filtering technique and the piston slap noise calculation method based on the dynamic model. The outcomes of the simulation and experimental study demonstrate the viability of the suggested approach.

C. H. Park et al. [8]the acoustic field from drone propellers is computed in the current work utilizing noise source modeling and the lattice Boltzmann technique, which is a novel computational tool. For a variety of drone propeller types, a straightforward mathematical model of constant loading noise is developed and verified to predict the blade passing frequency (BPF) tone and harmonics at low frequencies (100-1000 Hz). NASA's observed sound pressure level (SPL) for APC-SF and DJI-CF two-blade single drones propellers operating at 3600-6000 revolutions per minute is in reasonable agreement with the calculated result. With the first two BPF and harmonic peaks inside the SPL spectrum having a fading slope of -6, it accurately mimics the characteristic of an even number of BPF harmonics again for tested model propellers. Interestingly, the proposed constant loading noise model exhibits all RPS harmonic components with varying magnitudes for various rotor configurations and blade sizes, including tri-copter and quadcopter. The suggested technique may be used to a variety of open rotor systems, including multi-copters and distributed electrically powered vehicles, to forecast and analyze tones at low frequencies.

J. Zhang et al. [9] that study examines how the directivity of train noise sources affects the outcomes of a beamforming-based identification method that makes use of a microphone array. Typically, a single-microphone noise spectrum over a time frame equivalent to the length of the complete train, or of a single vehicle, is generated while doing pass-by noise testing. An algorithm for source quantification should be able to assess the contribution of each noise source throughout this time span in this situation. Yet it is shown that in order to obtain accurate source quantification, various railway noise sources must be taken into consideration since they have varied directivities. It is shown using monopoles, dipoles, and quadrupoles that a different compensation is necessary depending on the directivity. A microphone array can only partly capture the complicated directivity pattern of the noise generated by the rail in this specific scenario. It is shown that an incorrect interpretation of a

portion of the rail contribution from either the beamforming map may be responsible for the overestimation of a wheel contribution seen in earlier studies.

A. Etemadi et al. [10]one of the most promising methods for implementing Nano-scale communications with healthcare applications is diffusion-based molecular communication (DMC). The DMC systems may come into contact with biological entities that operate by releasing chemicals similar to those employed for signaling in in-vivo settings. According to the DMC system, these environmental elements serve as external noise sources. This work specifically models the release of molecules by external bio-inspired noise sources as a compound Poisson process. Investigation is done into how compound Poisson noise sources (CPNSs) affect a point-to-point DMC system's performance. In order to do this, the receiver-observed CPNS noise is described. The effectiveness of the DMC system in the presence of the CPNS is examined while taking into account a straightforward on-off keying modulation and creating a symbol-by-symbol maximum likelihood (ML) detector. The noise that is received from either the CPNS is approximated as a Poisson process with a normally distributed rate for the particular case of CPNS in a high-rate environment. In this instance, it is shown that the best ML detector is a straightforward single-threshold detector. Our findings show that, in general, if a CPNS is present, using the traditional basic homogeneous Poisson noise model could result in unduly optimistic performance forecasts.

DISCUSSION

Calculations for Total Output Noise

As we've previously said, any noise source that generates between a third and a fifth of the noise of another source may be disregarded. (The circuit's identical location must be used to measure both noise voltages.) The noise contributions of each component of the circuit must be evaluated to identify which are important before we can investigate the noise performance of an op amp circuit. The noise spectral density, which is frequently stated in V/Hz and is comparable to the noise in a 1 Hz bandwidth, will be used instead of real voltages in the calculations that follow in order to make them simpler.

Johnson noise exists in all resistors and has the following formula: where R is the resistance, T is the absolute temperature, B is indeed the bandwidth, and k is Boltzmann's constant (1.3810-23J/K). This is inherent unless operated at 0K, it is impossible to find resistors without Johnson noise.The three resistors' Johnson noise, the op amp's voltage noise, and the current noise from each of the op amp's inputs are three of the six distinct noise sources in the amplifier circuit, which consists of an op amp and three resistors (Rp represents this same source resistance at node A). Each one contributes in a different way to the noise at the amplifier output. Therefore, it is sometimes easier to compute the noise at the output and divide it by the signal gain (not the noise gain) of the amplifier to get the RTI noise. Noise is typically defined RTI or linked to the input.

The Johnson noise of R2 is buffered straight to the output over a bandwidth of 1/2 R2C2, and the amplifier by [2a] has these noninverting and inverting gains and bandwidths, accordingly, over a bandwidth of 1/2 R2C2. Negative feedback around the amplifier keeps the potential somewhere at inverting input unchanged, which is why a current flowing from such a pin is forced to flow in R2 only, resulting inside a voltage there at amplifier output of In-R2 over a bandwidth of 1/2R2C2 (we could equally well consider the voltage caused by In- flowing inside the parallel combination of R1 and R2 as well as the voltage caused by In- flowing in R2 alone).

If we take into account these six noise sources, then can see that if Rp and R2 are low, current noise and Johnson noise effects will be limited and the voltage noise of the op amp will become the dominating noise. Johnson noise and the voltage fluctuation brought on by noise currents both will grow as we increase resistance. Johnson noise will replace voltage noise as the main contributor if noise currents were low. Johnson noise, on the other hand, grows with the square root of resistance, but the voltage owing to noise currents climbs linearly with resistance. As a result, as resistance continues to rise, noise current voltage will eventually take precedence.

The noninverting gain (1 + R2/R1), which is perceived by the voltage noise of the op amp, Vn, is referred to as the "noise gain" of the amplifier since it is unaffected by whether the input is attached to node A or node B (the other being grounded or linked to another low impedance voltage source).Each of the six noise voltages must be multiplied by the proper gain and integrated over the appropriate frequency in order to get the overall output rms noise of the op amp. The total rms output noise is therefore represented by the root-sum-square of each of the output components. Thankfully, by making the necessary assumptions, this difficult procedure may usually be substantially reduced. It is relatively simple to carry out the voltage noise integration in two stages, but take note that owing to peaking, the high frequency region where the noise gain is 1 + C1/C2 will decide the bulk of the output noise caused by the input voltage noise. Second-order systems often exhibit this kind of reaction. Only across the bandwidth 1/2R2C2 is the noise from the inverting input current noise, R1, and R2 integrated. There are several further simplifications that may be done for high speed op amp applications. A first-order system designed for quick settling time often has a flat noise gain plot up to the closed-loop bandwidth frequency, with only a small gain peak. As a result, all noise sources may be combined throughout the closed-loop op amp bandwidth.

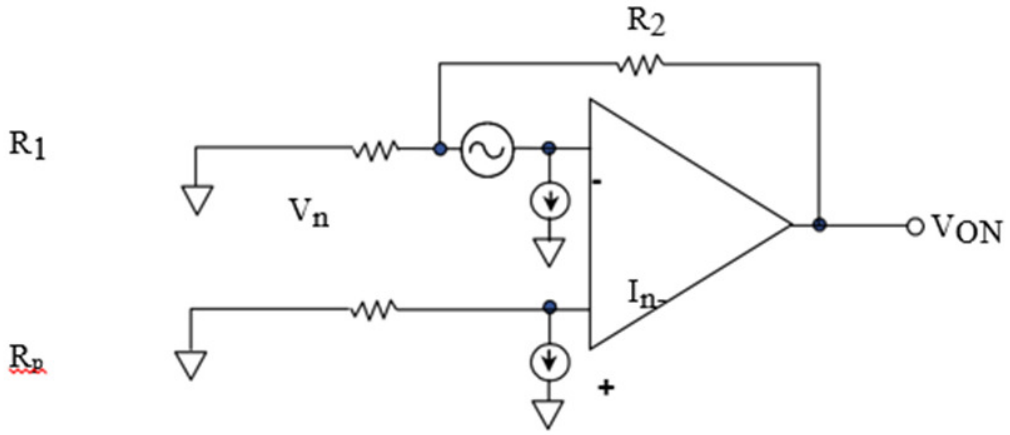

Figure 2: Illustrates the closed-loop op amp bandwidth.

Figure 2 shows that the primary causes of output noise in high speed current feedback op amplifier circuits are indeed the input voltage noise and the inverting input current noise.

Distortion

The dynamic range of an op amp may be described in a variety of ways. One of the most used techniques is to specify harmonic distortion, total harmonic distortion (THD), or total harmonic distortion plus noise (THD + N). Other related standards include those for intermodulation distortion (IMD), intercept points (IP), spurious-free dynamic range (SFDR), and multitone power ratio (MTPR), among others.

Total Harmonic Distortion (THD) (Total Harmonic Distortion)

Total harmonic distortion (THD), which is caused by amplifier nonlinearity, is the ratio of harmonically associated signal components (2X, 3X, 4X, and so forth depending on frequency components). Only harmonically coupled signals are included in the measurement. The distortion components that make up the overall harmonic distortion are often calculated as the square root of the sum of a squares of a fundamental's first five or six harmonics. Nevertheless, if just the third and second harmonics are considered, there is typically minimal error since the higher order components' amplitudes may sometimes be significantly reduced.

Total Harmonic Distortion plus Noise, or THD + N (Total Harmonic Distortion plus Noise)

THD + N is the signal that is still present after the fundamental has been removed. The measuring bandwidth must be utilized to integrate the noise into the THD + N measurement since the THD measurement doesn't really contain noise components, but the THD + N measurement does. In narrow-band applications, filtering may reduce the noise level, lowering the THD + N and increasing the signal-to-noise ratio (SNR). When a THD standard is specified, it is often a THD + N specification since most measuring techniques cannot distinguish harmonically linked signals from other signals. Typically, the fundamental signal is removed from the THD measurement, and the residual signal is then measured (the residual). The meanings of the words THD and THD + N.

1. V_S=SignalAmplitude(RMSVolts)
2. V_2=SecondHarmonicAmplitude(RMSVolts)
3. V_n=nthHarmonicAmplitude(RMSVolts)
4. V_{noise}=RMSvalueofnoiseovermeasurementbandwidth

Modulation Interference (IMD)

The primary causes of output noise in high speed current feedback op amp circuits are indeed the input voltage noise and the inverting input current noise.

Distortion

The dynamic range of an op amp may be described in a variety of ways. One of the most used techniques is to specify harmonic distortion, total harmonic distortion (THD), or total harmonic distortion plus noise (THD + N). Other related standards include those for intermodulation distortion (IMD), intercept points (IP), spurious-free dynamic range (SFDR), and multitone power ratio (MTPR), among others.

SlewRate

The slew rate is the greatest rate of voltage change at such an amplifier's output. V/s (or, more often, V/s) is the unit of measurement. Op amps may have different slew rates during positive- and negative-going transition due to circuit design, but for the purpose of this study, we'll assume that they do. The equation for the output voltage is as follows if we choose a sine wave with a frequency of f and a p-p amplitude of 2 Vp:

Many high-speed amplifiers can overshoot, so bear that in mind. The output will likely surpass the ultimate figure and then fluctuate steadily around it, according to this. To describe something as "ringing" How much overshoot and ringing there is will show the amplifier's phase margin. When overshoot and ringing increase, phase margin decreases. The slew rate is

normally measured between 10% and 90% of a final value, however 20% to 80% may also be used (Figure 3).

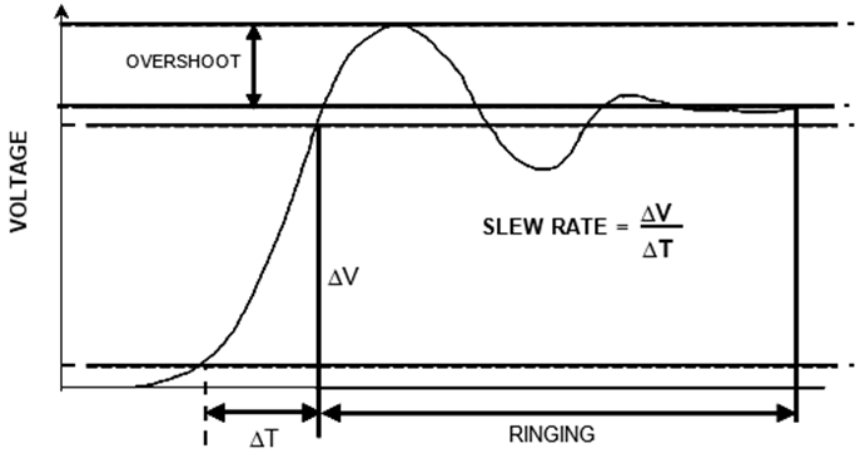

Figure 3: Illustrates the SlewRate

Power Bandwidth at Maximum

Inversely correlated with the signal's amplitude and directly proportional to the slew rate that's the greatest output frequency at which slew limitation occurs. This allows us to set the "full-power bandwidth" of an op amp (FPBW).

Flatness bandwidth of 0.1 dB

In demanding applications such professional video, it is ideal to maintain a reasonably constant bandwidth and linear phase until a maximum set frequency. This is true because a change inside the gain or phase of the system will affect the hue or intensity of the color. Just stating the 3 dB bandwidth is inadequate. Now a standard criterion, 0.1 dB bandwidth is often referred to as 0.1 dB bandwidth flatness. This shows that the ripple is contained to the stated 0.1 dB bandwidth frequency and no more. For video buffer amplifiers, the 3 dB and the 0.1 dB bandwidth are often specified. Remember that the 3 dB bandwidth is equivalent to around 400 MHz. This may be calculated using the response marked "GAIN" on the graph, and the corresponding gain scale is shown on the left-hand vertical axis (scaled at 1 dB/division). The response scale for "FLATNESS" is shown on the right-hand vertical axis with a scaling of 0.1 dB/division throughout this case. This enables the determination of the 0.1 dB bandwidth, which in the present case is around 65 MHz. the primary difference between the appropriate bandwidth of the 3 dB and 0.1 dB criterion. Standard tests reveal that in order to achieve the 65 MHz 0.1 dB flatness rating, a 400 MHz bandwidth amplifier is required.

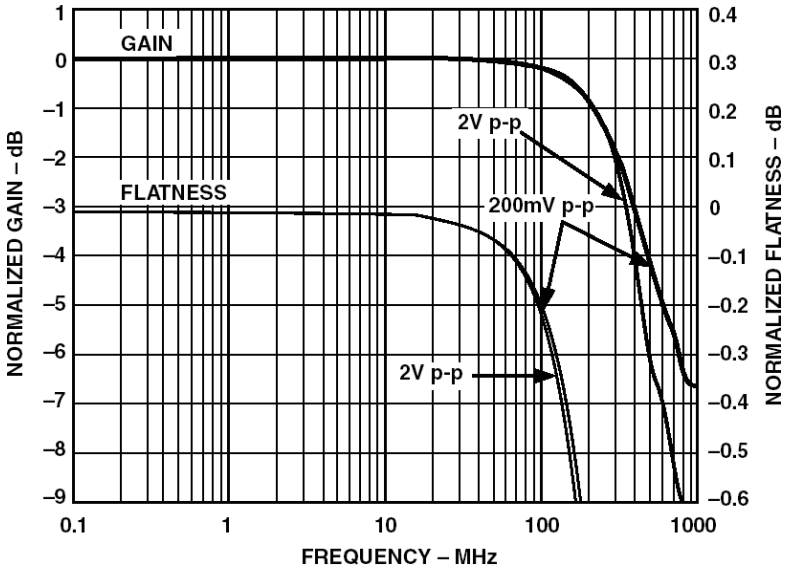

Figure 4: Illustrates the dB GainFlatness

One thing to keep in mind is that even these requirements hold true when driving a cable that's also terminated at 75 for the load and the source and 150 for the resistive load. The output of the amplifier should not have any capacitive loading since this might cause the frequency response to peak.

Gaining Bandwidth Product

With a VFB amplifier, the result of multiplying the gain at a specific frequency by this frequency is a constant. This is because increasing the frequency in a system of the first order causes the gain to decrease by two times. This result therefore becomes a relevant measure of quality when comparing the bandwidth of op amps.

Power supply rejection ratio, or PSRR (Power Supply Rejection Ratio)

The output of an op amp shouldn't change if the supply happens, yet it often does. The power supply rejection ratio specification, or PSRR, is developed in a manner similar to that of CMRR. If a change of X volts in the supply causes an output change equal to a differential input change of Y volts, then the PSRR for that supply is X/Y. As the PSRR formulation assumes that both supplies will alter equally and in opposite directions, the analysis becomes much more difficult. Alternately, the modification would bring about changes to the supply as well as the common-mode. This behavior is what causes the PSRR to seem to shift between positive and negative supplies. As op amp PSRR are frequency sensitive, op amp power supply needs to be appropriately segregated. Several devices may utilize a 10 F to 50 F capacitor on each supply at low frequencies, provided that it is no more than 10 cm distant from any of them (PC track distance). To decouple electrical supply lines at high frequencies, each IC has to have a low inductance capacitor with short leads and PC tracks that has an effective value of 0.1 F or less. Moreover, those capacitors are required to serve as a return channel for the HF currents inside the op amp load.

CONCLUSION

Noise is an unwanted signal that tampers with the primary message signal and tampers with its characteristics. Because of this change in the communication process, the message is changed. Most likely, it will be inputted at the receiver or the channel. Noise pollution, which

includes any distracting or undesirable sounds, has an impact on people's health and quality of life. Hearing loss and disorders connected to stress may be brought on by prolonged exposure to loud noise. An internalized feeling of congestion and confusion brought on by a range of stimuli, which makes it challenging for those who suffer from it to accept and order their experience due to their amount, intensity, and unpredictability.

REFERENCES

[1] P. Chiariotti, M. Martarelli, and P. Castellini, "Acoustic beamforming for noise source localization – Reviews, methodology and applications," *Mech. Syst. Signal Process.*, 2019, doi: 10.1016/j.ymssp.2018.09.019.

[2] O. Rikhotso, J. L. Harmse, and J. C. Engelbrecht, "Noise sources and control, and exposure groups in chemical manufacturing plants," *Applied Sciences (Switzerland)*. 2019. doi: 10.3390/app9173523.

[3] G. Burella, L. Moro, and B. Colbourne, "Noise sources and hazardous noise levels on fishing vessels: The case of Newfoundland and Labrador's fleet," *Ocean Eng.*, 2019, doi: 10.1016/j.oceaneng.2018.12.062.

[4] D. H. Kim, C. H. Park, and Y. J. Moon, "Aerodynamic Analyses on the Steady and Unsteady Loading-Noise Sources of Drone Propellers," *Int. J. Aeronaut. Sp. Sci.*, 2019, doi: 10.1007/s42405-019-00176-3.

[5] J. C. A. Gonçalves *et al.*, "Millimeter-wave noise source development on SiGe BiCMOS 55-nm technology for applications up to 260 GHz," *IEEE Trans. Microw. Theory Tech.*, 2019, doi: 10.1109/TMTT.2019.2926289.

[6] Y. Liu, S. Jiang, H. Wang, G. Wang, J. Yin, and J. Peng, "EMI filter design of single-phase SiC MOSFET inverter with extracted noise source impedance," *IEEE Electromagn. Compat. Mag.*, 2019, doi: 10.1109/MEMC.2019.8681368.

[7] J. Yao, Y. Xiang, S. Qian, and S. Wang, "Noise Source Separation of an Internal Combustion Engine Based on a Single-Channel Algorithm," *Shock Vib.*, 2019, doi: 10.1155/2019/1283263.

[8] C. H. Park, D. H. Kim, and Y. J. Moon, "Computational Study on the Steady Loading Noise of Drone Propellers: Noise Source Modeling with the Lattice Boltzmann Method," *Int. J. Aeronaut. Sp. Sci.*, 2019, doi: 10.1007/s42405-019-00177-2.

[9] J. Zhang, G. Squicciarini, and D. J. Thompson, "Implications of the directivity of railway noise sources for their quantification using conventional beamforming," *J. Sound Vib.*, 2019, doi: 10.1016/j.jsv.2019.07.007.

[10] A. Etemadi, P. Azmi, H. Arjmandi, and N. Mokari, "Compound Poisson Noise Sources in Diffusion-Based Molecular Communication," *IEEE Trans. Commun.*, 2019, doi: 10.1109/TCOMM.2019.2899092.

CHAPTER 5

ANALYSIS ON THE DIFFERENTIAL GAIN OF OP-AMP

Mr. Vivek Jain, Associate Professor,
Department of Electrical Engineering, Jaipur National University, Jaipur India
Email Id- vivekkumar@jnujaipur.ac.in

Abstract

Differential gain is a change throughout low frequency lama (brightness) amplitude that results in a change inside the color saturation point (amplitude of the color modulation). This modification clearly distorts the color by altering its intensity. In this chapter author is discusses Op-amp circuit noise

Keywords

Bandwidth, Gain, Operational Amplifier, Network, Signal.

INTRODUCTION

Differential Gain

Visual programs were the first to employ a standard known as differential gain. Early video processing systems showed that the amplifier's gain might sometimes alter with dc level. Differential gain is, technically speaking, a shift in low frequency luma (brightness) amplitude which affects the amount of color saturation (amplitude of the color modulation). By changing the color's intensity, this modulation obviously alters the color. Professional video editing software often strives to maintain a system-wide difference increase of 1% or less. Modern, high-performance video op amps have differential gain requirements of.01%.

Different Phase

Differential phase is the relationship between a change in low frequency luma (brightness) magnitude and a variation in hue (the phase of color modulation). This modulation, obviously a distortion, changes the colour of the color. Professional video editor software often strives to keep the system's total differential phase below 1°. For contemporary, high-performance video op amps, the differential gain parameters are.01°.

Phase Switching

Phase reversal is a condition when an op amp's input common-mode is exceeded. Since there is no longer a bias voltage given to it, another internal stage of the op amp turns off. The output waveform swings towards the opposing rail as a consequence up until the input returns to the common-mode area. This developed into a serious problem with the switch to single suppliers and lower supply voltages. Advances in circuit design have made it feasible to create op amps without phase reversal. If the op amp is designed to avoid phase reversal, it is often stated in the bullets or "Key Features" and not necessarily in the specification table.

Channel Switching

Channel separation or crosstalk refers to the signals that combine from one amplifier inside a package to some other amplifier within the same package. The typical path is the power

supply, which is something the amplifiers often share. The layout of the op amp chip may be carefully chosen to minimize crosstalk. Another option is to carefully externally bypass the power source.

Absolute Maximum Ratings

The op amp's absolute maximum ratings are its restrictions on voltage, current, and temperature. A failure of the op amp might result from exceeding the extreme limits. Applying overvoltage to the input pins is a pretty common method for killing an op amp. Conditions that include overvoltage include both ESD and overvoltage situations. 1000 volt ESD voltages are not uncommon. Most of us have experienced ESD. Simply touch a metal doorknob and tread on a nylon carpet, ideally one that is dry. Sparks will start to fly from your fingertips. CMOS electronics is highly vulnerable to ESD damage. Overvoltages occur when the op amp's maximum permissible voltage is exceeded. The maximum allowed voltage is typically determined by the supply voltage, with a few exceptions. When the inputs are overvoltages, generally via the substrate, the device drivers will often undergo a transformation into an SCR (silicon controlled rectifier) type structure.

Failure is brought on by the overvoltage's impact on the current, not the overvoltage itself. So, if indeed the current is limited, no permanent damage will occur. The current must not exceed 5 mA as per the standard. As overvoltage protection, current limiting resistors and diodes from either the input pins to the supply might be utilized. Due to its lower forward voltage, Schottky diodes are often used (typically 300 mV versus 700 mV for silicon). Therefore, it is best to utilize protection tools sparingly. Bias currents may have issues like leaky diodes. A few may also have fairly high capacitance, which might limit their frequency response. That is especially true for high-speed amplifiers. The current limiting resistors boost the noise floor. Current limiting is still required even though certain op amps, such as the OP-27, include protection diodes. If an op amp has protection diodes, the maximum differential input current for that amp will typically be indicated (Figure 1). The protection circuit should be included in the simplified schematic as well.

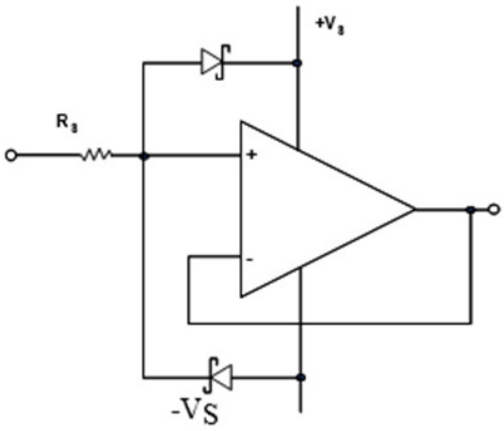

Figure 1: Illustrates the InputProtection.

Another characteristic of certain op amps is the presence of back-to-back diodes across the inputs. Instead of guarding against input overvoltage, they limit the differential voltage. If they are present, the differential input voltage will have a maximum specification of around 700 mV. The controlling temperature standard is a maximum junction temperature of 150 oC.

When this limit is reached, the amp's lifetime (in fact, the lifespan of any semiconductor) shortens. The temperature difference between the junction and the casing is determined by the thermal resistance of the package, abbreviated JC. Between the package as well as the environment, there is also a thermal resistance, CA. The total thermal resistance, JA, from the junction to the ambient is equal to JC + CA as a result of the linear sum of these thermal resistances.

The maximum operating temperature rating is less concerned with potential injury and more with the temperature performance range of the additional op amp requirements.There may be several entries for particular individual specs for various op amps. For this, there are many performance levels. Moreover, it could be for different temperature ranges (usually commercial, industrial, or military). Remember that specifications often provide three choices: Min, Typ, and Max. At Analog Devices, every stipulation in the min (minimum) and max (maximum) columns will be tested to ensure its accuracy. Testing one parameter in certain circumstances ensures testing another. In certain cases, it could be a straightforward test. Simply said, a typical specification would be that. Depending on the particular demand, the deviation from the norm might be substantial. Moreover, there is no way for you to ascertain the variation range of the typ standard. You may sometimes see a typ and a min for the exact same specification (or max). This suggests that even when the test limits have been set at a certain value (min or max), the typicals often outperform the test limits. Typing is harmful when used in design. It is far better to use mins or maxes for error budget analysis. Testing is one of the most expensive steps in the manufacture of op amps. As a result, a component with much more exact specs will often be more expensive than a component with less exact specifications. Nonetheless, the higher-specified component may be required in your system to guarantee circuit functioning.

The highest possible standards

The specification tables are always followed by a section listing the absolute maximum ratings. Voltage and temperature are often linked with this. The manufacturing process utilized to make the op amp often determines the maximum supply voltage. The maximum input voltage is typically the supply voltage. It should be made clear that the supply voltage is the present value, not the average or final value. Hence, if an op amp lacks a supply voltage while having voltages at its input. (Which may occur at system startup when certain components were powered but not others.) The op amp is overvoltaged even if everything is working within the parameters when power is applied.

The maximum input voltage requirement ranges from GND to VS. Six volts (V) is the maximum differential input voltage. Note that both of these conditions must be met. As a result, the input pins of both op amps need to be between 6 V and GND and VS. For semiconductor reliability, the junction temperature must remain below 150 °C. For each of the possible package choices, a ja will be given. This image displays the heat resistance. It uses a C/Watt scale. Determine the package's power dissipation before using this information. The supply voltage times the quiescent current would result in this. Then determine the maximum dissipation of the output stage (output current times the difference between the output voltage and the supply voltage). The dissipation of the complete system is equal to the total of these two, represented in Watts. By combining the thermal resistance and the dissipation, the temperature rise is computed. To get the junction temperature, multiply the increase calculated above by the ambient temperature (in degrees Celsius). Remember that you should feel comfortable where you are. Circuits packed in an enclosure, which is subsequently placed in a rack with other equipment, may have an internal ambient temperature that is much greater than the air temperature outside. This requires reflection.

Use the AD8534 as an example. It's assumed to be acting as a line driver. The required output voltage range is 500–5 V. With such a maximum output voltage of 5 V from every one of the four sections, we predict a maximum output current of 100 mA. This is the same as a load of 50 units. Assume that a 5.5 V supply will be used to power the circuit. The driver now has a bit extra headroom as a result. A plot of output voltage vs output current shows that the maximum consumption for such an amplifier with this type of resistive load is around 55% of a maximum. This is due to the fact that when the output voltage increases, even though the current keeps increasing, the dissipation voltage—the difference between both the output voltage as well as the supply voltage—decreases. Remember that the power dissipation of the package, not the load, will increase as the output voltage increases. The quiescent current (Iq) over temperatures is at its maximum of 1.75 mA.

LITERATURE REVIEW

W. Yang [1] et al. proposed to use a new, differential-fed, dual-polarized patch antenna. The dual-polarized antenna element's specific filtering response with radiation nulls will be first made possible by symmetrically loading defective ground structures (DGSs), a cross slot, but also eight shorting pins without the need for additional circuits. The DGS with pins may concurrently provide more in-band resonance for broad passband and produce a reduced edge radiation null for just a sharp roll-off rate. In the meantime, the cross slot with pins may provide both an in-band resonance and an upper edge null. The patch's intrinsic higher order-mode null may be used with it to dramatically increase skirt selectivity and cut off frequency suppressing at upper band. To obtain strong stopband suppressions, the |Sdd 11| there at upper and lower stopbands is near to 0 dB. As a consequence, it is simple to build a small, high-gain, dual-polarized patch antenna. The suggested approach is excellent for dual-polarized antennas since the performances for both polarizations is similar thanks to the perfect symmetry of the aforementioned structures. A prototype of the suggested antenna is created and measured for demonstration purposes. Indicating strong performance with a broad bandwidth of roughly 23%, a peak gain of up to 8.9 dBi inside the passband, and out-of-band suppression intensities of more than 20 dB, good agreements between both the measured and modelled findings are shown. The proposed filtering patch antenna, when compared to other filtering antennas that have been reported, not only displays good wideband dual-polarization radiation but then also high gain in such a compact structure for very high aperture performance and ultralow cross-polarization level because of the differential feed intake and complete symmetry.

According to the A. C. Duran [2] et al. It is questionable whether neighborhood foreclosures may affect the health of other residents, even if house foreclosure can cause deterioration in the mental and physical health of those experiencing it. We investigated whether exposure with neighborhood foreclosure filings was related to changes in objectively determined body mass index (BMI) over time using a racially and ethnically diverse sample of inhabitants of the Chicago metropolitan region connected to foreclosure data from 2008 to 2014. To evaluate the relationship between neighborhood foreclosures with BMI in >60,000 persons and for those who did not relocate during the follow-up period, we used fixed-effects regression models that adjusted for individual- and neighborhood-level factors. In order to test for robustness, we also made adjustments for the non-linear relationships between age, BMI, and comorbidities. For those who didn't move (nonmovers), a rise in BMI was linked in fully adjusted models to a standard-deviation increase in neighborhood foreclosure files within 500 m (mean = 0.03 BMI units, 95% confidence interval: 0.01, 0.06). For the whole sample, there was no correlation between changes in BMI and neighborhood foreclosure rates. Clarifying the possible health consequences of neighborhood foreclosures would assist

policymakers in developing measures to prevent home losses, predatory housing loans, and even that aim to much more effectively return foreclosed properties to productive uses, provided the potential negative effects of neighborhood foreclosures on individual people with longer exposure to the local area.

G. Muziol[3] et al. in that study, we demonstrate that a broad InGaN quantum well (QW) may function as the active area of laser diodes (LDs) more efficiently than a narrow one, even in the presence of a strong piezoelectric force. Study is done on the optical gain of LDs with a single broad QW. It is shown that an LD with a 10.4 nm QW has better differential gain than an LD with three QWs that are 2.6 nm thick. A broad QW's strong optical gain is thought to result from transitions via excited states. Moreover, it is discovered that the lasing spectra of LDs with broad and narrow QWs vary significantly from one another.

C. Ogbonnaya and J. Messersmith [4]the human resource management (HRM) literature is consistent with the notion that coherent systems of HRM procedures, when seen subjectively by workers, may have an impact on employees' attitudes. Current research suggests that sub dimensions of HRM systems emerge and explain variation in results. The effectiveness of three sub-dimensions of HRM practices improving employee skills, motivation, and opportunitieson innovative behaviors and overall wellbeing is examined in this research. Our predictions are based on the conflicting outcomes viewpoint, which relates HRM practices to increased work demands and stress, and the mutual gains approach, which identifies favorable linkages between HRM practices and employee performance. We provide evidence to support both the conflicting results and mutual benefits viewpoints using data from either the Finnish 2012 Practices of Working Life Survey. We also demonstrate that the impacts of the various subsets of HRM practices are varied.

M. Mudavath and K. Hari Kishore [5] discussed the differential Low Noise Amplifier (LNA) for 2.4GHz wireless receivers is described in this article. This differential offers strong stability, high gain, good reverse isolation, and lower noise figure (NF). A 180 nm CMOS process is used to simulate the intended LNA in the cadence virtuoso tool, and the results are simulated and used the SpectreRF simulator. The input reflection coefficient (S11) and output reflection coefficient (S22) of such a LNA are both 8.4 and 10 dB, respectively. It has a noise figure (NF) of 0.54dB, a high voltage gain (S21) of 30dB, strong reverse isolation (S12) of -48dB, with good stability with Rollet factor Kf> 1 and alternative stability factor B1f 1, respectively.

J. K. KasthuriBha and P. Aruna Priya [6]in 16 nm FinFET technology, two-stage differential operational amplifiers with low noise are shown. The suggested design would be used in high-speed chip systems (SOCs). Using a fundamental analog building block of a OP-AMP, the low leakage current, lower power consumption, and high current driving capabilities of the FinFET are realized. In the suggested design, a dynamic biasing mechanism is used to increase the OPAMP's slew rate. This method allows for an increase in the input common mode range (ICMR) and an improvement in gain stability. Using mixed mode device and circuit modeling on FinFET in sub-16-nm node technologies, the functionality of a differential amplifier is examined. It was found that the common mode rejection ratio of the FinFET-based OPAMP is 76 dB, and its size, power, and bandwidth performance have all improved. The suggested design may replace traditional MOSFET in reduced power Nano circuits since it performs better and has less 1/f noise.

A. Ballo[7] et al. low inherent gain and poor rejection to common-mode disturbances are characteristics of nanometer CMOS technology, which analog designers must overcome by using unconventional circuit designs capable of operating at sub-1-V supply voltages. In this

letter, a common-mode control loop for body-driven amplifiers is modified by substantially enhancing the small-signal performances of a source-coupled pair by cross-connecting the bulk terminals of an active-load transistors. The proposed approach provides a nominal 20-dB improvement in differential gain and a notional 29-dB increase in CMRR when compared to the conventional equivalent, according to a design example in a 65-nm process powered by 750 mV.

G. Srivastava and A. Mohan [8] in that communication, a dual-polarized, low-profile, small differential slot antenna with good common-mode rejection and isolation is shown. The antenna consists of a substrate integrated waveguide (SIW) cavity that is squarely supported by a cross-shaped slit. The differential signals are excited using the two differential pairings of the grounded coplanar waveguide. The diagonal TE120 and TE210 phases of the SIW cavities are excited by these differential signals. The suggested antenna has a front-to-back ratio of 22 dB and a differential gain of 7.4 dBi. As a proof of concept, a differential antenna prototype is constructed. The experimental findings demonstrate that the suggested antenna is a strong contender for a number of X-band applications.

H. Hu [9] et al. in order to improve the performance of such a conventional proportional integral differential controller and just a fuzzy proportional integral differential controller, that either consists of a genetic algorithm-based fuzzy gain tuner and just a conventional proportional plus integral differential controller, a fuzzy proportional plus integral differential control system of the proportional integral differential-type is presented in this research. The new fuzzy logic controller's gain settings for the traditional proportional integral differential controller are adjusted using the tuner. The suggested fuzzy logic controller uses a better evolutionary algorithm to adaptively adjust the membership functions but also control rules in contrast to the traditional fuzzy logic controller that relies on expert knowledge. The fitness value, the Euclidean distance, and the new reproduction operator of the genetic algorithm are also used to optimize the form of a membership functions and the elements of the rule base. Through extensive simulations under various operating conditions, including such varying set speed, constant load, and varying load conditions, this same performance of the genetic algorithm-based proportional integral differential-type fuzzy logic controller is assessed in terms of undershoot, undershoot, settling time, recovery time, and steady-state error. The outcomes demonstrate that the gain-tuned proportional integral differential controller, conventional fuzzy proportional integral differential control system, conventional fuzzy proportional plus integral differential control system, and scaling factor tuned fuzzy proportional integral differential controller are all outperformed by the genetic algorithm-based proportional plus integral differential-type fuzzy logic controller.

J. E. Pakaree and V. M. Srivastava [10] in that study, a differential amplifier using a Double-Gate (DG) MOSFET was developed. It may be used to electrical devices at the micro- and nanoscale. The DG MOSFET was chosen over Diodes, BJTs, and other MOSFETs owing to its low impurity dispersion, high current drive, and improved control of short channel effects. Several DG MOSFET differential amplifier configurations have been taken into consideration. The small signal model analysis of the DG MOSFET-based differential amplifier was followed by fabrication and testing for a variety of parameters, including differential mode gain, common mode gain, common mode rejection ratio (CMRR), but also frequency responsiveness. Results of the testing procedure include simulated frequency response of 32 MHz, differential mode gain (differential output) of 8.69 V/V, common mode voltage gain (single-ended) of 0.40 V/V, and CMRR of 19.06 dB.

DISCUSSION

Op-amp circuit noise

Typically, random signals that are unrelated towards the input signals may be found at an op-output. Amp's these unwanted impulses are known as noise. Theoretically, faults like drift error may be reduced to negligible amounts (by using, for example, a temperature-controlled environment), but noise error always occurs and reduces the available accuracy and resolution. Noise should be taken into account if the circuit being constructed must process low-level signals without high accuracy.Two types of noise that are fundamentally different may occur in a circuit. Interference noise is discovered outside the circuit. Noise is produced by the circuit itself. There are several causes of interference noise. Electromagnetism or electrostatic pickup form power sources running at mains frequency, broadcast radio, electrical arcing at switch contacts, and signals generated by digital electronic circuits are some examples. Fortunately, the circuit designer may often decrease interference noise by employing proper shielding and guarding, eliminating earth loops, and paying special attention to mechanical design.The amount of noise produced by a certain op-inherent amp depends on the circuit it is used in. The op-amp but also circuit components a designer picks are the only ways to control inherent noise. The range of an op-noise amp may be several orders of magnitude.

Characterization of random noise sources

An op-amp circuit's overall noise, or the noise in any circuit for that matter, may be thought of as a synthesis of an effects of several noise sources. Some inherent noise sources are essentially random signals. They generate an electrical signal with a waveform whose shape, amplitude, or frequency is not well defined. With amplitude and phase varying completely at random, they may be thought of as a superposition of signals at each and every imaginable frequency.

Value of the root mean square of a noise source (RMS)

When averaged over a sufficient amount of time, the RMS value of most random noise sources remains constant within a certain band width. So, a useful and informative method to define a random noise source is the RMS value in a specific bandwidth. The common definition is: where n is the instantaneous noise amplitude and rs is the RMS value of a noise source (current or voltage). For the RMS value of such a noise source to be helpful, the bandwidth must be well determined. When the bandwidth expands, the noise's RMS value rises.

Sources of noise are merged

Adding the RMS values of each noise source individually to the root sum of their squares gives an estimate of the overall influence of several random noise sources.

From a peak to a summit

Peak-to-peak noise may, in certain circumstances, actually determine the system's performance limit. Peak-to-peak noise is made up of the maximum positive and negative peak excursions that could be predicted over a certain amount of time. The probability of occurrence is lowest (but not zero) at the highest noise amplitudes, with the amplitude distribution for random noise basically Gaussian.

As a consequence, it may be difficult to measure peak-to-peak noise regularly, but a decent rule of thumb is to convert from RMS to peak-to-peak by doubling the RMS noise value by

the a factor of 6. Rarely (less than 0.25%) does a random noise signal with both the required RMS amplitude surpass the realized amplitude.

Spectral distribution of noise

Every source of random noise generates noise over the whole frequency range. Depending upon the frequency range being monitored, a source's contribution to noise varies. A noise density spectrum shows the frequency range across which noise from a certain source is distributed. The noise density n is often shown as a function of the frequency on log-log axes. Examples of noise spectra. In op-amp applications, the noise sources usually exhibit spectral distributions that fall into either of two categories: the first, where n is constant with respect to frequency; and the second, where n varies inversely with both the square root of frequency.""White noise" When n is constant with regard to frequency change, there is noise. White noise from a source is uniformly distributed over the frequency band. The heat agitation of a resistor's electrons causes random voltages to appear across it. The spectrum of this noise voltage is characterized by a noise density which is frequency invariant. Resistance noise, or "pink" noise

A density that varies inversely with both the square root of frequency is a defining feature of L/f noise. This noise is often referred to as "pink." The noise density for a pink noise source alone may be calculated using the equation of the form, wherein K is the value of n at f = 1 Hz. The log-log plot is a line with a slope of 10 dB/decade. In a graph of n2 vs. frequency, a straight line with a -20 dB/decade slope may be seen. One may calculate the contribution a pink source of noise makes to the RMS value of a noise in the frequency range between f to 2_ by substituting equation.

That used a noise density spectrum, RMS noise evaluation

Theoretically, by examining the integral, one may ascertain the contribution of a certain noise source towards the RMS noise in a specific bandwidth. Equations 2.33 and 2.35 provide the findings of these studies for the particular examples of a white noise source as well as a pink noise source. Bear in mind that evaluating the integral obviously requires knowledge of the equation defining the noise density as both a function of frequency. The noise density spectrum with both the appearance is often displayed by the noise generators used to replicate the influence of internally generated op-amp noise in the spectral regions of interest. A white noise component, which predominates at high frequencies, and a 1/f component, which predominates at low frequencies, may be thought of as the two components of this kind of spectrum. One may calculate the root sum of the squares (RMS) value of a noise each source provides in any given bandwidth by summing the RMS contributions of the two separate components in that bandwidth.

Op-amp noise specifications

The noise generated by an op-output amplifier is a combination of the amplified input noise and the noise the op-amp generates internally. A noiseless op-amp having noise voltage and noise current generators there at input terminal may easily replicate the noise produced internally by an op-amp.It is possible to use comparable noise generators connected to the op-input amp's terminals to replace the noise created by resistors at the input. In closed-loop op-amp applications, the multiple input noise contributions may be combined into a single input-referred noise source, which is then multiplied by the closed-loop noise gain to emerge at the output 1/ /3.

Similar to the approach used to evaluate offset and drift errors that was previously described in Section is the approach used to evaluate noise. The main contrast between the evaluation of a drift error and the evaluation of noise errors is the impact of noise on bandwidth. To assess the noise in an op-amp circuit, the designer needs use noise statistics from the op-amp data sheet.

Information about op-amp noise is shown numerically and visually. The voltage noise but also current noise models are typical graphical representations of numerical noise data that indicate the frequency dependence of the noise.The usual low-frequency peak-to-peak input current and voltage noise was provided by many manufacturers (say 0.01 to 1 Hz). For defining accuracy restrictions, this kind of peak-to-peak specifications is particularly useful when the signals of interest are predominantly DC or move very slowly (as restricted by noise). Wide bandwidth noise will unavoidably be present in the op-amp output, but it could be reduced by adding a suitable low-pass filter thereafter.The noise's RMS values may be used to determine peak-to-peak values. As a general rule, the previously mentioned multiplication factor of six is used.

Assessing noise defects using noise characteristics

The difficulty for the circuit designer is figuring out how noise affects the accuracy and resolution thresholds. It is evident that the noise has obscured the signal if the output noise level was equal towards the signal level. A useful statistic in wide band applications seems to be the signal-to-noise ratio (SNR), which quantifies how well the signal "stands out" from the background noise. The formula for computing the output signal-to-noise ratio is SNR = signal power out/noise power out.

Sometimes the connection will display the decibel ratio (dB). 10 log (P/P) is equivalent to SNR (dB). Peak-to-peak noise may be related to the limitations on accuracy imposed by noise in low frequency and DC applications. The connection allows us to express noise inaccuracy as a percentage.To determine the potential amount of noise in a particular circuit, noise data for the op-amp in use is employed. Comprehensive noise evaluations take time, and if they are predicated on "typical" noise data, they may not be particularly helpful in reality. It's crucial to be able to immediately assess the order of magnitude of the noise since one noise source may have a disproportionately significant influence on several applications.

Every noise evaluation should begin by determining the signal gain and noise gain in the circuit. Bode diagrams with their frequency dependency may be used to display the spectrum regions where significant noise contributions are expected. The noise performance of an op-amp used in a basic resistive feedback setup is evaluated as a starting point. The noise gain is 100 in this case, the 3 dB bandwidth limitation is 10 Hz, and the noise gain decays at a rate of 20 dB/decade beyond this frequency. The noise gain causes input noise sources to become more visible at the op-amp output.

Technology of analog integrated circuits

The op-amp-focused technology seen in analog integrated circuits. Also, it will outline the variations between voltage and current feedback. The kind of transistor utilized in the integrated circuit determines the technology (IC). Bipolar, bipolar with JFET inputs, LinCMOS (linear CMOS), and BiCMOS are among the varieties (incorporating bipolar and CMOS transistors). The vast majority of op-amps were built with voltage feedback in mind. Nevertheless, since they have a very broad bandwidth capacity, current feedback devices are currently used in radio frequency and video signal processing. Definitions of voltage feedback and current feedback may be helpful. In a closed-loop setup known as voltage

feedback, the error signal takes the form of a voltage. Conventional op-amps employ voltage feedback and respond to a variation in input voltage by producing an output voltage. In other words, as the voltage changes, so do their inputs. A voltage feedback op-amp with high input impedance and no input current is optimal. To maintain a zero differential input voltage, output power feedback is employed. Given by is a non-inverting voltage feedback amplifier's proportional gain.

$$\frac{V_o}{V_{IN}} = \left(1 + \frac{R_2}{R_1}\right) \frac{1}{1 + \frac{1}{LG}}$$

Here loop gain (LG) is given by $\frac{A_{OL}}{1 + \frac{R_2}{R_1}} = \beta A_{OL}$

Any closed-loop circuit that employs a current as the error signal is referred to as using current feedback. Current feedback devices feature an inverting input with a low impedance, unlike voltage feedback op-amps. Because of the low impedance, current may enter and exit the inverting input. Any current flowing into this input is just an error current, and the output voltage of the op-amp is proportional to the size of the error current. To keep the inverting input's error current at zero, current feedback is employed. A voltage feedback op-high amp's impedance non-inverting input has a high resistance. Transimpedance amplifiers are the brains of current feedback operational amplifiers. With a current input, the transimpedance amplifier generates a voltage output.The open-loop "gain," Vo/Iin, is given in ohms, as the function would imply. We shall examine this impedance either as a complex impedance Z or as distinct resistive (Rm) and capacitive (CC) versions (s). As a result, a current feedback opamp can sometimes be referred to as a transimpedance amplifier. Given by is a non-inverting current feedback amplifier's transfer function,

$$\frac{V_o}{V_{IN}} = \left(1 + \frac{R_2}{R_1}\right) \frac{1}{1 + \frac{1}{LG}}$$

In this case loop gain (LG) is given by $LG = \frac{Z(s)}{R_2}$

Voltage feedback op-amps

Bipolar transistor-based op-amp integrated circuits have been in use since 1965. The discrete "operational amplifiers" that were created using individual transistors, resistors, and capacitors were greatly improved by these op-amps. They were more compact, inexpensive, and easy to operate. Later, to enhance certain elements of the performance of bipolar op-amps, field effect transistors were included into some op-amps. In the late 1960s, devices were created that used bipolar transistors throughout but included JFET input transistors. The JFET input op-benefit amp's was that it required less input bias current. Texas Instruments referred to JFET input opamps as "BiFET" op-amps; this moniker is particularly apt given that it makes use of both bipolar and FET transistors. More recently, CMOS transistor-based op-amps have been employed to provide very low power operation. BiCMOS op-amps, which combine complementary MOSFET and bipolar transistors, are the result of further progress.

Bipolar op-amps

The input impedance of the first (1965) op-amp circuits was much less than optimal (about 200 k). Moreover, the offset voltages and input bias current were important. The performance of bipolar op-amps has continuously improved thanks to ongoing research efforts by numerous semiconductor manufacturers. Negative feedback may raise the input impedance of bipolar op-amps, which typically ranges from 10 M to 1 G or more. The bigger issue is that input bias currents are in the range of 10 nA, while the noise current that results is in the range of 0.3 pA/Hz. Bipolar op-amps cannot be used with high impedance sensors due to these bias and noise current values. The fast npn and pnp transistors used in bipolar op-amps. In Chapter 2, common input and output circuits were discussed (Figures 2.1 and 2.3). Because to them, the gadget may have a gain-bandwidth product of at least 10 MHz. Input offset voltage and drift with temperature and time are both reduced by good matching between the input transistors. Among all the available technologies, op-amps with such a bipolar input stage offer the best long-term stability. One explanation is because collector currents travel vertically through semiconductors, avoiding lateral tension and strain brought on by temperature changes. The emitter resistance, which is much lower than the corresponding resistance in JFETs or MOSFETs, is what causes the noise voltage in a bipolar transistor. As a result, a bipolar input stage's noise voltage is lower than a FET input stages. While low noise kinds have such a noise voltage below 5 nV/Hz, the typical noise voltage is 15 nV/Hz.

Adjunct bipolar technology (Excalibur)

Commercially accessible integrated circuit op-amps come in hundreds of distinct varieties, and the variety is growing virtually every day. By improving DC accuracy, accelerating AC performance, and reducing power consumption, the several producers of these various sorts are attempting to create the greatest products. The comparatively sluggish reaction of the pnp transistor in comparison to the npn is one challenge in enhancing the performance of op-amps. This is due to the majority carrier "holes" in the pnp transistor having lower mobility than the electrons in the npn transistor. PNP transistors are employed in many op-amp designs, especially in differential pair transistor input stages and emitter follower outputs. Yet, the pnp transistor's usual fT is just 5 MHz as opposed to the npn transistor's 150 MHz. Increasing the speed of the npn element causes the total speed to rise, which is one way to speed up sluggish complementary bipolar circuits. Many semiconductor makers take this stance. Transistors are often made using a vertical arrangement in the silicon chip. A p-type substrate and an n-type epitaxial layer will be present in annpn transistor. Theoretically, by merely flipping this design and using an n-type silicon substrate, it is possible to create quicker pnp transistors. While this technique effectively raises the speed of the pnp transistor, it lowers the speed of the corresponding npn transistor produced in the same integrated circuit. Texas Instruments, in contrast, has created a manufacturing procedure for a quick vertical pnp device structure that maintains the npn devices' speed. The Excalibur technology, developed by Texas Instruments, employs a deeply submerged n-region as an "artificial substrate" on top of which a buried p-region acts as the collector. Without having to worry about reducing the bandwidth or slew rate, the fast pnp Excalibur transistor may be inserted straight into the signal stream. In comparison to its predecessors, this often offers the additional benefit of needing less supply current. The TLE, a low power, precision op-amp, is an example of the Excalibur series of op-amps. The TLE reaches a slew rate of 0.9 V/s and a unity-gain bandwidth of more than 2 MHz. With an input voltage offset of under 100 V, the supply current is less than 200 A. The "phase reversal" that many op-amps experience is a typical issue. The output will change state and swinging towards the opposite rail if the input

swings near to the potential of the power rail. It is well known that many of the older bipolar and BiFET op-amps suffer from this issue. Several more recent products, including the TLE2020 series, have been made to prevent this.

CONCLUSION

A differential amplifier's main objective is to increase the voltage difference that results from comparing the two input signals provided to its inverting and non-inverting inputs. The basic purpose of differential amplifiers is to reduce noise. There are two types of noise: the normal differential noise and the common-mode noise, that latter of which is readily suppressed by an op-amp. Common mode interference, often known as noise, is produced when both signals are flowing toward the same direction. The direction of the signals differs in differential mode compared to common mode.

REFERENCES

[1] W. Yang, M. Xun, W. Che, W. Feng, Y. Zhang, and Q. Xue, "Novel Compact High-Gain Differential-Fed Dual-Polarized Filtering Patch Antenna," *IEEE Trans. Antennas Propag.*, 2019, doi: 10.1109/TAP.2019.2930213.

[2] A. C. Duran *et al.*, "Foreclosures and weight gain: Differential associations by longer neighborhood exposure," *Prev. Med. (Baltim).*, 2019, doi: 10.1016/j.ypmed.2018.07.009.

[3] G. Muziol *et al.*, "Optical properties of III-nitride laser diodes with wide InGaN quantum wells," *Appl. Phys. Express*, 2019, doi: 10.7567/1882-0786/ab250e.

[4] C. Ogbonnaya and J. Messersmith, "Employee performance, well-being, and differential effects of human resource management subdimensions: Mutual gains or conflicting outcomes?," *Hum. Resour. Manag. J.*, 2019, doi: 10.1111/1748-8583.12203.

[5] M. Mudavath and K. Hari Kishore, "A low NF, high gain of 2.4ghz differential LNA design for wireless applications," *Int. J. Sci. Technol. Res.*, 2019.

[6] J. K. Kasthuri Bha and P. Aruna Priya, "Low power & high gain differential amplifier using 16 nm FinFET," *Microprocess. Microsyst.*, 2019, doi: 10.1016/j.micpro.2019.102873.

[7] A. Ballo, A. D. Grasso, and S. Pennisi, "Active load with cross-coupled bulk for high-gain high-CMRR nanometer CMOS differential stages," *International Journal of Circuit Theory and Applications*. 2019. doi: 10.1002/cta.2684.

[8] G. Srivastava and A. Mohan, "A Differential Dual-Polarized SIW Cavity-Backed Slot Antenna," *IEEE Trans. Antennas Propag.*, 2019, doi: 10.1109/TAP.2019.2900380.

[9] H. Hu, T. Wang, S. Zhao, and C. Wang, "Speed control of brushless direct current motor using a genetic algorithm–optimized fuzzy proportional integral differential controller," *Adv. Mech. Eng.*, 2019, doi: 10.1177/1687814019890199.

[10] J. E. Pakaree and V. M. Srivastava, "Realization with fabrication of double-gate MOSFET based differential amplifier," *Microelectronics J.*, 2019, doi: 10.1016/j.mejo.2019.07.012.

CHAPTER 6

A COMPREHENSIVE STUDY ON THE CHOPPER STABILIZATION

Mr. Sunil Dubey, Associate Professor,
Department of Electrical Engineering, Jaipur National University, Jaipur India
Email Id- sunildubey@jnujaipur.ac.in

Abstract:

A DC or low-frequency signal is then converted to a high-frequency signal via a chopper. The high-frequency signal is modified and amplified by an AC amplifier. The frequency and intensity or DC signal is created by demodulating and filtering the amplified signal. In this chapter author is discusses the factors relating to AC

Keywords:

Bandwidth, Gain, Operational Amplifier, Network, Signal.

INTRODUCTION

Chopper stabilization

The TLC265X series of CMOS technology op-amps uses chopper stabilization, a method that improves DC performance. The chopper op-amp is intended to continually perform self-calibration throughout order to give a highly time- and temperature-stable, ultra-low offset voltage. The 1/f noise content is decreased while the CMRR is raised at the same time. A typical chopper stabilized op-amp is shown in Figure 1.

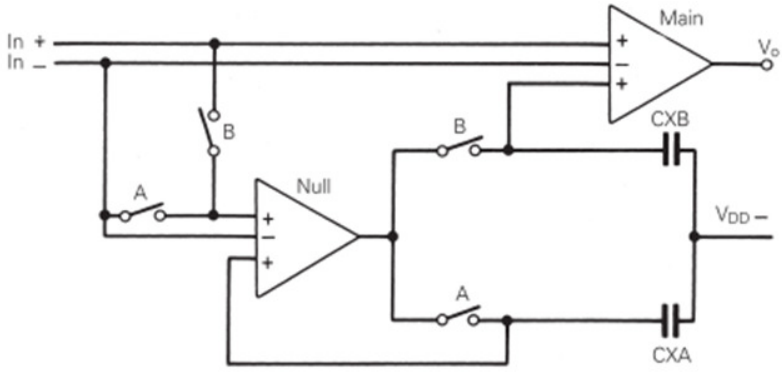

Figure 1 Chopper stabilized op-amp

Fundamentally, utilizing two op-amps results in the improved performance of a chopper stabilized op-amp. An oscillator, switches, two external (or internal) capacitors, a nulling op-amp, as well as a main op-amp are used to build a system that functions as a single op-amp. This method allows the TLC2652 op-amp to attain sub-microvolt input offset but also input noise voltages. The range of offset fluctuations with temperature is nV/°C. Two main clock phases are generated by the on-chip control logic: a nulling phase as well as an amplifying phase. Switch "A" is closed during the nulling phase, which shorts the nulling op-amp inputs

simultaneously. By sending its output signal back to an inverting input node, the nulling op-amp is able to lower the voltage at which it receives its own input offset. The offset voltage of a op-amp is simultaneously stored in the external capacitor CXA, allowing it to continue to be null throughout the amplifying phase. Switch "B" is closed during the amplification phase. This links the main op-non-inverting amp's input to the output of the nulling op-amp. The primary op-input amp's offset voltage is zeroed out in this design. Also, the main op-offset amp's is kept null throughout the following phase thanks to the external capacitor CXB's storage of the nulling potential. Offset voltage nulling is possible during temperature and time fluctuations because to this continual chopping procedure. Both the common mode input voltage range as well as the power supply voltage range are supported by the nulling procedure. Moreover, a very high gain is achieved since the low frequency signal channel passes through both the nulling and primary op-amps. The amount of component noise present before chopping determines the degree of low frequency noise output from the chopper op-amp. Also, it relies on how well the circuit can suppress noise when chopping. Low frequency noise is decreased by raising the chopping frequency. Intermodulation and aliasing are reduced by keeping the input signal frequency to under 50% of the chopping frequency.

Op-amps with JFET input

In an effort to lower the bias current and raise the input impedance of op-amp input stages, junction field effect transistors (JFETs) were included. Bipolar transistors were still used in the output and intermediate stages of the op-amp, as seen in Figure 2.

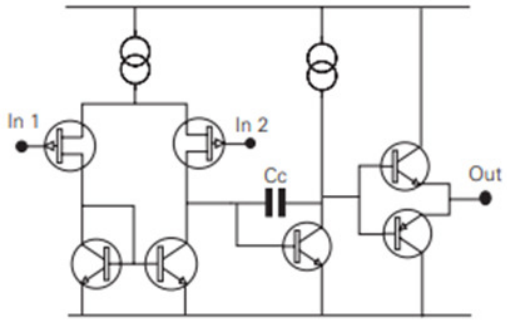

Figure 2: JFET input op-amp circuit.

Op-amps with JFET inputs generally have an extremely high input impedance of 1 T. Its noise current is normally 10 fA/Hz and their input bias current is 50 pA on average. Due to the high channel resistance, noise voltage is greater in JFET input op-amps than in bipolar devices. Typically, the noise voltage is 20 nV/Hz. JFET input op-amp input offset voltages are generally 500 V, which is roughly 10 times higher than bipolar input op-amp input offset voltages. A JFET input opamp has much less stability than a bipolar input device. The temperature causes stress and strain on the current flow via a lateral JFET channel, changing the current across the channel. In the "Texas Instruments" Excalibur method, special circuits that make use of bipolar transistors to lessen input offset voltage drift are employed. As opposed to a bipolar stage, the JFET at the input does not provide as much gain. As a result, higher slew rates may be reached than for an op-amp with a bipolar input and the same gain-bandwidth product. JFET input op-amps may be used in rectifier circuits, peak detector circuits, pulsed amplifying circuits, and sample and hold circuits due to their quick slew rate.

Op-amps for CMOS devices

CMOS transistors have been used in digital electronics for a long time to minimize circuit size and power consumption. Low quiescent (steady state) current needs along with low voltage have helped to minimize power usage. CMOS is now used by analog op-amps for identical reasons, as seen in Figure 3.

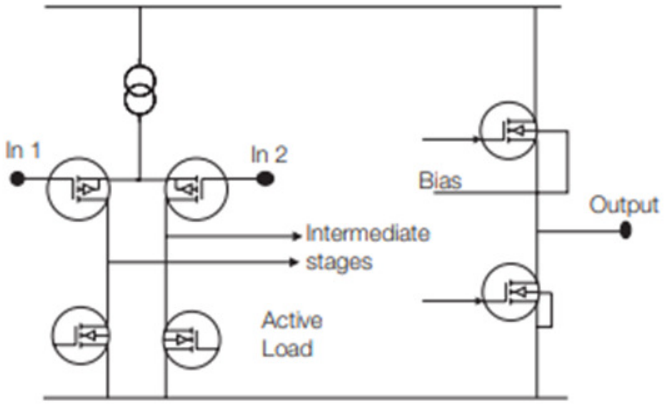

Figure 3: Illustrates the CMOS op-amp circuit.

There are op-amps on the market that need just 1 A of quiescent current from their supply rails. There are further devices that can run on supply voltages as low as 1.4 V. The majority of CMOS op-amps can only work at supply voltages of about 6 V, with many having a maximum operating voltage of 16 V. Since CMOS op-amps use p-channel MOSFETs on their input, they can function properly with input voltages as low as the negative supply rail. As a result, they may be used in circuits with a single supply in which the input voltage is referred to the negative rail. High input impedance and low offset and bias currents are provided by the MOSFET input. Typically, the input bias current is about 100 fA. Yet, this current doubles for every 10°C increase in temperature, much as the JFET input. As a result, the CMOS op-amp is subject to temperature drift. While some op-amps are built for offset voltages as low as 200 V, offset voltages are normally 1 mV. This is superior to many JFET input op-amps, but it falls short of what bipolar devices are capable of. High DC accuracy is achieved using CMOS op-amps with chopper stabilization, with a maximum offset voltage of around 1 V. In general, CMOS op-amps provide superior offset voltage stability than JFET input devices. The high noise voltage that CMOS op-amps experience is unfortunate. While certain devices have been built for minimal noise and generate a noise voltage of approximately 10 nV/Hz, noise voltage is normally 30 nV/Hz. Its noise level is lower than certain bipolar types and lower than JFET input op-amps. CMOS op-amps are perfect for portable equipment due to their single supply, low voltage, and low quiescent current needs. They are useful for integrating high input impedance transducers due to their low bias current and high input impedance. Care must be taken with all electrical equipment to avoid electrostatic discharge (ESD) damage. A high voltage supplied will cause the bipolar and JFET inputs to conduct. A pn junction will momentarily malfunction if reverse biased, much like a zener diode. As long as current flow is constrained, there is no long-term harm. MOSFET input op-amps are especially vulnerable to ESD damage because of their very high input impedance. A MOSFET gate will become permanently damaged if an input is overvoltaged because it will burn a hole in its surface (Figure 4).

BiCMOS op-amps

While BiCMOS technology has been utilized in logic integrated circuits for a while, there weren't many BiCMOS analogue devices available until the late 1990s. Nevertheless, the

need to employ single-rail low-voltage power sources has promoted the switch to BiCMOS. Op-amps are available that take very little current and work with a single-rail supply, generally between 2.7 V to 12 V. They are consequently appropriate for battery-powered machinery. The circuit's current is constrained by the current source linked to the V supply, and the bipolar transistors create an amplified current mirror. More current flows through the base of Q3 if the voltage at input IN1 is turned negative to increase the current through the MOSFET Q1. Q3 amplifies this current, which is then utilized to drive the bases of Q4 and Q5. The output voltage decreases as the current via Q5 increases. As a result, the amplified current mirror contributes to the stage's very high gain. The BiCMOS op-amp can run down to the negative supply rail, much as CMOS op-amps can, thanks to the usage of p-channel MOSFETs at the input. The input voltage is referred to the negative supply rail, making them perfect for single supply operation. Very high input impedance is provided by the MOSFET input, and bias currents of 1 pA are usual. BiCMOS has the benefit of having a high output bandwidth slew the rate while using minimal power from the supply. One component, the TS951, is designed to be used in cell phones. The gain-bandwidth product of this op-amp, which consumes 0.9 mA from the power source, is 3 MHz. With the LMV321, another op-amp, a gain-bandwidth product of 1 MHz may be delivered in only 0.1 mA.

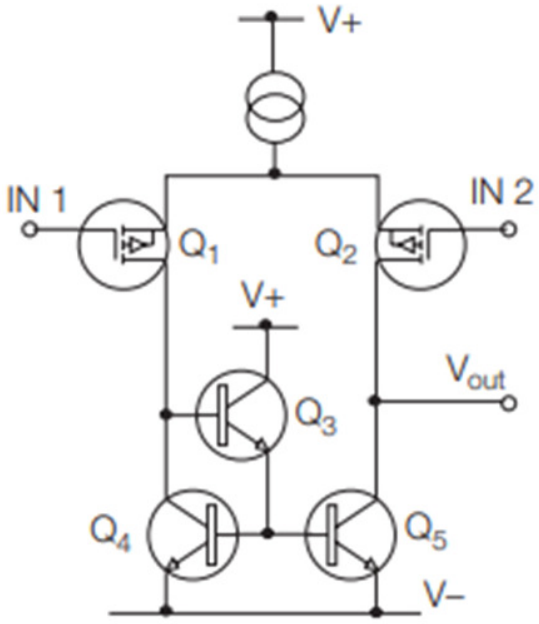

Figure 4:BiCMOS op-amp input stage.

BiCMOS capabilities

BiCMOS operates similarly to CMOS in the DC domain. Extremely low input bias and noise current that works with high impedance circuits and can be powered by single-rail, low-voltage sources. Comparing DC errors for several op-amp types reveals that the more recent bipolar designs outperform the more dated LM741 and LM301 devices. The openloop gain has been enhanced while the input offset and bias current have been significantly decreased. In comparison to bipolar devices, biFET op-amps often have greater input offset voltage and drift. As compared to bipolar devices, the input bias current of FET opamps was negligible. With every 10 degrees Celsius rise in temperature, the FET bias current doubles. Be aware that certain bipolar designs actually exhibit lower bias currents than FET input op-amps at

higher temperatures. Gate silicon Instable offsets in CMOS designs have been made less of a concern thanks to CMOS technologies like LinCMOS. A representative of the current generation of CMOS devices is the TLC2201, which was created using LinCMOS. It has the high input impedance and low noise current seen in the finest JFET devices, as well as incredibly low and steady offsets. The chopper stabilized op-amps, such the TLC2652, provide the lowest input offset and drift for high order DC accuracy.

LITERATURE REVIEW

H. Ko et al. [1]suggested to use resistive sensors with a low-noise analog front-end (AFE) and a multipath current-feedback instrumentation amplifier (CFIA). Chopper stabilization methods have been widely used in past research, and low-noise procedures are necessary for the functioning of accurate resistive sensors. Techniques that simply rely on chopper stabilization, however, have the drawback of having a limited bandwidth. In this study, a multipath operational amplifier is used to overcome this issue. Moreover, a multipath operational amplifier's low-frequency path uses the chopper stabilization approach. The offset voltage creates the "ripple" that is the result of this chopper stabilizing procedure. This ripple is eliminated via a ripple rejection loop in the low-frequency channel. Moreover, the measured analog signal is transformed into a digital output using a successive approximation register (SAR) analog-to-digital converter (ADC). The converter does have a signal-to-noise and distortion ratio (SNDR) of 75.68 dB and also an effective number of bits (ENOBs) of 11.02. The complementary metal-oxide-semiconductor (CMOS) design technique is used to create the resistive AFE with SAR ADC, which has an active area of 8.6 mm2. With a 1.8 V supply, it runs at 2.56 mW, and its input-referred noise ranges from 1 to 100 Hz and is 0.29 Vrms.

B. Lee [2] et al. proposed a capacitive humidity sensor with a low-noise 16-bit capacitance-to-digital convertor (CDC). The suggested sensor interface circuit directly translates the capacitance fluctuation of the humidity sensor into a 16-bit digital code using a first-order incremental delta-sigma architecture. The chopper stabilization approach uses a switched capacitor (SC) integrator of the delta-sigma modulation for a low-noise characteristic. The low-frequency flicker noise and offset of an amplifier may be eliminated using the chopper stabilization approach. The mismatched capacitance from of the parasitic capacitor and process fluctuations are removed using the offset cancellation programmed capacitance array of the input stage. To decrease the power consumption of both the back-end digital processing, the proposed delta-sigma CDC comprises an accumulator with a straightforward 16-bit dual counter that transforms the delta-sigma modulator outputs to a 16-bit digital code. The 0.18 m complementary metal-oxide-semiconductor technology is used to create the proposed sensor interface circuit, which has an active area of 0.66 mm2. The suggested delta-sigma CDC has an active energy consumption of 376 W with a 1.8 V supply, and the worst case effective resolution is 14.4 bits.

R. Chebli[3] et al. described the chopped LPGA circuits for EEG acquisition systems as well as a fully integrated low-noise, high common-mode rejection ratio (CMRR), logarithmic programmable gain amplifier (LPGA). A rail-to-rail true logarithmic amplifier (TLA) stage is the foundation of the suggested LPGA. In addition towards the lower common-mode gain of the suggested logarithmic amplification topology, the high CMRR attained in this study is the consequence of cascading three amplifying stages to build the LPGA. In addition, a chopper stabilization method is used to lessen the input transistors' intrinsic DC offset voltage and 1/f noise. The circuits are created using CMOS 180 nm standard technology. According to experimental findings, the integrated LPGA has an active area of 0.4 mm2, a CMRR of 140 dB, a differential gain of 37 dB, input-referred noise of 0.754 Vrms, and an energy

consumption of 189 W from 1.8 V power supply.

S. M. Lim and J. S. Park [4] discussed the sensitivity of CMOS Hall sensors is suggested to be increased via a low-noise offset-cancellation technique. Due to their large offset, flicker (1/f) noise, and chopper switching noise, conventional CMOS Hall sensors are not very sensitive. They need to lower noise production and extract the Hall signal from the noise in order to increase the sensitivity of Hall sensors. As a result, switching noise and harmonics are minimized in this research by adopting a low-noise offset-cancellation approach and fewer choppers. The offset noise of both the read-out circuits is also unaffected by the Hall signal since it does convert back to DC. The design and testing of a CMOS Hall plate-equipped Hall sensor system. We confirm that the signal-to-noise ratio (SNR) increases by 18.36 dB and the spurious free dynamic range (SFDR) improves by 9.02 dB whenever the Hall signal processed by the suggested technique is compared with the present system under the same circumstances.

According to the Y. C. Chen et al. [5]a low-noise chopper-stabilization potentiostat circuit based on current-mirror technology and an electrochemical sensor chip with only an integrated current-reducer pattern generator are shown. Without using any large-size passive components, the pattern generator generates a sub-Hz ramp signal for the cyclic voltammetric (CV) measurements using the current reducer approach and pseudo resistors. To minimize the impacts of amplitude noise and convert the sensing constant current to digital codes for the further data processing, the suggested design uses a counter-based time-to-digital converter, chopper-stabilization, and low-noise biasing techniques for the potentiostat. Using a 0.18-μm CMOS fabrication process, the design fabricates with a 41pA current resolution inside the current range of formula>tex>$pm. $</tex></formula> while keeping the Rformula>tex>, 5μA ^{2}</tex></formula> 0.998 linearity When a 5μA sensing current is measured, the system uses 16μW from a 1.2V supply. The readout interface's power efficiency is 0.31 and its sensing today's dynamic range was 108 dB. The design has been successfully evaluated in dual-mode (CA/CV) measurements using industry-standard gold electrodes in a potassium ferricyanide solutions at sub-millimolar concentrations.

Y. C. Chen [6] et al. discussed an electrochemical sensing front-end circuit with such a cyclic voltammetry potentiostat is shown in this research. A continuous offset current is supplied to allow for a broad and bidirectional current sensing region for the current-mirror based potentiostat. Chopper stabilization is an effective method for reducing the readout circuit's flickering noise. This research also suggests a charge-based oscillator to translate the current into the frequency for further data reading. The suggested reading IC has a current range of -2 A to 12.2 A, an R2 linearity of 0.992, and a minimum detectable current of 3.1 nA. It was constructed using a 0.18 m, 1.2 V CMOS technology. The chip uses 40.5 W at such a maximum sensing current of 12.2 A while the dynamic current range is 73.2 dB.

M. Mikawa[7] et al. proposed an analog-domain and digital-domain mixer-based delta-sigma modulator incorporating frequency division multiplexing (FDM). The suggested circuit has chopper stabilization to get rid of flicker noise and works well as the front-end of electroencephalogram (EEG) acquisition. The suggested method provides excellent space efficiency while not requiring additional digital signal processing for frequency-domain conversion. We assess dynamic range and adjust chopping frequencies to reduce crosstalk. The two-channel prototype made in 0.18 mm CMOS technology is measured and the performance is confirmed using MATLAB/Simulink simulation.

S. Zhang [8] et al. in that study, a switch-mode CMOS Hall sensor circuit is developed and

the offset voltage first from Hall component and amplifier is removed using the quadrature current approach and chopper stabilization methodology. The effective Hall signal may also be amplified at the same time using the chopper amplifier. Lastly, the offset voltage between the Hall component and the amplifier is removed using the modulation-demodulation technique. The simulation findings demonstrate that the sensor can successfully reduce lOmV offset voltage from either the Hall component and also the amplifier using a 0.18(1 CMOS modeling approach in a Cadence simulation environment. the ultimate voltage output from the hall with a level of 0.

S. Pokamisas[9] et al. conducted an analysis and design of a CMOS capacitive-coupled instrument amplifier are presented in this paper (CCIA). The amplifier is appropriate for portable devices for health monitoring since it has an ultra-low power consumption and a gain of 40 dB for frequency up to 100 Hz. By biasing the circuit's MOSFETs at the subthreshold region, the circuit's power consumption is reduced. It uses chopper stabilization to get rid of the predominant low-frequency noise. The Cadence® Custom IC Design Tools is used to implement the CCIA inside the TSMC 0.18 m process.

J. Lee [10] et al. presented a single-bit discrete-time (DT), switched-capacitor (SC), fourth-order cascade-of-integrators with feedforward (CIFF) delta-sigma modulator (DSM) for high-resolution applications. With a high-order modulator structure, this DSM is appropriate for high-resolution applications at low frequencies. In comparison to current designs, the suggested operational transconductance amplifier (OTA) used a feedforward amplifier technique that offered a high power efficiency, a broader bandwidth, and a greater DC gain. The initial integrator was stabilized using a chopper approach to get rid of the transistor's inversely frequency-proportional 1/f noise. Using complementary metal oxide semiconductor (CMOS) technology, the planned DSM was realized. The sampling frequency were 128 kHz, and the oversampling ratio (OSR) were 128. The signal-to-noise ratio (SNR), signal-to-noise distortion ratio (SNDR), and dynamic range (DR) were all 100.3 dB at a 500 Hz bandwidth. 99 W of total power consumption from a 3.3 V supply voltage was observed.

DISCUSSION

Accuracy in both AC and DC is needed for op-amps. Although bias currents and input offset voltages are important in DC applications, additional factors need to be taken into account while designing AC circuits. The purpose of the op-amp is to serve as an amplifier. However, phase shift that results from signal amplification often causes the device to become unstable. A Miller compensating capacitor is employed to avoid instability, but only at the cost of the op-gain amp's and slew rate. The unitygain bandwidth is ultimately defined by this compensating capacitor. The manufacturing process technology or the design methodologies utilized determine the AC performance of an op-amp. Devices with wide bandwidth often need a lot of supply current. While bipolar op-amps have strong gain and bandwidths, they have a poor slew rate for that bandwidth. There is a high transconductance (gm) constraint of the bipolar technology process that is difficult to build around. The usage of pnp transistors in bipolar op-amps imposes a speed restriction, as was covered in Section 3.1.1. Bipolar and JFET architectures are combined in the creation of biFET op-amps. The input stage uses P-channel JFETs, which have a substantially lower transconductance than bipolar transistors. The remaining component of the circuit is built using bipolar transistors. Op-amps made with this combination have much larger slew rates than those made with just bipolar designs. While they perform similarly to designs employing BiFETs, CMOS technologies, such as LinCMOS, are particularly well suited for low power or single supply applications. Although BiCMOS methods have many characteristics with CMOS, they offer a substantially greater dynamic response for a given supply current. They are commonly utilized in the audio

amplifier circuits with mobile cellphones because they have higher slew rate and gain-bandwidth products than a CMOS op-amp that consumes the same current.

Noise considerations

The input voltage noise of an op-amp is measured in nanovolts per root hertz (nV/ Hz). At extremely low frequencies, this level is greater than it is for the bulk of the op-operational amp's bandwidth. The 1/f corner frequency is the frequency at which the noise level 'flattens out'. The noise intensity increases inversely proportionally to frequency below the 1/f corner frequency. The 1/f corner frequency in a bipolar op-amp may be as low as 100 Hz, however this frequency can be significantly higher in FET input op-amps (several kHz). While other devices have substantially lower voltage noise levels (5 nV/Hz), bipolar devices usually give the lowest voltage noise among those that are commercially accessible (15 nV/Hz). Thermal noise from the base-spread resistance as well as the emitter resistance dominates the voltage noise from a bipolar input stage in the flat section of the band. Sadly, the shot noise brought on by the input bias current may be rather large. Hence, bias current cancellation circuits are occasionally employed to lessen this current noise. Shot noise is a result of the gate current and is what causes the input noise current of FET input op-amps. Compared to the base current in bipolar inputs, this is quite low at temperatures about 25 °C. Because of this, FET input op-amps provide excellent noise performance with high impedance sources and have little input current noise. In comparison to a bipolar input stage, a FET input stage has more voltage noise and higher 1/f corner frequency. Gate current is insignificant, and the input protection network reduces input current to leakage current. A MOSFET input device's noise sources resemble those of a junction FET. The relatively high voltage noise and high 1/f frequency of MOSFET input op-amps (i.e., CMOS and BiCMOS op-amps) are a typical drawback. Although some, like the Texas Instruments LinCMOS op-amp TLC2201, provide current noise levels that are comparable to the best junction FET input op-amps, other devices do the opposite. Moreover, their voltage noise levels are equivalent to those of many bipolar devices. The TLC2201 has an extremely low drift between time and temperature change and low input offset voltages. The gadget also has rail-to-rail output swing and can run off a single 5 V supply. In conclusion, bipolar input stages are ideal for interacting with low impedance sources since they have the lowest voltage noise and 1/f corner frequency. JFET, CMOS, and BiCMOS input stages may be employed with very high source impedances due to their small input current noise. For every 10°C change in temperature, the noise current, which is correlated with the input bias current, will increase by V2.

Considerations for the power supply

Op-amps are necessary for operation with a variety of sources. In instrumentation applications, circuits may need a 22 V or higher supply or they may be battery-powered and just need a single 1.5 V supply. Op-amp selection is influenced by the available power. When utilized with battery-operated equipment, single supply op-amps may require to function off a low voltage supply as low as 1.5 V. Moreover, they will need an output that swings close to ground and an input common mode range that extends to the negative rail. Op-amps with multiple supplies are often exempt from these limitations. With the aid of a bipolar method, an op-amp with a common mode range down towards the negative rail may be created with ease. PNP input transistors make sure that there won't be any issues if the input swings down to the positive rail or lower. A good output swing is difficult to attain. Many bipolar devices can source and sink current because they are designed for dual supply operation. Thus, the output won't often swing down to the negative rail. When a gadget is designed for single supply operation, crossover distortion occurs in its output when it is used with dual sources. It is rare to find bipolar devices that can operate with a single or dual power source.

BiFET op-amps are often inappropriate for single supply operation and have been built for dual supply operation. Its common mode input range approaches the positive supply rail potential, and in some cases even goes beyond it. The output will typically fluctuate between each source voltage by 2.5 V. They are designed for AC performance and work with a broad variety of supply (3 V to 22 V). BiCMOS and LinCMOS CMOS chips were created primarily for single supply operations. Typically, the supply voltage range is between 2 and 16 volts. The range of input voltages goes below the 0 V supply. With high impedance loads, the output voltage swing might go close to the power rails. CMOS devices having push-pull outputs, as opposed to bipolar designs, may also function effectively with two supply. Nevertheless, the low working voltage in certain dual supply systems is a drawback.

Op-amps with current feedback

The constant gain-bandwidth product of voltage feedback op-amps is a drawback. Gain is lost as the bandwidth is extended. A completely new gain-bandwidth product relationship exists for modern feedback op-amps. In actuality, independent of gain, the bandwidth is essentially constant. Figure 5 depicts the most basic form of a current feedback amplifier. In this arrangement, a buffer linked between the non-inverting and inverting inputs serves as the input of a current feedback amplifier. The buffer input is linked to the non-inverting input, which has a high impedance. Low impedance and connection to the buffering output characterize the inverting input. The low impedance inverting input allows current to enter and exit. A built-in amplifier detects current flow and generates an output voltage proportionate to the current. Positive output voltage results from current leaving the inverting input. A negative output voltage results from current flowing into the inverting input.

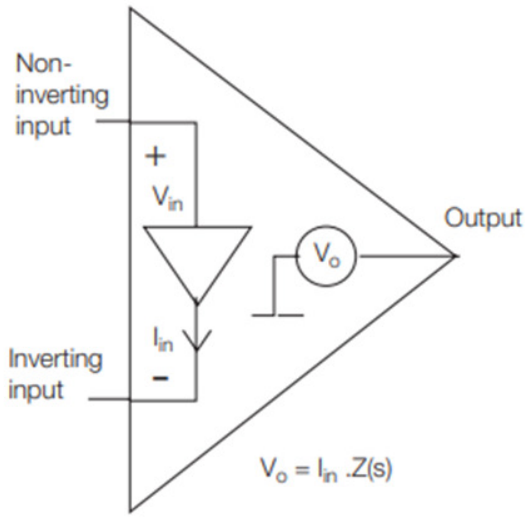

Figure 5: Illustrates the Simple current feedback op-amp model.

AC performance

By looking more closely at the amplifier, the bandwidth relationship of a current feedback op-amp may be explained. The small-signal model is seen in Figure 6. The output of the input buffer is linked to a current mirror. A same amount of current flows out of the equivalent circuit when current from the buffer exits the inverting input. The current mirror transforms the current flow into a proportionate voltage by applying a resistive load (Rm) across it. To guarantee the stability of the op-amp, a tiny frequency compensating capacitor (Cc) is attached across Rm.

A second buffer is used to output the voltage across Rm. The frequency response of this model may now be determined using the node equations. As a result of the input buffer's requirement that the inverting input match the voltage of the non-inverting input, V1 Vin,

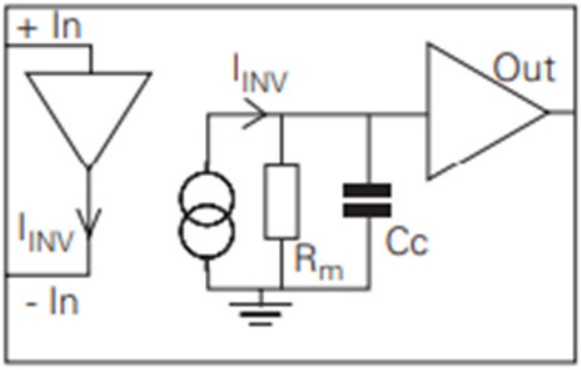

Figure 6: The small signal current feedback op-amp model.

The voltage across R_m is $V_2 = \frac{IR_m}{1 + j\omega C_C R_m}$

And $I = V_1\left(\frac{1}{R_1} + \frac{1}{R_2}\right) - \frac{V_{out}}{R_2}$

And since V_{out} is a buffered version of V_2, $V_{out} = V_2$.

Now these can be combined to find V_{out}.

$$V_{out} = \frac{\left[V_{in}\left(\frac{1}{R_1} + \frac{1}{R_2}\right) - \frac{V_{out}}{R_2}\right]R_m}{1 + j\omega C_C R_m}$$

If $R_m >> R_2$, this can be simplified to:

$$\frac{V_{out}}{V_{in}} = \frac{1 + \frac{R_2}{R_1}}{1 + j\omega C_C R_2}$$

The closed-loop gain is $1 + R_2/R_1$, therefore:

$$\frac{V_{out}}{V_{in}} = \frac{A_{VCL}}{1 + j\omega C_C R_2}$$

The closed-loop gain is $1 + R_2/R_1$, therefore:

$$\frac{V_{out}}{V_{in}} = \frac{A_{VCL}}{1 + j\omega C_C R_2}$$

When $1 = 2\pi f C_C R_2$, the closed-loop gain falls by 3 dB, thus:

$$f_{(-3dB)} = \frac{1}{2\pi C_C R_2}$$

R2 and the internal correction capacitor, thus, affect the bandwidth. The closed-loop gain is not reliant on R1 and, hence, is not reliant on the bandwidth. When we take the gain into account in terms of the complex impedance Z(s), we discover:

$$\frac{V_O}{V_{IN}} = \left(1 + \frac{R_2}{R_1}\right) \frac{1}{1 + \frac{1}{LG}}$$

In this case loop gain (LG) is given by $LG = \frac{Z(s)}{R_2}$

How about the circuit design presumptions that were stated in Chapter 1 for perfect opamps? In a circuit for a non-inverting amplifier, Figure 7 depicts a straightforward current feedback op-amp model employing the complex transimpedance Z(s).

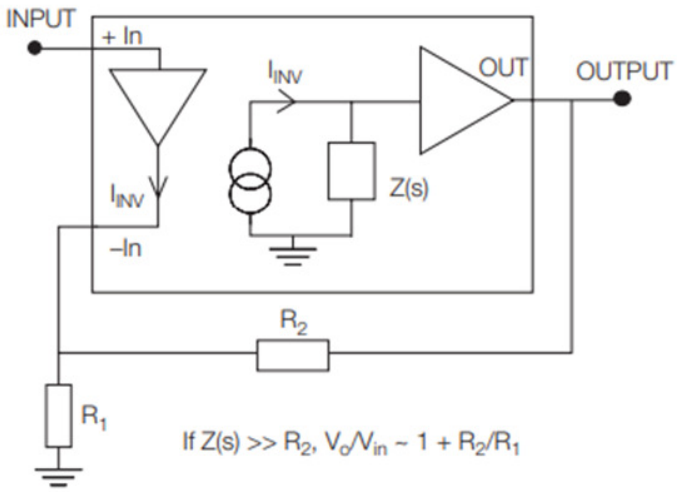

Figure 7: Non-inverting amplifier with ideal current feedback op-amp.

Think about what transpires when the input voltage VIN is increased over 0 V first. By increasing the voltage at the inverting input, the input buffer reacts to the rising input voltage. Then a current exits the inverting input. The transimpedance stage detects the current flow, and the output voltage increases. When a balance is attained, which occurs when the current fed back through R 2 equals the current flowing through R 1, the output voltage stops increasing. Hence, the current from either the inverting input is replaced by feedback current. The gain of a transimpedance stage determines how little the current from either the input buffer may be under steady state circumstances. It is safe to assume that the current from the

inverting input will be near to zero if the transimpedance stage has a high gain (high Z(s)). As the input buffer's voltage gain is almost equal to unity, the difference in voltage between inputs that are inverting and those that are not may be taken to be nearly zero. Hence, gain may be calculated using the ideal model, in this example AVCL 1 R 2 /R 1. The non-ideal output resistance (R o) of the input buffer will often range from 20 to 40 in reality, as illustrated in Figure 8. Due to the erroneous current flowing, the two input voltages will not be precisely equal, hence the added resistance will change the response. There will be a little voltage drop across R o. Due to the added resistance in the feedback line, the loop gain will actually be slightly influenced by the circuit's closed-loop gain. R2 is dominant at low gains, but as gains increase, the internal resistance becomes more significant, which lowers loop gain and narrows the closed-loop bandwidth. A non-ideal, non-inverting current feedback amplifier's transfer function is given by,

$$\frac{V_O}{V_{IN}} = \left(1 + \frac{R_2}{R_1}\right) \frac{1}{1 + \frac{1}{LG}}$$

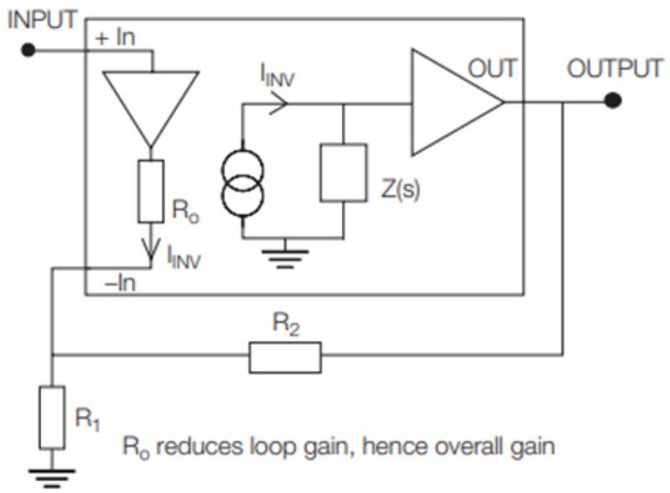

Figure 8: Non-inverting amplifier with non-ideal current feedback op-amp.

Loop gain (LG) is modified by the introduction of Ro, and becomes:

$$LG = \frac{Z(s)}{R_2 + R_o\left(1 + \frac{R_2}{R_1}\right)}$$

The gain error due to R_o is $\dfrac{R_o\left(1 + \dfrac{R_2}{R_1}\right)}{Z(s)}$

CONCLUSION

One of the two main methods for suppressing the low-frequency noise is chopping stabilization. Whenever the system is linear and low baseband noise is the primary objective, chopping stabilization is recommended over the other approach, auto zeroing. The reader

may process all that has transpired in a section by taking a chapter break. Consider chapters as brief apex points in your narrative. The reader becomes a step closer to the story's resolution with each accomplishment, which may be both inspiring and fulfilling.

REFERENCES

[1] H. Ko, H. Kim, B. Lee, J. Kim, D. il Cho, and K. Han, "Low-noise Analog Front-end with Chopper-stabilized Multipath Current-feedback Instrumentation Amplifier for Resistive Sensors," *Sensors Mater.*, 2019, doi: 10.18494/SAM.2019.2330.

[2] B. Lee *et al.*, "Low-noise 16-bit First-order Delta-sigma Capacitance-to-digital Converter for Capacitive Humidity Sensor," *Sensors Mater.*, 2019, doi: 10.18494/SAM.2019.2272.

[3] R. Chebli, M. Ali, and M. Sawan, "High-CMRR low-noise fully integrated front-end for EEG acquisition systems," *Electron.*, 2019, doi: 10.3390/electronics8101157.

[4] S. M. Lim and J. S. Park, "A Low Noise Offset Cancellation Method for Improving Sensitivity of CMOS Hall Sensor," *J. Electr. Eng. Technol.*, 2019, doi: 10.1007/s42835-018-00031-7.

[5] Y. C. Chen, S. Y. Lu, and Y. Te Liao, "A Microwatt Dual Mode Electrochemical Sensing Current Readout with Current Reducer Ramp Waveform Generation," *IEEE Trans. Biomed. Circuits Syst.*, 2019, doi: 10.1109/TBCAS.2019.2936373.

[6] Y. C. Chen, S. Y. Lu, J. H. Tsai, and Y. Te Liao, "A power-efficient, bi-directional readout interface circuit for cyclic-voltammetry electrochemical sensors," 2019. doi: 10.1109/VLSI-DAT.2019.8741529.

[7] M. Mikawa, S. Kawazoe, R. Fukuoka, and N. Nakano, "A delta-sigma modulator with frequency division multiplexing for multi-channel EEG acquisition front-end," 2019. doi: 10.1109/ICECS46596.2019.8965052.

[8] S. Zhang, S. Liu, C. Yuan, and N. Duan, "Design of the CMOS switching hall sensor circuit," 2019. doi: 10.1109/SNSP.2018.00072.

[9] S. Pokamisas, D. Baxevanakis, and P. P. Sotiriadis, "A 0.6V, 700nW Chopper Capacitively-Coupled Instrumentation Amplifier for Biomedical Applications," 2019. doi: 10.1109/MOCAST.2019.8741847.

[10] J. Lee, S. Song, and J. Roh, "A 103 dB DR fourth-order delta-sigma modulator for sensor applications," *Electron.*, 2019, doi: 10.3390/electronics8101093.

CHAPTER 7

OVERVIEW ON INSTRUMENTATION AMPLIFIER

Mr. Vivek Jain, Associate Professor,
Department of Electrical Engineering, Jaipur National University, Jaipur India
Email Id- vivekkumar@jnujaipur.ac.in

Abstract:

When there is significant noise present, an instrumentation amplifier (IA) is utilized to give a lot of gain for extremely low-level signals. High gain, a strong common-mode rejection ratio (CMRR), and extremely high input impedance are IAs' main characteristics.

Keywords:

Amplifier, Common Mode, Op-Amp, Offset, Wheatstone Bridge.

INTRODUCTION

The difference in voltage between the differential amplifier's inverting and non-inverting outputs is amplified. An operational amplifier appears to be a voltage subtract or that produces an output voltage which is proportional to the voltage difference between the two input incoming signal whenever two input signals are provided to the inputs of such an inverting and non-inverting terminal. They have thus far connected to the op amp utilizing only one of its inputs, perhaps the "inverting" or possibly the "non-inverting" terminal, amplified always one input signal, and grounded another input. However, because a normal operational amplifiers has two inputs—one for inverted signals and another for non-inverting warning signals may connect impulses to both of these channels at the exact same time to produce the differential amplifier, a more widely used kind of op amp. They learned in the first session on operational amplifiers that, essentially, all op amps were "Differential Amplifiers" because of the way that their inputs are configured. Although when one voltage signal is coupled between one inverting input and then a second voltage signal toward the opposite input terminal, overall power output would be proportionate towards the "Difference" between the two input voltages at V1 and V2. In contrast to a summing amplifier, typically adds or sums numerous input voltages, differential amplifiers turn this kind of operational amplifier circuits into a sub-tractor. This particular type of operational amplifier circuit, often known as both a differential amplifier arrangement, is shown in Figure 1:

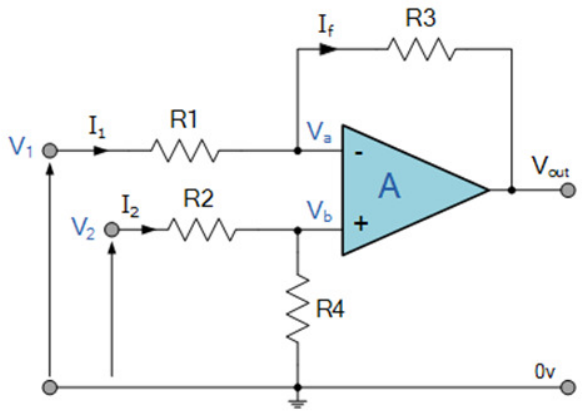

Figure 1: Illustrates the circuit diagram of a Differential Amplifier configuration.

Differential Amplifier Equation

$$V_{out} = \frac{R_3}{R_1}(V_2 - V_1)$$

When all of the resistances have the same ohmic frequency, or when R1 = R2 = R3 = R4, the circuit becomes a Unity Gain Differential Amplifier with a voltage gain of exactly one or unity. Therefore, the output formula would indeed be simple: Vout = V2 - V1. Be aware that if input V1 is larger than inputs V2, and vice versa, output voltage may total negative if input V2 is higher than input V1. By adding more parallel resistors, this Differential Amplifier circuits, an incredibly valuable op-amp circuit, may be set up to "Add" or "Deducts" the voltage supplied to each of its unique inputs. R1 and R3 are input resistor. One of the most common ways to achieve this is by connecting a "Resistive Bridges," also known as both a Wheatstone bridge, to the amplifier's inputs.

Wheatstone bridge Differential Amplifier

The typical differential amplifier circuit unexpectedly performs as a differential comparator circuit by "Trying to compare" one voltage level to another. The amplifier circuit can be employed to detect low or high temperatures or light levels, for example, by attempting to connect a further input to a reconditioned voltage reference installed only on one leg of both the resistive Wheatstone bridge circuit as well as the second to either an "Thermistor even though output voltage has changed into a linear transformation of the changes made to the active leg of something similar to the resistive overpass.

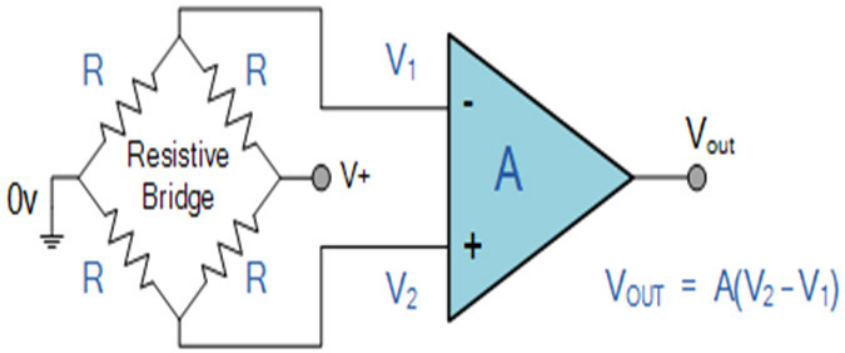

Figure 2: Illustrates the circuit diagram of a Wheatstone bridge Differential Amplifier.

Instrumentation Amplifier

Instrumentation amplifiers, sometimes referred to as in-amps, are differential amplifiers with either a single ended output or a very high gain. In motor coordination networks, instrumentation amplifiers are mainly used to amplify very small differential signals coming from strain gauges, thermocouples, and other current sensing devices. Contrary to conventional differential amplifier, which have their closed-loop gain determined by either an external series resistance feedback that can be connected between their own inverter output one and feedback station, whether in negative or positive, "instrumentation amplifiers" have always included an internal feedback load impedance that would be effectively separated from their inverting input also because input signal that is applied and across all two input variables, V1 and V2. The op-amp common mode rejection ratio (CMRR; negative emission when V1 = V2) is also quite strong, topping 100dB at DC. An example of an actual three-op-amp instrumentation amplifiers with just a high input impedance Zin.

$$V_{out} = V_2 - V_1[1 + \frac{2R_2}{R_1}](\frac{R_4}{R_3})$$

It is appropriate to refer to a class of genuine differential- input amplifiers with strong common mode rejection (CMR) and accuracy as "instrumentation amplifiers." Although using op amps as fundamental architectural "building blocks" in both instrumentation amplifiers and difference amplifiers, both amplifier types vary significantly from their op amp relatives. Op amps are "single-ended," and their feedback determines their functions. They are often designed to perform in a range of applications. Differential gain and common mode rejection are the main uses of instrumentation amplifiers and difference amplifiers. It is not meant to use feedback from output to input. There has been some widespread abuse of this phrase, which has made it unclear what an instrumentation amplifier really is (IA). One well-known manufacturer referred to their brand-new precision operational amplifier during the early days of monolithic operational amplifiers as an instrumentation amplifier. They really intended to state that the op amp was "instrumentation-grade." Instrumentation amplifiers have also been referred to as huge laboratory bench-top amplifiers and even traveling-wave tube (microwave) amplifiers. So, it is not surprising that there is so much misunderstanding over what an IA is and accomplishes. The three most popular IA types are the "Classical Three Op Amp Instrumentation Amplifier," the "Simple Difference Amplifier," and the "Two Op Amp Instrumentation Amplifier." These three designs are similar, as we will see, yet they function differently in several crucial ways. Let's consider the IA as a "black box" differential amplifier for the time being.

LITERATURE REVIEW

According to O. Ibrahim et al.[1]due to its quick reaction time, excellent accuracy, and cheap cost, thermometers are often employed to monitor temperature. Yet in order to construct a signal conditioning circuit for precise temperature monitoring, linearization is required because of the nonlinear resistance-temperature connection. The design of a Wheatstone bridge-based thermistor signal conditioning circuit is therefore presented in this work. The resistance response to temperature changes between 25 °C and 65 °C was measured in an experiment using an NTC thermistor and utilized for the model's linearization. The Wheatstone bridge signal conditioning circuit is designed using the linearized model's acquired parameters. Within the designated temperature range, the performance assessment of the developed measuring system showed a high degree of precision with just 1.1% non-linearity.

H. Jiang [2] et al. stated micro-electro-mechanical system (MEMS) technology was used in the design and fabrication of the PdNi film hydrogen sensors using Wheatstone bridge structure. PdNi alloy film resistors made up the four integrated sensors. Although the others were utilized for hydrogen sensing, the inside two were protected with silicon nitride sheet and served as reference resistors. The SiN and PdNi alloy films were created via magnetron sputtering. X-ray diffraction was used to study the PdNi films' morphology and microstructure (XRD). The output signal was transformed from resistance to voltage for effective data gathering. PdNi film hydrogen sensors with a Wheatstone bridge structure's hydrogen (H 2) detecting characteristics were examined at various temperatures (from 30°C to 70°C) and H 2 concentrations (from 10 ppm to 0.4%). In cycle testing with hydrogen concentrations as low as 0.4%, the hydrogen sensor showed unique response at various hydrogen concentrations and strong repeatability. The PdNi film hydrogen sensor has a visible and collected output voltage of 600 V toward 10 ppm hydrogen.

In study S. Gao [3] et al. for a 2-D wind sensor, a self-heated double Wheatstone bridge arrangement is given. Eight thermistors were symmetrically positioned in two orthogonal directions without a central heating source, and quartet of them in each direction form a Wheatstone bridge. The eight thermistors function as temperature sensors and heating sources at the same time. The terminal voltage from across bridge and also the bridge output voltage are used to determine the wind speed and direction, respectively, by applying the constant existing stock to the bridge. The 2-D wind sensor was mathematically generated and then physically constructed on the ceramic substrate. Studies show that after calibration, the measured speed ranges from 0 to 40 m/s with an error less than 2 m/s and the measured direction ranges from 0 to 360° with an error less than 3°. The measurement and control circuitry for the 2-D wind sensor are significantly streamlined by the twin bridge arrangement.

Y. J. Li [4] et al. discussed the single cell biomechanical characteristics have significant promise for early disease detection and efficient therapy. In this work, a microfluidic device for measuring a single cell's mechanical characteristics was created. A microfluidic device that resembles a traditional Wheatstone bridge circuit with micropipette aspiration built into it. We can efficiently change the flow direction for single-cell entrapment using this method, and we can also accurately adjust the pressure applied to the aspirated cells, which is similar to the ability of the Wheatstone bridge to perfectly control bridge voltage and current. We can efficiently capture Hela cells and micro-particles using the microfluidic device and the micropipette aspiration method, and we can also assess the deformability of cells. It was

determined that Hela cells had a Young's modulus of 387 77 Pa, which is similar to previous micropipette aspiration experiments. Our technology has high promise for biomechanical trials in clinical diagnostics and cell biology research because to its simplicity, accuracy, and usability.

Y. T. Ku [5] et al. presented a novel fully differential operational Trans resistance amplifier (FDOTRA)-based current-mode Wheatstone bridge (CMWB). With its benefits of low input and output impedances, input voltage calibration, high transimpedance (R m), a broad input range, and low input and output impedances, this suggested FDOTRA is an active component of the proposed CMWB. The performance of the proposed CMWB is unaffected by the usage of only one active component, the FDOTRA, and four resistors. The suggested CMWB features a straightforward design, excellent accuracy, a broad operating range, a compact volume, and cheap cost. Thus, the suggested CMWB has two distinct benefits. First of all, it lessens the quantity of passive and active sensing components. Second, compared to previous CMWB integrated circuits, the proposed CMWB circuit delivers a significant accuracy enhancement (IC). It has been evaluated, simulated, and implemented to use the suggested CMWB. The proposed FDOTRA was created using 2P4M CMOS technologies at TSMC's 0.35 mm pitch. 1.65 V is what its supply voltages are. The proposed FDOTRA has an open-loop gain of 69.2 dB and a 3-dB bandwidth of 16 MHz, respectively. The FDOTRA based CMWB has an open-loop gain of 24.6 dB and a 3-dB bandwidth of 16 MHz, respectively. The experimental findings indicate that the FDOTRA-based CMWB's accuracy is 92.4%.

F. Albouchi[6] et al. the electrical properties of liquids is measured using an electro-thermal technique in this study. This method is based on a Wheatstone bridge made up of eight heat-sensing resistors. The approach has been validated by measurements made on several liquids with a variety of thermal characteristics. Less than 3.8% was calculated to constitute the entire standard uncertainty of both the experimental findings. The measured values of the thermal characteristics and the values that have previously been published in the literature show good agreement. Moreover, this procedure takes less time to complete measurements than the conventional methods. Even when using external electric or magnetic fields, this method may be useful for the thermal characterization of complicated fluids.

F. Franco et al. [7]industrial demands are always pushing sensor boundaries to achieve greater signal-to-noise ratios in challenging conditions without increasing manufacturing costs via extra electronics. With the out-of-phase sensing components being replaced by passive elements, non-full resistive Wheatstone bridge designs emerge as a more portable and affordable alternative to full-bridge measurement systems, while having poorer output, linearity, and thermal drift immunity. Modern magneto resistive (MR) sensors combined with thermally compatible materials utilized as adjustable thin-film resistors at the wafer level, however, may result in competitive prototypes for applications with strict requirements. Thus, Cr, Ti, and TiW thin films were assessed for their resistivity and temperature coefficient of resistance (TCR) as prospective candidates for a thermally and electrically stable non-full MR bridge. A sin/cos magnetic encoder had been prototyped in a non-full-bridge architecture with a thermal mitigate drift of 51.48 0.25 nV/Vcc/°C and an offset voltage of 16 mV/Vcc, within such a TCR around 1059 12 ppm/°C for a spin-valve sensor lying between both the observed results for a Ti thickness range of 300 up to 500 (571.9 8.3 and 13

L. Safari [8] et al. emphasis of the current chapter's discussion on Wheatstone Bridges is the Current-Mode Wheatstone Bridge and the circuits that it is connected to for signal conditioning. Each circuit's functioning, benefits, and downsides are thoroughly explored. The idea of the standard Voltage-Mode Wheatstone Bridge is briefly explained at the beginning of this chapter to make it easier to compare it to the Current-Mode Wheatstone

Bridge. Read-out circuits and Mixed-Mode Wheatstone Bridge theories are also covered.

E. Alnasser[9] that work introduces a unique loss-less capacitive sensor estimating circuit with a completely analog signal conditioning architecture. The Wheatstone bridge is used in a unique way in the proposed circuit to build a novel null instrument. All of the components of the employed bridge, with the exception of the capacitive sensor, are standard resistors, in contrast to the usual ac Wheatstone bridge. The utilized bridge is thus inherently imbalanced. A completely analog feedback network has been developed to balance the bridge. The proposed circuit's key benefit over earlier null instruments is that the feedback loop is now implemented without the need for programmable components like voltage-controlled resistors. In the suggested circuit, the feedback network, which is made up just of an operational amplifier and a resistor, is used to balance the bridge in a straightforward and suitable manner. The suggested circuit has only been implemented using differential amplifiers and Op-Amp-based amplifiers. The design is so simple that it may be composed of discrete, low-cost pieces. The phase difference between the output and input voltages in the recommended signal conditioning circuit relies on the capacitive sensor value and is triggered by a sine voltage source. Measurement of the aforementioned phase difference may be used to estimate the capacitive sensor.

According to the L. K. Quynh [10] et al. increasing the form anisotropy of the film may significantly increase the magnetic field sensitivity of such an anisotropic magnetoresistance (AMR) sensor employing a single-layer Ni80Fe20 thin film. In this study, a practical method for increasing the sensitivity of an AMR Wheatstone bridge sensor and decreasing the magnetic coercive field as well as the contribution of thermal noise is suggested. This method involves combining numerous resistors in series-parallel combination circuits. Four different AMR sensor designs were created using Ta (10 nm)/Ni80Fe20 (5 nm)/Ta (10 nm) films started growing on thermally hydroxylated Si substrates in the presence and absence of a biasing magnetic field. These designs included a single resistor, three, five, and six resistors in series, as well as six resistors in series-parallel connection (900 Oe). The findings shown that the magnetic sensitivity (SH) of the sensors are based on series-parallel combination is 1.72 times greater than that of the sensors are based on series connection. With an estimated detection limit of magnetic moments of 0.56 emu, this enhanced sensor has increased capability of detecting varied concentrations of magnetic nanoparticles.

DISCUSSION

Sensor of the Wheatstone bridge

Let's take a closer look at the Wheatstone Bridge, one of the most widely used transducers in use today, to get a better understanding of the instrumentation amplifier and why its excellent common-mode rejection is so crucial. Figure 2a shows the bridge circuit in its typical form, but Figure 2b may be used to illustrate that the bridge is really just two voltage dividers that are driven by a single voltage (Vex) or current (I(ex) excitation source.One of the first instances of "radiometric" measuring was the Wheatstone bridge. Paradoxically, common mode voltage on the bridge did not cause any problems for early scientists. The galvanometer, which was simply attached to either side of the Wheatstone bridge, was the only sensitive measurement device they had at their disposal. Thankfully, this also allowed for a floating measurement of the output voltage of the bridge differential. The voltage divider potential covered the whole galvanometer. In comparison to bridge measurements made using the outdated galvanometer method, modern ground-referenced amplifiers have significantly improved sensitivity; however, since they are not "floating" like the outdated galvanometers, they have also introduced a common mode voltage (CMV) limitation to the

measurement. Linear operation is only feasible within the indicated operating limits for ground-referenced IAs but also difference amplifiers, and irreversible damage may result from operating beyond the "Absolute Maximum" device ratings. The resistance of one or even more resistors (bridge arms) will vary in response to a stimulus provided to the sensor. As it optimizes the sensitivity and linearity of the bridge sensor, "four active arm" designs are currently used in the majority of sensor designs. Early sensor designs only had one or two active arms, but current systems do not usually use them. When force is applied to the bridge with four active arms, R1 and R4 both grow while R2 and R3 drop. By doing this, the voltage on one side of the bridge rises while falling by the same amount on the other side. Let's look at an example where a little stimulus causes the sensor to become imbalanced, resulting in R1= R4= 4.999K and R2= R3= 5.001K. The current in either side will continue to be 1mA since the combined resistance on each side of the bridge (R1+R2 on one side and R3+R4 on the other) stays constant at 10K. Using the previous equations (3) and (4): Real-world instrumentation amplifiers are not perfect devices, thus it is important to take into account the error contributions of their imperfect parameters.

Poor common mode rejection in an amplifier may result in significant measurement mistakes. The applied CMV shifts the amplifier's input offset voltage V(os), which results in these CMR inaccuracies. The definition of common mode rejection is: A 500uV inaccuracy on a 2mV signal is obviously unacceptable, and our amplifier requires a far higher CMR. The input offset shift caused by CMV will be reduced by an amplifier with a 100 dB CMR standard to 50 uV, which may be a more tolerable inaccuracy of 2.5%. Another 20 dB of CMR from the amplifier will be needed to reduce this mistake by another ten years. The high degree of accuracy required by this kind of application is optimal for instrumentation amplifiers. Nevertheless, not every instrumentation amplifier is capable of delivering performance at this level. Only the finest equipment are capable of meeting the demanding CMR standards of 120 dB.

At the high strength needed by the little output signal from our sensor, a high-performance device like the Burr-Brown INA128 is claimed to have 120 dB minimum and 130 dB mean Common Mode Rejection. The overall measurement error of the amplifier will also be affected by other error factors, such as input offset voltage but also drift, power supply rejection (PSR), and input bias current. Naturally, we want to reduce these measurement mistakes, therefore we must choose an amplifier with sufficient performance requirements across the board. A shift in the amplifier's input offset voltage V(os) owing to a change in supply voltage results in power supply rejection problems. Rejection of a power supply is defined as: Let's say that we have a +/-15V amplifier that is being run on +/-12V supplies and has a power supply rejection standard of 80 dB in order to demonstrate amplifier power supply rejection and its contribution to measurement error. Equation (9 may be rearranged to determine the PSR error as follows:

Once again, we discover that a 300uV inaccuracy on a 2mV signal is intolerable and that our amplifier requires a much higher PSR. The input offset shift resulting from CMV will be reduced to 30uV by an amplifier with a 100 dB CMR standard. A simple to determine error source is input offset voltage: Vos is an input-referred standard, similar to CMR and PSR, therefore the IA offset voltage at the instrumentation amplifier's input may simply be added towards the differential signal voltage. The change in Value with every degree Celsius increase in ambient temperature is known as input offset voltage drift. The same procedures are used to handle input offset voltage error and drift error. The gain of the amplifier multiplies both the signal and all input-related mistakes (such as Vos, drift, CMR, and PSR), yet at the amplifier's output, the signal-to-errors ratio stays constant. Instead of the more

straightforward and well-known single value specifications seen in op amp and diff amp data sheets, instrumentation amplifiers may feature input-referred specifications that comprise gain dependant equations. As we shall see in a moment, there is a valid explanation for this. The extra offset voltage created by input bias current (Ib) passing through the amplifier's source resistance must be added to the input errors. Bipolar transistor input IAs may have severe offset issues as a result of high impedance signal sources. Low bias current FET input amplifiers are advised in these applications to reduce Ib errors with very high source resistances.

The operational temperature range, power supply control, common-mode voltage, source resistance, but also gain of the amplifier are taken into account while conducting an error analysis. Use the min/max specifications from the amplifier's data sheet to do a worst-case (although pessimistic) analysis. As all parameters are unlikely to exceed their spec limit simultaneously, an analysis of more probable "real world" mistakes is done using the data sheet's "typical" specifications. As most characterization measurements are made whenever the product is first introduced to production, any process improvements incorporated during routine manufacturing might well have skewed the statistical distribution from either the original tests. However, how reliable the "typical" specs are depends, in part, on the vendor's integrity. You should be aware that employing "typical" specs carries some risk; typicals are still not guaranteed since no semiconductor manufacture can ensure that the statistical distribution from his yields will stay constant over time. Only the min/max characteristics on the data sheet are guaranteed.

Avoiding Instrumentation Amplifier Pitfalls

Input Bias Current Effects

The source impedance N C H should not be disregarded as the influence of the amplifier input is represented by the current at its input. When choosing an MP lifer, this is one of the most crucial factors to look for, and if a big mistake is made, the impact will be felt on the CH between IA and its source. It will produce significant mistakes in c circuits.

Investigate the following "terrible example" of a poor source-to-IA mismatch:

Our inexperienced designer is attempting to create a low noise accelerometer preamplifier when they come across the INA103 Low Noise, Low Distortion Instrumentation Amplifier while browsing a catalog. He thinks to himself, "Excellent, it has less than 1nV per Hz noise, it’s very low distortion also indicates it has superb linearity, and it has outstanding CMR. There isn't a better amplifier I could ask for! He has just fallen victim to a very typical trap—the INA103, a self-generating piezoelectric accelerometer, is an utterly inappropriate option. To maintain the accelerometer's low-end frequency response, a very high load impedance is needed at the output, and this impedance is the root of many grave issues. As was previously mentioned, the accelerometer output needs a very high load impedance in order to maintain its low-end frequency response. This is due to a piezoelectric transducer's capacitive nature, which may be described as an AC current source coupled with a capacitor. The transducer capacitance and its load resistor RC time constant must be as big as feasible in order to extend the transducer & amplifier low frequency response. In order to achieve his low frequency response criterion, the accelerometer employed in this case needed a 1 megohm load resistor. An INA103 is designed to have an input bias current of 2.5 a average and 8 A maximum. The issue is with the 1 megohm load resistor.

The 1 megaohm load resistor must be connected in series with an RL network1, which has a negligibly low resistance of maybe 10 ohms, to draw the inverting input (-) bias current (V

OS-). It is a 2.5 voice input offset! (The offset caused by the 10 ohm resistance in the other input is negligibly tiny.) The amplifiers are forced into the rail as a consequence of this enormous offset being amplified by the INA103's gain of 100. This circuit will obviously not function at all. Therefore, in an effort to eliminate the bias current offsets, our inexperienced designer would try to balance the impedances seen by each IA input. "Good effort, but no cigar," we remark. We first notice that the input bias current of the (+) input is not equal to the input bias current of the (-) input when we examine the offset produced by adding a 1 megohm resistor from the non-inverting (+) input to ground. Right now, one input has a 2.5V offset, while the other has a 2.53V offset. Just the voltage differential (V) may be amplified thanks to the common mode rejection of the instrumentation amplifier. Hence, as opposed to his initial attempt, he is amplifying a considerably smaller input signal: Now, when we multiply by a gain of 100, the result is an output voltage of "just " 3V, which is still undesirable but is an improvement over the previous instance.

We can point out a math shortcut before continuing to explain why even hero actions like supplying 3VDC to the IA reference pin in an effort to zero this 3V output offset won't make this amplifier/transducer operate. We may simply reference the data sheet and utilize Input Offset Current rather than each individual input's Bias Current, even if the study of the impact of balancing input impedances to minimize offset voltage was determined for each input individually. Naturally, for this shortcut to work, the offset voltage at each input must not be higher than the amplifier's common mode voltage range. Despite the fact that we have demonstrated that this circuit has a significant DC offset, it may be tempting to counter that since the output of a piezoelectric transducer rolls off at low frequencies and has no DC response, the circuit is still valid if the amplifier's output is simply AC coupled to the stage after it with a capacitor. The reason why this "low noise" amplifier is not appropriate for high source impedances may be determined by computing the input noise voltage that results from the amplifier's high input bias current. While the amplifier's current noise density (in) of 2pA/Hz will produce substantial noise voltage (ein) across its source resistance as the source impedance increases, the INA103's input voltage noise density (e n) of 1nV/Hz will prevail with extremely low impedance sources. This is 2V/Hz, which is far more than the 1nV/Hz that our naive designer had anticipated. As we must also include the amplifier's input voltage noise spectral density in the equation, the overall amplifier noise will actually be a little bit greater than 2 V/Hz. In this situation, there won't be much of an increase in noise when the voltage noise component is added to the current noise contribution.

The resulting noise is still just a little bit more than 2 V/ Hz since the voltage noise density caused by the amplifier's current noise density (in this case) is so much more than the amplifier's input voltage noise density. The amplifier's overall noise will increase if the balanced input resistance arrangement is used! In this instance, each input has 2 V/Hz of uncorrelated noise. The input noise cannot be totally rejected by common mode rejection. When multiplied by 2, the two input noise voltages will sum arithmetically rather than vectorially. Similar to uncorrelated input noise, differential amplifier inputs cannot be used to remove it; rather, they simply add two identical noise voltages. These same uncorrelated input noise voltages are being added in this situation by the amplifier's CMR. Hence, the balanced impedance amplifier's total input noise is 4 VHz. The total equivalent input noise (eEQ) is caused by noise at the inverting input (eT-) as well as the non-inverting input (eT+). The output voltage noise density will therefore reach 400 V/Hz after this is amplified by the amplifier's gain of 100 V/V.

The RMS noise (E n) observed at the output is then calculated by multiplying the IA output noise voltage density by both the square root of the amplifier's bandwidth. The INA103 is a

wideband amplifier with a gain of 100V/V and a bandwidth of 800 kHz at -3dB. The noise measured at the INA103 output is 562mV rms, and because the amplifier's equivalent noise bandwidth is a factor of 1.57 times its -3dB bandwidth (presuming a single-pole response), we must multiply one more to reach our final result. Even worse, there will be a roughly six-fold increase in peak to peak noise! It is now clear that the INA103 performs badly when used improperly on a transducer with a very high source impedance, while being a superb option for low source impedances. For this application, a FET input instrumentation amplifier would be a much superior option. These calculations should be convincing when performed with an INA111 or INA121.

Simple advice: When choosing an amplifier, take your source impedance into account. Low source impedances need very low input noise (En) amplifiers, while high source impedances demand JFET or CMOS amplifiers.The reference pin of such a difference amplifier as well as the reference pin of a two op amp IA provide designers a lot of options, regardless of whether the difference amplifier is a standalone unit or the third op amp in a three op amp IA. This pin is most often used to provide output voltage offsets. The reference pin, in contrast to "trim" pins, enables the generation of extremely high offsets (up to several volts) without impairing the amplifier's input voltage drift. In order to prevent the CMR of the amplifier from being harmed, this pin must be driven with a "zero ohm" source resistance. In the study, it was determined that the internal network's extremely tight resistor matching was necessary for common mode rejection. A resistance mismatch and decreased CMR will result from added resistance between the reference pin and ground. R R RS only if RS 0, after all.

Whatever is connected to the reference pin must have a source resistance that is as near to zero as feasible. This requirement is sometimes disregarded when attempting to produce an offset voltage, as in the unsuccessful effort seen in Figure 14. This is a visual representation of "How Not to Do It." A 1k pot is utilized in this circuit to provide an offset voltage at the INA122 reference pin. The reference pin's strong resistance to ground severely hinders the IA's ability to conduct CMR. CMR is weakened even when the offset adjust pot wiper arm is rotated in the direction of the end that is grounded. But keep in mind that the potentiometer's end resistance is not zero—it might really be rather high. "1 ohm or 2%, whichever is greater" is a standard specification for potentiometer end resistance. Hence, the 1K pot's terminal resistance may reach 20 ohms, which would be high enough to noticeably lower amplifier CMR.

The values of the internal resistor network of the amplifier must be known in order to calculate the amount of CMR lost by the addition of resistance between both the reference pin and ground. After that, an analysis may be done and a precise response can be developed. It is more necessary to just remember that resistor mismatch is caused by additional resistance at the reference pin, which is seldom worth the work needed. Resistor mismatch is essential for amplifier CMR. Placing an op amp buffer between the pot and the reference pin is a much better way to create an offset. The output impedance of the op amp is reduced too much below one ohm using negative feedback. The amplifier's CMR won't be negatively impacted by this modest quantity of resistance connected in series with the internal resistor network of the IA.

Due to the extraordinarily high input resistance (1013 ohms) of the op amp's non-inverting input, the resistors' value may (optionally) be raised to reduce supply current. A further advantage is that by including a capacitor in the pot wiper output, an RC low-pass filter may be created. This will provide a low noise reference voltage and increase power supply noise rejection. The circuit shown in Figure 15 has the ability to produce significant offsets. The Offset Adjust pot may be adjusted to 100 if only a few millivolts of offset are needed, such as

when trimming the influence of the IA input offset voltage to zero.

The 40.2K resistor in Figure 15 may be attached to the output of a + 10V voltage reference (such a REF102) rather than being connected to either supply if a big offset voltage with very high stability is desired. The op amp may flip a +10V reference to produce a negative voltage reference. The 40.2k resistor might alternatively be replaced with a current source (REF200). Due to its adaptability, the REF200 current source may be connected to either supply or produce either a positive or negative voltage here on pot wiper arm.

Floating Inputs are a Frequent Error

This circuit detects a modulated LED light beam using two silicon PIN photodiodes. The detectors are reverse biased to provide the fastest reaction time and linearity. The outputs of the two detectors are compared, and the difference is amplified by an instrumentation amplifier. Capacitors block the DC bias voltage of the detectors while AC coupling the signals to the IA inputs. The circuit lacks a bias current return route, which causes the IA bias current to produce a significant offset and push its output to the rail. Think about Ohm's Law: The input offset Vos is determined by multiplying the input bias current (1nA) by the input resistance (1010 ohms), which is parallel to the insulation resistance of the 0.47-F capacitor (about 30,000 megohms microfarads for a metallized polypropylene film capacitor). Thankfully, it's simple to repair this circuit. This circuit would function properly if the two AC coupling capacitors were simply removed and a jumper was used in their stead. The photodiode DC bias voltage will now be shown on each input, but there is no need to panic since the little less than -5V bias at each input is well within the permitted common mode voltage (CMV) range for the INA118 when it is running on 15V supply. For further information, go to the CMV calculation section.

Due to its high CMR, the IA is able to reject both ambient light that is shared by both detectors and the diode DC bias voltage. A second strategy would be to connect each IA input to ground with a 10 megohm (or greater) resistor. As a result, the circuit will still entirely reject detector bias voltage and steady-state ambient light. This maintains the coupling capacitors' DC blocking function. The CMR of the instrumentation amplifier will continue to play a role in the rejection of noise from amplitude modulated ambient light, such as the output of fluorescent lights. Fluorescent bulbs often provide strong power line harmonic output. Lamps run on 60Hz lines exhibit modulation at 120Hz and 180Hz. The presence of unexpected optical noise is also possible. High frequency (50 kHz) light output modulation may sometimes be caused by Barkhausen oscillation in the tube's plasma discharge or even solid-state fluorescent bulb ballasts.

The resistance of the bias current return resistors should be high compared to the detector load resistance (10 megohms in this example) to reduce detector loading effects caused by these resistors, but an excessively high value can result in unacceptable input offset voltages due to input bias current. Using a FET- input instrumentation amplifier in lieu of the bipolar IA used in the original design is a suitable way to resolve this trade-off. The INA121 FET IA may be installed in the same socket as the INA118 bipolar IA, and because of its very low input bias current of 4pA, the bias current return resistors can be made as large as 100 megohms or more, if preferred. In Figure 18, several strategies for ensuring bias current return are shown. The bias current return channel for the IA inputs is provided by the center tap of the linear variable differential transformer (LVDT) in this circuit. This technique works with almost any kind of IA since the resistance of the majority of inductive sources is often just a few hundred ohms at most.

See the sensor's data sheet since certain sensors may need a specific load resistance (and sometimes, a specific capacitance, too). The inputs to the IA may be added in parallel with any required load. IA source loading won't be an issue since an instrumentation amplifier's typical input impedance is one gig ohm or more! With a comparable circuit, a simple difference amplifier could be sufficient in certain cases. With a difference amplifier, a few hundred ohms present no issues since the center tap will deliver an identical source resistance (within a few ohms) to each input. As there is no imbalance, the CMR of the diff amp is unaffected. You can put to rest concerns regarding bias current's potential negative impact on the magnetic core properties of the sensor. The net magnetic flux is substantially below a level that may lead to issues in the inductor core due to the low bias currents and opposing magnetic flux generated by the center-tapped secondary, respectively. Opposing currents cancel transformer core magnetic flux, which is one of the fundamental issues with single-ended Class A power amplifiers. This fact will be appreciated by those of us who are old enough to remember having to thoughtfully adjust a bias potentiometer to balance a pair of 6L6s or KT-88s in a "push-pull" audio power amplifier. In order to reduce distortion brought on by forcing the output transformer core into a nonlinear section of its B-H curve on current peaks, Class A amplifiers had to run their whole plate current via just one winding (the main) of their output transformer. Yes, sure, today's "high-end" audio designs use these ancient amplifiers.

CONCLUSION

A differential amplifier equipped with input buffer amplifiers that does away with the necessity for input impedance matching therefore make the amplifier especially well-suited to be utilized in measurement and test equipment, is known as an instrumentation amplifier (commonly abbreviated as in-amp or In Amp). Very low-level signals are amplified by an instrumentation amplifier, which filters out interference and noise. Heartbeats, heart rate, temperatures, earthquakes, and other examples are only a few.

REFERENCES

[1] O. Ibrahim, S. M. Hassan, A. Abdulkarim, M. F. Akorede, and S. A. Y. Amuda, “Design of Wheatstone bridge based thermistor signal conditioning circuit for temperature measurement,” *J. Eng. Sci. Technol. Rev.*, 2019, doi: 10.25103/jestr.121.02.

[2] H. Jiang *et al.*, “Low concentration response hydrogen sensors based on wheatstone bridge,” *Sensors (Switzerland)*, 2019, doi: 10.3390/s19051096.

[3] S. Gao, Z. Yi, Y. Ye, M. Qin, and Q. A. Huang, “Configuration of a Self-Heated Double Wheatstone Bridge for 2-D Wind Sensors,” *J. Microelectromechanical Syst.*, 2019, doi: 10.1109/JMEMS.2018.2883131.

[4] Y. J. Li *et al.*, “A microfluidic micropipette aspiration device to study single-cell mechanics inspired by the principle of wheatstone bridge,” *Micromachines*, 2019, doi: 10.3390/mi10020131.

[5] Y. T. Ku, Y. S. Hwang, J. J. Chen, C. C. Shih, and D. Cheng, “A new current-mode wheatstone bridge based on a new fully differential operational transresistance amplifier,” *AEU - Int. J. Electron. Commun.*, 2019, doi: 10.1016/j.aeue.2019.01.032.

[6] F. Albouchi, F. Mzali, S. Saadaoui, and A. Jemni, “Thermal conductivity measurements of liquids with transient hot-bridge method,” *Instrum. Mes. Metrol.*, vol. 18, no. 1, pp. 25–30, 2019, doi: 10.18280/i2m.180104.

[7] F. Franco, S. Cardoso, and P. P. Freitas, "Reconfigurable Spintronics Wheatstone Bridge Sensors with Offset Voltage Compensation at Wafer Level," *IEEE Trans. Magn.*, vol. 55, no. 7, 2019, doi: 10.1109/TMAG.2019.2896379.

[8] L. Safari, G. Ferri, S. Minaei, and V. Stornelli, "Current-Mode Wheatstone Bridge," in *Analog Circuits and Signal Processing*, 2019, pp. 29–57. doi: 10.1007/978-3-030-01343-1_3.

[9] E. Alnasser, "A Novel Fully Analog Signal Conditioning Circuit for Loss-Less Capacitive Sensor Estimation," *IEEE Sens. J.*, vol. 19, no. 18, pp. 8019–8026, 2019, doi: 10.1109/JSEN.2019.2917029.

[10] L. K. Quynh *et al.*, "Design Optimization of an Anisotropic Magnetoresistance Sensor for Detection of Magnetic Nanoparticles," *J. Electron. Mater.*, vol. 48, no. 2, pp. 997–1004, 2019, doi: 10.1007/s11664-018-6822-4.

CHAPTER 8

ANALYSIS OF THE LIMITS ON COMMON MODE VOLTAGE

Mr. Sunil Dubey, Associate Professor,
Department of Electrical Engineering, Jaipur National University, Jaipur India
Email Id- sunildubey@jnujaipur.ac.in

Abstract:

Line voltages present in or close to a particular circuit are often the source of common mode voltages. A line's stray capacitance may charge up to the line voltage peak if there is any. There might be 400 volt potential peaks if indeed the line voltage was 240 VRMS.

Keywords:

Amplifier, Common Mode, Gain, Network, Signal.

INTRODUCTION

A designer can be in for an unpleasant surprise if he or she does not pay close attention to the instrumentation amplifiers they choose. When a common mode voltage is provided to an instrumentation amplifier's inputs, there are significant external impacts on how it operates. The supply voltage(s), voltage gain, and reference pin voltage of the IA all have an impact on the common mode voltage working range. An IA or diff amp may become utterly worthless if it is operated outside of its "envelope"; the amplifier may not have been harmed, but one or more internal nodes may have been forced into a nonlinear state or even into saturation. A 2 or 3 op amp IA could be your best option, depending on your specific application. Amplifier topologies define an amplifier's linear envelope.

The most crucial factor to take into account when selecting an instrumentation amplifier is the common mode input voltage range; other IA specifications come in second. All other factors are irrelevant if an amplifier cannot be used in a certain application. It is not simple to determine the common mode input voltage working range (also known as the "envelope") of an instrumentation amplifier. The IA's internal op amps' input and output ranges must be determined in order to calculate a "envelope," which requires a thorough circuit analysis (which may be done as shown in a previous chapter). Although "do-it-yourself" circuits may allow for this, the majority of IA suppliers do not provide enough details to allow for an exact computation.

The majority of manufacturers do provide one or two graphs in their data sheets that show the operating "envelope" of the amplifier's CMV under certain operating situations. This is OK if those circumstances apply to your specific application, but they seldom do. We need to ascertain if the amplifiers under consideration will function effectively in our specific application. We may assess the amplifier's performance under the real operating circumstances of our application by creating a graph of the amplifier input CMV range vs. output voltage swing. A "Trump Plot1" is a particular kind of graphical display of CMV range.

It is feasible to manually compute the CMV if you know the maximum internal op amp node voltage swing restrictions. There are two ways to avoid having to carry out this horrible chore, so do not be alarmed.

The CMV range of the amplifier may be directly determined by building a test circuit. The amplifier's CMV range may be seen on an oscilloscope by introducing a triangle wave to the differential input of the IA and a second unrelated triangular wave as a common mode signal to the two IA inputs. The scope must be powered in an X-Y mode in order to do this, with the X input linked to the amplifier output and the Y input connected to the common mode triangle wave input. A set of curves that represent the amplifier's CMV range and the operating conditions that were imposed on it will be produced by the unsynchronized input signals. It is simple to view and quantify the impact of different supply voltage combinations, amplifier gains, and reference pin voltages on the CMV range.

One word of caution is in order: it seems that even the most sophisticated digital oscilloscopes are unable to accurately show the family of curves that this approach necessitates. The X-Y display on an earlier Tektronix 7000 series (7834) analog storage scope was judged to be the finest of all those that were tested. There is just another justification for keeping that "vintage" analog scope in the lab's corner. Analog scopes don't have an issue with aliasing.

Common Mode Voltage Range Calculation Painlessly

The CMV range of an instrumentation amplifier may be determined considerably more simply by letting your computer handle the laborious task of determining the working envelope of the IA. A freeware computer utility for calculating IA and difference amplifier CMV range is available on the Burr-Brown Corp website. To use the application, just download the files and then create a new directory on computer hard drive called something like "CMV Range." Just add the three files to your newly created directory. The following items need to be in your directory:

The CMV working envelop of the IA is shown graphically by the executable program cm range.exe, which runs under Microsoft Windows and overlays plots of every one of the internal op amp inputs and outputs nodes of the IA. Hence, both the instrumentation amplifier's total CMV range and the position of the CMV limitation inside the IA are displayed. Use the pull-down menu to choose an instrumentation amplifier components number, together with its supply voltages, voltage gain, and reference voltage. Positive and negative power supply voltages were input separately to demonstrate the effect of asymmetrical supply voltages upon that amplifier's CMV range. If the voltage on the amplifier's V- pin is negative, enter the value with a negative sign, such as -15. Likewise, provide the voltage on the amplifier's reference pin. Add the amplifier's voltage gain last. If the voltage gain you provided is less than the minimum specified gain, the gain is adjusted automatically to that value. The amplifier's common mode voltage range is determined and shown on a graph (called a "Trump plot"). A "Trump plot" of an instrumentation amplifier for such INA118. The selected operating conditions are shown at the top of the graph as +Vs= 15.00, -Vs= -15.00, Vref= 0.00, and G= 100.00. Node limits for these operating conditions are calculated and shown for every one of the three internal op amps inside the INA118. Operational amplifiers are designated as A1 and A2, while output difference amplifiers are designated as A3. The input and output limits of all three internal op amps may be superimposed to reveal the whole common mode voltage range of the INA118. The amplifier will work well if it is switched on anyplace in the plot's spacious, white interior. Due to internal node constraints, an amplifier may only be utilized inside the hatched area of the plot, which is also its proper operating envelope. If you utilize an instrumentation amplifier outside of its proper working envelope, the IA output could not only be incorrect, but it might also have the opposite polarity in certain cases! Go to page 40 for further details on this behavior. Figures 19 (a) and 19 (b) exhibit the effects of IA gain on an INA118's

CMV range when operated under similar conditions with the exception of gain. The positive CMV range is dramatically decreased when the IA gain is decreased from 100V/V (a.) to 1V/V (b.). A closer look at the hatching in this region reveals that the input of node A2 is the precise node responsible for this CMV limitation. Only an INA118 operating under the specified conditions is appropriate for this design. There will be a "Trump plot" for each particular amplifier or IA.

Truth in Output upholding

Users need to be aware of a very challenging feature of three op amp instrumentation amplifiers. Any three op amp IA on the market is impacted by this feature because of the architecture of the device you lose any sense of "which way your signal should just go" at the output of both the third amplifier if you go beyond the output swing range of either one of the two input amplifiers (the IA output). Examining IA CMV plots, as discussed in the section above under "Common- Mode Voltage Limits," as well as other 3 op amp IA data sheets, might help one forecast this phase- confusing behavior. It goes without saying that the only way to prevent the amplifier's internal nodes from exceeding their voltage swing limit is to restrict the amplifier's input, gain, and CMV. In certain systems, it would be conceivable to use a window comparator composed of two op amps and a number of resistors to keep an eye on the outputs of both the two input op amps. The user may at least determine if the instrumentation amplifier output can indeed be trusted by detecting the two input op amp outputs.

Phase reversal may have detrimental effects on systems like servo amplifiers. In a servo system operating a heavy structure, oscillation brought on by unintentional positive feedback may be harmful and destructive. Be cautious and thoroughly examine each active part of a closed-loop control system for the potential for phase inversion in overdriven circumstances. Noise the incorrect IA input filtering creates an undesirable situation.

High levels of radio frequency interference (RFI) on a signal input line to an instrumentation amplifier may result in conducted RFI, which can lead to unforeseen issues like DC offset voltage, offset voltage "drift," or mysterious "jumps" in the amplifier's DC output. In many circumstances, an unstable circuit's input amplifier is held responsible while, in reality, the amplifier is not the root of the issue. The IA inputs may correct and produce tiny DC changes in the operating point of the amplifier if high amplitude, high frequency interference is introduced into the wire between a sensor and a low level amplifier input, with the external wiring functioning as an antenna. Consequently, transmissions that reach hundreds of megahertz might have a negative impact on even modest bandwidth equipment. After being corrected, RF manifests as DC. The output of the amplifier will additionally display the modulation envelope of the problematic RF signal if it is amplitude modulated. Connecting another audio amplifier to the IA output may occasionally help identify the interfering RF source when RF rectification is suspected. If a loud and clear local AM radio station can be heard, don't be shocked! This method also effectively distinguishes RFI from TV stations, although it does not distinguish FM broadcast stations. The buzz of radar interference may be recognized. IA topologies of different sorts are more or less susceptible to RFI rectification. An effective RF detector is the forward-biased emitter-base junction of a bipolar transistor, whereas a reverse-biased gate-source junction of a JFET is a rather ineffective detector. This is due to the fact that a signal with a high amplitude is required to drive the JFET gate-source diode before it can conduct in forward direction (rectify).

- JFET- input amplifiers perform well in severe RFI situations, as a general rule of thumb.
- Filter each and every lead—input, output, and power.

Protect everything

The use of a low pass filter somewhere at instrumentation amplifier inputs is the single most effective way to get rid of RFI. The first step in resolving conducted RFI issues is to keep RF away from the instrumentation amplifier inputs, but this must be done properly. At first glance, applying a simple RC low pass filter (LPF) to each IA input seems to be the best course of action. The issue is resolved if the RC LPF pole frequencies were low enough to significantly diminish the loudness of an interfering RF signal at the IA inputs.

Sadly, this is incorrect. The lowest pole frequency that an input LPF may use without impacting the IA differential signal bandwidth is a restriction. This approach may be effective if the offending RFI has a frequency that is significantly higher than the necessary signal bandwidth, but it must perfectly match the LPF pole frequencies of R1 and C2 in order for it to be effective. This is because real-world component tolerances cannot be used in an RFI filter. The worst-case scenario for RFI filter component mismatches with 1% resistors and 5% capacitors. Although R2 and C2 are in this instance at their lower tolerance limits, R1 and C1 are above their higher tolerance limits. As a consequence, the inverting input's LPF pole frequency is lower than that of the non-inverting input. This discrepancy is the root of all the issues. There is a filter mismatch issue. This graph displays the amplitude of the signals somewhere at inverting and non-inverting inputs as a 1V RMS common mode signal (Vcm) is scanned from 100 kHz to 1GHz. The input RFI filters subsequently convert the common mode signal into a differential signal because the two filter pole frequencies (time constants) are not matched. Hence, by converting a part of the interfering common signal to a differential signal, we have actually made the RFI situation worse since even an IA with infinite CMR cannot refuse the interfering common signal. The intended input signal is now amplified together with it as a result.

The circuit's reaction to frequency. Due to two considerations, the INA118 response (upper curve) abruptly drops off over 1MHz: the amplifier's gain-bandwidth restriction (about 150 kHz BW in a gain of 50V/V) and the placement of the RFI filters' poles. The differential input signal caused by the RFI input filter pole mismatch is seen by the bottom curve. The impact of bias current in the resistors must be taken into account when using a passive RC filter. High resistance reduces input offset voltage an extremely low input bias current instrumentation amplifier, such the FET-input INA121, is necessary for RC filters. The two pole frequencies may be adjusted to match if C1 is a trimmer capacitor and C2 is a fixed capacitor (or the other way around). Try connecting a fixed capacitor in combination with a smaller trimmer capacitor for simpler adjustment. Any RFI input filter capacitors should possess a low temperature coefficient regardless of the method used. It is advised to use COG (NPO) ceramic dielectric types, polypropylene film, or polystyrene film.

Replacing the resistors with inductors will allow you to RFI filter IAs with larger bias current. If the inductance is chosen properly, an RC filter will have low DC resistance but high RF impedance. Be cautious that fixed inductors with 1% tolerance are not cheap. In course, an LC filter with a variable inductor may be employed in one input so that it can "tune" its pole frequency to match an LC filter with a fixed inductor in the other input. Pole matching over temperature must be maintained by low TC filter components. Better passive filtering techniques exist that don't depend as much on filter component matching. Comparing this input filters and the other's instrumentation amplifiers' frequency responses

can help. Using this filter, there is less common mode voltage into differential voltage conversion even if the R1C1 and R2C2 mismatch are unchanged. I'll admit it now that you've been forewarned against it: input filtering is possible with modest signal bandwidth requirements. The differential error signal resulting from the input filter RC pole mismatch as well as the higher frequency common mode signal will travel far down the attenuation roll off curve if indeed the input filter RC pole is sufficiently low that it will not significantly affect the CMR error.

Application Circuits

The INA117 monolithic difference amplifier operates on ordinary +/-15V power sources, but it can handle +/-10V differential input signals with up to +/-200V common-mode. An amplifier with the +/-200V common-mode capabilities as well as a wider differential input range is necessary for many applications. With an application circuit, the differential input range may be increased to +/-20V.The INA117's excellent common mode rejection capabilities is a consequence of the inbuilt resistor dividers that are about 20-to-1 provided to the op amp's inputs. A +/-200-V common mode signal is reduced to +/-10 V at the op amp's two inputs thanks to such attenuation. The common-mode signal is rejected by this configuration, while differential signals are passed at unity gain. The gain of the diff amp is separately controlled by suitable resistors in the internal op amp circuit of the INA117. Therefore, the ratios of R1/R 2 and R3/R 4 must track with ratio R1/ for the gain to stay steady with temperature fluctuations (R 2 in parallel with R5). Excellent matching but also TC tracking are achieved using an on-chip metal film resistor network with precision laser trimming.

It is feasible to create a comparable circuit using a few discrete resistors and an op amp, but it is challenging at best to achieve the required precision with non-matching resistors. Yet, the original INA117 circuit's differential input range is just +10V since it has unity gain. The output swing is regulated by it’s +/-15V power supply. The INA117's differential input range might be expanded by lowering the gain; for instance, lowering the gain to 0.5V/V would expand the circuit's differential input range to +/-20V. The use of an external op amp (0PA27) circuit to reduce the gain is preferable than just lowering the gain using external resistors. The exceptionally accurate internal-resistor matching of the INA117 is preserved as a result, maintaining the circuit's common mode rejection minimizing temperature drift. Moreover, the output noise is actually made better by the gain reduction the external op amp circuit produces. That wouldn't change if we used the less complicated resistor-only strategy. The voltage gain of the diff amp is decreased by using the 0PA27 to invert the output of the differential amplifier and sending a tiny portion of its output signal back towards its reference pin (pin 5). Even with the additional OPA27 op amp inside the feedback line, the final circuit in Figure has remarkable stability (Figure 1).

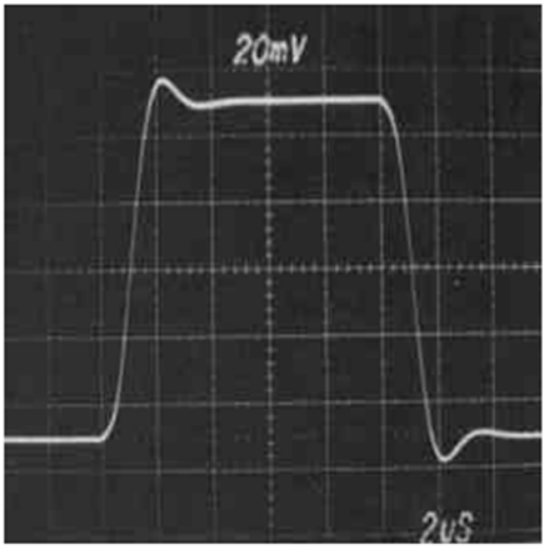

Figure 1: Even With The 0PA27 Op Amp feedback circuit gain of 0.5V/V and l000pF load, the stability of the INA117 circuit is excellent.

Consider the INA117 as being a four-input device, with E 2 being the signal at pin 2, E 3 at pin 3, E 5 at pin 5, and so forth and better understand how the circuit operates. E0=E 3-E2+19E 5–18E 1 is the output voltage. A = 1/[1+19/(R 6/R 7)] is the decreased differential gain having E1 grounded (equal to 0 V). And R6/R7 = 19 for A = 0.5. The crucial resistor matching, gain, and common-mode rejection of the INA117 are maintained as a result of the low output impedance of the 0PA27 circuit and the low impedance at pin 5 of the INA117. Add a 20 ohm variable resistor in series with pin 1 as well as a 10 ohm fixed resistor throughout series with pin 5 to modify the common-mode rejection for important applications. Short pins 2 and 3 together, and use a 500Hz square wave to drive them. Rather than employing a sine wave test signal, use a square wave to examine and modify the DC CMR. This enables the AC signal to level off. Trim the circuit using a variable resistor of 2 ohms to the minimal output when the scope gain is high. This CMR reduction might somewhat alter the gain. If so, change the R6/R7 ratio to change the gain. The CM1R will not be impacted by this alteration.

Uses for two and three op amps

A two-op amp IA would be the most appropriate for a wider CMV range or single supply. Another application would benefit from a three-op amp IA for a higher CMR.

LITERATURE REVIEW

B. Tan et al. [1] in that work, a three-phase PWM inverter technique called third harmonic injection sinusoidal pulse width modulation (THISPWM) based on alternating carrier polarity (ACP) is developed. Lower low-frequency common mode voltage is a benefit of the THISPWM over space vector pulse width modulation (SVPWM) (CMV). Nevertheless, the third harmonic must be precisely synchronous in phase with both the reference voltage when it is injected. The third harmonic generation that is inserted will be challenging due to the synchronization. To get a real-time conversion technique and fix the synchronization issue,

the relationship between the injected third harmonic and the reference voltage of both the PWM inverter output is first investigated. Next, a modulation technique based on ACP is suggested to get rid of the PWM inverter's zero switch states. The carrier with negative polarity is chosen using the middle amplitude-modulated voltage. In addition, consideration is given to the low-frequency and high-frequency CMV, which are defined individually based on the carrier frequency and the modulated fundamental voltage frequency. The analysis's findings therefore show that the suggested approach has the same voltage usage as SVPWM and can suppress both high- and low-frequency CMVs. Ultimately, an FPGA-based three-phase PWM inverter circuitry was created, and the experimental findings supported the suggested approach.

Y. Liu et al.[2]for the active power filter (APF) integrated single-phase quasi-Z-source inverter (qZSI) based photovoltaic (PV) power system, a common mode voltage (CMV) reduction approach is suggested. By retaining low qZS inductance and capacitance, the APF integrated qZSI entirely compensates the dc-side double-line-frequency (2) ripple via the APF capacitor. The CMV amplitude is cut in half by the suggested approach compared to the conventional sinusoidal pulse width modulation (SPWM). Analyses are done on the conduction and switching power losses. Results from simulations and experiments show that the suggested solution lowers CMV without compromising the effectiveness and performance of the APF integrated single-phase qZSI.

A. S. Zalhaf et al. [3]the incorporation of wind energy into power networks is growing daily in an effort to minimize the usage of fossil fuels and, as a result, greenhouse gas emissions. When wind turbine generators, especially doubly-fed induction generators, use pulse-width modulated (PWM) power converters, a common-mode voltage is produced (CMV). This generator structure's stray capacitances allow the common-mode current (CMC) that's also produced by this common-mode voltage to seep out. These currents subject the generator bearing to a voltage that might damage it. The CMV generated by a PWM converter is eliminated in the present work by the development of an active common-mode voltage canceler (ACMVC). In order to remove the CMV and thus lessen the voltage stress here on generator bearing, the ACMVC creates a compensatory voltage there at converter terminals. The polarity of this compensatory voltage is the opposite of CMV's, but it has the same amplitude. The PSCAD/EMTDC (Electromagnetic Transient Design and Control) software suite is used to simulate the ACMVC model. Findings show that ACMVC is successful at canceling not just the CMV but also the CMC and bearing voltage. Investigation is being done into the connection between the peak value of CMC and the increase time of CMV.

T. T. Tran et al. [4]a modified three-phase, two-level inverter for voltage sources is suggested in this study. The suggested inverter's DC-link voltage is doubled in comparison to the input DC voltage by integrating a switching capacitor voltage doubler network with a traditional three-phase H-bridge inverter. The output voltage of the suggested inverter may thus be greater than the DC input voltage. Also, by regulating the two extra switches based upon that space vector pulse-width modulation, the common-mode voltage (CMV) of a proposed inverter may be decreased. Just 16.6% of the DC-link voltage may vary in CMV when compared to the current modulations and topologies. Additional switches and diodes are subject to a voltage stress that is equivalent to half of the DC-link voltage. The suggested three-phase two-level inverter for voltage sources is compared to the traditional three-phase voltage source inverter (vsi via mathematical analysis, operational principles, and comparison. The PLECS-based simulation results attest to the proposed inverter's successful operation. Last but not least, a lab prototype built around a TMS320F280049 DSP is created,

and experimental tests are run to confirm the viability of the suggested three-phase inverter design.

S. Du et al. [5]A grid-tied MMC is often installed in a transformer-less modular multilevel converter (MMC)-based drive system to connect to a medium-voltage ac utility. The grid-tied MMC is anticipated to immediately defend the common-mode voltage (CMV) against asymmetrical grid failure and switch the functioning of converters for the maximum protection of the medium-voltage motor as no front-end transformers is installed. A control method to reduce the CMV of both the grid-tied MMC is presented in this research. By placing the arm-voltage pulses end-to-end, the switching ripples brought on by MMC switching operation are decreased while the CMV resulting from an asymmetrical grid failure is cancelled. Moreover, the impact of MMC counterpart voltage upon phase-leg power deviation is examined, and a feed-forward control-based solution is created as a result. The suggested technique reduces the grid-tied system's maximum CMV from 1/3 per unit (p.u.) to (1/3N) p.u. under severe asymmetric grid conditions, where N is the number of the per-arm submodule. In the meantime, balanced phase-leg power, continuous dc-bus voltage, and unified power factor are also accomplished. Experiments and simulations back up the validity of the concept.

T. Jin et al. [6] proposed a unique double vector optimum selection approach for model predictive control (MPC). The major goal of this technique is to reduce the high common-mode voltage of a two-level inverter while it is in a balanced state, enhance output current tracking capability, and lower the high output current harmonic distortions rate. This approach manages two voltage vectors within every sample period to improve the output current's ability to follow voltage vectors in order to address the issue of the total harmonic distortion (THD) growing in magnitude due to the lowering of the available voltage vector. The suggested approach for determining the selection range of a second voltage vector simultaneously reduces switching losses in comparison to the adding virtual vector MPC technique, which leads in high switching losses. To significantly lower the switching frequency, only two voltage vectors that are close to the initial voltage vector may be used. For further confirming the efficacy of the suggested control strategy, an experimental control allows for the development on Simulink-Real-Time system is given. The modeling and practical findings demonstrated that the suggested strategy may successfully lower the inverter's output common-mode voltage. The switching loss and THD value are both significantly decreased simultaneously.

According to the A. Salem [7] et al. a cutting-edge architecture with fewer switching devices than a traditional diode clamped converter is the dual T-type multilevel converter (MLC). In this study, a simplified switching phase model predictive control (MPC) of a dual T-type drive system is proposed. It takes into account the torque management of an open-ends induction motor, common-mode voltage (CMV), and balancing of the DC link capacitor. The proposed research examines the CMV under two distinct scenarios, namely the CMV Reduction (CMVR) and the CMV Elimination (CVE) (CMVE). For the suggested driving system, a MATLAB simulation is shown. Design, implementation, and testing of a dual T-type converter prototype based on discrete Silicon-Carbide MOSFET switches are performed in the lab. The suggested MPC technique effectively balances the twin DC connections and executes the torque instruction.

When compared to the CMVR, the CMVE is shown to have several limitations, especially when operating at rated speed. It is important to note that the suggested decreased switching states approach might cut the calculation time for CMVR and CMVE from 5.5 ms to 140 s and 70 s, respectively. Moreover, the findings show that, in comparison to the CMVE

scheme, the CMVR scheme is more successful at minimizing harmonic contents, torque and flux ripples, and converter switching losses.

Z. Quan and Y. W. Li [8] stated the voltage source converters (VSCs) for three-phase interleaving are often used in industry. Up until now, literature has mostly focused on the prevailing topical problem. The common-mode voltage (CMV) produced by interleaved VSCs, which is also a significant element affecting the system's performance, has not yet undergone much research. This study examines how pulse width modulation (PWM) techniques affect the CMV of interleaved two-level VSCs. The analysis is carried out using the extended double Fourier integral theory and taking into account any number of interleaved converters. The interleaved sinusoidal PWM (ISPWM), interleaved space vector modulation (ISVM), interleaved discontinuous PWM (IDPWM), and newly introduced interleaved carrier phase-shift PWM (ICPS PWM) and interleaved carrier phase-shift SVM are five PWM schemes that are taken into consideration (ICPS SVM). With each approach, the magnitude and harmonic content of CMV are investigated. The investigation shows that the CMV may be decreased using ISPWM, ISVM, ICPS PWM, and ICPS SVM. For drive applications employing linked architecture, interleaving is less desirable since it has minimal effect on the CMV using IDPWM, which is constantly at VDC/2 because of excessive low-order harmonics. Since its low-ZSCC peak value, ICPS PWM and ICPS SVM are preferable for modular design. The findings of the experiments are used to validate the research.

Y. Xiang et al.[9]in order to reduce common-mode voltage (CMV) and eliminate electromagnetic interference, this research provides an enhanced H8 power converter. The enhancement of the structure and the control technique are primarily responsible for the proposed H8 converter's ability to achieve zero CMV variation while entering and departing the zero state. To float the ac portion of the three-phase converter inside the zero state for the system structure, switching devices are added to the dc bus. More capacitors are utilized to provide controlled CMV. For the H8 converter's control technique, a straightforward control method is suggested. It has the ability to automatically adjust to the load current's direction of flow in order to achieve synchronous changeover of the power switches, thereby eliminating the influence of dead time. A comparison between the suggested H8 converter and the traditional H6 converter is carried out via analysis, simulations, and testing. Findings confirm the H8 topology's efficiency.

In study U. Subramaniam et al. [10]common mode voltage (CMV) and common mode current (CMC) produced by power inverters result in high-frequency electromagnetic interference (EMI) noise, leakage currents in applications involving electrical drives, and grid-connected systems, which significantly reduce the efficiency of the system. By creating appropriate EMI filters and/or researching the impacts of various modulation techniques, this CMV may be reduced. This study examines the effects of different modulation strategies on CMV and CMC for two- and three-level inverters. It has been shown that the CMV and CMC inside the system were decreased by 60% using the modified third harmonic injection approach. EMI chokes are used in conjunction with this modified pulse width modulation (PWM) technology, which reduces system distortion.

DISCUSSION

Amplifiers used in Single- Ended Applications Vary

Commercially available monolithic diff amps may be utilized for fascinating and practical single ended gain applications while being initially designed for differential amplification. To

provide accurate and steady gains, the majority of these applications make use of the precision resistor network that is built into the device. A precision inverter with a gain of -1.000V/V is created by connecting a difference amplifiers. In the original design, the inputs and feedback resistors were precisely laser trimmed to get a high CMR, but in our application, they use this exact ratio to provide a highly accurate and steady gain. The voltage gain of the circuit is increased to +2.000V/V by a simple wire modification. The non-inverting gain is now set using the same ratio resistors that were previously used to adjust the inverting gain. The parallel resistors connected in series with both the input and the op amp's non-inverting gain have no effect on the signal since they are connected to an input impedance of around 109 ohms, hence their existence causes no mistake. These resistors do provide a little offset voltage as a result of the bias current flowing through that input, but this is advantageous since it balances out the offset caused by the other op amp input's bias current.

An average value amplifier is produced by once again rearranging the difference amplifiers connections. A voltage divider involving two inputs is now created via precise resistor ratios. For with this divider, the op amp functions as a high-impedance unity-gain buffer. Connecting using feedback resistor in Figure to get a 2V/V op amp gain. Changes the difference amplifier into a two-input summing amplifier after compensating for the voltage divider ratio of one-half (Figure 2).

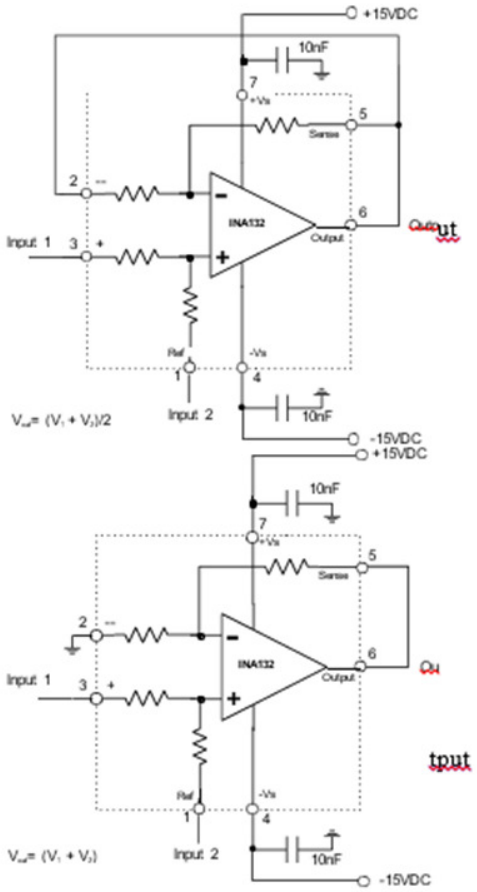

Figure 2: A Difference Amplifier Connected As (a.) An Average Value Amplifier.(b.) A 2- Input Summing Amplifier.

Using the average value circuit with one input grounded gives us an amplifier with a precision gain of +0.500V/V. This variant is shown in Figure 3.

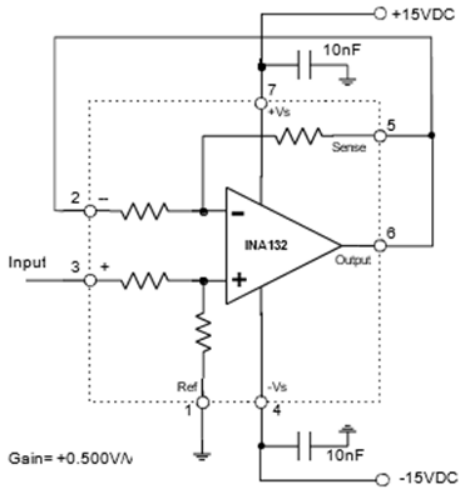

Figure 3: Illustrate A Precision Gain Of +0.500V/V.

The output signals of two INA134 unity gain difference amplifiers appears 180 degrees out of phase when their inputs are connected in an anti-parallel configuration. This is an amplifier with differential input to differential output, in other words. The iPhone input is grounded, therefore it may also be utilized as a single-ended input to differential output amplifier. Due to the fact that one output of this amplifier swings positively while the other swings negatively, two advantages result: the output voltage swing has been doubled to +/-20V, and the amplifiers' slew rate has been increased from 14V/us to 28V/us.

The behavior of the circuit is not as intuitively clear whenever the potentiometer is turned to its completely clockwise position, or c(w). As opposed to being linked to ground in the previous situation, the non-inverting input of the op amp is now connected to the signal. There is no current flowing through the resistors in this instance, but the negative feedback route is still there. According to op amp theory, the inverting input of an op amp must be driven by feedback such that it is equal to the non-inverting input. The input signal voltage may be seen on the non-inverting input because there is no voltage drop inside the two parallel resistors inside the differential amplifier's + input. Feedback requires both the inverting input and the input signal voltage to be equal. The current flowing through the - input resistor is zero because there is a equal voltage (signal) across it. As there is no current flowing into the inputs of a perfect op amp, there is also no current flowing through into the negative feedback resistance. This negative feedback circuit is only "going along for the ride" and making no gains if there is no current flowing through it. With such a gain of +1V/V, this link now functions as a straightforward voltage follower.

As we've seen, the wiper position of a pot may choose between a +1V/V gain connection and a -1V/V gain connection. In reality, if we center the wiper position here on potentiometer, the amplifier will have a gain of zero (no output) since its -1V/V gain will precisely cancel out its +1V/V gain.

We get a constantly adjustable gain by rotating the potentiometer, which changes the proportion of inverting to non-inverting gain. In order to create a useful general-purpose reference circuit which can be changed to any output voltage between -10V and +10V, this

circuit may be paired with a precise +10VDC reference, such as a REF101. This voltage reference is really "universal (Figure 4).

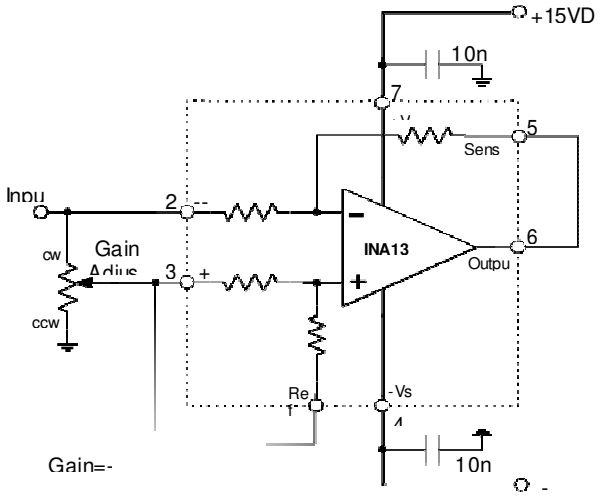

Figure 4: Illustrates an Amplifier with A Continuously Adjustable Gain Range of -1.000V/V To +1.000V/V.

CONCLUSION

The voltage that a circuit's two output terminals on average. The ac voltage that results from applying input terminals with identically phased and amplitude ac signals to two output terminals, or perhaps the output terminals and ground in circuits with just one output. Since the direction of the noise currents upon that positive (+) and negative (-) sides of both the power supply are the same, this noise is referred to as "common mode" noise. There is no noise voltage observed across the power supply cables. As previously stated, these noises are conducted emissions.

REFERENCES

[1] B. Tan, Z. Gu, K. Shen, and X. Ding, “Third harmonic injection SPWM method based on alternating carrier polarity to suppress the common mode voltage,” *IEEE Access*, 2019, doi: 10.1109/ACCESS.2018.2890014.

[2] Y. Liu, B. Ge, X. Li, and Y. Xue, “Common mode voltage reduction of single-phase quasi-z-source inverter-based photovoltaic system,” *IEEE Access*, 2019, doi: 10.1109/ACCESS.2019.2949026.

[3] A. S. Zalhaf, M. Abdel-Salam, and M. Ahmed, “An active common-mode voltage canceler for PWM converters in wind-turbine doubly-fed induction generators,” *Energies*, 2019, doi: 10.3390/en12040691.

[4] T. T. Tran, M. K. Nguyen, T. D. Duong, J. H. Choi, Y. C. Lim, and F. Zare, “A Switched-Capacitor-Voltage-Doubler Based Boost Inverter for Common-Mode Voltage Reduction,” *IEEE Access*, 2019, doi: 10.1109/ACCESS.2019.2930122.

[5] S. Du, B. Wu, and N. Zargari, "Common-mode voltage minimization for grid-tied modular multilevel converter," *IEEE Trans. Ind. Electron.*, 2019, doi: 10.1109/TIE.2018.2881939.

[6] T. Jin, J. Guo, M. A. Mohamed, and M. Wang, "A Novel Model Predictive Control via Optimized Vector Selection Method for Common-Mode Voltage Reduction of Three-Phase Inverters," *IEEE Access*, 2019, doi: 10.1109/ACCESS.2019.2928440.

[7] A. Salem, M. Mamdouh, and M. A. Abido, "Capacitor balancing and common-mode voltage reduction of a sic based dual T-type drive system using model predictive control," *IEEE Access*, 2019, doi: 10.1109/ACCESS.2019.2907021.

[8] Z. Quan and Y. W. Li, "Impact of PWM Schemes on the Common-Mode Voltage of Interleaved Three-Phase Two-Level Voltage Source Converters," *IEEE Trans. Ind. Electron.*, 2019, doi: 10.1109/TIE.2018.2831195.

[9] Y. Xiang, X. Pei, M. Wang, P. Shi, and Y. Kang, "An Improved H8 Topology for Common-Mode Voltage Reduction," *IEEE Trans. Power Electron.*, 2019, doi: 10.1109/TPEL.2018.2870039.

[10] U. Subramaniam, S. M. Bhaskar, D. J. Almakhles, S. Padmanaban, and Z. Leonowicz, "Investigations on EMI mitigation techniques: Intent to reduce grid-tied PV inverter common mode current and voltage," *Energies*, 2019, doi: 10.3390/en12173395.

CHAPTER 9

APPLICATION OF PHASESENSITIVEDETECTOR

Dr.Pradeepa P, Professor
Faculty of Engineering and Technology, Jain (Deemed-To-Be University), Bengaluru, Karnataka, India
Email id- p.pradeepa@jainuniversity.ac.in

Abstract:

When there is a lot of noise present, phase-sensitive detection is an effective technique for detecting extremely tiny signals. The lock-in amplifier1 is the device that allows this experimental approach, which was created and has now been widely used, feasible.

Keywords:

Amplifier, Detector, Gain, Phase Sensitive, Noise.

INTRODUCTION

If a switch is used in its stead, we may drive the pot from one end to the other electronically. This results in the amplifier circuit of with a gain of +/-1V/V. A strong signal detecting instrument, a synchronous detector (sometimes called a phase sensitive detector) is created by this amplifier circuit. It excels at extracting weak signals from noise (Figure 1).

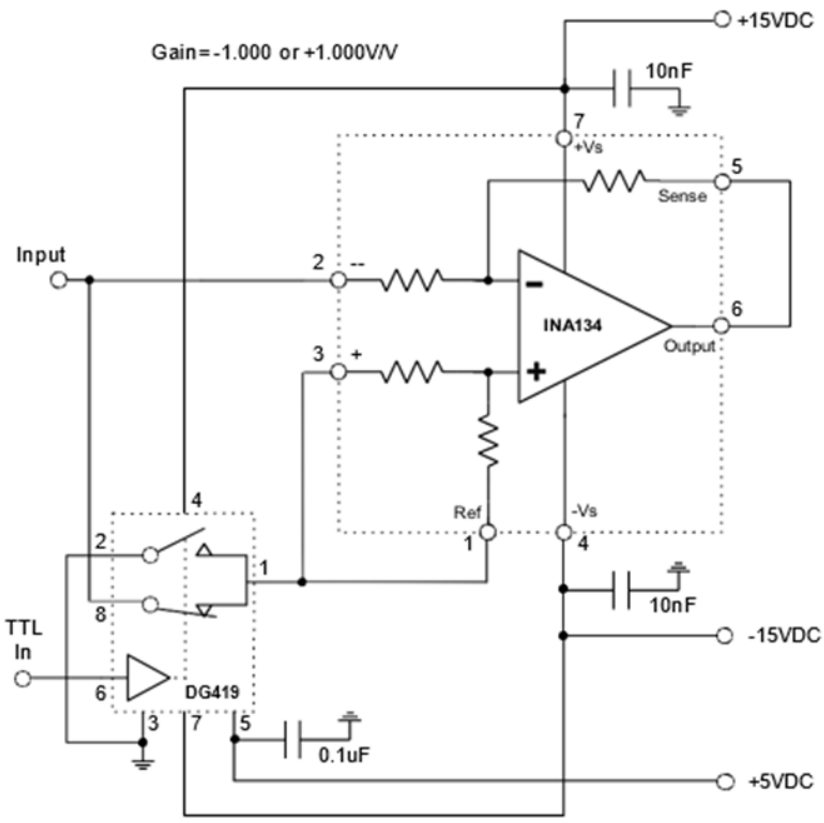

Figure 1: Illustrates the Adding a Switch to a Difference Amplifier Creates Turns It into a Synchronous Detector, a.k.a. Phase Sensitive Detector.

The difference amplifier's input offset voltage must be low, the positive and negative gains must match very well, and the difference amplifier's negative and positive slew rates must be tightly matched in order to provide accurate carrier suppression. An INA134 satisfies these criteria. In order to maintain effective carrier suppression, it is also important to match the duty cycle of the TTL switch drive, often known as the "reference signal," to that of the input signal we are trying to recover. In order to ensure that both the signal and detector get an accurate 50% duty cycle reference voltage, the sync is derived by splitting a free-running oscillator with a D-Q flip-flop. This ensures that the majority of input signals will employ a 50% duty cycle (square wave modulation).

By seeing a synchronized detector as an RF mixer, its functioning may be better understood. The "input" is the RF input, while the "reference" is the LO input. Instead of the typical band pass filter (BPF) found in a radio receiver, we discover a low pass filter (LPF) at the mixer's intermediate frequency (IF) output. The synchronous detector functions precisely as the RF mixer does. Although the mixer creates sum and difference imaging frequencies (sidebands) that are spread out from the LO at a certain spectral distance, these frequencies are centered on the mixer's carrier, or the LO frequency. Its sidebands extend symmetrical from either the carrier to something like a frequency that is dictated by the LPF corner frequency since the IF stage used after a synchronous detector uses an LPF. A synchronous detector, its reference, and LPF together may create a "receiver" that has an exceedingly small bandwidth. Thankfully, the reference signal that powers the detector also establishes the frequency of the input signal. This maintains the input signal's position in the synchronous detector's restricted

passband. Therefore the "synchronous" detector gets its name. The signal-to-noise ratio (SNR) is enhanced by lowering the LPF filter corner frequency such that less and less noise power passes through the detector system. A synchronous detector can quickly recover a signal that, on such an oscilloscope, seems to be completely buried in white noise with bandwidths as small as 0.01Hz, which is feasible. The ability to identify a signal with an SNR of just -30 to -40dB is impressive.

The Integrator Amplifier

The output voltage of something like the integrator Op-amp is proportional to the input transmitter magnitude and duration. The ideal op-amp integrator simulates mathematical integration by having an inverting amplifiers for whom the voltage output is proportionate to the input voltage's negatives integral [1]. Operational amplifiers may be utilized in adder or subtracted circuits, with positive or negative feedback amplifiers, or even circuits with just pure resistance values in the inputs and feedback loop. To replace the solely resistive (R) feedback component of such an inverting amplifier with something like a frequency-dependent complicated element having a reactance, (X), for instance a capacitor, C. the impact of this complex permittivity on the voltage gain fourier transform of the op-amp across its frequency spectrum [2]. As seen in Figure 2, by swapping out this feedback resistance for a capacitor, they have created a different sort of op amp known as an Op-amp Integrator circuit by connecting an RC Network throughout the operational amplifiers feedback route.

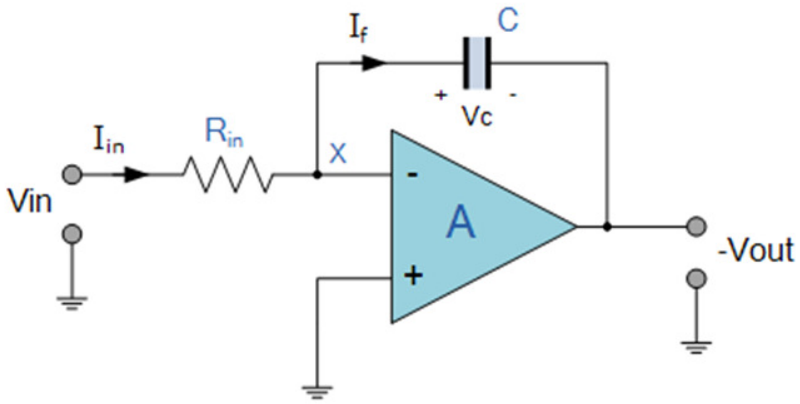

Figure 2: Illustrates the circuit diagram of the Integrator Amplifier.

Op-amp Integrator Circuit

Since the op-amp integrator generates an output voltage that is proportional towards the integral of an input voltage, it functions as an operational amplifier circuit that completes the mathematics process of integration. As a result, one can have the output react to changes in the input output power over time. In other words, the current through into the feedback loop charges or discharging the capacitance as the necessary negative feedback happens via the capacitor, determining the output signal's amplitude depends on how long a voltage is maintained at the input. The unindicted capacitor C has a very low resistance and behaves much like a short circuit that whenever a step voltage, Vin, is initially supplied to an integrated amplifier's input, enabling the greatest current to flow through the input resistor, Rin, as voltage differential occurs between the two plates. Zero output results from point X being a virtual earth and no current flowing into the amplifier's input. Given that the

capacitor's capacitance at about this point is extremely low and that XC/gain RIN's ratio is likewise very modest, the total voltage gain is less than one (voltage follower circuit). The input voltage's effect causes the feedback capacitor, C, to start charging up, and as it does so, the impedance Xc gradually rises in proportional to the rate of charge.

The series RC network's () RC time constant governs how quickly the capacitor charges. The op-amp is compelled by negative feedback to create an output voltage which preserves a virtual ground at the inverting input of the op-amp. The capacitor is placed between both the op-inverting amp's input, which has a virtual earth potential, and the op-amp output, which is currently negative. As a result, the potential voltage, Vc, developed throughout the capacitor gradually rises, causing the current flowing to drop significantly as the capacitor's impedance rises. As a consequence, the Xc/Rin ratio rises, providing an output voltage ramp that increases linearly again until capacitor is completely charged. The capacitor now functions as just an open circuit, stopping further DC current flow. Now that the relationship between the feedback capacitor and the input resistor (XC/RIN) is infinite, the gain is limitless. The output of an amplifier becomes saturation as a consequence of the high gain (comparable to the open-loop gain of op-amps). (Saturation happens when there is little to no control between the extreme swings in the amplifier's output voltage to either of the voltage supply rails).

Continuous Op-amp Integrator

The Op-amp Integrator behaves less as an integrator it's more like an active "Low Pass Filter," passing signals with low frequencies whilst attenuating this same high frequencies, if we swap the output waveform input signal mentioned above for a sinusoidal waveform of changing frequency. Owing because of its reactance, the capacitor behaves as an open switch at zero frequency (0Hz) or DC, suppressing any output voltage feedback. As a consequence, very little negative responses is sent from the amplifier's outputs back to its input. Therefore, at zero frequency, the op-amp is firmly connected as a typical open-loop amplifier with an extremely high open-loop gain using only a single capacitor, C, in the feedback line. The op-amp becomes unstable as a consequence, leading to unacceptable output voltage circumstances and potential voltage rail saturation. In this circuit, a continually discharging and charging capacitance is connected in parallel with a high value resistance. This feedback resistor, R2, when added across the capacitor, C, transforms the circuit into an inverting amplifier with such a limited closed-loop voltage gain determined by: R2/R1. Because of the consequences of capacitive reactance lowering the amplifiers gain, the capacitor burns out another feedback resistor, R2, at high frequencies (Figure 3). The circuit functions as a typical integrator at operational frequencies, however at very lower frequency around 0 Hz, when C opens up owing to its reactance, the size of the voltage gain was constrained and regulated by the proportion of: R2/R1.

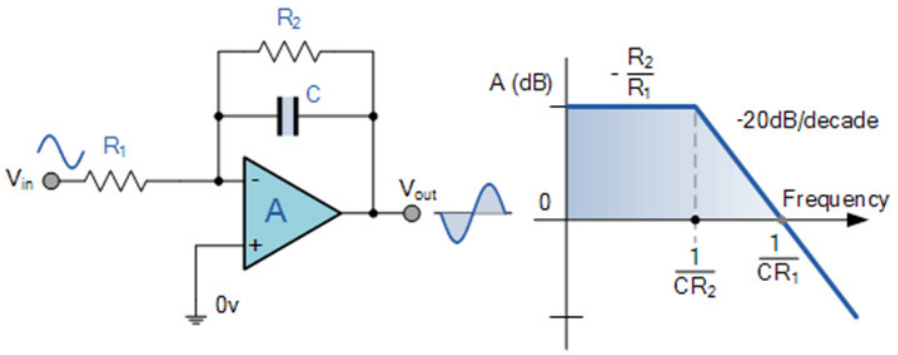

Figure 3: Illustrates the circuit diagram of p-amp Integrator with DC Gain Control.

LITERATURE REVIEW

According to the S. Shukla [3] et al. A small photoacoustic spectrometer (PAS) based on a microcontroller has been created. Helmholtz resonator type photoacoustic (PA) cell with provision to assess sample behavior as a function of temperature was created for the current investigation. An electret microphone is used in this system to produce a high signal-to-noise ratio. In order to prevent heating from affecting the electric microphone that picks up the photoacoustic signal, the microphone compartment is separated from the sample compartment. A low noise op-amp LM308 has been used to construct a high-gain, low-noise, two stage preamplifier, second order bandpass, and adjustable narrow band-pass filters. The amplitude and phase of the photoacoustic cell signal have been measured using a phase sensitive detector based on the C8051F060 microprocessor. For selected samples, the PAS applications for phase transition research are provided. The device that was created is inexpensive, very portable, and perfect for carrying out tests to examine a sample's thermal characteristics.

Y. Liu et al. [4] discussed the photoelectric detecting system's capacity to identify weak signals in environments with higher levels of background noise may be enhanced using two-dimensional spatial modulation and demodulation technologies. The demodulation of a 2D spatial amplitude-modulated signal with great accuracy is suggested in this study using a two-dimensional phase-sensitive detector. Using a 2D phase-sensitive detector, we demonstrate how to extract modulating signals from 2D amplitude modulated pictures while simulating the detector's capacity to suppress noise and extract signal from amplitude-modulated images covered in noise. The methods of filtering in the frequency domain, rectifying plus filtering, and two-dimensional phase sensitive detector are used to remove noise the mesh amplitude-modulated image, and the effects of extracting deformities and suppressing noise are compared in in order to remove the influence of grid concept testing by metal wire mesh sandwiched among both two layers of glass on the detection of shielding glass defects. Also offered are the theoretical underpinnings and experimental findings for the flaw detection of common glass utilizing an external carrier. The modeling and detection findings demonstrate that the spatial two-dimensional amplitude-modulated picture generated by optical modulators may be demodulated by a two-dimensional phase-sensitive detector to provide two-dimensional measurement signals. The amplitude-modulated picture buried in noise may be used to extract modulating signals from the 2D phase-sensitive detector, which can also significantly boost detection accuracy and the signal-to-noise ratio of both the output image.

I. Haïk Dunn [5] et al. proposed a technique for measuring the thermoelectric Thomson coefficient that is straightforward, quick, and accurate. The approach involves dynamically heating a hanging wire with an alternating current. We discover that the response somewhere at second harmonic of the stimulation frequency is precisely proportional to the Thomson coefficient by creating a temperature gradient across the wire. So, by using a phase sensitive detector, the absolute thermoelectric coefficient of such a single material may be retrieved with great accuracy. Using platinum and nickel wires, we test our methodology, and we create analytical and numerical models to identify the main causes of mistake.

G. F. Zhao et al. [6]that study describes a technique for improving an eddy current sensor's resolution (ECS). The theory is explained using a standard ECS based on an AC Bridge and an orthogonal phase sensitive detector, and it is then tested via experiments. The noise inside the excitation voltage provided to the bridge for this form of ECS is thought to have a significant impact on the sensor's resolution. Design and analysis are performed on a high-Q passive LC bandpass filter that is used to reduce excitation voltage noise. According to experimental findings, the filter significantly increases the sensor's resolution. The operating range of the sensor is 20 m, and its resolution is increased from 0.35 nmrms to 0.05 nmrms with a bandwidth of 7.2 Hz.

I. V. Gorbenko et al. [7] stated a plasmon-assisted DC current is induced by a phase difference between terahertz signals linked to a field effect transistor's gate and source and gate and drain terminals (a TeraFET), and that this current is significantly amplified in the region of plasmonic resonances. We report a TeraFET operation with such a phase-shift-induced asymmetry but equivalent radiation amplitudes there at source and drain antennas. In this domain, the TeraFET functions in the sub-terahertz and terahertz frequency ranges as a tunable resonating polarization-sensitive plasmonic spectrometer. We also suggest a practical design for a phase-sensitive homodyne detector that operates in this phase-asymmetry mode, allowing for a markedly improved response. These regimes may be applied to silicon as well as other types of material systems. The 200 to 600 GHz environmental windows might be supported by the p-diamond TeraFETs, which is crucial for beyond 5G communication systems.

According to the J. Song et al. [8]recent years have seen a significant increase in interest in electron ptychography for high resolution phase-sensitive imaging. The electron dosage needed to record a ptychographic database is too large for usage with beam-sensitive materials, hence investigations to date have mostly been restricted to radiation resistant samples. Here, we describe defocused electron ptychography, which reconstructs the transmission function—which, in turn, is connected to the electrostatic potential of such a two-dimensional material at atomic resolution—under a variety of low dosage situations.

According to the B. Chen et al. [9]the development of two instrumental procedures has led to the current capacity of rare earth element (REE) analysis. The ability of spectroscopic technologies to find and identify REE traces in diverse materials has been greatly enhanced. Although chromatographic methods are particularly effective instruments for the separation of REEs, the detection of REEs often rely on the preconcentration and separation of REEs. Several challenging analytical jobs may be completed by combining with sensitive detectors. The method that is employed the most often is liquid chromatography. Ion exchange chromatography, ion - exchange chromatography, ion-pair reverse-phase chromatography, and other methods may use various combinations of stationary phases and mobile phases. Gas chromatography can only separate volatile components of REEs, which restricts its applicability. The applicability of thin-layer and paper chromatography were constrained since these methods cannot be connected directly with appropriate detectors. Capillary

electrophoresis, which has a very high separation efficiency, may be used to conduct separations for specific requirements.

In study S. M. Mousavi et al.the heart of observational seismology is the detection of earthquake signals. A good detection algorithm should be effective for processing huge data volumes, sensitive to tiny and weak events with a range of waveform patterns, and resilient to background noise and non-earthquake signals. Here, we present the deep neural network-based detector Cnn-Rnn Earthquake Detector (CRED). Convolutional layers plus bi-directional long-short-term memory units are combined in a residual structure by CRED. Using the three component data that were captured on different stations, it learns the time-frequency characteristic of the major phases in an earthquake signal. We developed the network using 500,000 seismograms collected in Northern California, 250k of which were linked to tectonic earthquakes and 250k to noise. Applying the trained model to a collection of semi-synthetic signals demonstrates its resilience with regard to noise level and non-earthquake signals. In order to show the model's effectiveness, generalizability, and sensitivity, we also apply it to a month's worth of continuously collected data from Central Arkansas. More than 800 microearthquakes smaller than 1.3 ML caused by hydraulic fracturing remote from the training zone have been detected by our model. We evaluate how well the model performs in comparison to the STA/LTA, template matching, and FAST algorithms. These findings point to CRED's effective and dependable functioning. The detection threshold might be lowered with the help of this framework while reducing the number of false positive detections.

U. Adiyan et al. discussed the thermal imaging applications have expanded quickly thanks to uncooled infrared detectors. The majority of these detectors are bolometers, which interpret a pixel's temperature change caused by infrared light as a change in resistance. Transducing infrared photons into a mechanical resonator's frequency shift is another uncooled sensing technique. Here, we introduce thermos-responsive shape memory polymer-based very sensitive resonant infrared sensors. Our method improves the temperature coefficient of frequency by two orders of magnitude by using the phase-change polymer as a transduction mechanism. With f/2 optics, a noise equivalent temperature difference of 22 mK throughout vacuum and 112 mK in air is produced. By employing high-Q silicon nitride membranes as that of the substrates again for shape memory polymers, the noise equivalent difference in temperature is further increased to 6 mK in vacuum. Due to its great performance in air, infrared sensors won't need to be hermetically sealed and will instead be flexible.

G. Blaney et al. [10]provided non-invasive, bilateral optical measurements of 0.1 Hz oscillatory hemodynamics induced either by paced breathing or by cyclic inflating of pneumatic thigh cuffs upon that forehead of five healthy adult volunteers. Frequency-domain near-infrared spectroscopy was used to measure the optical intensity and phase of photon-density waves at seven source-detector distances (11-40 mm). Oxyhemoglobin (O) and deoxyhemoglobin (D) concentration phasors and the vector D/O, which indicates the amplitude ratio and phase difference of D and O, are used to describe coherent hemodynamic oscillations. We discovered that, on average, the phase difference ((D/O)) and amplitude ratio (|D/O|) obtained with single-distance intensity at 11-40 mm rise from 0.1° and -330° to 0.2° and -200°, respectively. At distances higher than 20 mm, the single-distance phase as well as the intensity slope produced values of roughly 0.5 and -200° for |D/O| and (D/O), respectively, and showed a decreased reliance on source-detector separation. The main conclusions are as follows: (1) Single-distance phase and intensity slope are much more sensitive to deeper tissue than single-distance frequency; (2) Deeper tissue hemodynamic

fluctuations, which more closely resemble the brain, have D and O phasors that are consistent with a higher relative flow-to-volume charitable donations in brain tissue than extra cerebral, superficial tissue.

DISCUSSION

The Differentiator Amplifier

The output signal from the fundamental operational amplifier differentiator circuitry is indeed the input signal's first derivatives. The position of both the capacitor and resistor throughout the differentiator power amplifier has been switched, causing the reactance, XC, to be connected to the output terminals of a inverting amplifier whereas the resistor, R, still serves as the typical negative feedback element throughout the op amp. This op amp circuit carries out the mathematical process of differentiating, producing an output voltage that is "exactly proportional to the change rate without respect to time of the voltage level ". In other words, overall output voltage will fluctuate more quickly or dramatically in response to changes in the input signal generator and input current, creating more of an "spike" in form. Similar to the integrator circuit, the op amp is connected to a capacitance and resistor through an RC network, as well as the reactance (Xc) of the capacitor has a significant impact on how well the Op-amp Differentiator performs.

Op-amp Differentiator Circuit

The capacitors in Figure4 receives the input signal towards the differentiator. A zero output voltage results from the capacitor's suppression of any DC content, which prevents current from flowing to the amplifier's summation point, X. The capacitor's frequency is dictated by the input signal's rate of fluctuation and only permits changes in voltage regulator of the AC type.

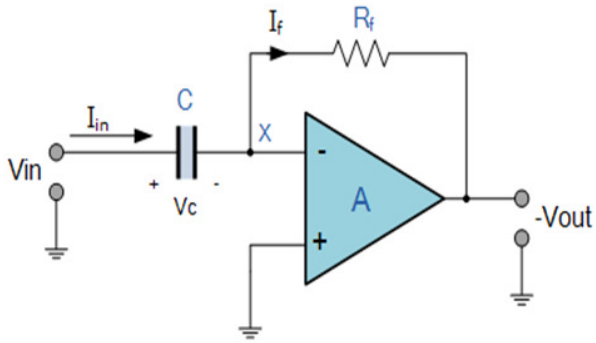

Figure 4: Illustrates the circuit diagram of Op-amp Differentiator Circuit.

The capacitor's "High" characteristic impedance at low frequencies causes a low gain (R/Xc) and lower power voltage from either the op-amp. The capacitance of the capacitor is significantly less at higher frequencies, increasing the gain and power output of the differentiation amplifier. Unfortunately, an op-amp differentiator circuit develops unstable and begins to oscillate with higher frequency. This is primarily caused by the first-order impact, which establishes the op-amp circuit's resonant frequency and results in a second-order response that, at high frequencies, produces an output voltage that is far greater than anticipated. In order to prevent this, the circuit's high frequency gain must be decreased by connecting a second, small-value capacitor throughout the feedback resistor R. The operational amplifier's inverting input contact has zero node voltage, hence the current

through into the capacitor, I will indeed be expressed as:

$$I_{IN} = I_F$$

$$I_F = -\frac{V_{out}}{R_F}$$

The capacitor's charge is equivalent to Capacitance multiplied. Cross-capacitor voltage.

$$Q = C * V_{IN}$$

Consequently, this charge's rate of change is:

$$\frac{dQ}{dt} = C\frac{dV_{IN}}{dt}$$

But $\frac{dQ}{dt}$ is the capacitor current, i

$$I_{IN} = C\frac{dV_{IN}}{dt} = I_F$$

$$-\frac{V_{out}}{R_F} = C\frac{dV_{IN}}{dt}$$

This yields the following optimum voltage output for the op-amp differentiator:

$$V_{out} = -R_F C\frac{dV_{IN}}{dt}$$

As a result, the input voltage VIN's time-dependent derivative is equal to -R*C times the output voltage Vout. Also because input data is linked to the operational amplifier's inverting terminal wire, the negative sign (-) denotes a 180o phase shift. One last thing to note is that, as compared to the prior operational amplifier integrator circuit, the Op-amp Voltage divider has two significant drawbacks. The capacitive input makes it particularly vulnerable to random noise signals, as well as any noise or harmonics existent in the source circuitry will indeed be amplified greater than the input signal itself. This causes the device to be unstable at high frequency, as was already described. This is due to the fact that the output is proportionate to the gradient of the input voltage, hence some kind of bandwidth limitation is necessary to guarantee closed-loop stability.

Improved Op-amp Differentiator Amplifier

Due to the two fundamental flaws described above, "Instability" and "Noise," the simple single resistor as well as single capacitor op-amp differentiator circuitry is not often used to reconstruct the mathematical formula of differentiation. Therefore, an additional resistor, Rin, is connected to the input of both the circuit in order to decrease its total closed-loop gain at higher frequency. The circuit now functions as a differentiator amplifier with shorter wavelengths and an amplifier without resistive feedback during high frequencies, delivering significantly better sound rejection. Introducing the input resistor RIN restricts the differentiator's growth in gain at a ratio of R/RIN. The differentiator responses resistor, R, and a capacitor, C, are connected in parallel to further attenuate higher frequencies.

Op-amp Multivibrator

The Operational Amplifier, or Op-amp as it is more often known, is an extremely adaptable component that may be used in a wide range of electronic circuits as well as applications,

including voltage amplifiers, filters, and signals conditioners. However, the Astable Op-amp Multivibrator is an extremely uncomplicated and incredibly useful op-amp circuit built around in any multipurpose op amp. Multivibrator circuitry may be created using transistor, logic gates, or specialized chips like the NE555 timer, as we learned in our courses on sequential logic. They also observed that, without any external triggering, the as stable multivibrator alternates continually between its 2 unstable modes. However, the issue with using these components to create a stable multivibrator circuit is that more and more additional materials are needed for transistor-based stables, digital stables seem to be typically only usable in integrated electronics, as well as the utilization of a 555 timer may not always produce a symmetrical production without supplemental biasing elements. Furthermore, the Op-amp Multivibrator circuit just needs three resistors, a timing capacitor, plus four other parts to produce a decent rectangular wave signal.

An RC timing network linked to the operational amplifier's inverting input and a potential divider network attached to the second non-inverting input make up the Op-amp Multivibrator, a stable oscillator circuitry which produces a rectangles output waveform. This astable multivibrator, in contrast to the monostable as well as bistable, contains two states, both of which are permanent since it alternates between them continually. The duration of each condition is regulated by the capacitor's loading or discharge via a resistor. The op-amp functions as an analog comparator throughout the op-amp multivibrator circuit. When two input voltages are compared, an op-amp comparator determines if the input voltage is larger or lower than just a reference value, VREF, and outputs either a positively or negatively signal depending just on result.

However, anytime the input voltage becoming measured is close to the reference signal, VREF, the outputs might abruptly flip between its positive, +V(sat), as well as negative, -V(sat), supply rails. This happens due to the open-loop op-amp comparator is particularly sensitive towards the input voltages on its own inputs. The multivibrator circuit's op-amp is set up as a closed-loop Schmitt Trigger circuit to prevent any unpredictable or uncontrolled shifting activities. Think about the circuit.

Op-amp Schmitt Comparator

In Figure 5, the Schmitt trigger op-amp comparator circuit makes advantage of the positive feedback given by resistors R1 and R2 to produce hysteresis. A positive voltage is supplied to the op-non-inverting amp's input whenever Vout is saturating there at positive supply rail because this resistance network is linked between the amplifier's output its non-inverting (+) input. The non-inverting input of the op-amp receives a negative voltage when Vout is connected to the negative positive supply. The measured value, Vref, will depend on the percentage of output voltage supplied back towards the non-inverting input since the two transistors are set up as just a voltage divider network throughout the op-amps output. The provided value for this feedback percent is:

$$\beta = \frac{R_2}{R_1 + R_2}$$

$$V_{out} = V_{SATURATION}$$

$$V_{REF} = V_{out}\frac{R_2}{R_1 + R_2} = \beta V_{SAT}$$

Therefore:

$$\frac{+V_{REF}}{-V_{REF}} = \frac{+\beta V_{SAT}}{-\beta V_{SAT}}$$

Where +V(sat) and -V(sat) represent the positive and negative op-amp DC saturation voltages, respectively. The maximum positive number for the voltage somewhere at inverting input, also known as the positive or upper reference signal, +Vref, is then provided as +Vref = +V(sat), while the maximum significant decline again for voltage there at inverting input, or the lowering reference voltage, is given as -Vref = -V(sat). Therefore, the output voltage lowers to its negative DC saturation voltage if Vin exceeds +Vref, causing the op-amp to flip states. Similarly, the power output will transition from the negatives saturation potential back towards the positive DC saturation value whenever the input voltage drops below –Vref (Figure 5). The difference between both trigger voltage waveform defines the amount more built-in hysteresis provided by the Schmitt comparator because it transitions between both the two saturation concentrations as: Hysteresis equals +Vref -. (-Vref).

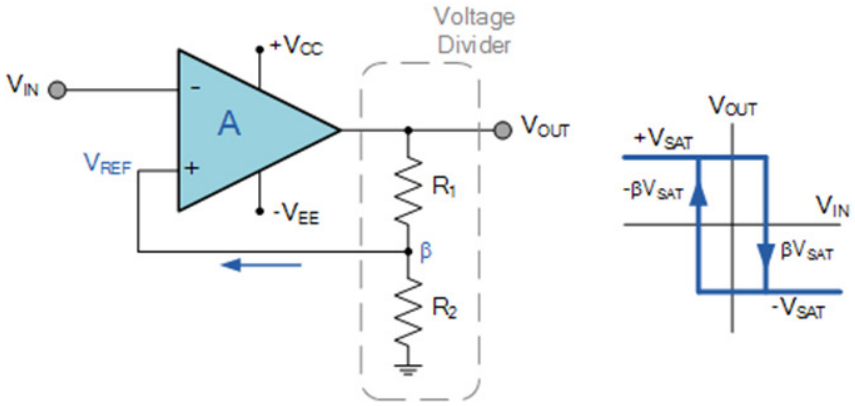

Figure 5: Illustrates the circuit diagram of Op-amp Schmitt Comparator.

Sinusoidal to Rectangular Conversion

Schmitt trigger comparators have various applications outside of their employment as op-amp multivibrator, and one of them is the ability to transform any periodical sinusoidal wave into something like a rectangle waveform so long as the sinusoid's value above the voltage point of reference. In actuality, regardless of the waveform of the input signal, the Schmitt comparator always outputs a rectangular output waveform. In those other words, every voltage input may be any wave structure including complex waveform; it is not required to be a sinusoid. A common operational amplifier, like the 741, may be used to build an Op-amp Multivibrator circuitry along with a few other parts. So because op-amp lacks the necessary frequency, these voltage-controlled non-sinusoidal relaxing synthesizers are often restricted to a few hundred kHz, although they nonetheless make great oscillators.

Op-amp Comparator

In the comparator's open-loop configuration, an electrical decision-making circuits, a very high gain op amp is used (i.e., without a feedback resistor). The Op-amp comparator generates an output signal based on a voltage comparison between two analogue input voltages or a preset reference value, VREF. In other words, to determine which of two power converters is bigger, the op-amp voltage voltage comparator their orders of magnitude. The operational amplifier may be employed with negative feedback to regulate the size of its

output signal throughout the linear area, performing a number of different tasks, as we have seen in earlier courses. It also found that the output voltage, indicated by the formula VOUT = AO(V+ - V-), is controlled by the voltages at the non-inverting and inverting terminals respectively, as well as the open-loop gain (AO) of a standard op amp serves as little more than a defining feature. Voltage comparators, on the other hand, switch their outputs between a number of saturated stages whether using positive feedback or even none feedback at all (open-loop mode), because in the latter situation the amplifier's switching frequency is virtually equal to AV. Due to this large open loop gain, according to the application of a fluctuating input signal which exceeds a specified threshold value, the output from each comparator thereafter swings wholly to either its positive supply rail, +Vcc, and fully toward this negatives positive supply, -Vcc. The open-loop op-amp comparison may appear to be an analog circuit which operates in its nonlinear region because variations in its two input or output, V+ and V-, allow it to behave as a digital bistable device since triggered causes it to have two possible output states, +Vcc or -Vcc. Because the input current was analog but the output is digital, the voltage comparator may well be thought of as a 1-bit electronic to analogue conversion.

Op-amp Comparator Circuit

Let's first assume that, with reference to the op-amp comparison circuit shown in Figure 6, VIN is lower than the DC voltage level close to VREF, or that (VIN VREF). Due to the fact that the non-inverting (positive) input is less than the inverting (negative) output, this same comparator's output will in fact be LOW and located at the negative voltage source, -Vcc.

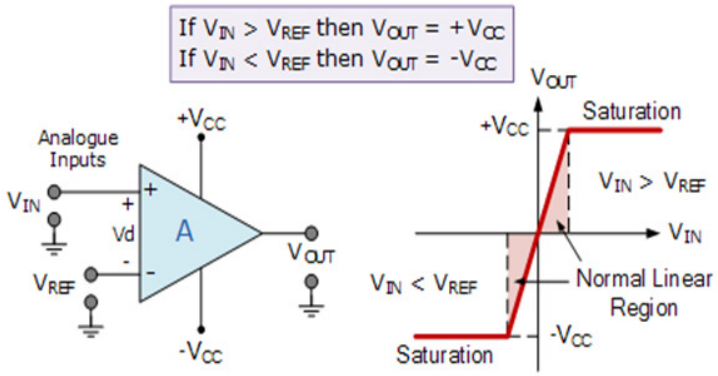

Figure 6: Illustrates the circuit diagram of Op-amp Comparator.

If we now increase the input voltage, VIN, such that its value is greater than the recorded voltage VREF upon the same inverting input, the output voltage soon climbs HIGH forward towards the positive supply voltage, +Vcc, resulting in a negative saturation of the output. If they again reduce the input voltage VIN until it is just less than the reference voltage, the output of the op-amp, acting as a threshold detector, moves back towards to the negative saturation value. The op-amp voltage comparator's output is HIGH whenever the electricity supply on the non-inverting input is greater than the voltage here on input terminal but instead LOW however when the voltage just on non-inverting understanding is lower. This output appears to be dependent on the magnitude of something like the voltage level, VIN with respect to some DC voltage level. This condition is true regardless of whether the input data is connected to the comparator's inverted or non-inverting output. I can also see that the output reference voltage is solely dependent on the op-amps' power supply voltage. Due to the op-high amp's open-loop gain, whose output voltage may potentially go indefinitely high

in both directions (). The op-amp supply wires, which produce VOUT = +Vcc or VOUT = -Vcc, are what restrict it realistically and for obvious reasons. As stated earlier, the basic op-amp comparator compares the input voltage to the predefined DC reference voltage to ascertain that whether output value is positive or negative. A resistor voltage divider is commonly employed to establish the reference input prospective of a comparator, although alternative possibilities include a battery source, a zener diode, or even a potentiometer for a movable reference signal.

CONCLUSION

Owing to the operational amplifier's very high open-loop gain, when it is used with positive feedback—or even without any feedback at all the output saturates to its supply rail, generating one of two separate output voltages depending here on relative values of its own two inputs. Operational amplifiers known as comparators are created specifically to operate in unstable and non-linear open-loop or positive feedback modes. Just two possible values, which roughly correlate to the voltages of the power source, may be produced by them.

REFERENCES

[1] K. You en H. Choi, "Wide bandwidth class-S power amplifiers for ultrasonic devices", *Sensors (Switzerland)*, 2020, doi: 10.3390/s20010290.

[2] J. Nebhen, P. M. Ferreira, en S. Mansouri, "A chopper stabilization audio instrumentation amplifier for iot applications", *J. Low Power Electron. Appl.*, 2020, doi: 10.3390/jlpea10020013.

[3] S. Shukla, J. Immanuel, en P. Bhaskar, "Design and implementation of microcontroller based photoacoustic spectrometer and its applications", *Int. J. Adv. Res. Eng. Technol.*, 2019, doi: 10.34218/IJARET.10.1.2019.001.

[4] Y. Liu, S. Z. Hao, Y. L. Tian, en G. Z. Liu, "Two-dimensional phase sensitive detector and its application to demodulating amplitude modulated image", *Wuli Xuebao/Acta Phys. Sin.*, 2019, doi: 10.7498/aps.68.20190803.

[5] I. Haïk Dunn, R. Daou, en C. Atkinson, "A straightforward 2 ω technique for the measurement of the Thomson effect", *Rev. Sci. Instrum.*, 2019, doi: 10.1063/1.5055826.

[6] G. F. Zhao, J. Ying, L. Wu, en Z. H. Feng, "Eddy current displacement sensor with ultrahigh resolution obtained through the noise suppression of excitation voltage", *Sensors Actuators, A Phys.*, 2019, doi: 10.1016/j.sna.2019.111622.

[7] I. V. Gorbenko, V. Y. Kachorovskii, en M. Shur, "Terahertz plasmonic detector controlled by phase asymmetry", *Opt. Express*, 2019, doi: 10.1364/oe.27.004004.

[8] J. Song *et al.*, "Atomic Resolution Defocused Electron Ptychography at Low Dose with a Fast, Direct Electron Detector", *Sci. Rep.*, 2019, doi: 10.1038/s41598-019-40413-z.

[9] B. Chen, M. He, H. Zhang, Z. Jiang, en B. Hu, "Chromatographic Techniques for Rare Earth Elements Analysis", *Physical Sciences Reviews*. 2019. doi: 10.1515/psr-2016-0057.

[10] G. Blaney, A. Sassaroli, T. Pham, N. Krishnamurthy, en S. Fantini, "Multi-distance frequency-domain optical measurements of coherent cerebral hemodynamics", *Photonics*, 2019, doi: 10.3390/photonics6030083.

CHAPTER 10

OVERVIEW ON WINDOW COMPARATOR

Dr. Trupti VN, Assistant Professor
Faculty of Engineering and Technology, Jain (Deemed-To-Be University), Bengaluru, Karnataka, India
Email id- n.trupti@jainuniversity.ac.in

Abstract:

A device that is often made up of two voltage comparators, whose output shows whether the measured signal falls within such a voltage range defined by two distinct thresholds (an upper threshold and a "lower" threshold). In this chapter author is discussesnegative and positive feedback systems.

Keywords:

Feedback System, Operational Amplifer, Signal, Window Comparator.

INTRODUCTION

To create a window comparator, the preceding inverted and non-inverting conditional operators are effectively combined into a single comparator phase. The window comparator examines input voltage ranges that fall within the set range or windows of values rather than indicating whether a particular voltage is higher or lower than a predefined or fixed voltage point of comparison. This time, instead of only one reference voltage value, every window comparator will additionally have previous two polarities given by a few voltage comparators. One that does so when a specific higher voltage threshold, VREF (Top half), and another one that does so when a specific lower voltage threshold, VREF, are detected (LOWER). Figure 1 windows show the output voltages between some of these two waveforms of greater and lower voltage.

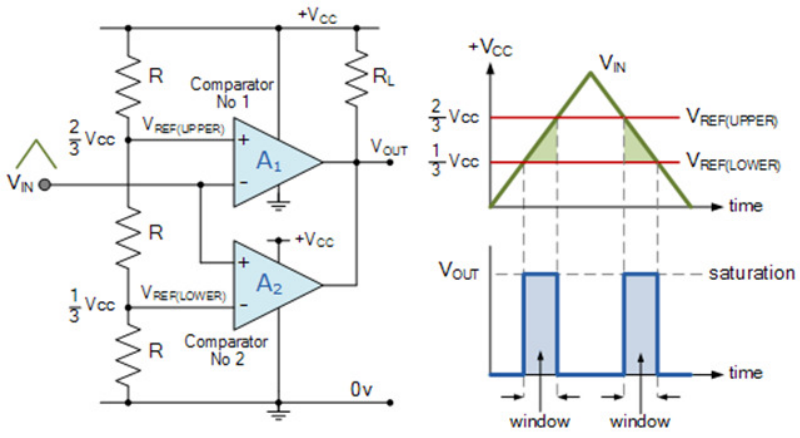

Figure 1: Illustrates the circuit diagram of Window Comparator.

Utilizing the voltage divider network we previously established, we can construct a pretty simple windows comparator circuit through using three resistors of identical value, R1 = R2 = R3 = R. Since all of the resistive character traits are equal, the voltage drops across each resistor will also be the same at 1/3Vcc, the voltage supply. For ease of usage, one may set

the lower output voltages to 1/3Vcc and the higher reference voltage to 2/3Vcc in this basic windows comparison example.

Op-amp Monostable

Op-amp whenever externally triggered, monostable multivibrator are electrical circuits that generate a single timed rectangle output pulse. Creating monostable circuits employing discrete components using digital logic gates is simple, but operational amplifiers may also be used to build monostable circuits, as shown in Figure 2. Op-amp Positive-feedback (or regenerative) switching circuits called monostable multivibrator (one-shot multivibrator) circuitry contain only one stable state and generate output pulses with a predetermined T duration. The monostable circuit changes direction whenever an external trigger signal is applied, and after a predetermined amount of time—either in microseconds, microseconds, or seconds—that is ascertained by RC components, this same monostable controller returns to its initial stable state, where it stays until the subsequent trigger input signal arrives [1].

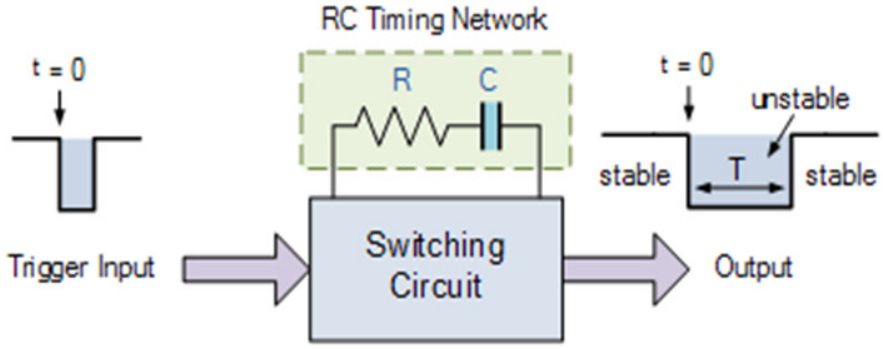

Figure 2: Illustrates the block diagram of Op-amp Monostable.

Op-amp Monostable Circuit

In this design of an inverting op amp, a portion of the output signal—referred to as the feedback fraction—is given back through the resistive network towards the operational amplifier's inverting input. The feedback percentage is consequently negative since it is transmitted back towards the inverting input throughout this fundamental inverting arrangement. The differential voltage level is forced toward zero by this negative feedback setup between both the output as well as the inverting terminal wire [2]. The op-amp generates an enhanced output signal that is 180 degrees out of phase with both the input signal as a consequence of this negative feedback. The result is a balanced as well as stable amplifier working within its linear zone as a result of a drop throughout the output voltage, VO, and a rise in the inverting voltage magnitude, -V, fed back from either the output. Now imagine the same operational amplifier circuit, but with the op-inverting amp's and non-inverting inputs switched [3]. It produces a simple op-amp comparator circuit featuring built-in hysteresis when the feedback signal is sent back towards the non-inverting input as well as the evaluation system is now positive. The operational amplifier that forms the basis of the closed-loop Schmitt trigger circuit for the op-amp monostable multivibrator circuitry employs positive feedback given by the resistors R1 and R2 to generate the necessary hysteresis. The application of positive feedback results in regenerative feedback that supplies the necessary

state dependency, thereby converting the op-amp into something like a bi-stable memory device.

Basic Op-amp Monostable Circuit

Basic op amp monostable in Figure 3 will saturation toward either the positive rail (+Vcc) or the negatives rail (-Vcc) at initial power on (that is, t = 0), because these are the only two solid states permitted by the op-amp. For the time being, let's suppose that the output has shifted in favor of the positive voltage rail (+Vcc). When that happens, the voltage at the non-inverting output, VB, will be equivalent to +Vcc*, where is the feedback percentage.

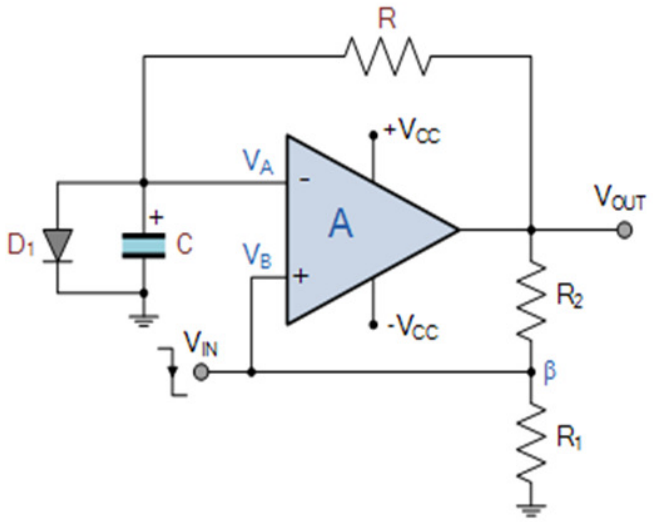

Figure 3: Illustrates the basic circuit diagram of Op-amp Monostable.

The forward volt drop from diode D1 holds the inverting input at 0.7 volts and clamps it to ground (0 volts) to stop it from getting any further positive. The output is therefore steady at +Vcc and the prospective at VA is much lower than that at VB. The forward-biased potential difference of the diode holds the capacitor, (C), which charges up to the same potential of 0.7 volts, there. The 0.7v voltage at VA would now be larger than the voltage at VB because VB is now negative if we were to deliver a negative pulses to the non-inverting input. As a result, the output of the op-amp with a Schmitt configuration changes state and saturates in the direction of the negative supply rail, -Vcc. As a consequence, VB's potential has now become equal to -Vcc*.

The capacitor charges exponentially in the opposite way via the feedback resistor, R, from +0.7 volts downwards to the saturated output that it has just switched to, -Vcc, as a result of this momentary meta-stable condition. Diode D1 develops reverse bias and is hence ineffective. At a constant value t = RC, the capacitor C will discharge. The op-amp changes to its original permanently stable state with the output saturated at +Vcc as soon as that the capacitor voltage at VA reaches the same voltage as VB, or -Vcc*. Note that the capacitor attempts to charge up in reversed to +Vcc but is only able charge to a maximum value of 0.7v provided by the diodes forward voltage drop after the timing interval is through and the op-amps output goes back to its steady position and overwhelms towards to the positive input rail. As shown in this lesson, an Op-amp a multipurpose operational amplifier, such as a 741, plus a few more parts may be used to build a monostable circuit. Even though building

monostable (one-shot) circuits using special devices, digital logic gates, or the widely used 555 IC chip may be simpler, there are occasions when building monostable with op-amps for use in analogue circuits is necessary.

Op-amp Monostable

Op-amp whenever externally triggered, monostable multivibrator are electrical circuits that generate a single timed rectangle output pulse. Creating monostable circuits employing discrete components using digital logic gates is simple, but operational amplifiers may also be used to build monostable circuits. Op-amp Positive-feedback (or regenerative) switching circuits called monostable multivibrator (one-shot multivibrator) circuitry contain only one stable state and generate output pulses with a predetermined T duration. The monostable circuit changes direction whenever an external trigger signal is applied, and after a predetermined amount of time—either in microseconds, microseconds, or seconds—that is ascertained by RC components, this same monostable controller returns to its initial stable state, where it stays until the subsequent trigger input signal arrives (Figure 4)[1].

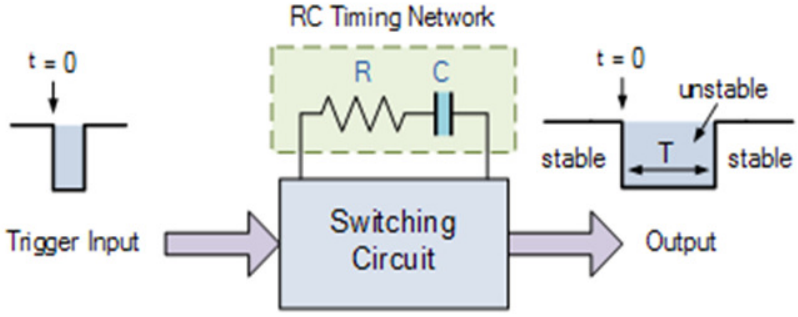

Figure 4: Illustrates the block diagram of Op-amp Monostable.

LITERATURE REVIEW

According to the C. Summatta[4] et al. a window comparator circuit is used in industrial settings to verify the input DC signal level and is connected to safety systems for the identification of false signals. The AND logic circuit serves as the design's foundation. Analogue circuit depending on transistor oscillation, which is defined by the values of impedance and that each input voltage, and window comparator using op-amp or module ICs made up of two distinct comparators and an AND gate were the first two approaches for the window comparator. Based on the characteristics of digital switching levels using MOSFET-resistor voltage references, this research presented a window comparator with digital logic IC. The circuit creates window borders using a potential voltage divider circuit that makes use of a resistor, an N-channel MOSFET, and the threshold voltage of a CMOS logic IC. As it is a relatively simple circuit, no further components are needed. The circuit may be utilized with fast-changing inputs and low voltage. Simulation and experimental data were used to evaluate and assess the performance.

H. Toyokawa et al. [5]created aluminum Schottky diode sensors, CdTe pixel detectors, and photon-counting ASICs. The 200 by 200 pixel hybrid pixel detector has an area of 19.0 mm by 20.0 mm and a pixel size of 200 by 200 mm. Preamplifiers, shapers, 3-level window-type comparators, and 24-bit counters are all features of the photon-counting ASIC SP8-04F10K.

We have carried out energy-resolved X-ray diffraction feasibility investigations. Energy dispersive Laue fellow creatures were used to calculate the lattice spacings of a polycrystalline copper alloy. The dual-window comparator mode was used to conduct simultaneous X-ray diffraction measurements with 61.4 and 122.8 keV X-ray beams on an amorphous silica sample.

J. Song et al. that study describes a background timing-skew calibration method for time-interleaved (TI) ADCs based on mean absolute deviation (MAD). It chooses input samples close to the zero crossing and calculates their MAD value, which is utilized as a measure of the temporal skew, using a single comparator-based windows detector. As the suggested method just calls for taking the absolute value and averaging, it has a minimal computational cost. When used in the background using unknown random inputs, it also offers a quick convergence rate since the MAD value can be precisely predicted with a few amount of samples. In order to validate the suggested method, a 40-nm CMOS prototype 10-bit 2-way TI-SAR ADC is constructed. The SNDR it obtains throughout the whole Nyquist band is above 52 dB. It uses 4.7 mW when operating at 600 MS/s, giving it a Walden figure-of-merit of 24-fJ/conversion-step [6].

In study K. Vasanth et al. [7]to eliminate salt and pepper noise in rank ordering applications, an effective VLSI design for a reduced sorting network (Vasanth sorting) is given. Rank ordering is the fundamental step in the salt and pepper noise reduction process. This paper proposes Vasanth sorting, a unique 2D sorting approach for a fixed 3 3 window. To sort the nine window components using Vasanth sorting, just 25 comparators are needed. Using 25 comparators, a parallel architecture is created for Vasanth sorting. An 8-bit data comparator serves as the parallel architecture's processing component (Two cell comparator). The effectiveness of the suggested sorting method is contrasted with another method that is intended for the XCV1000-5bg560 on XILINX 7.1i and the XC7V2000T-2flg1925 on XILINX 14.7 project manager, accordingly, using Modelsim 10.4a for simulation and the XST compiler tool for VHDL synthesis. As compared to currently used sorting methods, it was discovered that the parallel architecture created for Vasanth sorting only needs a quarter of the space on an FPGA. The suggested architecture's combinational latency was also two times smaller than that of its competitors. The logic required 7mw of electricity to operate. Vasanth sorting is thus a preferable option when compared to other rank ordering approaches because of the aforementioned performances.

Z. Ding et al.[8] presented a successive approximation register (SAR) analog-to-digital converter (ADC) with a comparator based on a voltage-controlled oscillator (VCO). In order to determine a VCO-comparator choice, the connection between the input voltage and also the number of oscillations cycles (NOC) is investigated, suggesting an inherent coarse quantization in addition to the standard comparison. The NOC is presented and examined as a design parameter while taking noise, metastability, but also tradeoff factors into account. The NOC is used to increase the power efficiency of VCO-based SAR ADCs by skipping a fixed amount of SAR cycles. An adaptive bypassing strategy is put forward to deal with the process, voltages, and temperature (PVT) fluctuations by monitoring and modifying window widths in the background. The ADC reaches a high effective number of bits at 9.71 b at 10 MS/s while being manufactured in a 40-nm CMOS technology. A broad variety of supply voltages and sampling speeds result in a typical figure of merit (FoM) of 2.4-6.85 fJ/conv.-step. The proposed ADC is shown to be resistant across PVT changes without any off-chip calibration or tuning by measurement under normal, fast-fast, and slow-slow process conditions over a temperature ranging from 0 °C-100 °C.

I. Stojkovićet al.[9]the possibility of directly measuring the concentration of 14C activity in wastewater without subjecting samples to chemical pretreatment is investigated in this paper. This approach would have the advantages of rapidity, low cost, and simplicity of radio analysis, which are desirable in nuclear emergency situations. A methodology using liquid scintillation counting (LSC) has been put into practice and refined. The procedure presupposes combining a scintillation cocktail (Permafluor E+ and Ultima Gold AB cocktails were tried) with the water sample. The Wallac 1220 Quantulus Ultra Low Level Liquid Scintillation Spectrometry was used to conduct the measurements. The approach was optimized by choosing the best water-to-cocktail volume ratio, the best counting window, adjusting the PAC (Pulse Amplitude Comparator) parameter based on the greatest FOM (Figure of Merit) value obtained, and evaluating the detection limit and efficiency. It has been noted that interference with those other beta emitters, which are often found in wastewater samples, is the major issue with such a technique. It is also possible to quantify the contribution of additional high-energy beta emitters to the findings of the 14C content experiment and to remove low-energy counts which would arise from 3H. The limitations of the method, as well as its accuracy and precision, have been taken into account by analyzing the data from measurements made on wastewater samples. Its use is restricted to 14C screening of samples with 14C activity that are much greater than those of the ambient (surface and ground) waters. The findings that have been presented might serve as guidelines for the development, improvement, and use of the quick 14C screening approach in other labs.

M. Jahns et al.[10] determined the resonance energy range from a measured -ray spectrum is an important aspect of Mössbauer (MB) spectroscopy. The selection of the photons with the MB transition energy necessitates quick processing since the detection of the complete -ray source spectrum creates significant count rates. The primary electronics board of the MIMOS II instrument, designed and constructed by the GöstarKlingelhöfer group at the TU Darmstadt with JOGU Mainz, implements numerous sets of two comparator units that use fast operational amplifiers that establish a specific energy window. Reasonably stable reference voltages are used to establish the thresholds in these analog circuits. Modern rapid microcontroller-based analogue-to-digital converters (ADC), like the Arduino Due, exhibit improved signal-to-noise ratio and the potential to extend Mössbauerspectroscopy to two dimensions.

N. Liakopoulos et al.[11] conducted a research on a class of naturally occurring long-term budget restrictions on online convex optimization algorithms with reliability assurances or total consumption limitations. Prior research by Mannor et al. (2009) has shown that in this general scenario, obtaining 0% regret is impossible if indeed the functions determining the agent's budget are selected by an opponent. By adding the concept of a "K-benchmark," or a comparator that fulfills the issue's given budget for any window of length K, we improve the agent's regret meter to get around this difficulty. For K = T, Mannor et al. (2009)'s impossibility analysis is recovered; however, for K = o (T), we demonstrate that it is feasible to reduce regret while still satisfying the problem's long-term budget restrictions. We do this using a careful online Lagrangian descent-based online learning algorithm (COLD) for which we develop precise constraints for the incurred regret for residual budget violations.

According to the S. Chang et al.[12]A 12-bit asynchronous successive approximation register (SAR) analog-to-digital converter (ADC) built using 40nm CMOS technology is shown in this work. A comparator built on a VCO is used to adaptively modify the noise level, and its oscillations number is used to skip superfluous cycles to save energy. To overcome the settling concerns and improve the bypass window size, a 1-bit split-and-

recombination redundancies and a digital error correction are suggested. The ADC's sampling rate, which is one of highest among SAR ADCs with such a single time-domain comparison, is up to 30 MS/s. The ADC generates a figure of merit (FoM) of 5.69 fJ/conversion-step with an SFDR of 85.35 dB and 11.12-bit ENOB using Nyquist input requiring 0.38mW at a 1.1V supply.

T. Marukameet al. [13]a resistive synaptic device-based, low-power, "static-type" neural network (NN) circuit was created and tested. The circuit consists of current sources, cross switches for inputs, comparator firing functions for binary output, and variable resistors for synaptic weights. With regard to the kinds of current sources and also the resistance-change ratios of the variable resistors, nonlinearity analysis of operation conditions in such circuits was carried out. So, it was made clear what operating window was required to achieve both operation stability and low energy consumption of less than 1 mW for 1024 synapses. Memristive synaptic devices using WOx/MgO were created and studied in terms of spike-timing-dependent neuroplasticity and nonlinear switching enabling learning in order to enhance NN performance.

DISCUSSION

Op-amp Monostable Circuit

In this design of an inverting op amp, a portion of the output signal—referred to as the feedback fraction—is given back through the resistive network towards the operational amplifier's inverting input. The feedback percentage is consequently negative since it is transmitted back towards the inverting input throughout this fundamental inverting arrangement. The differential voltage level is forced toward zero by this negative feedback setup between both the output as well as the inverting terminal wire [2]. The op-amp generates an enhanced output signal that is 180 degrees out of phase with both the input signal as a consequence of this negative feedback. The result is a balanced as well as stable amplifier working within its linear zone as a result of a drop throughout the output voltage, VO, and a rise in the inverting voltage magnitude, -V, fed back from either the output. Now imagine the same operational amplifier circuit, but with the op-inverting amp's and non-inverting inputs switched [3]. It produces a simple op-amp comparator circuit featuring built-in hysteresis when the feedback signal is sent back towards the non-inverting input as well as the evaluation system is now positive. The operational amplifier that forms the basis of the closed-loop Schmitt trigger circuit for the op-amp monostable multivibrator circuitry employs positive feedback given by the resistors R1 and R2 to generate the necessary hysteresis. The application of positive feedback results in regenerative feedback that supplies the necessary state dependency, thereby converting the op-amp into something like a bistable memory device.

Basic Op-amp Monostable Circuit

Basic op amp monostable in Figure 5 will saturation toward either the positive rail (+Vcc) or the negatives rail (-Vcc) at initial power on (that is, t = 0), because these are the only two solid states permitted by the op-amp. For the time being, let's suppose that the output has shifted in favor of the positive voltage rail (+Vcc). When that happens, the voltage at the non-inverting output, VB, will be equivalent to +Vcc*, where is the feedback percentage.

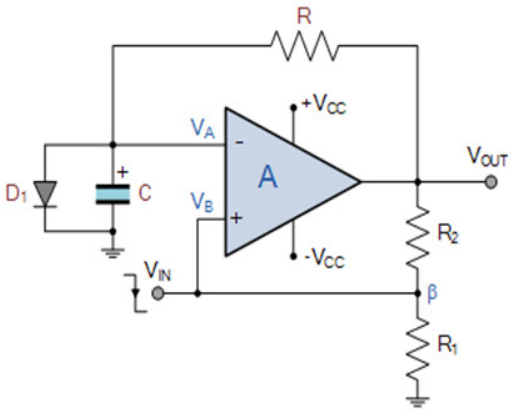

Figure 5: Illustrates the basic circuit diagram of Op-amp Monostable.

The forward volt drop from diode D1 holds the inverting input at 0.7 volts and clamps it to ground (0 volts) to stop it from getting any further positive. The output is therefore steady at +Vcc and the prospective at VA is much lower than that at VB. The forward-biased potential difference of the diode holds the capacitor, (C), which charges up to the same potential of 0.7 volts, there. The 0.7v voltage at VA would now be larger than the voltage at VB because VB is now negative if we were to deliver a negative pulses to the non-inverting input. As a result, the output of the op-amp with a Schmitt configuration changes state and saturates in the direction of the negative supply rail, -Vcc. As a consequence, VB's potential has now become equal to -Vcc*.

The capacitor charges exponentially in the opposite way via the feedback resistor, R, from +0.7 volts downwards to the saturated output that it has just switched to, -Vcc, as a result of this momentary meta-stable condition. Diode D1 develops reverse bias and is hence ineffective. At a constant value t = RC, the capacitor C will discharge. The op-amp changes to its original permanently stable state with the output saturated at +Vcc as soon as that the capacitor voltage at VA reaches the same voltage as VB, or -Vcc*. Note that the capacitor attempts to charge up in reversed to +Vcc but is only able charge to a maximum value of 0.7v provided by the diodes forward voltage drop after the timing interval is through and the op-amps output goes back to its steady position and overwhelms towards to the positive input rail. As shown in this lesson, an Op-amp a multipurpose operational amplifier, such as a 741, plus a few more parts may be used to build a monostable circuit. Even though building monostable (one-shot) circuits using special devices, digital logic gates, or the widely used 555 IC chip may be simpler, there are occasions when building monostable with op-amps for use in analogue circuits is necessary.

Feedback Systems

Whether the output voltage is either positive or negative, a feedback system sends part or all of it back to the input. Although they handle signals, feedback systems called signal processors. The processing portion of a feedback system may be electrical or mechanical, with circuits ranged from being very simple to being highly complex. Simple digital feedback systems may well be constructed utilizing microprocessors and electronic components, while more complex digital feedback systems could be constructed using discrete or isolated components like transistors, resistance, capacitance, etc (ICs) [14]. As people have seen, open-loop systems are merely that—open ended—and do not attempt to take into account changes in circuit conditions or changes in load conditions caused by variations in circuit

characteristics, including such amplifier and consistency, temperatures, supply voltage fluctuations, and/or external disturbances. However, the addition of Feedback could entirely eliminate, or at the very least greatly reduce, the effect of these "open-loop" variations [15]. An error signal is produced by sampling the output signal and then feeding it backwards into the inputs in a feedback loop. In the previous step on closed-loop systems, creators discovered that feedback has been typically composed of a sub-circuit that allows a portion of the output voltage from such a framework to keep changing the effective incoming signal in in order to generate a response that may be noticeably different from either the reaction produced in the apparent absence of such feedback. Feedback systems are useful and often used in high power applications, oscillators, logic controllers, as well as other types of electronic systems. However, for feedback to be a valuable tool, it must be under control because an uncontrolled system could fluctuate or cease to function. The following is a basic description of a feedback system:

Feedback System Block Diagram Model

There are a number of compelling reasons why feedback is applied and exploited in electronic circuits, starting with the fundamental feedback loop of sensing in Figure 6 and moving on to control and actuation. One can accurately regulate circuit features like the system gain and responsiveness [16]. It is possible to make circuit characteristics independent of environmental factors like supply voltages and temperature changes. The non-linear properties of the components employed may significantly minimize signal distortion. A circuit or system's frequency response, gain, and bandwidth may be readily modified to fall within certain parameters. Negative feedback and positive feedback are the sole two primary forms of feedback control, despite the fact that there are several more types of control systems.

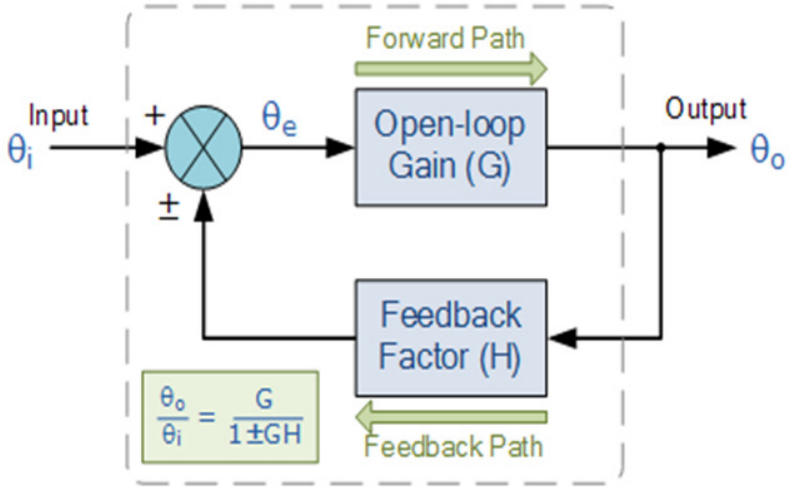

Figure 6: Illustrates the block diagram of Feedback System.

Positive Feedback Systems

A "positive feedback control system," where another feedback is "in-phase" with both the input, uses a controller to establish the set point and corresponding outputs. Positive (or regenerative) feedback seems to have the effect of "raising" the system's gain, meaning that the gain will be greater overall with supplied feedback than one without input. For example,

if someone complements him or gives us constructive criticism, you could feel energized and more upbeat about yourself. However, excessive praising and positive feedback may elevate the system gain disproportionately in electromagnetic and control systems, which might cause oscillatory circuit reactions since it increases the power of the useful original signal. Figure 7 shows an electrical amplifier focused on an op amp, also known as an op-amp., might be an instance of a positive feedback mechanism.

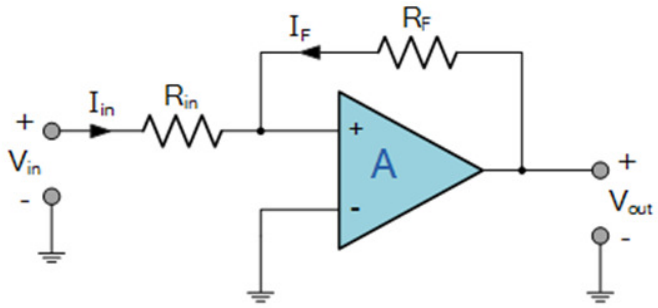

Figure 7: Illustrates the block diagram of Positive Feedback Systems.

Positive feedback control of the op-amp is achieved by sending a small fraction of the output voltage signal from Vout directly to the non-inverting (+) input terminal via the feedback network, RF. When the input voltage Vin is positive, the op-amp enhances the positive signal to produce a more positive output. A portion of this power output is returned to the input through the feedback network. As a consequence, the output voltage rises more, the input voltage changes to the positive side, and so on. The positive supply rolling stock saturation of the output finally occurs. Whenever the input voltage Vin also goes negative, the op-amp reaches saturation at its negative power source. One can clearly see that positive feedback prohibits the circuit from functioning as just an amplifier since even when using positive feedback loops, "more goes to more" and "fewer leads to less" as the output voltage quickly saturates between someone positive supply or the other.

If the loop gain is positive for just about any system, the frequency response will indeed be Av = G /. (1 – GH). If GH = 1, the circuit will start to self-oscillate, which is useful if you want to build an oscillator because no input signal is needed to maintain oscillations at that point. Although it is generally considered undesirable, such characteristic is used in electronics to provide a very rapid switching response to a situation or signal. Positive feedback is used in hysteresis, which is when a device or system maintains a certain state until an input crosses a particular threshold. The term "bi-stability" refers to this sort of behavior, which is often connected to digital switching components like multi-vibrator and logic gates. Positive feedback, also known as regenerative feedback, is often employed in oscillatory circuits like oscillators as well as timing circuitry since it has been shown to enhance gain and the potential for instability in a system, which may result in self-oscillation.

Negative Feedback Systems

The feedback is "out-of-phase" with both the initial input, which causes the set point as well as output values of the "negative control system" to be subtracted from each other. Gain "reduces" as a result of negative (or degenerative) feedback. For example, people could feel depressed and lack energy if someone criticizes you or gives others unpleasant feedback about something [17]. Because although negative feedback produces strong circuit responses,

improves stability, and increases a system's operating bandwidth, the majority of control and feedback systems were degenerative, reducing the effects of the gained. Even during feedback process, a component of the output voltage, for example a voltage or a current is used as an input. Whenever the feedback portion is in the opposite amplitude or phase ("anti-phase") of an original signal, it is referred to as negative feedback.

Positive feedback increases or decreases the input signals, which seems to have various advantages for control system stability and design. Negative feedback, for instance, affects the input in such a way that the alteration is cancelled out if the system's outputs changed for any reason. Feedback reduces a system's overall gain, with the degree of reduction variable based on the system's open-loop gain. Negative feedback also reduces distortion, noise, and change sensitivity while increasing system bandwidth reducing input and output impedances. Inside of an electrical system, either positive or negative feedback is unidirectional in its direction. Signaling that signals emanating from either the output or the input may only go in one way in the system. As a consequence, the system's loop gain, G, is unaffected by the load and source inductance and capacitance. Feedback necessitates a closed-loop system, necessitating the presence of a summation point. In certain types of systems having negative feedback, the summing point plus junction was at its input subtracts the signal is generated from the receiving feedback signal to produce an error signal, which is what propels the system. The feedback signal, as illustrated in Figure 8, must be eliminated from either the input signal if the system seems to have a positive gain in condition for the response to be negative

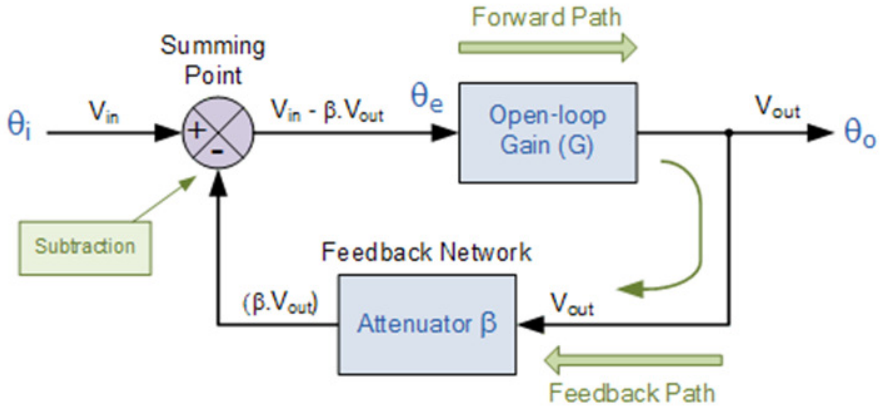

Figure 8: Illustrates the block diagram of Negative Feedback Systems.

The circuit shows a system having positive feedback and gain, G. The summing junction creates the error signal Vin-G, whose controls the system, was at its input by deducting the feedback path from the input signal.

Negative Feedback System circuit

Negative feedback control of an amplifiers is achieved by applying a small amount of the output signal generated at Vout back to the inverting (-) input terminal via the feedback network, Rf (Figure 9).

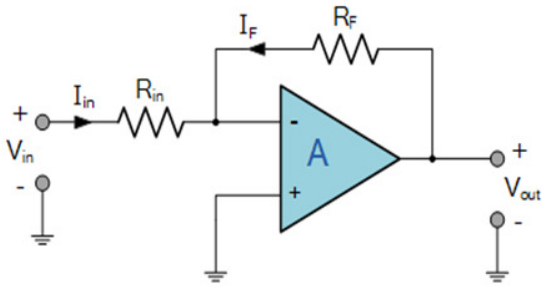

Figure 9: Illustrates the circuit diagram of Negative Feedback Systems.

Whenever the input voltage Vin remains positive, the op-amp amplifies a positive signal, but because it is connected to the inverting terminal of an apparatus like an amplifiers, the output is much more negatively polarized. A portion of this output voltage is returned to the input via the Rf feedback network. Since the input voltage is decreased as a consequence of the negative feedback signals, the output voltage is also decreased, and vice versa. The output will eventually stabilize and arrive at a value determined by the performance gain of Rf Rin. The op-output amp's is reversed and then becomes positive in a same way if the inputs voltage Vin changes to the negative, amplifying the negative incoming signal. Thus can see that negative feedback makes it possible for the circuit to function as an amplifier as soon as the output surpasses the saturation limits. Because more leads to much less in negative feedback mechanism and less contributes to more in positive feedback loops, it is evident that the feedback mechanism controls and remains stable the voltage output.

The frequency response will be if the frequency response is positive for any system:

$$A_V = \frac{G}{1 + GH}$$

Since negative feedback systems are frequently more stable then positive intervention programs, they are commonly utilized in amplifier industrial process control applications. That whenever a negative feedback system doesn't oscillate on its own at any frequency until a certain circuit condition is present, it is said to be stable [18]. A further advantage of negative feedback is that it increases the robustness of control systems to inputs and component values that fluctuate erratically. Naturally, nothing else is free, therefore it should be used with caution since negative feedback significantly alters how a system functions.

Effects of Negative Feedback

If the open-loop gain, G, is actually quite large, the combined gain of the two systems will be almost equal to 1. G will be substantially more than 1 if this is the case. As long as G is still a significant number, even if the open-loop gain decreases due to frequency or simply the effects of systems ageing, the overall system gain does not change much. Negative feedback thereby helps to reduce the effects of gain change, leading to gain stability.

CONCLUSION

Positive feedback happens to accelerate change or output: a reaction's outcome is amplified to accelerate its occurrence. Negative feedback is used to lessen change or output, which helps the system return to a stable condition by reducing response results. Positive feedback amplifies changes such that modest disturbances may lead to significant changes. A system is considered to be in an unstable equilibrium if there is positive feedback to any alteration from its present state while it is in equilibrium.

REFERENCES

[1] K. Fan, J. Hao, Q. Tan, en M. Cai, "A monostable hybrid energy harvester for capturing energy from low-frequency excitations", *J. Intell. Mater. Syst. Struct.*, 2019, doi: 10.1177/1045389X19873420.

[2] K. Fan, M. Cai, H. Liu, en Y. Zhang, "Capturing energy from ultra-low frequency vibrations and human motion through a monostable electromagnetic energy harvester", *Energy*, 2019, doi: 10.1016/j.energy.2018.12.053.

[3] Z. Xie, S. Zhou, J. Xiong, en W. Huang, "The benefits of a magnetically coupled asymmetric monostable dual-cantilever energy harvester under random excitation", *J. Intell. Mater. Syst. Struct.*, 2019, doi: 10.1177/1045389X19879999.

[4] C. Summatta, T. Phurahong, W. Rattanangam, en W. Chaiyong, "Low-cost and Compact Window Comparator Circuit with MOSFET-Resistor Voltage References", 2019. doi: 10.1109/ICPEA.2019.8818512.

[5] H. Toyokawa *et al.*, "Development of CdTe Pixel Detectors for Energy-Resolved X-ray Diffractions", 2019. doi: 10.7566/jpscp.24.011015.

[6] J. Song, K. Ragab, X. Tang, en N. Sun, "A 10-b 600-MS/s 2-Way Time-Interleaved SAR ADC with Mean Absolute Deviation-Based Background Timing-Skew Calibration", *IEEE Trans. Circuits Syst. I Regul. Pap.*, 2019, doi: 10.1109/TCSI.2019.2907581.

[7] K. Vasanth, E. Sindhu, en R. Varatharajan, "VLSI architecture for Vasanth sorting to denoise image with minimum comparators", *Microprocess. Microsyst.*, 2019, doi: 10.1016/j.micpro.2019.102880.

[8] Z. Ding, X. Zhou, en Q. Li, "A 0.5-1.1-V Adaptive Bypassing SAR ADC Utilizing the Oscillation-Cycle Information of a VCO-Based Comparator", *IEEE J. Solid-State Circuits*, 2019, doi: 10.1109/JSSC.2018.2885554.

[9] I. Stojković, N. Todorović, J. Nikolov, I. Krajcar Bronić, G. Bátor, en T. Kovács, "Investigation of fast screening LSC method for monitoring 14C activity in wastewater samples", *Radiat. Meas.*, 2019, doi: 10.1016/j.radmeas.2018.12.004.

[10] M. Jahns *et al.*, "An Arduino based Mössbauer spectrometer", *Nucl. Instruments Methods Phys. Res. Sect. A Accel. Spectrometers, Detect. Assoc. Equip.*, 2019, doi: 10.1016/j.nima.2019.06.003.

[11] N. Liakopoulos, A. Destounis, G. Paschos, T. Spyropoulos, en P. Mertikopoulos, "Cautious regret minimization: Online optimization with long-term budget constraints", 2019.

[12] S. Chang, X. Zhou, Z. Ding, en Q. Li, "A 12-bit 30MS/s SAR ADC with VCO-based comparator and split-and-recombination redundancy for bypass logic", 2019. doi: 10.1109/ISCAS.2019.8702448.

[13] T. Marukame *et al.*, "Nonlinear operation of static-binary neuron circuits and dynamic memristive devices for STDP learning", 2019. doi: 10.1109/ISCAS.2019.8702643.

[14] P. Zangheri, T. Serrenho, en P. Bertoldi, "Energy savings from feedback systems: A meta-studies' review", *Energies*. 2019. doi: 10.3390/en12193788.

[15] J. Reszel *et al.*, "Use of a maternal newborn audit and feedback system in Ontario: A collective case study", *BMJ Qual. Saf.*, 2019, doi: 10.1136/bmjqs-2018-008354.

[16] T. O'Neill *et al.*, "Introducing a scalable peer feedback system for learning teams", *Assess. Eval. High. Educ.*, 2019, doi: 10.1080/02602938.2018.1526256.

[17] P. Anand en B. Bhuvan, "An alternate, discrete-time approach to the analysis of continuous-time negative feedback systems", 2019. doi: 10.1109/TENCON.2019.8929536.

[18] L. Keviczky, R. Bars, J. Hetthéssy, en C. Bányász, "Negative feedback", in *Advanced Textbooks in Control and Signal Processing*, 2019. doi: 10.1007/978-981-10-8321-1_4.

CHAPTER 11

AUDIO DIFFERENCE AMPLIFIER INPUT RESISTANCE

Dr. Raghu N, Associate Professor
Faculty of Engineering and Technology, Jain (Deemed-To-Be University), Bengaluru, Karnataka, India
Email id- n.raghu@jainuniversity.ac.in

Abstract:

The input stage emitter connected logic gates and switch are both implemented as differential amplifiers. While acting as a switch, the "left" base/grid serves as the signal input while the "right" base/grid remains grounded; this same right collector/plate serves as the output. In this chapter author is discusses frequency amplifiers for audio and amplifiers for intermediate frequency.

Keywords:

Amplifier, Circuit, Gain, Input Resistance, Signal, Signal Sources.

INTRODUCTION

When a difference amplifier circuit is carefully examined, one oddity of its inputs becomes apparent: the resistances to ground are different. This is not an issue for signal sources with extremely low output impedances, but in other cases this "imbalance" is cause for worry. With the aid of an analog circuit modeling computer application like P- Spice, we can quickly examine a difference amplifier. The outcome amply Illustrates how the two inputs are interdependent. Input resistance is often defined as a change in input voltage divided by a matching change in input current (Rin). But, in this instance, we are talking to the product of the input voltage and the accompanying change in input current brought about by the application of a voltage to the other input. Since there doesn't seem to be an industry-accepted name or phrase to express this, the author has rather arbitrarily chosen to use the term "source load resistance" (SLR) for this discussion. If any readers are photographers and misunderstand this to refer to a "single lens reflex" camera, they should be excused. Imagine a unity-gain difference amplifier built in P-Spice with an AC sine wave (4 kHz, 1 V peak) on the non-inverting input and 1 VDC on the inverting input (INV) (NI), as shown in Figure 1.

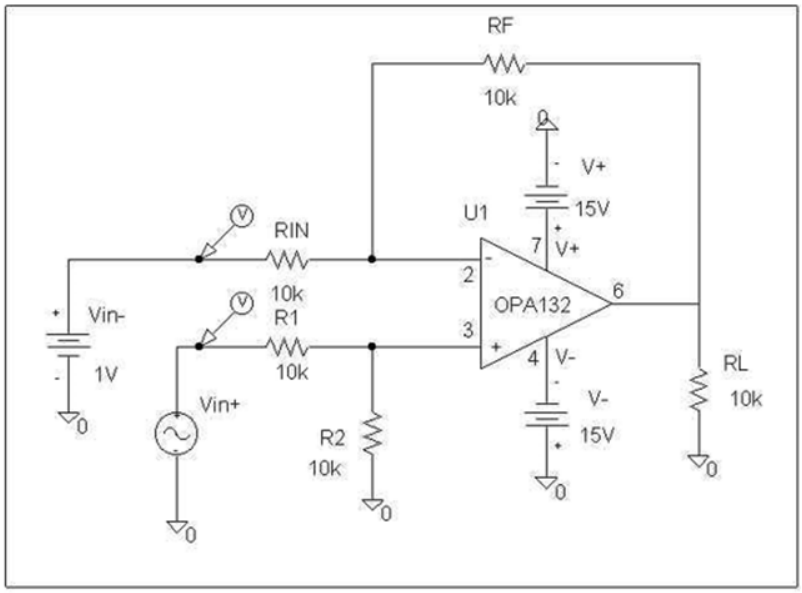

Figure 1: Illustrates the Schematic Capture Drawing: Simulated Unity- Gain Difference Amplifier with Two Independent Signal Sources.

The AC voltage that appears on the op amp's NI (+) input causes the INV (-) input to be equal to it, as predicted, as a result of the op amp's negative feedback or servo action. This AC voltage mostly on INV input causes a fluctuating voltage drop from across input resistor RIN since one end of it is connected to a fixed 1VDC signal source. The input resistor RIN's current fluctuates along with changes in the voltage across it. The burden on the signal source of this input varies. Surprise

When the "resistance" of the load experienced by that of the source connected to the inverting input of the differential amplifier is computed using "Ohm's Law," the "resistance" of the INV input exhibits a significant fluctuation because of the voltage provided to the other input. Given the numbers employed in this example, the diff amp's inverting input offers a load to its source that ranges between 20k and around 6k ohms. The input SLR for both inputs. In reality, there won't be any voltage drop from across input resistor if the voltage upon that NI input is double that on the INV input (assuming R1 and R2 have identical values in this case). The INV input SLR becomes infinite when there is no current flowing through this resistor. Any more voltage upon that NI input will result in current flowing backwards and a negative SLR calculation. These factors only apply when two separate single-ended signal sources are powering a difference amplifier's inputs. Another tale is the differential input resistance. The NI signal source will modify the output of the INV signal source unless the INV signal source has a particularly low output impedance. In contrast, the NI input behaves nicely and remains consistent, in this case at 20k ohms.

An amplifier is used to increase the amplitude of a signal, without changing other parameters of the waveform such as frequency or wave shape. Amplifiers are one of the most commonly used circuits in electronics and perform a variety of functions in a many electronic systems. The amplifier symbol gives no detail of the types of amplifiers described, it only gives the direction of signal flow and can be assumed as flowing from left to right of the diagram. Different types of amplifiers are also often described in system or block diagrams by name.

LITERATURE REVIEW

Deepak Kumar et al.[1] in that study discusses a unique through-line, weakly coupled, broad band (300–700 MHz), high power, and directional sensor including measured performance and large-scale deployment. The measurement of the forward and reflected powers in the center of high-power solid-state radio frequency amplifiers called for a significant amount of them. Instead of requiring an external level detection and processing device, unlike ordinary directional couplers, its output data may be displayed directly in dBm units using a PC or any controller with a serial port. The primary line of the coupler is built with a robust coaxial construction and an aperture connected to a secondary line that resembles a micros trip in order to determine high power. A microcontroller circuit internally processes the signals at coupled and isolated ports in preparation for streaming them over serial interface. Repeatable performance, low insertion loss (0.05 dB), suitability for thru-line high-power operation (1 kW average and 5 kW pulse power), direct power reading using internal identification and digital circuit, simplicity of fabrication, wideband operation (more than 1 octave), excellent directivity (minimum 20 dB), and a compact design are the benefits gained in this design (palm sized).

Ahmed NabihZaki et al.[2], [3]based on frequency spacing and an optimization approach for the amplifier section stage, the research offers the average power model of optical Raman fiber amplifiers. The frequency spacing is chosen from 0.2 to 1 nm, and the amplifier section phase is taken from 25 to 75 km. Variations in operational wavelength range but also bit time period are assessed in relation to input/output Raman signal fluctuations. The optical transmitter's acceptable input signal strength is set to -10 dBm, and a return to zero modulation code is used with the available data rate of 10 Gb/s. 64 channels are combined to provide a variety of users with appropriate power levels.

Lee, Y. H. et al. [4]Precision physics investigations may benefit from the low-noise performance of radio-frequency (RF) amplifiers that use direct current (DC) superconducting quantum interference devices (SQUID). The operating circumstances and various SQUID parameters affect the gain curves of SQUID RF amplifiers. In order to analyze very weak RF signals from microwave cavities with ultra-low temperatures and strong magnetic fields in axion search studies, we are constructing SQUID RF amplifiers. In this work, we developed, made, and analyzed SQUID RF amplifiers using various SQUID parameters, including coupling capacitance inside the input coil, the number of input coil turns, and the shunt resistance value of both the junction. We then compared the outcomes.

According to HoomanRashtian et al. [5]the difficulties of building distributed amplifiers under frequencies near to the transistor fmax are addressed in this study. In comparison to low-pass transmission lines, bandpass transmission lines enhance the distributed amplifier's maximum operating frequency. Moreover, a unique gain-boosted cascode structure with internal feedback is used to increase the amplifier's bandwidth and maximum operating frequency while also canceling some of the loss in the input line. The suggested amplifier works at frequencies up to 0.67 times the transistors' maximum operating frequency. A 0.13-m SiGe method is used to create two proof-of-concept prototypes with a maximum frequency of 210 GHz. The first prototype has a bandwidth of 90 GHz at the central frequency of 97 GHz as well as an average gain of 14.4 dB from 52 to 142 GHz, while the second one reaches an average gain of 18.6 dB between 48 to 135 GHz (bandwidth of 87 GHz at the center frequency of 91.5 GHz).

Toniato, A. et al.[6]using Weyl semi-metals, such as WP2 and MoP2, authors suggest and simulate a new amplifier in this study. It has been shown that these topological materials

have an extremely high magnetoresistance at freezing circumstances. In the suggested device, a gate current creates a local magnetic field that regulates the Weyl semi-metal channel's resistivity and the output current that results. Thermal modeling is used to assess the consequences of self-heating and magnetic field simulations are performed to enhance the device design. An analytical 3D model of magnetic fields, resistivity, and a small-signal model are used to simulate device functioning. Findings indicate that the suggested device could provide high gain (20–30 dB) while using just 40 W of DC power and having high transition frequencies. Given that it can be integrated under lower cryostat temperature stages and has a low power dissipation, this kind of device has the potential to replace HEMTs in quantum computers.

MaryamSajedin et al. [7]the most advanced microwave and radio frequency power amplifiers for next-generation wireless communication standards are included in this study. We'll go through the Doherty amplifier's fundamental working theory and its flawed behavior, which has its roots in transistor properties. Additionally, advanced design architectures for improving the Doherty power amplifier's performance in terms of greater efficiency and broader bandwidth characteristics, in addition to the compact design techniques of Doherty amplifier that satisfy the needs of legacy 5G handset applications, will be discussed.

Neumeyer, S.et al.[8] the two-to-one frequency ratio between both the parametric and direct excitation as well as the relationship between the direct excitation frequency and the system's inherent frequency may alter in frequency tuned parametric amplifiers. Theoretically, these effects are examined using a Duffing-Mathieu equation as that of the model system, and practically, they are examined using a macro cantilever beam. The approach of varied amplitudes is used to determine the approximate analytically steady-state vibration amplitudes, which are then compared to the results of direct numerical integration and demonstrate excellent agreement. According to theoretical expectations, several of the amplitude-frequency curves seem to collapse with detuned super threshold parametric amplification. In certain regions of the amplitude-excitation detuning domain, experiments reveal a reduction in the maximum steady-state vibration amplitude, whilst in other regions frequency detuning may result in an increase in the maximum steady-state vibration amplitude. So, depending on the application, such as for sensors or energy harvesters, frequency detuning is a trait that may be intentionally avoided or used. We provide bitable magnified steady-state responses that were achieved experimentally, which also confirm theoretical conclusions.

AkaninyeneObot et al.[9] presented the design and analysis of a multistage common emitter (CE) amplifier that has a higher voltage gain than a single stage CE amplifier. The single - phase CE amplifier design served as the starting point for the design process. The CE amplifier's design requirements were laid forth. The single stage CE amplifier that was built served as the basis for the creation of the multistage CE amplifier. The linear technology simulation software with a focus on integrated circuits was used to model the planned single stage and multistage CE amplifiers (LT SPICE). According to the findings, a voltage gain of 45 dB for the single stage and 54 dB for the multistage was achieved using analytical methods, whereas the LT SPICE simulation program produced values of 44 dB for the single stage and 54 dB for both the multistage. Applications for the suggested amplifier might include low-frequency devices like those used to process audio signals. Also, based on these findings, it is advised to couple additional transistor amplifier stages in order to increase voltage, current, and power increases.

DISCUSSION

Types of Amplifiers with their Workings

Several of the different stages that make up the TV are amplifiers in the analog TV receiver. Also, you'll see that the names indicate the kind of amplifiers. Some amplifiers are actual amplifiers, while others include additional components to change the fundamental amplifier architecture for a particular use. All electronic systems share the technique of creating huge, complicated circuits out of very simple electronic circuits. Millions of logic gates and other parts, which are just specialized amplifiers, are what make up computers and microprocessors. The first step in learning about electrical projects is to identify and comprehend fundamental circuits, such as amplifiers. There are several amplifier types available for various uses. The sort of signal that an amplifier is intended to amplify determines its classification. Typically describes a range of frequencies at which an amplifier will be able to carry out the task that has to be done inside an electrical system.

Frequency amplifiers for audio

Signals in the 20 Hz to 20 kHz range, which is the range of human hearing, are amplified using audio frequency amplifiers. Although most audio amplifiers may limit the high frequency limit to 15 kHz or less, certain Hi-Fi audio amplifiers may increase this range up to around 100 kHz ranges. Low level signals from microphones, disk pickups, etc. are amplified using audio voltage amplifiers. Amplification devices may additionally adjust tone, balance signal levels, and blend various inputs thanks to additional circuitry. In general, amplifiers have high output resistance and high voltage gain. These power amplifiers for audio are used to take the amplified input from a number of voltage amplifiers and then provide enough power to drive loudspeakers.

Amplifiers for Intermediate Frequency

Amplifiers with an intermediate frequency were tuned amplifiers used in radio, TV, and radar equipment. Before the audio or visual data conveyed by a TV or radar signal is separated or decompressed from the radio signal, the main goal is to supply the bulk of the voltage amplification needed. Amplifiers operate at a frequency that is lower than the radio waves that are being received but higher than with the audio or video signals that the system will ultimately create. Intermediate Frequency is the frequency at which.

Amplifier for Intermediate Frequency

These amplifiers work, and their bandwidth varies depending on the tools they're using. Home TV typically utilizes 6 MHz bandwidth for the I.F Signal at roughly 30 to 40 MHz, whereas radar may use a bandwidth of 10 MHz. AM radio receivers and I.F amplifiers operate from about 470 kHz and their bandwidth is typically 10 kHz, or 465 kHz to 475 kHz.

Infrared amplifiers

A tuned circuit device controls the operating frequency of radio frequency amplifiers, which are tuned amplifiers. Depending on the amplifier's intended use, this circuit might or might not be programmable. Its bandwidth might be quite large or small depending on the purpose. Amplifier typically, input resistance is little. Certain RF amplifiers are mainly used as a buffer between a receiving antenna and subsequent electronics to stop any high-level undesired signals from the receiver circuits from reaching the antenna port, where they might be re-transmitted as interference. These amplifiers may have little or no gain. The early stages of a receiver employ RF amplifiers because of their low noise performance. Since the

amplifier will be processing extremely low amplitude signals from of the antenna, background noise caused by any electrical equipment should be kept to a minimum. Low noise FET transistors are often utilized in these stages.

Amplifying ultrasonic sound

A form of audio amplifier that can handle frequencies in the 20 kHz to 100 kHz ranges is called an ultrasonic amplifier. They are often made for particular uses, such as remote control systems, metal fatigue detection techniques, ultrasound scanning, and ultrasonic cleaning. Each kind will function within a very small band of ultrasonic frequencies (Figure 2).

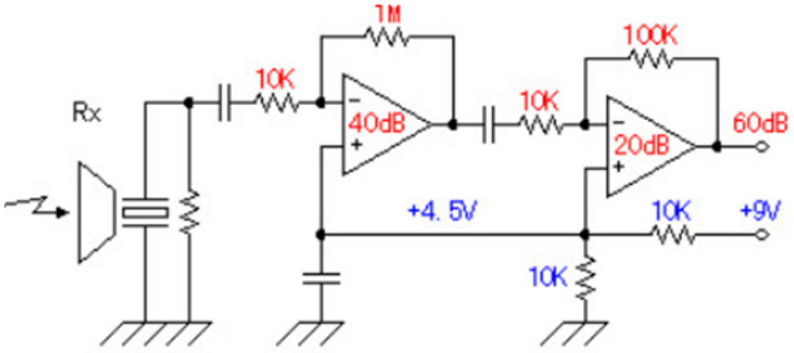

Figure 2: Illustrates the circuit diagram of ultrasonic sensor.

Wide ranging amplifiers

From DC to a few tens of MHz, wide band amplifiers must maintain a consistent gain. Measurement tools like oscilloscopes employ these amplifiers as power sources. The extraordinarily wide bandwidth and low gain of signals need reliable measurement across a broad frequency range.

Drive Amplifiers

When a signal's DC level is a crucial factor, DC amplifiers are used to magnify DC (0 Hz) voltages or extremely low frequency signals. They are typical in plenty of electrical measuring devices and control systems.

Video Boosters

Wide band amplifiers are employed particularly for signals that are to be applied to CRTs or other video equipment, and video amplifiers are a special sort of wide band amplifier that also maintains the DC level of the signal. All of the visual data on TVs, video, and radar systems is carried via video signals. The usage affects the video amplifiers' bandwidth. It spans from 0 Hz (DC) to 6 MHz in TV receivers, and it is much broader in radar.

Amplifying buffers

Within any of the aforementioned category kinds, buffer amplifiers are an often seen specialized amplifier type that are positioned between two other circuits to prevent the performance of one circuit from impacting the operation of the other circuit. They keep the circuits apart from one another. Buffer amplifiers are impedance matching devices because they have a very high input impedance as well as a low output impedance, which allows them to have a gain of one and produce an output wave with the same amplitude as their input wave. Buffer prevents signal attenuation across circuit characteristics, which occurs when a

signal is sent straight from one circuit with a maximum output impedance to another with a low input impedance.

Operational Boosters

The circuits used in the first analog computers to perform mathematical operations like addition and subtraction gave rise to operational amplifiers. They are often incorporated into complicated integrated circuits for certain purposes and are available in a single or multiple amplifiers packages in integrated circuit form, where they are commonly employed. Based on a differential amplifier circuit, which seems to have two inputs as opposed to one, the design. In proportion towards the difference between the two inputs, they generate an output. Op-amps have a very high gain efficiency, often in the hundreds of thousands, when there is no negative feedback supply. Negative feedback diminishes the gain efficiency of the op-amps while increasing their bandwidth, allowing them to function as wide band amplifiers with a bandwidth inside the MHz range. These simple resistor networks can provide this external feedback, and many other external networks can change how op-amps operate.

The Amplifiers' Output Characteristics

Amplifiers are used to boost a voltage, current, or the amount of power that is typically accessible from an AC signal wave. There are three types of amplifiers that correspond to the characteristics of their output in every activity. The amplifier may be categorized in three distinct ways.

Voltage amplifiers, Current amplifiers and Power Amplifier

While the amplitude of the output current may be more or lower than that of the input current, the fundamental goal of a voltage amplifier is to make the output voltage waveform larger than the input voltage waveform. While the output voltage may be larger or lower than the input voltage, this difference is less significant for the amplifier's intended use. The primary goal of a current amplifier would be to increase the amplitude of an output current waveform relative to the input current waveform. The output voltage and current product of such a power amplifier is bigger than the input voltage and current product. The product of the two is greatly raised when either voltage or current is smaller at the output than that at the input. There are several amplifier types, such as class A, class B, class AB, and class D, accessible in power amplifiers.

REFERENCES

[1] D. K. Sharma, A. Jain, K. Pathak, en M. Lad, “Compact dual-channel radio frequency power sensor for solid state amplifiers”, *Nucl. Instruments Methods Phys. Res. Sect. A Accel. Spectrometers, Detect. Assoc. Equip.*, 2019, doi: 10.1016/j.nima.2019.162559.

[2] S. Bhattacharya, S. Sae-Tia, en B. C. Fries, “Candidiasis and mechanisms of antifungal resistance”, *Antibiotics*. 2020. doi: 10.3390/antibiotics9060312.

[3] Y. Guo, G. Song, M. Sun, J. Wang, en Y. Wang, “Prevalence and Therapies of Antibiotic-Resistance in Staphylococcus aureus”, *Frontiers in Cellular and Infection Microbiology*. 2020. doi: 10.3389/fcimb.2020.00107.

[4] Y. H. Lee *et al.*, “Gain characteristics of SQUID-based RF amplifiers depending on device parameters”, *Prog. Supercond. Cryog.*, 2019, doi: 10.9714/psac.2019.21.1.010.

[5] H. Rashtian en O. Momeni, “Gain boosting in distributed amplifiers for close-to-fmax operation in silicon”, *IEEE Trans. Microw. Theory Tech.*, 2019, doi: 10.1109/TMTT.2019.2894671.

[6] A. Toniato, B. Gotsmann, E. Lind, en C. B. Zota, “Weyl Semi-Metal-Based High-Frequency Amplifiers”, 2019. doi: 10.1109/IEDM19573.2019.8993575.

[7] M. Sajedin, I. T. E. Elfergani, J. Rodriguez, R. Abd-Alhameed, en M. F. Barciela, “A survey on RF and microwave doherty power amplifier for mobile handset applications”, *Electronics (Switzerland)*. 2019. doi: 10.3390/electronics8060717.

[8] S. Neumeyer, V. S. Sorokin, M. H. M. van Gastel, en J. J. Thomsen, “Frequency detuning effects for a parametric amplifier”, *J. Sound Vib.*, 2019, doi: 10.1016/j.jsv.2018.12.036.

[9] D. E. Dan-Abia, A. Obot, en K. M. Udofia, “Design and Analysis of a Multistage Common Emitter Amplifier for Low Frequency Applications”, *Eur. J. Eng. Res. Sci.*, 2019, doi: 10.24018/ejers.2019.4.10.1431.

CHAPTER 12

STUDY ON THE NON-INFINITE OPEN-LOOP VOLTAGE GAIN

Savitha R, Assistant Professor
Faculty of Engineering and Technology, Jain (Deemed-To-Be University), Bengaluru, Karnataka, India
Email id- r.savitha@jainuniversity.ac.in

Abstract:

Our approach to designing analog systems has undergone a profound and ongoing change thanks to the operational amplifier. The availability of low-cost, high-performance devices affects a wide range of circuits and systems, from simple, mass-produced circuits to extremely complicated machinery intended for intricate data collecting or processing tasks. In this chapter author discusses the parameters of real operational amplifier and their output limitations.

Keywords:

Circuit, Capacitor, Gain, Operational Amplifier.

INTRODUCTION

This lesson on the fundamentals of operational amplifiers will show that these devices are linear and have all the characteristics needed for almost perfect DC amplification. To execute arithmetic computations including addition, subtraction, integration, and differentiation as well as control signal as well as filtering, they are often utilized. A voltage-amplifying machine called an operational amplifier, and op-amp for short, is essentially designed to be utilized with external feedback elements like resistors and capacitors in between output and the input connections. By virtue of the many feedback topologies, whether resistive, capacitive, or both, the amplifier may perform a number of different operations, going to give birth to its moniker of "Operational Amplifier." These feedback characteristics dictate the resultant function or "operation" of an amplifier. In essence, an operational amplifier is a three-terminal instrument with two high increased likelihood. The Inverting Input is one of the inputs, and it is identified by a "minus" or negative sign (–). The second input is referred to as the Non-inverting Input and is denoted by a plus sign (+). The output port of the operational amplifier is represented by a third terminal, which may source and absorb either current or voltage. In a linear operational amplifier, overall output signal equals the amplification factor, called amplifiers gain (A), and multiplied by the magnitude of the original signal. There are four main types of operational amplifier gains, depending on the characteristics of the gate and source.

Operational Amplifier Basics of Classification

1. Voltage: Voltage “in” and Voltage “out”
2. Current: Current “in” and current “out”
3. Transconductance: Voltage “in” and Current “out”
4. Transresistance:Current “in” and Voltage “out”

Since voltage amplifiers are often used in operational amplifier circuits, we will restrict the lessons in this part to simply covering voltage amplifiers (Vin and Vout). The differential

between the signals supplied to an operational amplifier's two separate outputs is the signal's output voltage. In other terms, an operational amplifier's output voltage is the differences between the two incoming signal because the operational amplifier's input stage is really a differential amplifier.

The Differential Amplifier: Operational Amplifier Fundamentals

Figure 1 of a circuit depicts a differential amplifier through its generalized version with two inputs denoted V1 and V2. The emitters of the two consecutive transistors TR1 and TR2 are coupled together and returned towards the common rail, -Vee, through a resistor Re. They are both biased towards the same operating frequency. The dual supply +Vcc and -Vee used by the circuit guarantees a steady supply. Due to the fact that the different base inputs are out of sync phase with one another, the value that is seen at the amplifier's output, Vout, is the difference between both of the input signals. Transistor TR1's forward bias is raised while transistor TR2's forward bias is decreased, and vice versa. The current that flows through into the common emitter resistance, Re, will stay constant if the switching devices are precisely matched.

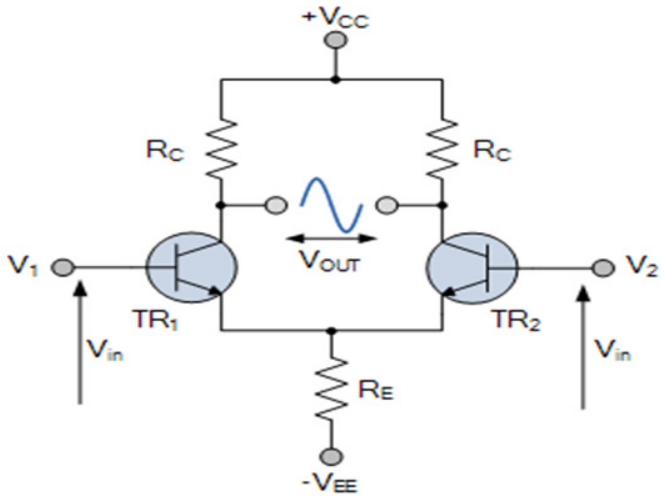

Figure 1: Illustrates the circuit diagram of a generalized form of a differential amplifier with two inputs marked V1 and V2.

The output signal is balanced, just like the input signal, and because the collector voltages whether in swing in the identical direction (in-phase) or opposite instructions (anti-phase), respectively, the output voltage signal, chosen to take from between the 2 different collectors, is, in the case of a perfectly balanced circuit, the zero contrast between the different collector voltages. This is referred to as the "Common Mode of Operation," and the amplifier's "common mode gain" is its output gain whenever the input is zero. Operational amplifiers also feature a low-impedance output with something like a common ground comparison that should completely disregard any common mode signals, meaning that the output should not change if the same signal has been applied to each of the inverting and non-inverting inputs (although some models have an additional differential output).

The Common Mode Rejection Ratio, or CMRR for short, measures how much an amplifier's terminal voltage changes in relation to how much its common mode source voltage changes in actual amplifiers. Operational amplifiers possess an extremely high open loop DC gain on their own, and when negative feedback is employed, we may create an operational amplifier

circuitry with a highly accurate gain characteristic that depends solely on the kind of feedback used. The phrase "open loop" refers to the feedback channel or loop being open since there are no feedback components being employed in the area surrounding the amplifier. An operational amplifier simply reacts to the "Differential Input Voltage," often known as the voltage difference between the two input terminals; it does not react to the potential difference between them. Following that, if the same electrical potential is supplied to both terminals, the output will be zero. The Open Loop Differential Gain, often known as such an Operational Amplifiers gain, is denoted by the symbol (Ao). The use of operational amplifiers is constrained by the fact that they comprise analog circuits and need a designer with knowledge of analog basics including loading, resonant frequency, and stability. A relatively simple op amp circuits may be designed, but when it is turned on, it often oscillates. The designer must be aware of how some of the previously covered critical factors affect their design, which usually requires a moderate to high degree of knowledge in analog design.

LITERATURE REVIEW

Y. Y. Qian et al.[1]in that work presents an instrumentation amplifier (IA) targeting biomedical applications that is based on operational amplifiers (op-amps). Such IA maintains low energy consumption, high power supply rejection ratio (PSRR), as well as other design limitations, while achieving high gain and high common-mode rejection ratio (CMRR). There at input and output stages, the IA employs three identical two-stage telescoping cascode op-amps. In contrast to the capacitors and resistors used in the traditional voltage mode IA, feedback networks use resistors. Capacitive feedback is utilized in the output stage for filter unwanted frequency components and boost the IA's gain, while resistive feedback is used in the input stage to improve stability. Using the Cadence Spectre tool, this same IA schematic is developed and tested using 180 nm CMOS technology. The single op-amp has a gain and CMRR of 100.45 dB and 94.8 dB, respectfully. At a supply voltage of 0.9 V, so every op-amp uses 12.96 mu W of power. The RC Miller compensating approach aids in the op-achievement amp's of a 60° phase margin. This IA has a gain of 101.61 dB and a power consumption of 38.88 muW and 147.68 dB. Because of its significant gain and high CMRR, the suggested approach is appropriate for a number of biological applications.

In study R. Shi et al.[2] the single pulse power and narrow linewidth of a fiber amplifier using a large mode area (LMA) Yb-doped double cladding fiber (YDCF) amplifier and just a solid state seed laser were reported. The YDCF amplification method used a twostage large diameter fiber amplifer even though opposed to the customary onestage fiber amplifer using solid state laser seed source. The process of connecting the spatial seed illumination into to the fiber was significantly easier with the two-stage fiber amplifer. Various techniques were used to prevent nonlinear effects while the signal was being amplified. With the SNR above 30 dB, obvious exponential effects like SBS and SRS were not seen in the output. The output average power were increased to 10.07 W after the YDCF amplification system. Their output was raised by 14.23 dB in comparison to the seed's power, which was roughly 0.38 W. The pulse energy is approximately 1 mJ, with a pulse width of 50 ns, at such a repetition rate of 10 kHz. The output laser's beam quality M2 is 3.72. Numerous real-world applications, including laser remotely sensed, laser measurement, nonlinear frequency conversion, and others, will greatly benefit from the pulsed fiber amplifier's small linewidth with high pulse energy.

According to the R. Shi [3] et al. a potential approach for stroke rehabilitation has been created using assistive robots and brain-computer interface (BCI). However, the majority of recent research rely on pricey, large, and complicated system setups. In this study, we created

a wearable BCI device based on electroencephalography (EEG) to help stroke victims regain their hand function. The device comprises of a lightweight hand exoskeleton, a tiny, commercial amplifier, and a personalized EEG hat. Additionally, a user-friendly interface with visualizations was created. To confirm the security and efficiency of our suggested approach, we enlisted the help of six healthy volunteers and two stroke victims. Online BCI classification accuracy up to 79.38% on average was attained. This research serves as a proof-of-concept and suggests possible therapeutic uses in outpatient settings.

According to the S. Chauhan and L. M. Saini [4] one of the most crucial components of an ECG recording system is the instrumentation amplifier (IA). An IA that achieves low power consumption and minimal noise is provided in this study. A chopper stabilized approach has been used to lessen the impact of noise while regulating the output DC level. The operational transconductance amplifier (OTA) was designed as a low power device. The suggested IA requires a 1.8 V supply to function. Incorporated within CADENCE 180 nm CMOS technologies is the suggested IA.

According to the Z. Chen et al.[5]a GaN Doherty amplifier with a 160 MHz LTE signal bandwidth that is suited for multi-carrier aggregating including DPD correction was created. Results indicate that when tested with such a pulse signal, an amplifier's saturated output power is over 54 dBm, its back-off efficiency is above 40%, its average output power was 44.8 dBm, and its average power gain stands 13.5 dB. The amplifier's initial ACPR is -33 dBc, and a DPD platform can optimize it by around 20 dBc. The amplifier eventually achieves an ACPR of less than -51 dBc, fulfilling the criteria for system use.

X. Zhuet al. stated the transition technique between W-band waveguide and microstrip was examined, a W-band solid-state combining power amplifier were detailed, and it was confirmed that the structure of the microstrip probe for W-band power combining technology would work. Last but not least, eight GaN MMICs are paired with a high efficiency wave guide power combiner to provide an output power of higher than 6 W from 92 to 98 GHz, a peak power of 7.4 W at 98 GHz, and a PAE of higher than 11%[6].

X. Zhu et al.[7] that research presents a monolithic RF receiver for Wireless Local Area Networks (WLANs) 802.11ac applications that integrates a Low Noise Amplifer (LNA) and Single Pole Double Throw (SPDT) switch inside a single 0.25 mu mathrm m GaAs pHEMT process. The LNA having bypass function was developed to prevent saturation and overload again for component in the following step. In order to achieve low Noise Figure (NF) for the RX route and high power handling capabilities for the TX path, a low Insertion Loss (IL) SPDT antenna switch is also accomplished. In the 5.15–5.85GHz frequency band, the constructed RF receiver with both the die size of 1.6x0.8 textmm2 displays an NF of 2dB with 11dB average gain including the SPDT switch loss.

J. Du et al.[8]the ultra-wide band (UWB) low noise amplifier (LNA) for 3–10 GHz applications is presented in complete integration in this work. It uses current recycling and self-biased resistive feedback to provide broad input matching and low power features. In order to get a higher gain-compensation performance, a better biased design is chosen in the second stage. The design is validated using the RF CMOS standard 1P6M 0.18 m process from TSMC. The test findings demonstrate that the transistors' parasitic issue at high frequencies has been resolved. In the intended frequency region, a high and flat S21 of 9.71.5 dB and the lowest NF of 3.5 dB are attained. Under a 1.6 V supply, the power usage is merely 7.5 mA. The suggested LNA offers simultaneous bandwidth flat gain, noise canceling, and good linearity performance, making it suitable for 3-10 GHz UWB applications.

A. Popp et al.[9]the single-mode output of ytterbium-doped laser cutting amplifiers is noted for its high single-pass gain and average outputs up to the kilowatt range. Transverse mode instabilities place an upper limit on the output power that may be produced (TMI). Above a specific threshold, chaotic power transfer takes place, which lowers the beam quality. This is caused by interference with higher order modes, which results in a thermally generated long period grating. It has been shown that altering the grating strength may change the effect. Additionally, it has been shown that in order to effectively transmit power or prevent the impact via phase disruption, a certain phase relation of the grating towards the guided modes is required. The pump or seed source in a fiber amplifer introduces noise, which results in a natural phase disruption. In this work, we experimentally analyze and connect the basic shot noise limit to the intensity noise present in a fiber-pre-amplifer, which would be frequently used in kW studies (SNL). A single-frequency external cavities excitation wavelength was employed in the trials as a low noise source, and its output power was increased by 30 dB from 10 mW to 10 W. Before such sources may be amplified to the kW level, this is a common pre-amplifier arrangement. The fiber amplifiers is a double-clad fiber with such a 10/125 m shape that is pumped at 976 nm by a pump diode that has its wavelength regulated using a monolithic pump coupling. The seed laser is expanded to 50 GHz linewidth and phase modulated by such a sinusoid as well as white noise combination to avoid stimulated Brillouin dispersion. The noise measurements are carried out using improved photodiode readout circuits covering several frequency bands and balanced self-homodyne detection. To look at each component's role in this arrangement, the fiber amplifier, phase modulator, and seed source have been individually described. Both co-pumping and counter-pumping configurations for the fiber amplifier are studied. All provided spectra are obtained at optical powers in the mW range, which equate to around 30 dB of amplifier attenuation, due to detector constraints.

B. Lu and Q. Li[10] study used a 130-nm silicon-germanium (SiGe) heterojunction bipolar transistor (HBT) technology to build two broad tuning signal sources operating at roughly 300 GHz, and both with and without a buffer. The Colpitts voltage-controlled oscillator (VCO) and doubler used to create the 300-GHz signal source exhibit -2.89 dBm output power at 302 GHz, -81.5 dBc/Hz phase distortion at 1-MHz offset, 7.98% tuning ranges, and 0.96% DC-to-RF efficiency. It displays a slightly higher working frequency, between 290.8 to 316.6 GHz, as well as a better -85.1 dBc/Hz phase distortion at 1-MHz offset, but with lower output power of -5.2 dBm but also efficiency of 0.33% after adding a differential common-emitter amplifer between both the VCO and doubler. Each oscillator's layout size, including DC but also RF pads, is 524 times 495 mu mathrm m2 and 524 times 540 mu mathrm m2.

DISCUSSION

A high-gain, direct-coupled amplifier, an operational amplifier is often employed in feedback connections. The transfer function of the amplifier with feedback may often be regulated solely by the steady and well-known values of passive feedback components provided the amplifier characteristics are good. The name "operational amplifier" originated in analog computing, when these circuits were used to sum and integrate numbers, among other mathematical functions. Modern operational amplifiers are employed as all-purpose analog data-processing components because they provide performance and financial benefits that go well beyond the original uses. Early in the 1950s, excellent operational amplifiers were readily available. These amplifiers often only worked with analog computers and lacked the adaptability of more contemporary devices. In the early 1960s, when several manufacturers created modular, solid-state circuits, the range of operational-amplifier use started to broaden toward the current variety of applications. Compared to earlier amplifiers, these ones were

more compact, durable, affordable, and used less power from the power source. These discrete-component circuits come in many varieties now, and when compared to previous models, their performance characteristics are amazing. As monolithic integrated-circuit amplifiers with decent performance characteristics emerged in the late 1960s, utilization saw a tremendous leap. The superior discrete-component circuits still outperform these devices in terms of several performance parameters, but the integrated ones are substantially cheaper, with numerous designs selling for about $0.50. The availability of operational amplifiers often justifies the inexpensive replacement of two- or three-transistor circuits without regard to any accompanying performance benefits. The days of a discrete-component circuit, except for specialties with low manufacturing needs, are probably numbered as processing and designs advance and the integrated circuit expands into previously regarded purely discrete design territory. Investigating operational amplifiers in further depth is worthwhile for a number of reasons. Instead of just giving a fair sample of these devices' uses, we must examine both the theoretical and practical elements of them. Since almost all operational-amplifier connections require some kind of feedback, an in-depth knowledge of this procedure is essential for the effective use of the tools. For everyday needs, partly understood rules of thumb could be enough, but this design approach fails when performance goals get closer to the amplifier in question's maximum useful range. Similar to this, a serious user must have a thorough understanding of the internal design and operation of operational amplifiers because this knowledge is required to identify various constraints and to suggest modifications or connections that can be made to a unit to ensure optimum performance in a particular application. Thus, even though he may never construct one, the current analog circuit designer must grasp how operational amplifiers work internally for the same reason why his predecessor ten years ago needed to be familiar with semiconductor physics. Additionally, there has been a tremendous advancement in good design practice in this field, and many of the circuit approaches discussed in the following chapters are applicable to the design of various kinds of electronic circuits and systems.

Real op-amp performance parameters

Op-amps are available in a wide variety of configurations. Additionally, there are several technologies, including CMOS, BiFET, and bipolar. Additionally, bipolar may be classified as either voltage feedback or current feedback. Therefore, it is necessary to take the performance factors of each device into account. It might be difficult to choose the optimal op-amp for a certain application, particularly for a beginner. The designer is first confronted with a vast array of requirements and several op-amp kinds while looking through manufacturer catalogs. Economic factors are likely to influence the op-amp selection. A general-purpose op-amp will often be less expensive than a product that satisfies a stringent need. This is because general-purpose gadgets sell in bigger numbers, which allows the maker to spread out the development expenditures across a larger number of units. Typically, the op-amp with the lowest cost that satisfies the design requirements should be used. In order to make this option the design goals must be thoroughly specified. The designer must also be aware of the connection between the impacts of published op-amp settings on the overall performance of the circuit for the intended application. The numerous op-amp specs that are often included in a manufacturer's data sheet are described in this chapter. The relevance of these characteristics will be addressed. It's critical to comprehend the precise circumstances under which a certain parameter is defined. Later chapters, when op-amp applications have been discussed, will return to the crucial topic of op-amp selection. The user should then have a clearer understanding of the design goals and *how the op-amp settings prevent them from being achieved*.

Limitations on Op-amp input and output

An op-input amp's circuit often consists of a long-tailed pair. Transistors connected at their emitters form the long-tailed pair (in the case of a bipolar input op-amp). A constant current circuit serves as the link between the emitters and also the supply rail. One transistor will conduct more via its collector if its base is primed at a little higher potential than the other transistors, whereas the other transistor in the pair would conduct less as a result. In Figure 2, a resistor or, more often, a constant current generator is used to connect each transistor's collector to the opposite supply rail.

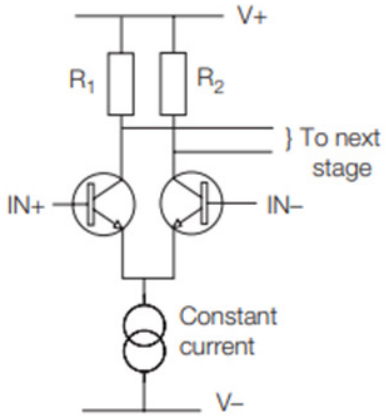

Figure 2: Illustrates the circuit diagram of Op-amp input circuit.

Maximum voltage between inputs

Negative feedback often keeps the voltage between an op-input amp's terminals at a very low value during operation. Figure 3 shows what would happen if negative feedback is not employed when the differential input voltage may surpass this low value and the op-output amp's saturates.

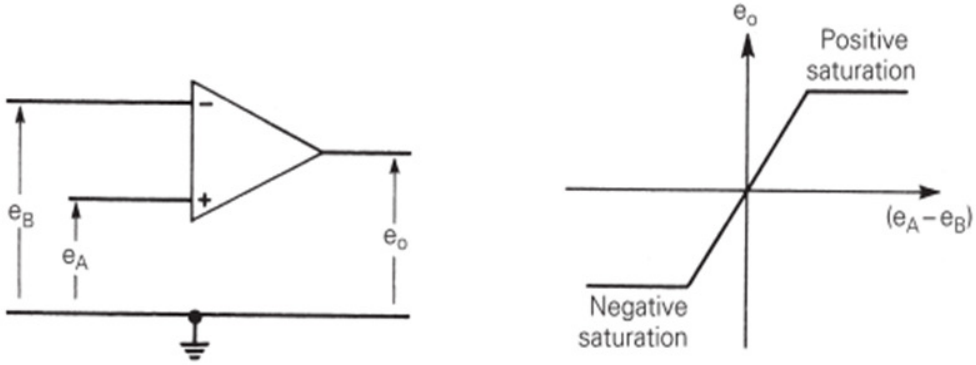

Figure 3: Illustrates the Idealized transfer curve for an op-amp.

Care must be taken to make certain that the maximum permitted value is not exceeded if the circuit design permits the application of multiple volts between the input terminals; otherwise, the op-amp risk suffering irreparable damage. Others are internally protected against input overload circumstances, whereas many op-amps permit the differential input voltage to be equal to the supply voltage. When an op-input amp's terminals don't have this inherent safety, diodes might be connected externally to fill the gap.

Swing in maximum output voltage

Two transistors are typically present at the output of an op-amp, one of which is wired to the positive rail and the other to the negative rail (see Figure 4). This circuit adjusts the output voltage by raising the driving on one transistor whereas lowering it on the other. Constant current circuits are employed in the base drive among these transistors, because then quiescent supply current (the current with no signal) is reduced. The greatest output voltage swing is limited by the need that both transistors in this circuit have a certain voltage between collector and emitter. The largest output voltage variation eo max is the greatest change throughout output voltage (positive and negative), measured with relationship to the mid-rail supply, that can be obtained without clipping the signal waveform. When an op-amp is operating into a specific load and with defined values for op-amp power supply, values for eo max are stated (sometimes at the maximum rated output current). Supply voltage maximums are often mentioned and shouldn't be exceeded. It will be discovered that values for eo max depend upon that supply voltage used. Except when running from high supply voltages, BiFET and CMOS op-amps feature FET outputs that enable the output voltage to be located within 200 mV of a supply voltage.

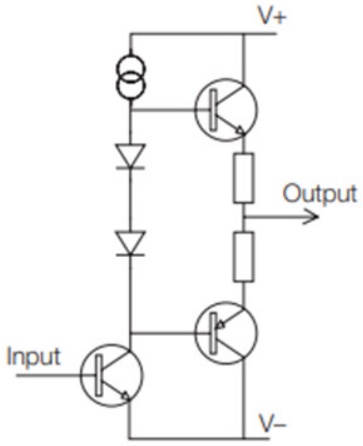

Figure 4: Illustrates the circuit diagram of Op-amp output circuit.

Maximum common mode voltage T

The average voltage between the two inputs in relation to ground is known as the common mode voltage. Ecm, or the maximum common mode voltage, is the highest voltage that can be employed without causing output saturation or non-linearity. The common mode voltage range of so many devices is around 2 V or less from the supply rails. Input circuits for single supply op-amps often let the common mode voltage spectrum to reach the negative supply rail. In a perfect world, the output is unaffected by the common mode input voltage. eo AOL (eAeB) In actual use, the output is impacted by the common mode input voltage. A good pair of zener diodes may provide safety if an op-amp is to be utilized in circumstances where an excessive common mode voltage might harm it. The anodes of the diodes should indeed be united and they should be connected "back to back." The two op-amp inputs should be linked to the two cathodes.

Non-infinite open-loop voltage gain

The open-loop voltage gain, AOL, of an op-amp may be defined as the ratio

$$\frac{\text{change of output voltage}}{\text{change of input voltage}}$$

The voltage measured between the inverting and non-inverting input terminals is the input voltage. AOL is often given for signals that fluctuate extremely slowly, and it is theoretically possible to calculate it from the slope of the input/output transfer curve's non-saturated region. The op-amp load and the quality of the power sources have an impact on the AOL's size for a certain op-amp. AOL values are often given for supply voltages and loads that are defined. An open-loop setup never employs op-amps. They are infrequently employed in circuits with positive feedback, but they are considerably more often utilized in circuits with negative feedback that specify exact functioning. Open-loop gain is significant since it establishes the accuracy thresholds for these applications. Studying the basic concepts of feedback op-amp functioning is necessary in order to evaluate the quantitative consequences of the open-loop gain size. A signal is sent back from the output to the input in a negative feedback op-amp circuit. The input signal supplied from outside is opposed by this feedback. After subtracting two signals, the signal that really drives the op-input amps is produced. The signal voltage supplied between the op-amp input terminals decreases with increasing open-loop gain (the gain of the op-amp without feedback). Negative feedback drives the op-differential amp's input signal to zero if the open-loop gain is infinite (as is anticipated for a perfect op-amp). A little input signal must exist between the op-input amp's terminals due to the enormous but limited open-loop gain. Because the genuine op-amp has a limited open-loop gain, it is useful to conceive of this as an input error voltage.

Input impedance that is not infinite

The circuit analysis based here on ideal op-amp made the assumption that no current entered the input terminals of the op-amp. In actuality, the differential input impedance is substantial yet limited. Input capacitance contributes to some of this impedance, which has an impact on high frequency performance. The input resistance may have an impact on performance in the majority of applications. The input resistance of op-amps with FET inputs varies from the order of 1012. The resistance of bipolar input devices is lower, yet it is often larger than 106. It is possible to essentially disregard the common mode input resistance to earth, which is much higher than this and generally 100 times higher (i.e. 108 for a bipolar input device).

Output resistance that is not 0

Op-amp output resistance is not zero ohm. A typical gadget has an output resistance of 50. The greatest output voltage swing into something like a low resistance load, when a significant voltage drop occurs across the internal resistance, is limited by this resistance. The effects of output impedance may be lessened via feedback, which causes the op-amp to produce more internal voltage to make up for any drop brought on by the output resistance. The effective output impedance when there is feedback is often less than 1 m.

A non-inverting amplifier's impact

For a non-inverting amplifier, the impacts of finite open-loop gain, finite input resistance, and non-zero output resistance would be taken into consideration. Each parameter must be taken into account independently in order to analyze the impacts. First we must determine a few general relationships for the non-inverting amplifier in respect of the non-infinite open-loop

gain. Figure 5 depicts a differential input op-amp with applied series negative voltage feedback. The differential input voltage of the op-amp is e. The output of the op-amp is represented by the circuit of its Thévenin equivalent. When connected in series with the output impedance of the opamp, the output acts as a source of EMF (AOLe). (Note that the negative sign merely results from the differential input signal's e's presumed positive direction.) To the op-inverting amp's input terminal, a voltage, ef, that is precisely in proportion to the output voltage, eo, being fed back (negative feedback):

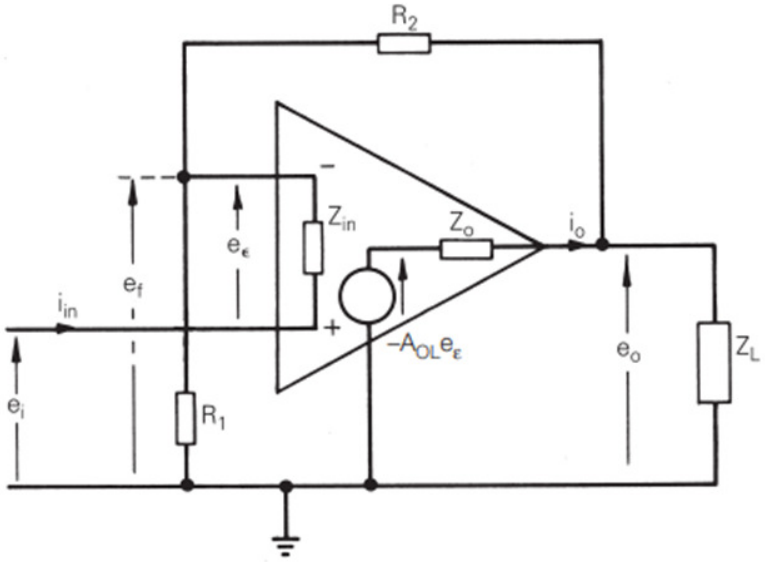

Figure 5: Illustrates the circuit diagram of Series voltage feedback.

CONCLUSION

In a wide range of applications, including the biomedical sector and data gathering systems, the instrumentation amplifier was utilized as an input stage. The rationale for the new IA's design, which places a focus on low power consumption, silent operation, and high common mode rejection ratio [CMRR], is the increased interest in and ongoing advancement in integrated systems for bio-potential monitoring. The flicker noise, which is important in the low frequency region, is the most important element. By choosing the right doping material and temperature, flicker noise may be decreased. On the other side, several methods have been employed to reduce noise, including linked double sampling and chopper stabilization. A low power, low noise instrumentation amplifier has already been suggested in this study. The power dissipation has been kept to a minimum via an OTA. To stabilize the output DC level, a common mode feedback (CMFB) circuitry has been utilized. A chopper controlled circuit has indeed been employed to reduce noise.

REFERENCES

[1] Y. Y. Qian, Z. G. Wang, Y. K. Liu, and Z. J. Zhou, "A High Gain and High CMRR Instrumentation Amplifier for Biomedical Applications," 2019. doi: 10.1109/ICICM48536.2019.8977189.

[2] R. Shi *et al.*, "1 mJ narrow linewidth Yb-doped pulsed fiber amplifier," *Hongwai yu Jiguang Gongcheng/Infrared Laser Eng.*, 2019, doi: 10.3788/IRLA201948.S105001.

[3] Z. Qin, Y. Xu, X. Shu, L. Hua, X. Sheng, and X. Zhu, "EConHand: A Wearable Brain-Computer Interface System for Stroke Rehabilitation," 2019. doi: 10.1109/NER.2019.8716940.

[4] S. Chauhan and L. M. Saini, "Low Power and Low Noise Instrumentation Amplifier," 2019. doi: 10.1109/ICCONS.2018.8662917.

[5] Z. Chen, A. Li, R. Zeng, C. Zhu, L. Zhang, and X. Chen, "Design of a 30 W 40% Efficiency GaN Doherty Power Amplifier for 3.5 GHz LTE Application," *Guti Dianzixue Yanjiu Yu Jinzhan/Research Prog. Solid State Electron.*, 2019.

[6] X. Zhu, H. Cheng, F. Guo, and W. Wang, "W-band Solid-state Combining Power Amplifier Research," *Guti Dianzixue Yanjiu Yu Jinzhan/Research Prog. Solid State Electron.*, 2019.

[7] L. Zhong, Z. Zhang, J. Li, Z. Liu, Z. Liu, and G. Zhang, "A dual mode integrated LNA and switch for WLAN receiver," 2019. doi: 10.1109/APMC46564.2019.9038821.

[8] J. Du, C. Fan, Z. Wang, and J. Xu, "Fully-integrated ultra-wide band LNA in 0.18 μm CMOS technology for 3-10 GHz applications," *High Technol. Lett.*, 2019, doi: 10.3772/j.issn.1006-6748.2019.04.003.

[9] A. Popp *et al.*, "Investigation of noise sources down to the shot-noise limit in Yb-doped fiber amplifers for TMI investigations," 2019.

[10] B. Lu and Q. Li, "Two 300-GHz Wide Tuning Signal Sources in 130-nm SiGe BICMOS Process," 2019. doi: 10.1109/ICMMT45702.2019.8992201.

CHAPTER 13

INVERTING CONFIGURATIONS OF OPERATIONAL AMPLIFIER

Dr.Pradeepa P, Professor
Faculty of Engineering and Technology, Jain (Deemed-To-Be University), Bengaluru, Karnataka, India
Email id- p.pradeepa@jainuniversity.ac.in

Abstract:

Both the inverting and non-inverting op-amp configurations only need one operational amplifier but also two resistors. Because of the negative gain produced by the inverting design, a single circuit may both amplify and reverse the polarity of a signal between positive to negative or vice versa. In this chapter author is discusses effect on inverting amplifer and characteristics of real op-amp frequency response.

Keywords:

Feedback, Gain, Operational Amplifier, Signal.

INTRODUCTION

The non-inverting input of an inverting operational amplifier circuit is connected to ground, whereas the signal is transmitted toward the inverting input. The outputs of this kind of amplifiers is 1800 from out phase with the input, thus if a positive signal is transmitted toward the circuit, the result will be negativity. The idea of a virtual short could be employed at the Op-input Amp's terminals providing the Op-Amp is flawless. The voltage at an inverting terminal is thus equal to the voltage at a non-inverting termination. The inverted op amp is basically a continuously or fixed-gain amplifier which produces a negative output voltage since its gains has consistently been negative. The previous instruction showed that the open loop gain (AVO) of an op amp might be as high as 1 million (120 dB). However, due to the instability and difficulty in controlling the amplifier caused by the extremely high gain, even for the smallest input signals—a just several microvolts (V)—would be sufficient to prompt the voltage output to saturate though rather than swing toward a particular voltage supply rails, rendering the output totally and utterly uncontrollable.

Because the open loop DC gain of this kind of op amp is unusually large, it is possible to restrict and control the total strength of the signal by connecting an appropriate resistor throughout the amplifier either through the downstream secondary terminals or even the transistor base. This results in what is frequently referred to that as negative feedback, resulting creates an amplifier-based systems that is very stable in terms of both maintenance and operation. Then, using an external feedback resistance called R, it must be sent back more toward the negative terminal of the op-amp in order to make the receiving feedback negative. The process of "feeding back" a part of the output voltage towards the input terminal is known as negative feedback. This feedback loop between the output and the inverting input terminals forces the differentiating input voltage toward zero.

Due to the effect of a closed loop circuit upon that amplifier, the gain of the device is now referenced to as its Closed-loop Gain. The amplifier's gain is then decreased by a closed-loop inverting amplifier at the price of properly managing the amplifier's overall gain. Since the input voltage as well as the negative feedback potential are summed together, providing the

terminal the moniker of a summation point, the inverting terminal endpoints are given a signal depending on the negative feedback that is distinct from either the input voltage. In order to separate the real incoming signal from either the operational amplifier, they must employ an input resistor (Rin). We are not utilizing the positive non-inverting component, thus it is connected to a common grounding or negative half cycle terminal. To construct a Virtual Earth summation argument since it will be at the same potential as the level headed reference voltage, the action of this type of closed loop feedback circumstance that can cause output voltage available at the inverting input should become equivalent to that situated at the non-inverting input. In other words, the op-amp becomes a "differences in the effects (Figure 1).

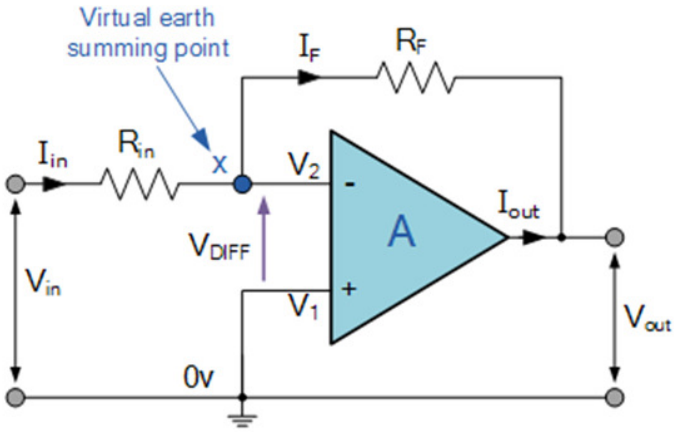

Figure 1: Illustrates the circuit the operational amplifier is connected with feedback to produce a closed loop operation.

In this inverting amplifier circuit, the op amp is linked with feedback to generate a closed loop. When using operational amplifiers, there's many two very important rules for inverting amplifiers that you must follow: It is accurate to state that "V1 always equals V2" and "No current is entering the input terminal." However, in practical op-amp circuits, both of these rules are slightly distorted. This is so that the input-feedback signal junction (X), which carries the same charge as that of the positive (+) input and is situated at zero volts or ground, may act as a "Virtual Earth." Both of the input impedance of the amplifier and the closed loop gain of an inverting amplifier may well be changed by adjusting the proportion between the two loading resistances. Both become proportional to the diameter of the input resistor owing to this "virtual ground node."

Two rules are essential to remember when using inverting amplifiers or another operational amplifier, for just that matter. Since V1 = V2 = 0, there is no current flowing through the input terminals, and the differential battery voltage is also 0. (Virtual Earth).Thus, using these two conditions, the formula for the inverting amplifier's closed-loop gain might well be calculated from the ground up. Current flows via the resistor connector (I), as shown.

$$i = \frac{V_{in} - V_{out}}{R_{in} + R_f}$$

Therefore $i = \frac{V_{in}-V_2}{R_{in}} = \frac{V_2-V_{out}}{R_f}$

The closed loop gain is given as, $\frac{V_{out}}{V_{in}} = -\frac{R_f}{R_{in}}$

The equation's negative sign indicates that the output signal is inverted since it is out of phase by 180 degrees with both the input. This is due to the poor value of the feedback. The computation for a variable such as output voltage Vout, for example, shows that the circuitry was linear in construction for a particular amplifier gain because Vout = Vin x Gain. This characteristic may be extremely helpful for increasing the voltage from a smaller sensor signal.

LITERATURE REVIEW

L. Safari et al.[1] second generation voltage conveyor (VCII) was first conceptualized more than twenty years ago, but its uses and capabilities were just recently investigated by writers in a paper. In this study, a comparison between circuits implementable using either Op-Amp or VCII is made in light of the fact that VCII-based circuits are likewise realizable using Operational Amplifiers (Op-Amps). The transfer function and essential features of each implementation are described. Spice simulations carried out in 0.18 m CMOS technology with a supply voltage of 0.9 V are offered to support the validity of the hypothesis put forward. The obtained findings demonstrate that extremely high gain for this active block, to be traded off with bandwidth, is needed in circuits based on Op-Amp. Therefore, VCII can effectively replace Op-Amp in high frequency applications. In addition, the output of Op-Amp based circuits seems to be of inverting (or non-inverting) type whereas both inverting and non-inverting outputs are feasible in the VCII based circuits. More significantly, utilizing VCII to construct non-inverting voltage summing circuits is an efficient way to eliminate the undesirable cross-talk issue that happens in Op-Amp based ones. Other advantages are realized. The comparison is done using PSpice simulations.

S. Joshyet al.[2] the purpose of that work was to show how circuit analysis may be used to forecast an electronic circuit design's resistance to humidity. There aren't many design techniques that can anticipate humidity-related problems, particularly the impact of humidity on the electrical operation of circuits. This study offers a way for utilizing circuit simulation tools to find defects in a circuit design linked to humidity using data on surface insulation resistance or empirically determined leakage current obtained from test patterns or model circuits. The experimentally discovered SIR value was used as a parasitic resistance between two circuit nodes during circuit simulation. This approach was used to analyze widely used circuits like differential amplifiers and non-inverting comparators. Circuits with greater humidity robustness have been offered as examples to show the value of this technique based on the study. Last but not least, a connection between the characteristics of the water layer on the SIR pattern and real components was carried out, thus proving the methodology's applicability.

P. Y. Kuo and Z. X. Dong [3] aimed to lessen the RuO2 urea biosensors' drift impact. With the benefit of having a straightforward construction, a novel calibration circuit (NCC) based on the voltage regulation approach was introduced. The suggested NCC was made up of a voltage calibrating circuit and a non-inverting amplifier to maintain its simplicity. A ruthenium oxide (RuO2) urea biosensor was created to evaluate the calibration properties of the proposed NCC's drift rate. The experiment conducted for this research was broken down into two key phases. A reliable RuO2 urea biosensor testing environment was built up for the first step. The voltage-time (V-T) measurement apparatus and the suggested NCC were used to measure the response voltage after submerging the RuO2 urea sensing film in the urea solution for 12 hours. The RuO2 urea biosensor was successfully manufactured, as shown by the first stage's findings, which indicated that it had an average sensitivity of 1.860

mV/(mg/dL) and a linearity of 0.999. The findings showed that the suggested NCC lowered the RuO2 urea biosensor's drift rate to 0.02 mV/hr (98.77% reduction) in the second stage of the experiment, which proved the proposed NCC's functionality.

According to the F. Fauzy and S. Kasmungin[4] the stability of the system is the key aim for Control System Design criteria. The one control that may increase the system's ability to remain stable against disturbance effects is PID control with a closed loop system. In this work, a closed loop feedback system for DC motor speed control is created using PID LabVIEW 2010 software and just a proximity sensor. The technology enables the user to regulate the DC motor's speed from the LabVIEW front panel, which automatically stabilizes when a load—which typically reduces the motor's speed—is applied. PID LabVIEW 2010 creates voltage output of 0-5Vdc and operates a DC motor through with an analog output channel from an NIDAQ 600, which is then amplified to 0-12Vdc output by a non-inverting amplifier. The speed response second order of such a DC motor may be dampened by PID Control using a Closed Loop system to have a value of overshoot number? 0 with steady state error of 2%. This state may be stabilized via system feedback to prevent outside intervention. Overshoot (Mp) = 0 and Error Steady State (Ess) = 0.82% are success criteria for this speed control system's output.

M. Masud et al.[5]offer a brand-new voltage mode first order active optionally tuneable all pass filter (AOTAPF) circuit design. 0.7 V, 16 nm carbon nanotube field effect transistor (CNFET) technology was used in the creation of the AOTAPF. The design utilizes an inverting amplifier with unity gain and a CNFET-based varactor (UGIA). Three N-type CNFETs are used to implement the AOTAPF that is being discussed; no further passive parts are used. It should be noted that the actual circuit is appropriate for low-voltage operation since it only requires two CNFETs as its supply rails. By adjusting the voltage-controlled capacitance of the used CNFET varactor, the electronic tunability is obtained. A large adjustable range of pole frequency between 34.2 GHz and 56.9 GHz is accomplished by adjusting the varactor tuning voltage. The suggested circuit is appropriate for multi-GHz frequency applications and does not need any matching constraints. Utilizing the well-known Stanford CNFET model and the HSPICE simulation tool for the 16 nm technology node, the reported AOTAPF performance is supported. Results from the AOTAPF simulation validate the hypothesis across a broad frequency range.

I. M. Pandiev and E. C. Stoimenov[6] For engineering instruction, a low-power multistage amplifier laboratory kit has been created and put to the test. A multistage amplifier constructed using the fundamental transistor stages seen in operational amplifiers is included in the lab kit. There are separate components used to accomplish each level. The input stage of the circuit's main functional unit is a differential amplifier, which is followed by an output stage and a common-collector amplifier as a buffer. The output stage consists of two complementary bipolar transistors and a common-emitter amplifier component with a current-source load. The functioning of the individual amplifier stages and the impact of the negative feedback on even a multistage voltage amplifier during non-inverting operation may also be studied. The Technical University of Sofia's second-year undergraduate "Electronic Engineering" students are the target audience for the proposed laboratory kit.

While adjusting for the effects of other demographic factors, this study used a laboratory experiment with financial incentives to test the effects of three personal factors moral reasoning, value orientation, and risk preference and three situational factors the presence and otherwise absence of audits, tax inequity, but also peer reporting behavior—on tax compliance. All of the primary factors that have been examined are statistically significant & strongly impact tax compliance behavior, according to analysis of covariance (ANCOVA).

These findings emphasize the significance of gaining a thorough understanding of these factors in order to develop policies that effectively increase the level of compliance, and they suggest that standard enforcement policies based solely on punishment should indeed be supplemented by an information system which would inform taxpayers about the level of compliance of other taxpayers, reaffirm the idea that the tax system is equitable among taxpayers, and develop programs that enhance and improve compliance by O.Auou[7].

According to the S. Kumar [8] et al. in order to achieve greater pressure sensitivity, a piezoresistive pressure transducer was designed and simulated in this study employing an operational amplifier (op-Amp) in summer mode. Piezoresistors are employed as the sensing components that track changes in piezoresistors' resistance across a pressure range of 0 to 1 MPa in steps of 100 KPa. These piezoresistors are mounted on high-stress areas of a square silicon diaphragm. Utilizing the T-Spice simulation tool, an operational amplifier circuit has been created using five micron CMOS technology parameters. The readout circuit of both the pressure transducer, which transforms the resistance change of piezoresistors towards output voltage, uses a non-inverting op-Amp in summer mode. The analytical model that defines the whole behavior of the pressure transducer using both p-Type and n-Type piezoresistors because as sensing components has been simulated using the Intellisuite software. The output of the simulation clearly demonstrates that the p-Type and n-type piezoresistors used in the op-Amp in summer configuration pressure transducer have sensitivity values of 187 mV/MPa and 1047 mV/MPa, respectively.

In study V. S. Bendre[9] et al. due to its very fast throughput and wide range of applications in many analog/mixed signal applications of the current high-speed age, carbon nanotube (CNT) is one of the emerging technologies among recent advancements towards the downsizing of semiconductor devices. Future generations of integrated circuit (IC) devices are expected to be stimulated by carbon nanotube field effect transistors (CNFETs). Widespread consideration is being given to CNFETs as a potential alternative for silicon MOSFETs. The low-power folded cascode operational amplifier (op-amp) implemented using CNFET is used in this paper to implement a variety of analog signal processing applications, including inverting amplifier, noninverting amplifier, summer, subtract or, differentiator, implementer, half-wave and full-wave rectifiers, clipper, clamper, inverting and noninverting comparators, maximum detector, and zero crossing detector. Applications for CNFET-based analog signal processing are being developed at the 32 nm technology node. The intended applications are successfully achieved utilizing innovative folding cascade operational amplifiers (FCOAs) constructed using CNFETs, according to simulation findings.

B. Chaturvedi [10] et al. proposed a brand-new, adaptable universal biquadratic arrangement that doesn't need input matching conditions and is based on two completely differential second-generation current conveyors. Two completely differential second generation current conveyors, four resistors, and two grounded capacitors make up the proposed circuit. All five common filtering responses low-pass, high-pass, band-pass, band-reject, and all-pass in voltage-mode, Tran’s admittance-mode, current-mode, and trans impedance-mode—are offered by the proposed biquad architecture. The suggested circuit is a single-input multiple-output design, allowing for simultaneous access to all replies. Additionally, the suggested circuit does not need an additional inverting amplifier or a double-type amplifier for any filtering response. Investigations have also been done on the nonideal and parasitic effects of completely differential second or third generation current conveyance on the suggested circuit. Results from the HSPICE simulation have been integrated to support the concept.

DISCUSSION

Effect on inverting amplifier

The implications of finite open-loop gain, finite input impedance and non-zero output impedance will indeed be studied for the inverting amplifier. Each parameter must be taken into account independently in order to analyze the impacts. In order to understand a non-inverting amplifier in terms of the non-infinite open-loop gain shown Figure 2, AOL, one must first identify a few general correlations.

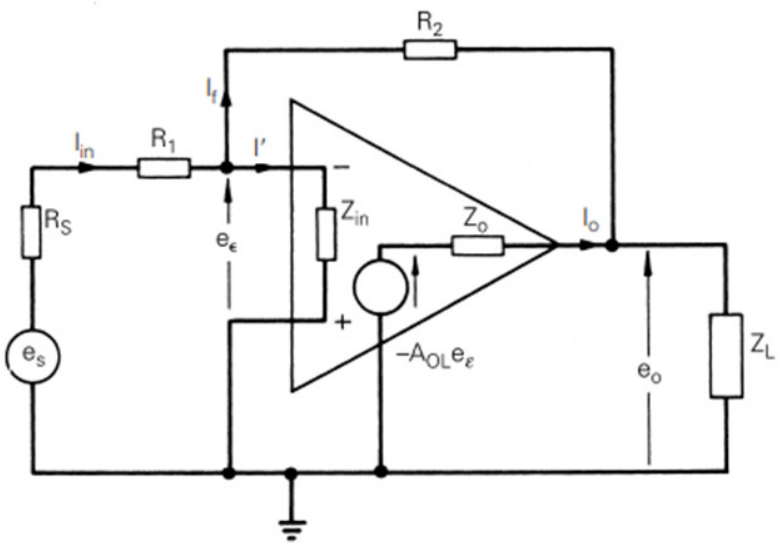

Figure 2: Illustrates the circuit diagram of Shunt voltage feedback.

The output voltage e o and the externally provided input signal voltage e s are actually applied in parallel towards the differential input of the op-amp. The effects of the signals e s and e o are superimposed to create the signal e, which drives this same differential input.

$$e_\varepsilon = e_s \frac{R_2}{R_1 + R_2 + R_s} + e_o \frac{R_1 + R_s}{R_1 + R_2 + R_s}$$

It is assumed that Zin >> R 1 R s and that Zo << R 2.

The feedback fraction,

$$\beta = \frac{R_1 + R_s}{R_1 + R_2 + R_s}$$

Let's now investigate the impact of output impedance that is not zero. You might write the output voltage as,

$$e_o = -A_{OL} e_\varepsilon - I_o Z_o$$

Substitution for e and rearrangement gives,

$$e_o = -\frac{R_2}{R_1 + R_2 + R_s}\frac{A_{OL}}{1 + \beta A_{OL}} e_s - i_o \frac{Z_o}{1 + \beta A_{OL}}$$

The closed-loop signal gain of the circuit is thus,

$$e_o = -\frac{R_2}{R_1 + R_2 + R_s}\frac{A_{OL}}{1 + \beta A_{OL}} = -\frac{R_2}{R_1 + R_s}\left[\frac{1}{1 + \frac{1}{\beta A_{OL}}}\right]$$

For large values of AOL, the term,

$$\left[\frac{1}{1 + \frac{1}{\beta A_{OL}}}\right]$$

The closed-loop gain is really near to unity and,

$$\frac{R_2}{R_1 + R_s}$$

The closed-loop output impedance is,

$$Z_{oCL} = \frac{Z_o}{1 + \beta A_{OL}}$$

In many circuits, an op-closed-loop amp's output impedance is a negligibly small portion of the open-loop impedance, generally less than 1 m under low frequencies.

Real op-amp frequency response characteristics

It has not yet taken into account the op-amps' dynamic reaction. Gain is described as the slow change in input voltage divided by the change in output voltage. Rapid change's impact hasn't yet been thought about. It is typical to differentiate between sinusoidal and transient response characteristics. An op-reaction amp's to sinusoidal impulses is described by its sinusoidal response parameters. They specifically demonstrate how the frequency of the signal affects the op-response. Amp's an op-reaction amp's to a step or square-wave input signal is described by its transient response parameters. The need to discriminate between small signal and big signal response characteristics adds another layer of complexity; these variations result from dynamic saturation effects which happen with large signals. Small signal sinusoidal response characteristics are covered in this section. Although a practical op-gain amp's does exhibit frequency dependency, it is thought that an ideal op-open-loop amp's gain is frequency independent. The open-loop gain is frequency dependent in both amplitude and phase. The closed-loop performance is significantly impacted by this frequency dependency.

Closed-loop frequency response for small signals

Op-amp circuits' favorable properties result from the incorporation of negative feedback. The loop gain AOL has a relationship with the quantitative consequences of negative feedback. The AOL of real op-amps is frequency dependent, and in certain cases, the feedback fraction is as well. As a result, the frequency dependent loop gain present in real-world op-amp circuits significantly affects closed-loop performance. A both magnitude change and a phase

shift with frequency are implied by frequency dependency. Positive feedback may be applied to a circuit that is employing negative feedback with only a phase change of 180 degrees in the feedback loop; this can lead to significant issues. If the feedback loop's phase shift exceeds 180 degrees and the loop gain is larger than unity, an op-amp feedback circuit will start to self-sustain oscillations. This should never be allowed to happen. Sustained oscillations are not produced by feedback loop phase changes higher than 90° but much less than 180°. Nevertheless, they may result in a frequency response that rises to the bandwidth limit and then begins to decline. The circuit will display overshoot and ringing through its transient response as a result of this closed-loop gain peaking. A step or square-wave input signal causes variations in the output known as a transient response. A closed loop op-amp circuit's relative peace is described by the concept of phase margin. The phase margin is the difference between the phase shift at the frequency where the size of the loop gain is unity and 180° or less. Gain peaking is not seen in a closed-loop circuit with such a 90° phase margin. Gain peaking becomes apparent with decreasing phase margins at around 60 ° phase margins (about 1 dB peaking), and it gets increasingly pronounced with decreasing phase margins (20 ° phase margin yields roughly 9 dB of gain peaking). The open-loop frequency response of the majority of general-purpose op-amps has a first order decay characteristics. With increasing signal frequency, the open-loop gain decreases proportionately. As a result, they are guaranteed to be invariantly stable for any magnitude of resistive feedback. This kind of response, which was covered in the section before, has a phase shift of no more than 90 degrees and a 20 dB/decade roll-off down to unity gain. Therefore, the phase margin is not ever less than 90 degrees for whatever amount of resistive feedback. The closed-loop response is also impacted by the gain frequency dependency of the open-loop response. Drawing the necessary Bode plots allows for the most convenient graphical representation of the influence on closed-loop gain. We investigate how AOL affects loop gain before examining how loop gain affects the gain error factor. We could write:

$$|\beta A_{OL(jf)}| = \left| \frac{A_{OL(jf)}}{\frac{1}{\beta_{(jf)}}} \right|$$

Which when expressed in decibel form gives,

$$\text{loop gain (in dB)} = \text{open-loop gain (in dB)} - \frac{1}{\beta}\text{ (in dB)}$$

In other words, the difference between the open-loop gain magnitude in dB and 1/ in decibels seems to be equal to the magnitude of a loop gain in decibels at any frequency. Consider one first order frequency response op-amp with resistive feedback in a follower configuration as an illustration of the graphical technique. Figure 3 depicts the circuit and associated Bode charts. We simply superimpose the plot of 1/ (in dB) over the op-open-loop amp's frequency response plot throughout order to show the frequency dependency of the loop gain. Feedback that is solely resistive, as it is in this case, is frequency independent, therefore 1/ is a straight line that runs parallel towards the frequency axis. In this instance, the open-loop gain's frequency dependency is the only factor contributing to the loop gain's frequency dependence.

The open-loop gain, AOL, decreases with increasing frequency. The gain error, AOL, and loop gain all decrease in lock-step with each other. Keep in mind that gain error is proportional to the gain error factors [1/ (1 1/AOL)] deviation from unity. The phasor nature

of both the loop gain will be used to calculate the gain error if it is necessary to do so for frequencies that are close to or greater than the open-loop bandwidth fc.

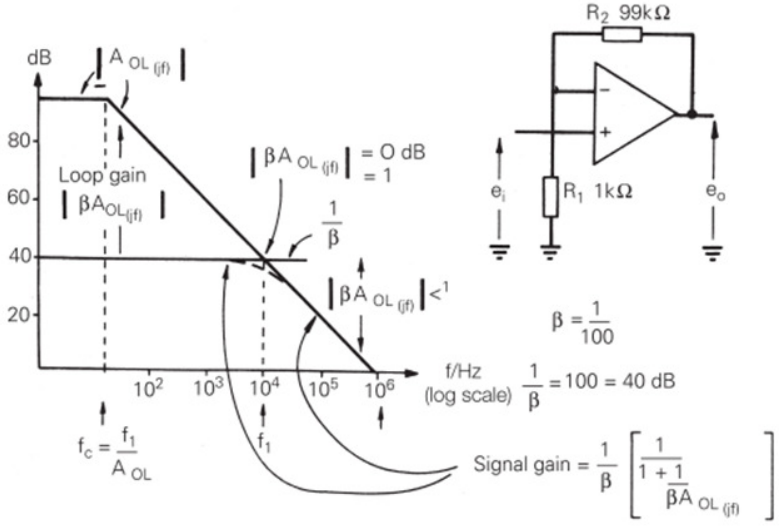

Figure 3: Illustrates the Bode plots show frequency dependence of loop gain.

Not to be overlooked. Let's assess the gain error for the circuit shown in Figure 3 at 103 Hz. The phase shift inside the loop gain is over 90 degrees at this frequency, where |AOL(jf)| is 20 dB 10. Thus,

$$\left|\frac{1}{1+\frac{1}{\beta A_{OL(jf)}}}\right| = \left|\frac{1}{1+\frac{1}{-j10}}\right| = \frac{1}{\sqrt{1+0.01}} = 0.995$$

Compare this with the value obtained by neglecting the phasor nature of the loop gain, which is,

$$1/(1 + 1/10) = 0.909, \text{ a 9\% gain error!}$$

The magnitude of the loop gain equals unity at frequency f1′ where the open-loop and 1/ magnitude charts overlap (0 dB). The two figures close at a 20 dB per decade pace, indicating a loop gain phase shift of 90° and just a residual phase margin equal 90°. The gain error at frequencies f1 is on the order of magnitude:

$$|1/(1 + 1/-j1)| = 1/\sqrt{2}$$

Thus, the amplitude of the closed-loop gain is 3 dB lower than its ideal value of 1 at the frequencies f1′. At frequencies higher than f1′, the amplitude of the closed-loop gain approaching the magnitude of both the open-loop gain. F1′ stands for the closed-loop bandwidth. The closed-loop gain but also closed-loop bandwidth combination, 1/ (f1′) f1, stays constant for various values of if AOL (o) >> 1. The closed-loop bandwidth is bigger than that of the open-loop bandwidth when there is negative feedback. Greater closed-loop gain results in lower closed-loop gain, however broader closed-loop bandwidth.

CONCLUSION

By applying the input towards the positive terminal of the op- amp and applying the op-output amp's voltage signal providing feedback towards the input of the inverting terminal, an op-amp may be utilized as a noninverting amplifier. Thus, this is everything about an explanation of inverting op-amp or inverting operational amplifier. Operational amplifiers are often employed as fundamental parts in analog electrical equipment. As a result, it is used in filtering, signal conditioning, and a variety of mathematical operations. To increase the voltage level for the applied signal, several electrical components are placed between both the operational amplifier's two terminals.

REFERENCES

[1] L. Safari, G. Barile, G. Ferri, and V. Stornelli, "Traditional Op-Amp and new VCII: A comparison on analog circuits applications," *AEU - Int. J. Electron. Commun.*, 2019, doi: 10.1016/j.aeue.2019.152845.

[2] S. Joshy, V. Verdingovas, M. S. Jellesen, and R. Ambat, "Circuit analysis to predict humidity related failures in electronics - Methodology and recommendations," *Microelectron. Reliab.*, 2019, doi: 10.1016/j.microrel.2018.12.010.

[3] P. Y. Kuo and Z. X. Dong, "A new calibration circuit design to reduce drift effect of RuO2 urea biosensors," *Sensors (Switzerland)*, 2019, doi: 10.3390/s19204558.

[4] F. Fauzy and S. Kasmungin, "Perancangan Sistem Kontrol Kecepatan Motor DC Dengan PID Labview 2010," *Manutech J. Teknol. Manufaktur*, 2019, doi: 10.33504/manutech.v9i02.42.

[5] M. Masud, A. A'ain, I. Khan, and N. Husin, "Design of voltage mode electronically tunable first order all pass filter in ±0.7 V 16 nm CNFET technology," *Electron.*, 2019, doi: 10.3390/electronics8010095.

[6] I. M. Pandiev and E. C. Stoimenov, "Design and Development of Low-Power Multistage Amplifier Laboratory Kit for Electronic Engineering Education," 2019. doi: 10.1109/ELECTRONICA.2019.8825602.

[7] Ö. Äüôú *et al.*, "Anupam shukla," *J. Chem. Inf. Model.*, 2019.

[8] S. Kumar, G. D. Ropmay, P. Kumar Rathore, and P. Rangababu, "An idea of implementing CMOS operational amplifier in summer configuration for the designing of highly sensitive pressure transducer," 2019. doi: 10.1109/IESPC.2019.8902445.

[9] V. S. Bendre, A. K. Kureshi, and S. Waykole, "Design of analog signal processing applications using carbon nanotube field effect transistor-based low-power folded cascode operational amplifier," *J. Nanotechnol.*, 2018, doi: 10.1155/2018/2301421.

[10] B. Chaturvedi, J. Mohan, and A. Kumar, "A New Versatile Universal Biquad Configuration for Emerging Signal Processing Applications," *J. Circuits, Syst. Comput.*, 2018, doi: 10.1142/S0218126618501967.

CHAPTER 14

NON-INVERTING OPERATIONAL AMPLIFIER: A REVIEW

Dr. N. Raghu, Associate Professor
Faculty of Engineering and Technology, Jain (Deemed-To-Be University), Bengaluru, Karnataka, India
Email id- n.raghu@jainuniversity.ac.in

Abstract:

An operational amplifier circuit with such a non-inverting op amp has an output voltage that coincides phase with both the input voltage. The inverting op amp, which generates an output signal that is 180 degrees out of phase, is its counterpart. In this chapter author discusses closed loop stability consideration and phase margin determines closed loop gain peaking.

Keywords:

Gain, Inverting, Operational Amplifier, Network.

INTRODUCTION

The input voltage signal (VIN) is applied directly towards the non-inverting (+) output terminals in a non-inverting operational amplifier arrangement, causing the output source impedance to change to "Positive" in comparison to the "Inverting Amplifier" circuit people saw in the previous tutorial, with whom the output gain is negative. The end consequence is that both the output signal and the input signal are "in-phase." Applying a tiny portion of an output voltage signal down to the inverting (-) inverting input through an R - R2 voltage divider network generates negative feedback, which is used to regulate the non-inverting op amp. Since no current starts flowing through into positive input terminal (ideal circumstances), this closed-loop arrangement creates a non-inverting operational amplifier with extremely strong reliability, a very higher current resistance, Rin approaches infinity, as well as a low output impedance Rout, as illustrated in Figure 1.

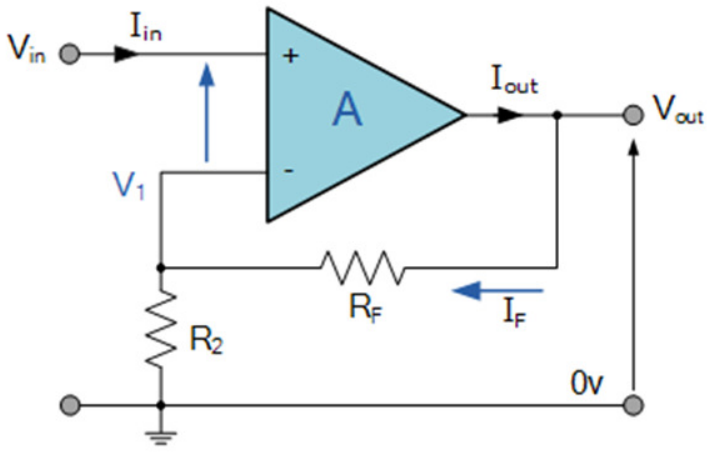

Figure 1: Illustrates the circuit of Non-inverting Operational Amplifier.

Equivalent Potential Divider Network

In the last instruction on inverting amplifiers, we said that "V1 always equals V2" and that "No current can flow through into input terminal" of the amplifiers for a perfect op-amp. This occurred as a result of the input signal as well as feedback signal's junction (V1) being at the same voltage. The intersection serves as a "virtual earth" summation point. Because of this virtual earth node the resistors, Rf and R2 form a simple potential divider network across the non-inverting amplifier with the voltage gain of the circuit being determined by the ratios of R2 and Rf as shown in Figure 2.

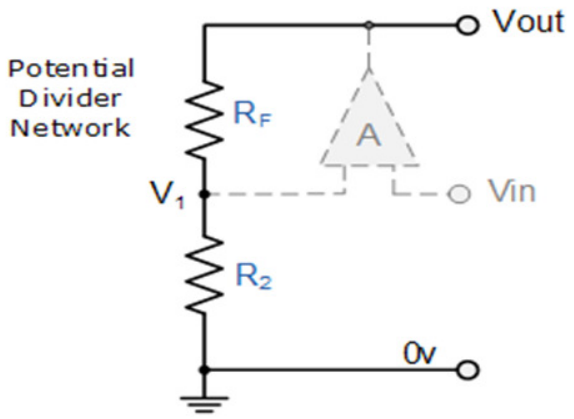

Figure 2: Illustrates the circuit diagram of Equivalent Potential Divider Network.

Then using the formula to calculate the output voltage of a potential divider network, we can calculate the closed-loop voltage gain (AV) of the Non-inverting Amplifier as follows:

$$A_v = 1 + \frac{R_F}{R_2}$$

The equation above demonstrates that the combination of the values of R and R2 determines the total closed-loop gain of a non-inverting amplifier, which is naturally positive and will remain larger but never less than one (unity). The gain achieved by the amplifier will indeed be precisely equal to one when the feedback resistance R has a value of zero (unity). However, in reality, the gain will be restricted to the operating amplifier' open-loop differential increase if resistance R2 is zero (AO).

Voltage Follower (Unity Gain Buffer)

As all of the terminal voltage is given back towards the inverting input wire, the circuit would achieve a fixed gain of "1" (unity) if we set the feedback resistance, R, to zero (R = 0), as well as the resistor, R2, to infinity (R2 =). (Negative feedback). An electrical impulses, commonly referred to as a "unity gain buffer," is a specific kind of non-inverting amplifier circuit that would be created by this setup. This output signal is not reversed since it is linked directly towards the amplifier's non-inverting intake, hence Vout = Vin because the output voltage is the same as the input voltage. As a result of its input-to-output isolation qualities, the voltage follower circuitry is thus perfect as a voltage source in series or voltage regulator. Since the unity gain voltage follower arrangement retains the input signal voltage was at its output terminal, it may be employed in situations where circuit isolation or susceptibility matching are more critical that power or current augmentation. Additionally, since the input impedance of a voltage follower circuits is equal to the corresponding resistance occasions

the gain of an operational amplifier, it is very high, frequently exceeding 1M. (Rin x AO). Since a perfect op-amp condition is maintained, the op-output amp's impedance is extremely low and is thus unaffected despite changes in load.

Non-inverting Operational Amplifier Voltage Follower

The feedback impedance R has been lowered to zero in this non-inverting circuit arrangement, while the input impedance Rin is reached infinity. Since the output is directly coupled towards the negative inverting input, there is 100% feedback hence Vin precisely equals Vout, giving the system a fixed gain of 1, or unity. Since there is no current flowing into the non-inverting output terminals due to the infinite input impedance (ideal circumstances), there will be no current flowing through the feedback loop when the input voltage Vin is applied to the non-inverting input. Since no current flows through the resistance, there is minimal voltage drop between it and no power is lost as a consequence, any amount of resistance may be used in the feedback loop while changing its properties. As a result of the exceptionally high input impedance, the unison gain buffer (voltage follower) may be utilized to give a significant power gain since the additional power is sent to the load through into the op-amps' output as well as supply rails rather than directly from the input. However, leakage currents and parasitic capacitor values are common in genuine unity gain buffer circuits, therefore a low value (usually 1k) resistor is needed in the feedback loop to assist mitigate their effects and provide stability, particularly if the op amp is a reference current type. The voltage follower, also known as a unity gain buffer, is a unique and highly practical type of non-inverting operational amplifier that is frequently used in circuit boards to disconnect circuits from one another, particularly in high-order system variables passive filters or Sallen-Key active filters to differentiate one filter phase between them. The 74LS125 Quad 3-state buffer and the more prevalent 74LS244 octal buffer were typical digital cushion ICs that are readily accessible.

LITERATURE REVIEW

In study G. Mulberry[1] et al. in biosensor applications, such as in vivo dopamine measurements, single-cell electrophysiology, photoplethysmography, pulse oximetry, and Nano pore recordings, high-throughput recordings of tiny current are becoming increasingly prevalent. Thus, there is a need for a Tran's impedance amplifier design that is extremely scalable. By sharing the operational amplifier design's non-inverting side across many inverting halves, half-shared amplifier designs are one technique to increase scalability. Comparing this way to employing separate operational amplifiers, silicon area and power are reduced by over 50%. In this study, we investigate the trade-offs associated with expanding the number of inverting half amplifiers sharing a single non-inverting half while analyzing the scalability of a straightforward half-shared amplifier structure. To reduce the size of each amplifier, a Tran's impedance amplifier is developed utilizing a half-shared structure. A capacitor's current integration serves as the foundation for the trans impedance amplifier. Because the integration amplifier is a non-stationary circuit and does not attain a steady state, doing a noise analysis on it might be difficult. An estimation approach to determine the noise characteristic in the simulation is given for frequency analysis. To verify the accuracy of the aforementioned analysis, the array design of 1024 Trans impedance transistors is constructed using a conventional 0.35 m method and tested. The amplifier array has a low mismatch of 1.65 mV over the full 1024 amplifier array, very low noise, and great linearity in Trans impedance gain (7.00 mV/pA for high gain and 0.86 mV/pA for low gain). The method will be essential for allowing the creation of bigger arrays so that greater throughput measuring equipment for biosensor applications may be used.

T. M. Mishonov et al.[2]as a crucial tool for the study of modern circuits with operational amplifiers, the time-dependent master equation from the original publication by Ragazzini, Randall, and Russell (Ragazzini et al 1947 Proc. of the I.R.E. 35, 444–452) is retrieved. The relationship between the time-dependent output voltage U0(t) and the difference between the input voltages (U+(t) and U-(t)) is given by this equation. In this equation, the time constant stands in for the crossover frequency f0. Two common examples are used to demonstrate how the 0 master equation works: a) the stability requirement for devices with negative resistance converters, which we regard to be a novel result b) without using the time-dependent equation, the frequency dependency of the operational amplifier amplifiers is stated in the technical requirements. The approach is shown by determining the crossover frequency for the low-noise and fast ADA4898 operational amplifier. A simple circuit is proposed for determining f0. It is determined that the 70-year-old master equation is a valuable approach implicitly integrated in the modern software for a precise calculation of pass bandwidth for amplifiers with active filters. For the situation of non-zero conductivity between the operational amplifiers' inputs, the equations for the amplification coefficient both inverting and non-inverting amplifiers are provided.

S. F. Wang et al.[3] that study introduces a flexible three-output voltage-mode biquadratic filter with five inputs. Five single-ended output operational transconductance amplifiers (OTAs) and two grounded capacitance are features of the proposed filter. It is simple to convert the filter into a quadrature oscillator. The grounded capacitor filter has no resistors and may be electrically adjusted. By properly choosing input and output terminals, a voltage-mode single-input three-output biquadratic filter or a voltage-mode five-input single-output biquadratic filter may be controlled. By applying the input voltage signals properly, it is possible to realize the non-inverting low pass, non-inverting bandpass, inverting band pass filter, inverting high pass, non-inverting band reject, inverting band reject, and non-inverting all pass filtration responses when the five-input single-output biquadratic filter is operating. The non-inverting/inverting low pass, bandpass, and band reject filtering responses may be implemented concurrently in the operation of a single-input three-output biquadratic filter. High input impedance, independent modification of the resonance rayleigh number and quality factor, and the absence of input voltage signals of the inverting type are all features of the circuit. The use of a quadrature oscillator demonstrates separate electronic tuning properties for the oscillation frequency and condition. Through OrCAD PSpice and further experimental data, the theoretical analysis has been confirmed.

S. F. Wang et al.[4] suggested voltage-mode multifunction biquadratic filter in this study uses a high-input impedance current feedback operational amplifier (CFOA), and it is combined with a voltage-mode quadrature oscillator. Three CFOAs, three resistors, and two grounded capacitors are used in the proposed high-input impedance CFOA-based voltage-mode multifunction biquadratic filter, which has two inputs and output unit. Whereas the inverting band-pass and non-inverting high-pass filtering functions may also be obtained by using another high-input impedance terminal, the filter could indeed simultaneously realize non-inverting low-pass, non-inverting band-pass, and non-inverting band-reject filtering functions there at high-input impedance terminal. Resonance angular frequency but also quality factor may be controlled orthogonally by the filter. It is possible to create a voltage-mode quadrature oscillator with separately regulated oscillator frequency and oscillations state using the suggested high-input impedance CFOA-based voltage-mode multifunction biquadratic filters. The experimental findings of the commercially available integrated circuit, AD844AN, and OrCAD PSpice simulation were utilized to verify the features of the proposed filter and oscillator.

Novel current feedback operational amplifier-based two first-order all-pass filters (CFOAs) are developed by E. Yuceet al. [5]. Two CFOAs are used in the first planned APF, whereas three CFOAs are used in the second. The use of a grounded capacitor, the ability to change gain, and having a low output impedance are the major characteristics of both of the proposed APFs. Both of the proposed APFs need to have a single passive element matching condition for optimal functioning, despite the second suggested APF's high input impedance and ability to concurrently give both inverting and non-inverting APF responses. Applications of the suggested APFs are shown by the inclusion of single-phase and multiphase oscillators. To test the notion, a number of simulations and tests using commercially available hardware, including AD844s, are conducted.

S. F. Wang et al.[6] in that work, a novel voltage-mode universal filter based on five single-ended operational transconductance amplifiers (OTAs) containing two grounded capacitors as well as a quadrature oscillator is described. By properly applying various five input voltage signals, the suggested circuit may provide non-inverting lowpass, frequency response, highpass, bandreject, and allpass filters, as well as inverting bandpass and highpass filters. This same circuit only uses five single-ended OTAs but also two grounded capacitors to maintain this same following benefits: high input impedance, no additional inverting or non-inverting amplifiers needed for special input signals, low active and passive hypersensitivity, orthogonal automated tunable resonance angular frequency, and quality factor without control parameter matching conditions. Additionally, a quadrature sinusoidal oscillator having separately regulated oscillation condition and oscillation frequency may be implemented using the suggested filter. The suggested voltage-mode universal filter and quadrature sinusoidal oscillator's properties are verified using OrCAD PSpice simulation and experimental findings of commercially available OTAs, LT1228.

S. F. Wang et al.[7] five single-ended output operational transconductance amplifiers (OTAs), two grounded capacitors, and a voltage-mode biquadratic filter with five inputs and three outputs are used in this research. Different approaches may be used to connect the suggested circuit to the input terminals to create a lowpass, bandpass, high pass filter, bandreject, and allpass filter. The suggested circuit, in contrast to other efforts, can implement both non-inverting and inverting lowpass, bandpass, but also bandreject filtering responses. The suggested circuit accomplishes independent controllability of a parameters o and o/Q without the necessity for control factor matching conditions, as well as orthogonal controllability of both the resonance angular frequency (o) and quality factor (Q). The novel circuit has the following benefits: a single-input three-output function that returns filter or a five-input single-output topology biquadratic filter with a single output, high input impedance, resistorless construction, and no requirement for inverted input signals. Additionally, utilizing the suggested filter, a quadrature sinusoidal oscillator with fully-uncoupled electrically adjustable oscillation frequency and condition is created. Experimental findings and the OrCAD PSpice simulation tool serve to confirm the suggested circuits' viability. The outcomes are in line with what is predicted by theory.

M. Dogan and E. Yuceet al.[8]in that study, new simulators for five grounded emittance functions were presented. One inverting buffers plus-type second-generation current conveyor is all that is needed for the first suggested circuit, a positive lossless grounded inductor simulator, but just one non-inverting current feedback operational amplifier was required in each of the other four circuits. The second and third versions are simulators of grounded inductors with negative loss. The final component is a negative capacitance multiplier, while the fourth one is a positive inductance with such a series positive resistor. Every suggested circuit, with the exception of the first, consists exclusively of grounded

capacitors (s). Nevertheless, a single passive component matching condition is required for each of the suggested circuits. The first suggested circuit is used in a band-pass filter as an example. Additionally, frequency dependent non-ideal gain impacts on each circuit's performance are provided. When doing several SPICE simulations, 0.13 m IBM technology parameters are used, and 0.75 V DC symmetrical power supply polarities are used. An example of an experimental outcome is provided to show how well the first suggested circuit performs.

Research proposes a study of the non-inverting amplifier using a two stage CMOS unbuffered current-feedback operational amplifier (UCFOA) byH. Barthélemy[9] et al. The closed loop gain is theoretically explained using just a small-signal equivalent circuit (macro-model) of the non-inverting amplifier. According to the quality factor Q of resonance and also the unique Operational Transconductance Conveyor description of the UCVFOA input stage, the op-amp phase margin and its bandwidth have indeed been determined (OTC). One may think of the OTC description as a development of type II second-generation current conveyors. A theoretical method is presented in this research that shows how to exactly determine the value of the UCFOA compensatory capacitance based on the core characteristics of the proposed OTC. The both theoretical macro-model and the CMOS arrangement from a 0.35 m typical BSIM3V3 transistor models were simulated using PSPICE.

Low measurement throughput is a typical issue in single-cell experiments byG. Mulberry [10] et al. Because of the combination of electrodes and amplifiers onto a single chip, monolithic CMOS microsystems have made it possible for several parallel tests to be performed concurrently to boost throughput. This study investigates a CMOS device that utilizes a "half-shared" operational amplifier design and has an array comprising 1024 parallel trans-impedance amplifiers. The inverting half and also the non-inverting half of a conventional 5-transistor operational amplifier are divided into two by this construction. By dividing an amplifier in two, the die space needed with each individual amplifier may be decreased since the non-inverting half can be "shared" with numerous inverting halves. This makes it possible to integrate more amplifiers onto a single chip; in this scenario, 32 amplifiers may occupy the same area as 17 conventional 5-transistor differential amplifier. The amplifiers show strong linearity throughout trans-impedance gain and low mismatch of 1.65 mV over the full 1024 amplifier array. Future designs will be able to make bigger arrays thanks to the technology, giving access with even higher-throughput measuring tools to electrophysiologists and others.

DISCUSSION

Closed-loop stability considerations

The majority of op-amps have had an open-loop frequency response with such a 20 dB/decade roll-off and therefore are internally frequency adjusted. In theory, a response of this kind guarantees that the op-amp will be closed-loop stable even under resistive feedback situations. The usage of an internally frequency adjusted op-amp does not always guarantee closed-loop stability, it is vital to be aware of this. Even now in resistive feedback circuits, phase changes brought on by capacitive loading at such an op-output amp's or stray capacitance between both the inverting input terminal and ground may result in instability. An internally adjusted op-amp displays instability in differentiator applications when the feedback fraction is purposefully made frequency dependent. Externally frequency compensating op-amps are those that have a final roll-off in characteristic open-loop frequency response of more than 20 dB/decade. When a circuit requires a large closed-loop

bandwidth as well as a gain higher than unity, these rapid roll-off op-amps are often utilized. For them to be closed-loop stable, a capacitor must be connected outside. Bode graphs may be used to describe the closed-loop frequency response achieved with rapid roll-off (externally frequency adjusted) op-amps. The response is a result of the phase shift and gain error brought on by the fading open-loop gain. Take the response of an op-amp, for instance, which has three gain stages, each of which has a distinct cut-off point for the frequency response. Figure 3 shows the open-loop gain's phase and magnitude characteristics. To get the magnitude and phase characteristic features for a given feedback fraction, a plot of 1/ is superimposed over the open-loop frequency response chart. It is frequency independent with resistive feedback. By looking back at the graphs, it is possible to deduce that the phase shift throughout the open-loop gain determines the phase shift inside the closed-loop gain.

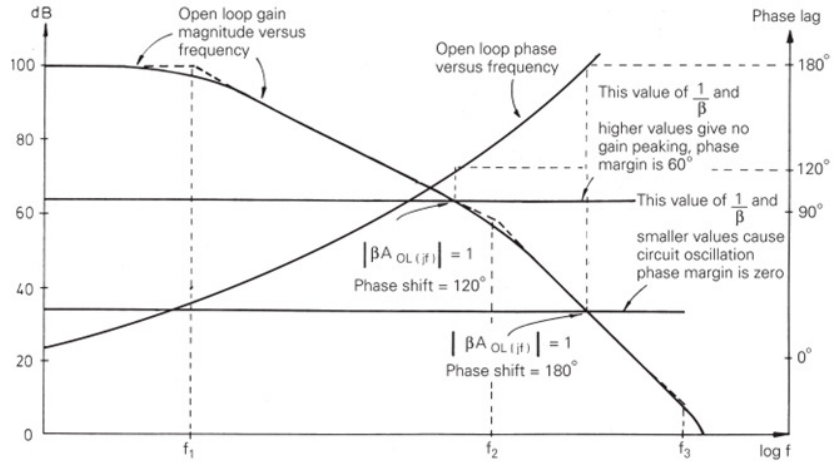

Figure 3: Illustrates the Gain magnitude and phase characteristics of op-amp with three-pole response.

Phase margin is the difference between this phase shift and 180° at the frequency when the loop gain is at its maximum (0 dB). Keep in mind that rising causes the phase margins to become narrower and smaller. The closed-loop gain peaks when phase margins are smaller than 60 degrees (see Figure 4). As the phase margin is progressively lowered, the gain peaking rises until, at zero phase margin, whole circuit erupts into prolonged oscillations.

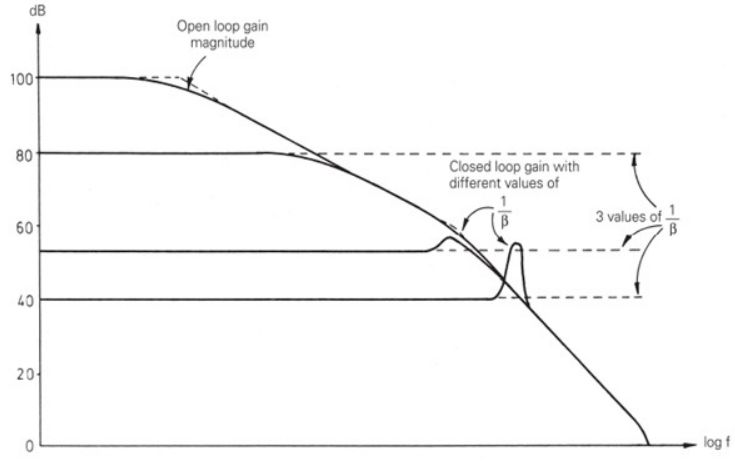

Figure 4: Illustrates the too much feedback gives gain peaking with uncompensated fast roll-off op-amps.

Phase margin determines closed-loop gain peaking

Positive feedback is the root cause of the gain peaking, which happens as a consequence of insufficient phase margin. Whenever a component of the feedback signal has been in phase with the input signal delivered externally, positive feedback occurs. The circuit oscillates if the gain is larger than unity when the phase shift inside the loop gain exceeds 180°. We must look at the impact of the loop gain magnitude/phase behavior upon that gain error factor when evaluating the amount of the gain peaking (obtained as a consequence of insufficient phase margin).

$$\beta A_{OL(jf)} = |\beta A_{OL(jf)}| e^{-j\theta}$$

The value of the gain error factor may then be expressed as,

$$\frac{1}{1+\frac{1}{\beta A_{OL(jf)}}} = \frac{1}{1+\frac{e^{j\theta}}{|\beta A_{OL(jf)}|}}$$

$$\frac{1}{1+\frac{\cos\theta + j\sin\theta}{|\beta A_{OL(jf)}|}}$$

The magnitude of the gain error factor can then be written as,

$$\left|\frac{1}{1+\frac{1}{\beta A_{OL(jf)}}}\right| = \sqrt{\left(\frac{1}{1+\frac{1}{|\beta A_{OL(jf)^2}|}+\frac{2\cos\theta}{|\beta A_{OL(jf)}|}}\right)}$$

We have the potential of a gain error factor magnitude bigger than unity for values of more than 90° since the cosine of angles between 90° and 180° is negative. Closed-loop gain peaking is caused by this change in the gain error factor. Gain peaking often results from a phase shift, the frequency of which is governed by a simple first order function. The difference between this break frequency and other break frequencies is more than ten years. There are two examples of scenarios. This scenario's projected link between closed-loop gain peaking but also phase margin is also demonstrated visually in (see also Appendix A2). The 1/ graph (in dB) is overlaid on the open-loop response to determine the phase margin in a specific circuit. The frequency f1′ at which the amplitude of the loop gain equals unity is determined by the intersection of the two curves. The phase margin is 180°, and the phase shift at this frequency would then be calculated from either the phase/frequency variation in AOL. The graph may be used to determine how much gain peaking there is. Keep in mind that the gain peaking really happens at frequencies that are a little lower than f1′. The gain peak, however, grows in magnitude as the phase margin shrinks, and the frequency during which it occurs approaches frequency f1.

Frequency compensation (phase compensation)

The technique of adjusting the loop gain magnitude/phase characteristics of a feedback op-amp circuit to provide an acceptable phase margin is known as frequency compensation or

phase compensation. Closed-loop stability and immunity from closed-loop gain peaks are guaranteed by an adequate phase margin. The stability and frequency sensitivity of feedback circuits may be evaluated using Bode diagrams, and examples will be presented along with their respective Bode diagrams. Ordinarily internal frequency adjusted and providing unconditional stability including all amounts of resistive feedback, general-purpose op-amps. For all frequencies where another open-loop gain magnitude is more than unity, the phase shift throughout their open-loop gain is commonly managed to be 135° or less, ensuring a minimum phase margin of 45° for any and all levels of resistive feedback. Internal frequency compensation makes things easier for the user at the cost of closed loop bandwidth but also speed (slew rate - see below), which would otherwise been available when the op-amp is operated at greater closed-loop gains than unity. It is essential to remember that if the load was sufficiently capacitive, even frequency adjusted op-amps might become unstable. At the output terminal of the op-amp, the input impedance and external capacitance lead to a phase shift. Oscillation may occur even if the op-amp does have a phase margin of 45° period of at least because of a phase shift that is bigger than this at the output. This is because the output of the op-amp is used as feedback. Phase shift there at output and consequently in the feedback loop are both decreased by an external resistor placed between the op-output amp's and the load. In Section 10.5, the topic of correcting both capacitive loads but also capacitive inputs is further upon. External frequency compensating components are necessary for op-amps without internal frequency correction. They provide the user the option to choose a frequency compensating strategy suitable for the specific closed-loop circuit. Any frequency compensating mechanism used has an impact on the closed-loop bandwidth, slew rate, maximum energy response, and noise performance (see later). Due to variations in internal circuitry, different compensation techniques are recommended for various op-amp types. For all op-amps, the fundamental concepts behind frequency correction are the same. Active loads allow the amplifying stages of an op-amp to obtain extremely high gains. In many situations, employing only two internal voltage gain circuits, the total gain may be suitably big. Op-amps of this kind often use a single feedback capacitor linked around the second inverting gain stage to adjust for frequency. The method simply needs tiny quantities of frequency compensating capacitors (10 pF–30 pF). This size of capacitor may be produced on the same integrated circuit chip as both the rest of the op-amp circuitry due to its compact size. This is how general-purpose op-amps compensate for internal frequency: Figure 5 shows a simplified schematic of the internal circuit.

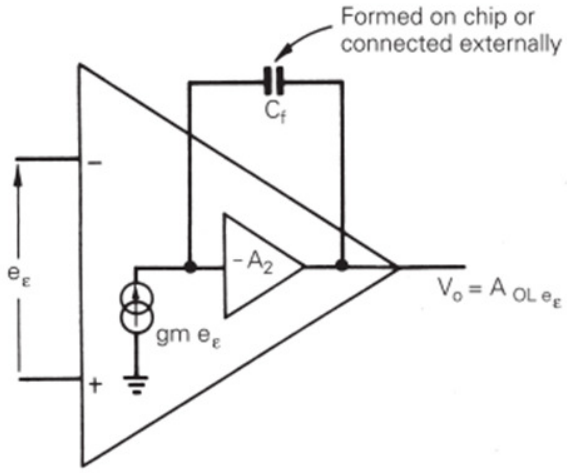

Figure 5: Illustrates the Equivalent circuit for frequency compensation.

CONCLUSION

Operational amplifiers are crucial in the creation of the fundamental elements of several electronic circuits. Because of external components that are connected to the system characteristics, certain operational amplifier components are involved. The reason the op-amp shifts the output signal's phase angle precisely 180 degrees out then of phase without regard to the input signal is why it is known as just an inverting amplifier. The same as previously, let's build a closed loop circuit from across amplifier using two external capacitors to form a feedback circuit.One op amp and two resistors may be used to create both inverting and non-inverting op amps, only in distinct manners.

REFERENCES

[1] G. Mulberry, K. A. White, and B. N. Kim, "Analysis of Simple Half-Shared Transimpedance Amplifier for Picoampere Biosensor Measurements," *IEEE Trans. Biomed. Circuits Syst.*, 2019, doi: 10.1109/TBCAS.2019.2897287.

[2] T. M. Mishonov *et al.*, "Master equation for operational amplifiers: Stability of negative differential converters, crossover frequency and pass-bandwidth," *J. Phys. Commun.*, 2019, doi: 10.1088/2399-6528/ab050b.

[3] S. F. Wang, H. P. Chen, Y. Ku, and Y. C. Lin, "Versatile tunable voltage-mode biquadratic filter and its application in quadrature oscillator," *Sensors (Switzerland)*, 2019, doi: 10.3390/s19102349.

[4] S. F. Wang, H. P. Chen, Y. Ku, and P. Y. Chen, "A CFOA-based voltage-mode multifunction biquadratic filter and a quadrature oscillator using the CFOA-based biquadratic filter," *Appl. Sci.*, 2019, doi: 10.3390/app9112304.

[5] E. Yuce, R. Verma, N. Pandey, and S. Minaei, "New CFOA-based first-order all-pass filters and their applications," *AEU - Int. J. Electron. Commun.*, 2019, doi: 10.1016/j.aeue.2019.02.017.

[6] S. F. Wang, H. P. Chen, Y. Ku, and C. M. Yang, "A voltage-mode universal filter using five single-ended OTAs with two grounded capacitors and a quadrature oscillator using the voltage-mode universal filter," *Optik (Stuttg).*, 2019, doi: 10.1016/j.ijleo.2019.162950.

[7] S. F. Wang, H. P. Chen, Y. Ku, and C. M. Yang, "Independently tunable voltage-mode OTA-C biquadratic filter with five inputs and three outputs and its fully-uncoupled quadrature sinusoidal oscillator application," *AEU - Int. J. Electron. Commun.*, 2019, doi: 10.1016/j.aeue.2019.152822.

[8] M. Dogan and E. Yuce, "Supplementary single active device based grounded immittance function simulators," *AEU - Int. J. Electron. Commun.*, 2018, doi: 10.1016/j.aeue.2018.07.016.

[9] H. Barthélemy, R. Vauché, V. Giès, S. Bourdel, and J. Gaubert, "Two-stage unbuffered CFOA based non-inverting resistive-feedback amplifier: a study based on the description of the operational transconductance conveyor (OTC)," *Analog Integr. Circuits Signal Process.*, 2018, doi: 10.1007/s10470-018-1219-0.

[10] G. Mulberry, K. A. White, and B. N. Kim, "A Half-Shared Transimpedance Amplifier Architecture for High-throughput CMOS Bioelectronics," 2018. doi: 10.1109/BIOCAS.2018.8584792.

CHAPTER 15

A COMPREHENSIVE STUDY ON SUMMING AMPLIFIER

Savitha R, Assistant Professor
Faculty of Engineering and Technology, Jain (Deemed-To-Be University), Bengaluru, Karnataka, India
Email id- r.savitha@jainuniversity.ac.in

Abstract:

A voltage output from the summing amplifier generally equal to the amplified sum of more than two input voltages. The output voltage of a summing amplifier is frequently an inverting amplifiers, meaning it is negative when measured against grounding. In this chapter author is discusses frequency compensation with slew rate consideration.

Keywords: Circuit, Inverting, Network, Summing Amplifier.

INTRODUCTION

Having previously observed that the inverting op amp seems to have a single input voltage (Vin) supplied towards the inverting input wire. A different operational amplifier circuitry known as a summing amplifier is produced in Figure 1 if more input resistor are added to the input, each with a magnitude equivalent to the original input resistor (Rin). The output voltage (Vout) in this straightforward summing amplifier circuit has now become proportional to the product of the input voltages (V1, V2, V3, etc.). Therefore, to account for these extra inputs, we may change the original calculation again for inverting amplifier:

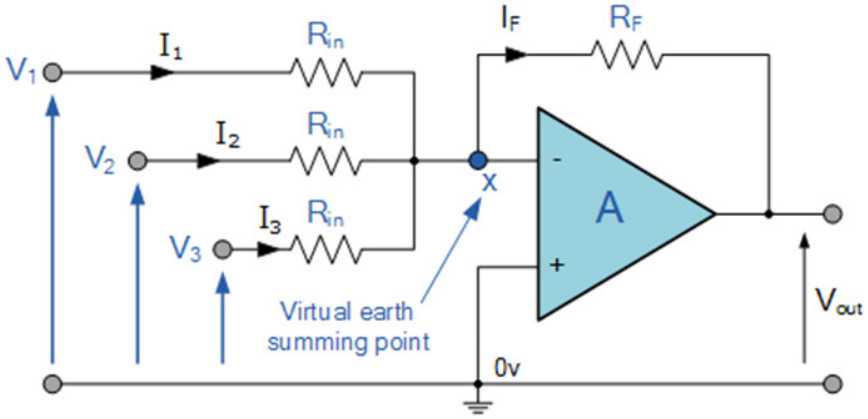

Figure 1: Illustrates the circuit diagram of summing amplifier.

Summing Amplifier Equation

They now have a functional amplifier circuit which will boost each individual voltage source and generate an output voltage that is proportional towards the algebraic "SUM" of a three distinct input voltages V1, V2, and V3. Because each input "sees" its own resistance, with Rin acting as the single input impedance, one may easily add additional inputs if necessary.

$$-V_{out} = \frac{R_F}{R_{IN}}(V_1 + V_2 + V_3 \ldots . V_n)$$

This happens because the "virtual earth" node at the op-inverting amp's input effectively isolates the input signals from one another. When all the resistances have the same value and R = Rin, then direct voltage addition might also be produced. Keep in mind that any amount of input voltages would create the negative total whenever the summing point is linked to the op-inverting amp's input. The summing point will also generate the positive sum of the input voltages whenever it is attached to the op-non-inverting amp's input.

Non-inverting Summing Amplifier

The non-inverting setup's benefit over the inverting summing amplifier configuration, then the biggest benefit of a non-inverting summing amplifier throughout Figure 2 is because there is no simulated earth condition throughout the inverting input, its input resistance is much higher compared to a typical inverting amplifier configuration. This is in addition to the obvious actuality that perhaps the op-amps output voltage VOUT seems to be in phase with some of its and the output. voltage is the weighted combination of all its inputs, something that themselves are established by about their resistance ratios [1]. The circuit's input summing portion is also unaffected by changes to the op-amps' closed-loop voltage gain. Nevertheless, choosing the weighted gains on every input somewhere at summing junction requires additional arithmetic, particularly when there are greater than two inputs, each with a distinct weighting factor. However, there will be far less arithmetic required if all of the inputs possess the same resistive values.

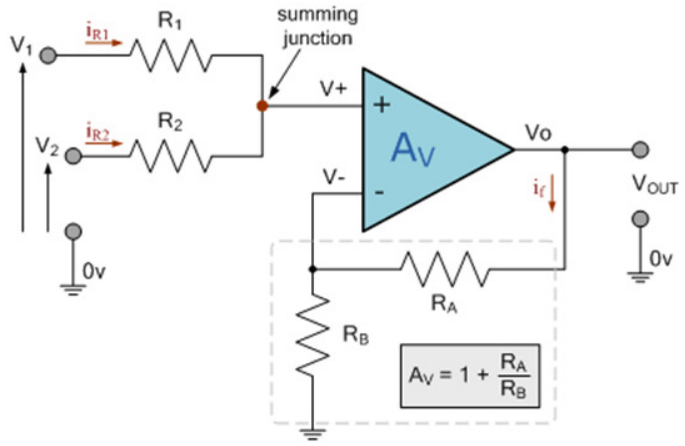

Figure 2: Illustrates the circuit diagram of Non-inverting Summing Amplifier.

The output voltage of a non-inverting op amp will be precisely equal to the total of all the voltage sources if indeed the closed-loop gain of the op-amp is set to correspond to the number of summing inputs. That is to say, the op-amps gain is equivalent to 2 for an input signals non-inverting summing amplifier, 3 for a three control summing amplifier, and so on. This is due to the fact that the voltage at each input resistor determines the current that flows there. Even though they can enter the high impedance, non-inverting input of both the op-amp, the increase in current equal out and the output voltage equals the sum of the input resistances if the input reactance are all set to the same value (R1 = R2). Consequently, the currents streaming into in the input terminals of a two-input, non-inverting operational amplifier may be characterized as:

Summing Amplifier Applications

It utilizes either inverting or non-inverting summing amplifiers. The degree by which the various input signals were mixed together may be controlled by connecting potentiometers towards the input resistance values of a summation amplifier. When measuring temperature, for instance, individuals could add a negative counterbalanced power output to start making the voltage output or showcase read "0" so at freezing point, or maybe you could create an audio mixer to incorporate or add independent output waveform (sounds) from various source touchpoints (vocals, instruments, etc.) rather than having to send the resulting mix to an audio amplifier.

Digital to Analogue Converter

The output step voltage throughout this DAC summing power amplifier is ultimately determined by the number decoding different pieces that make up the original data word—in this case, four bits—as a proportion of a full-scale analogue - to - digital voltage. That full-scale analogue output's precision is also reliant on the input bits' voltage levels, which must constantly be 0V for "0" and 5V for "1," in addition to the accuracy of a resistivity values utilized for something like the input resistors, RIN. Furthermore, commercially accessible Digital-to-Analogue and Analogue-to-Digital devices were widely available with very precise resistor ladder connections already built-in to circumvent these flaws, at least from our end.

LITERATURE REVIEW

I. Yeo et al.[2]presented a circuit method and training algorithm that reduce the impact of stuck-at-faults (SAFs) in a memristor crossbar array of neural networks (NNs). A standard trans-impedance amplifier, that is responsible for total the currents flowing through the memristors, is changed to make sure the amplifier output is located within the proper working range in order to optimize the network performance when the presence of SAFs. Using the suggested training approach, which trains the network using the positions and values of defective mersisters, further enhances the performance of the network. To demonstrate how the suggested circuit approach and training procedure increase the performance of NNs, a feedforward NN utilizing 32 x 32 memristor crossbar arrays was developed.

In this work, a brand-new ultra-low voltage, ultra-low power completely differential current conveyor (FDCCII) that is appropriate for use in analog signal circuits with very low voltage, low power is presented. The suggested structure uses two differential pairs that provide minimal complexity and low power consumption because to the multiple-input bulk-driven MOS transistor technology. The suggested circuit's rail-to-rail input common-mode range is also provided by the bulk-driven MOS method circuit. The circuitry has been used to construct summing/subtracting amplifiers as design examples to demonstrate the viability of the planned FDCCII[3]. With such a 0.18 m TSMC n-well CMOS process as well as a 0.4 V supply voltage, PSPICE simulations are used to show the proposed FDCCII's performance and design examples by M. Kumngernet al.

An amplifier that uses output transistors for switches is referred to as a class D amplifier by B. Murtianta et al.[4]A transistor has no current flowing through it while it is off, and when it is on, it has a minimal, preferably zero voltage across it. Because of the very low power dissipation, the amplifier only needs a modest heat sink. Class D amplifiers operate according to analog principles; the signal is not digitally encoded. The common classes prior to the development of class D amplifiers were class A, class AB, class B, and class C. Utilizing a comparator is the traditional technique for producing signals that drive a transistor MOSFET. An audio signal is used to drive one input, while a triangle wave or sawtooth wave at the

desired switching frequency drives the other. A triangle or sawtooth wave must have a frequency greater than the audio input. MOSFET transistors function as switches thanks to their complementary operation. Square waves fed into the integrator circuit often produce triangle waves. The integrator and comparator are thus crucial components in the PWM (Pulse Width Modulation) processing of audio signals. In this study, the summing integrator technique, which serves as the major component of a class D amplifier system, would be discussed.

An innovative analog to digital converter (ADC) design called noise-shaping SAR (NS-SAR) provides great resolution and high energy efficiency by L. Jie et al.[5]Despite these benefits, oversampling places restrictions on the NS-SAR ADCs' useable bandwidth. This article presents an interleaving design that circumvents this bandwidth restriction. A realizable time-interleaved noise-shaped (TINS) system is made possible by midway feedback to several successive-approximation conversion stages. Utilizing the natural channel delay, a high-order noise-transfer function is developed (NTF). The NTF coefficients' redundancy and optimization prevent the possibility of quantization overload, resulting in reliable operation. The design is kept simple by realizing error feedback (EF) using a summing pre-amplifier and just a shared feedback bus. The pre-amplifier is easily built as a single-stage open-loop amplifier because of the low necessary gain. The measured SNDR for a prototypes 40-nm CMOS TINS-SAR ADC with a 50-MHz bandwidth is 70.4 dB. It just uses 13 mW and takes up 0.06 mm2. Evaluation of various devices and assessment of their performance under varying supply and temperature conditions show reliable performance requiring calibration.

E. T. Sung and S. Hong [6] presented is a wideband, 28-nm RF CMOS process-implemented, 6-bit vector-sum based active phase shifter. A differential I/Q generator and just a vector-summing amplifier featuring differential input and output buffering to employ virtual grounds for high frequencies make up the proposed phase shifter. To produce precise I/Q signals, the I/Q generator was built using a differential hybrid coupler construction, and also the mismatch through its differential input should really be minimal. There at common-gate stage of the cascade input buffer, source cross-coupling capacitors were added to lessen the differential mismatch there at I/Q generator input. Over a broad frequency range of 76 GHz to 104 GHz, the measured findings show a root mean square (RMS) gain inaccuracy of 0.69-0.98 dB but also RMS phase error of 6.8-9.3 degrees. At 82 GHz, the total average peak gain among all 64 states is 3.5 dB. The manufactured phase shifter uses 26 mW of power and has a chip area of 0.32 mm2.

According to the K. R. Namrathaet al.[7]modern society is dominated by wireless communication. The term "wireless" plays a significant role in all forms of communication, including satellite and telephone. In recent years, the right design of a Low Noise Amplifier (LNA) in receiver front ends has become a need for modem wireless communication in broadcast radio microwave radio. The design of a radio frequency regime high performance amplifier with low noise is presented in the study. The LNA has been built using a.18um CMOS process at 1.6 GHz, its operational frequency. Due to its ability to enhance unstable Radio Frequency (RF) signals without adding further noise, LNA are often employed in wireless communication receiver’s leading-ends. The LNA design was implemented using the Cadence Virtuoso tool, and operating frequency performance metrics were examined.

A. D. R. Martinez [8] the construction and transistor-level design of a CMOS front-end amplifier for reading out vast areas of SiPM at LAr temperature are shown in this study (87 K). Using industry-standard 110 nm CMOS technology, a trans-impedance amplifier and just a summing amplifier were constructed for the front-end circuit; the simulation results obtained using the foundry PDK are presented in this study. Each stage is built as a Folded

Cascode Operational Trans-impedance Amplifier (OTA) with just an open-loop gain of more than 100 dB, a power rail of 1.25 V and -1.25 V, and a 95 mW power consumption. The target sensor is indeed a SiPM tile of 24 cm2 that was created as part of the Darkside cooperation project. It has a capacitance of 6 nF/cm2 and a quenching resistance of 6 M. The front-end can produce a signal-to-noise ratio over 12 and jitter better that 45 ns for just a single photoelectron (250 fC).

P. Zhang et al.[9]a 16-bit, 1 MS/s pseudo-differential Successive-Approximation-Register Analog-to-Digital Converter (SAR ADC) with a 15-bit ENOB is presented in this study. The design of a differential DAC that makes use of both monotonic and conventional switching allows for the pseudo differential input. Three methods are suggested for improving static and dynamic performance. To get rid of capacitor mismatch faults, a foreground digital self-calibration approach is first given. The bit weights of additional capacitors are measured and calculated using some of the LSBs capacitors. Second, a method for DNL improvement is described. Before the conversion is complete, an analog voltage is subtracted from the DAC using fractional value capacitors. This balances out the impact that would result from discarding the fractional portion of the digital output before final output. A low-offset, low-noise comparator is developed in the third step. It is suggested to use a reset timer in conjunction with a DAC settling replica to trigger the comparator's pre-amplifier to begin amplification of the DAC summing node voltage as soon as the DAC has finished settling. In a 0.18-m, 5-V CMOS fabrication method, an ADC prototype is created. It registers a 107.9-dB SFDR and an SNDR of 92.3 dB. The distance between the DNL and INL is between 0.3 and 0.72 LSB, respectively. The total amount of power used, which is supplied by the 5 V power source, is 40 mW.

D. G. Aller et al.[10] presented a high efficiency linear-assisted Visible Light Communication (VLC) LED driver that doubles as a transmitter. Based on the concept of employing high efficiency but bandwidth-restricted circuitry to give the majority of the power and just a low efficiency but quick linear amplifier (linear aid), a linear-assisted transmitter compensates the signal distortion. In contrast to the conventional approach used during Envelope Tracking (ET) and Envelope Elimination and Restoration (EER) techniques, the proposed solution makes use of the light inside a VLC system by summing the contribution of the linear amplification in light rather than electrically, leading to an electrical isolation between these stages and a reduction of the complexity. The design of a linear-assisted Class E amplifier that delivers a 16-PSK phase digital modulation with such a 1 MHz carrier is provided as experimental findings. On the one hand, the linear amplifier merely transmits the error signal at lesser efficiency whereas the Class E amplifier transmits the majority of the power (92% of the signal power) with high efficiency (81%). The signal circuitry's efficiency is up to 75%, while the overall system efficiency, which takes into account the signal and also the LED biasing circuitry, is up to 85%.

D. G. Aller et al.[11]stated the DA-VSPS, a novel digitally aided vector-summing phase shifter with excellent precision and improved linearity. It starts out by pointing out how standard DA-VSPSs operating at millimeter-wave frequencies suffer from poor RF performance because of their many unit cells and extensive underlying parasitic. Then, a novel DA-VSPS architecture with analog variable-gain amplifiers and digitally assisted current sources is suggested to prevent this cause of performance deterioration. In order to choose the best parameters (number of unit-cells and load impedance) which enhance RF performance while reducing implementation complexity, a study of the accuracy and linearity of both the proposed DA-VSPS is done. In 45 nm silicon-on-insulator CMOS technology, a proof-of-concept prototype was put into use. The test findings showed a 1-dB RF bandwidth

between 27 and 33 GHz, root-mean-square magnitude, and phase errors of 0.1 dB and 0.5° to 0.6°, respectively, despite covering 360° of phase shifts at 5° resolution. Additionally, for all phase shift settings, the observed group delay and input 1dB compression point are kept within 4 ps and > 2.2 dBm, respectively.

DISCUSSION

Frequency compensation and slew rate considerations

The slew rate, or rate at which an op-output amp's voltage may shift, has a maximum value. Slew rate, which is defined as the maximum rate at which the output voltage changes in response to a significant input step, is often given in volts per microsecond. The primary controlling factor of slew rate is capacitor charging. The maximum current that may be used to charge the capacitance at any given point in a circuit limits the pace of voltage change at that location. The charging of a frequency compensating capacitor, whether internal or external, determines the output slew rate in many op-amp applications. Op-amps made with low supply current needs are often slower and have a smaller bandwidth as a result. The output current provided by the op-initial amp's gain stage charges the frequency compensating capacitor. Due to the first stage output current capabilities, the charging rate is consequently limited:

$$\text{Slew rate} = \left|\frac{de_o}{dt_{max}}\right| \cong \frac{I_o}{C}$$

Io is the initial operational current in the stage. The first stage operating current may be simply increased to increase the slew rate, however this is not the case for op-amps with bipolar transistor input stages. An increase in operating current in standard bipolar transistor op-amp stages results in a proportional rise in the stage's electrical characteristics:

$$\text{Transconductance } g_m = \frac{I_o}{\frac{2kT}{q}}$$

Where T is the temperature in Kelvin (K), q is the electrical charge, and k is the Boltzmann constant. The transconductance equation using bipolar transistors has been modified:

$$\text{Transconductance } g_m = \frac{I_C q}{kT}$$

Which, at ambient temperature, is 40 IC V1. Accordingly, gm = 40 mA V1 for a transistor with such a collector current of 1 mA, and a change in VBE of 1 mV results in a change in collector current of 40 A. Due to the differential input's effect on transconductance, which is reduced by half in the input stages of an op-amp, a differential input of 1 mV results in an output current of 20 A. To fix a certain value for f, the rise in transconductance that comes along with any increase in operational current necessitates a matching increase in Cf.

$$\text{Slew rate} = \left|\frac{de_o}{dt_{max}}\right| \cong \frac{2kT}{q} 2\pi f_1$$

The frequency of the input stage current seems to have no effect on slew rate. The majority of

internally compensated general-purpose bipolar input op-amps have slew rates on the order of 1 V/ s, which is explained by our approximation technique. When corrected down to unity gain, bipolar input op-amps with external frequency compensation have the same slew rate restriction. The lower amount of the necessary frequency compensating capacitor results in a higher slew rate when the capacitors are frequency adjusted for closed-loop gains larger than unity. There are bipolar input op-amps with high slew rates that include specialized input stage circuitry that increases current output without also increasing the stage's transconductance. Although FETs, unlike bipolar transistors, are not subject to their transconductance directly reliant upon operating current, they do not have the aforesaid restriction on slew rate. The slew rate of FET input op-amps is often greater than that of bipolar input op-amps.

Compensated feed-forward frequency

For usage with feed-forward frequency adjustment, a few op-amps are appropriate. Compared to conventional lag compensation approaches, this method may provide a large bandwidth and slew rate boost. The first stage in the majority of op-amps contributes the most to total gain, although its frequency response is often quite constrained. The high-gain, low-bandwidth first stage is bypassed somewhere at higher signal frequencies in feed-forward frequency correction, and these frequencies are delivered straight to the op-second amp's stage with a broader bandwidth. By using this method, the phase shift caused by the high-gain low bandwidth stage is removed, leaving the phase shift somewhere at higher frequencies solely attributable to the wide band stage. Figure 3 depicts the core premise of the plan.

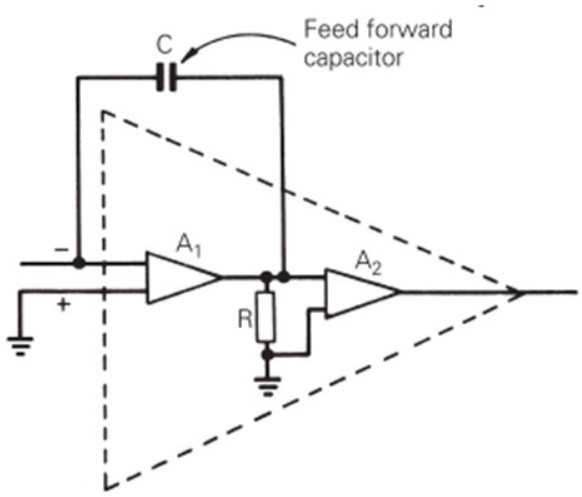

Figure 3: Illustrates the Principle of feed-forward frequency compensation.

The overall gain due to both stages may be expressed as,

$$A_{OL(j\omega)} = \left[A_{1(j\omega)} + \frac{R}{R + \frac{1}{j\omega C}}\right] A_{2(j\omega)} = \left[A_{i(j\omega)} + \frac{1}{1 + \frac{1}{j\omega CR}}\right] A_{2(j\omega)}$$

C is selected such that, when f > 1/2 CR, the first stage's gain has decreased to below unity, roughly matching the second gain stage's total gain. The total gain is reduced to unity by the second stage 20 dB/decade roll-off. The response having feedforward compensation and the

uncompensated response's Bode graphs are shown. Only inverting feedback topologies utilizing externally adjusted op-amps are subject to feed-forward frequency correction.

Compensation for lead

A method for enhancing the phase margin is lead frequency correction. In order to correct for the op-amp phase lag, which would normally result in inadequate phase margin, a capacitor is added to a feedback loop. Connecting a capacitor Cf in parallel with both the feedback resistance is an easy method to do this. This technique of lead compensation is used in a circuit, and the corresponding Bode charts are displayed. We write

$$\frac{1}{\beta} = 1 + \frac{R_2}{R_1}\left(\frac{1}{1 + j\omega C_f R_2}\right) = \left[1 + \frac{R_2}{R_1}\right] 1 + \frac{1 + j\omega C_f (R_1 // R_2)}{1 + j\omega C_f R_2}$$

Other frequency compensating techniques

There are situations when methods other than those mentioned in the aforementioned sections are employed for frequency adjustment in Figure 4. The fundamental idea is the same regardless of the approach. In order to compensate for frequency, the loop gain must be reduced to unity while avoiding an excessive phase shift that might cause closed-loop instability. Simply shunting a signal point inside the feedback loop with a capacitor allows for frequency correction. The additional capacitor adds a 20 dB/decade frequency of attenuation, which begins at the break frequency 1/2 C1Ro, assuming the output resistance somewhere at signal point is Ro. A CR lag network may cause a phase shift as large as 90°. The capacitor value must be selected to bring the loop gain magnitude downward to unity at a frequency lower than that of other attenuating phase break frequencies.

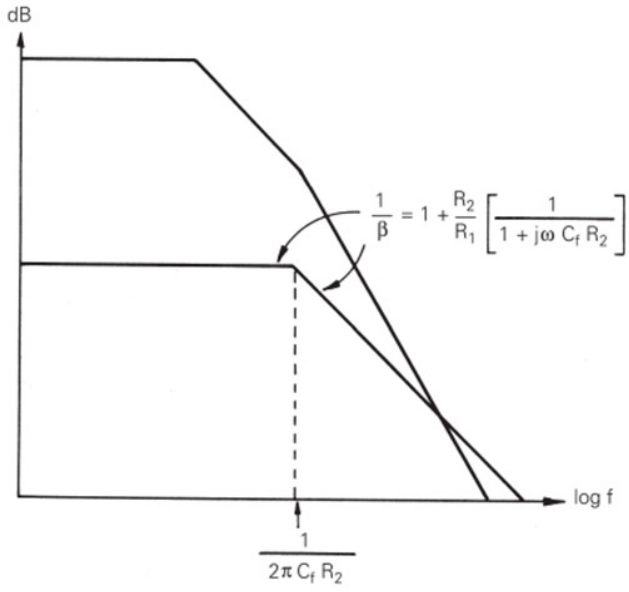

Figure 4: graphical representation of frequency compensating techniques.

Transient response characteristics

It has been focused on variables affecting the op-amp feedback circuits' tiny signal frequency response properties in Figure 5. Now, focus is placed on the variables affecting their temporal behavior, namely their transient responses to large and tiny input step or square-wave signals. By doing out transient tests, students may better comprehend op-amp transient behavior and

the lingo used to explain it. Closed-loop transient behavior is influenced by the amount of the frequency compensation component, the load capacitance, the input capacitance, as well as any stray feedback capacitance.

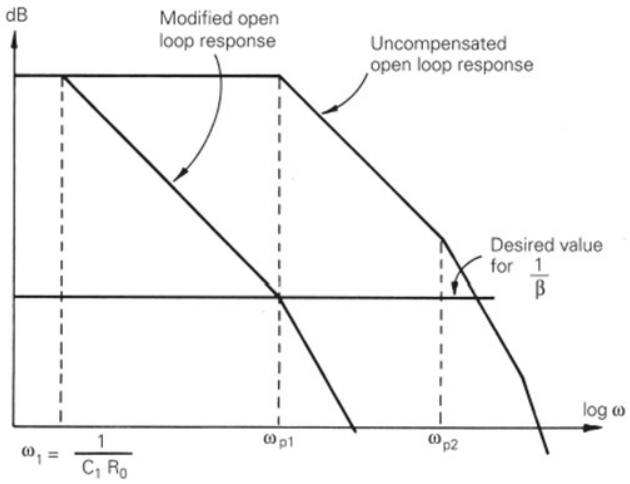

Figure 5: Illustrates the Simple lag compensation with single capacitor.

Small-signal transient response

When there aren't any saturation effects (no slew rate limiting output) and the op-amp circuit is functioning in its linear range, small-signal properties are attained. Circuit relationships in small-signal operation are unaffected by the magnitude of the current and voltage output as well as by their prior history. A circuit's small-signal sinusoidal resonance frequency and small-signal transient behavior are closely connected. We differentiated between two separate closed-loop scenarios in our earlier discussion of small-signal closed-loop frequency response in Figure 6.

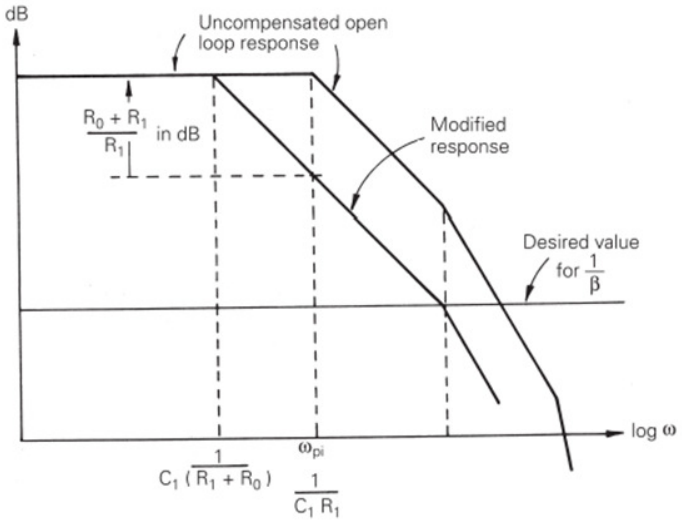

Figure 6: Illustrates the Frequency compensation with RC shunt.

CONCLUSION

An inverting or non-inverting design may serve as the foundation for a summing amplifier. The inverting summing amplifier is much more popular since its output is a simple weighted

sum, but the non-inverting summing amplifier might produce an in-phase output signal with high input impedance. Analog signals are often processed with summing amplifiers. Summing amplifiers are a component of audio mixers. It enables audio professionals to aggregate and replicate sounds from numerous channels into a single recording. The output may be individually set for each and every audio input.

REFERENCES

[1] J. Tang *et al.*, "In Situ Oxygen Doping of Monolayer MoS2 for Novel Electronics," *Small*, 2020, doi: 10.1002/smll.202004276.

[2] I. Yeo, M. Chu, S. G. Gi, H. Hwang, and B. G. Lee, "Stuck-at-Fault Tolerant Schemes for Memristor Crossbar Array-Based Neural Networks," *IEEE Trans. Electron Devices*, 2019, doi: 10.1109/TED.2019.2914460.

[3] M. Kumngern, "0.4 V fully differential current conveyor using multiple-input bulk-driven MOST technique," *Microelectronics J.*, 2019, doi: 10.1016/j.mejo.2019.05.019.

[4] B. Murtianta, "PENGUAT KELAS D DENGAN METODE SUMMING INTEGRATOR," *Elektrika*, 2019, doi: 10.26623/elektrika.v11i2.1693.

[5] L. Jie, B. Zheng, and M. P. Flynn, "A Calibration-Free Time-Interleaved Fourth-Order Noise-Shaping SAR ADC," 2019. doi: 10.1109/JSSC.2019.2938626.

[6] E. T. Sung and S. Hong, "A Wideband W-band 6-bit Active Phase Shifter in 28-nm RF CMOS," 2019. doi: 10.1109/RFIT.2019.8929156.

[7] K. R. Namratha, N. G. Goudar, M. R. Nandish, V. Patil, and N. Thangadurai, "Performance analysis of cascode and inductive regenerative low noise amplifier for wireless applications," *Int. J. Innov. Technol. Explor. Eng.*, 2019, doi: 10.35940/ijitee.i7646.078919.

[8] A. D. R. Martinez, "4-Channel Front-End Integrated Circuit For Readout of Large Area of SiPM under Liquid Argon," 2019. doi: 10.1109/PRIME.2019.8787758.

[9] P. Zhang, W. Feng, P. Zhao, X. Chen, and Z. Zhang, "A 16-Bit 1-MS/s Pseudo-Differential SAR ADC with Digital Calibration and DNL Enhancement Achieving 92 dB SNDR," *IEEE Access*, 2019, doi: 10.1109/ACCESS.2019.2937384.

[10] D. G. Aller, D. G. Lamar, P. F. Miaja, J. Y. Rodríguez, and J. Sebastián, "Design of a Linear-Assisted VLC-LED Transmitter Based on Summing the Light," 2019. doi: 10.1109/IECON.2019.8927718.

[11] J. Xia and S. Boumaiza, "Digitally Assisted 28 GHz Active Phase Shifter with 0.1 dB/0.5° RMS Magnitude/Phase Errors and Enhanced Linearity," *IEEE Trans. Circuits Syst. II Express Briefs*, 2019, doi: 10.1109/TCSII.2018.2872865.